ON THE SUCCESS OF THE HADAL SNAILFISHES

The Influence of Trophic Ecology, Life History, and Pressure Adaptation on Depth Zonation in the Planet's Deepest-Living Fishes

A Dissertation Submitted to the Graduate Division of the University of Hawai‘i at Mānoa in Partial Fulfillment of the Requirements for the Degree of

DOCTOR OF PHILOSOPHY

IN

MARINE BIOLOGY

MAY, 2017

By

Mackenzie Gerringer

Dissertation Committee:

Jeffrey Drazen, Chairperson
Brian Popp
Allen Andrews
Craig Smith
Anna Neuheimer

Keywords: hadal zone, Liparidae, otoliths, stable isotopes, enzymes, stomach contents analysis

This dissertation is dedicated to the teachers who challenged and inspired me.

ACKNOWLEDGEMENTS

I would like to sincerely thank my advisor, Dr. Jeff Drazen, for his enthusiasm, support, and understanding throughout this process. Your unadulterated love for fish, your tireless passion for education, and your graceful work-life balance are inspiring. I express my gratitude to my committee members, Drs. Allen Andrews, Brian Popp, Craig Smith, and Anna Neuheimer, who have taught me so much, have provided fruitful insights and discussions on this work and on science, and have been highly supportive of my education. I also especially thank Dr. Paul Yancey for his mentorship, example, encouragement, and friendship over the years. Thank you for teaching me and believing in me, working with you has been a great joy.

Science, especially hadal science, is by necessity highly collaborative and I am extremely grateful those with whom I have had the opportunity to work on this research. I thank those involved in the HADES program for all their hard work, without whom this research would not have been possible. I am very grateful for those that have set such a wonderful example of grace, kindness, and professionalism in research collaborations, particularly Bruce Mundy, Ashley Rowden, Adam Summers, Andrew Stewart, Malcolm Clark, Dmitri Davydov, and Gary Huss. My sincere thanks to Alan Jamieson for scientific insights, compelling discussions, and support. I also thank Thomas Linley, who has been a wonderful nemesis, collaborator, and friend, and has contributed so much to this research.

I am extremely grateful for the support of the National Science Foundation Graduate Research Fellowship, as well as to the other agencies that made this work possible, including Schmidt Ocean Institute and NOAA. I would like to especially thank the captains and crews of the

research vessels that have supported this research – of the *R/Vs Kaharoa*, *Falkor*, *Thompson*, *Okeanos Explorer*, *Centennial*, and *Shinyo-maru*.

I extend my sincere gratitude to the administrative and support staff in the Oceanography Department who have been so kind and helpful facilitating this work, particularly Anne Lawyer, Phil Rapoza, Catalpa Kong, Kristin Momohara, and Pamela Petras. Kindest thanks also to Lindsay Root and Xuan Tran, Marine Biology Program Coordinators and Tasha Ryan, Fellowships and Professional Development Coordinator, for all their hard work and support.

My deepest thanks to my family and friends for their love and support throughout my life. Thanks to the 2013 Marine Biology Cohort, the 2014 Friday Harbor Fish Class, and the members of the Drazen lab for their friendship and support, especially Astrid Leitner, Chris Demarke, and Kristen Gloeckler. I also thank my friends outside of science, for their encouragement, support, and humor, which have kept me grounded throughout this process. Thank you, Amanda Ziegler for being such a wonderful office mate and friend, and for your shared wit, wisdom, support, and coffee. My heartfelt thanks to Logan Peoples for your support, understanding, insights, and encouragement. Thank you, Madison Gerringer, my sister and friend, for your love and your laughter. Finally, I thank my parents, Teresa and Michael Gerringer, for teaching me the value of education, dedication, and pursuing your dreams. I am so lucky to be your daughter and so grateful for all your support and love.

ABSTRACT

The snailfishes, family Liparidae (Scorpaeniformes), have found notable success in the hadal zone from ~6,000–8,200 m, comprising the dominant ichthyofauna in at least five trenches worldwide. The hadal fish community is distinct from the surrounding abyss where solitary, scavenging fishes such as rattails (Macrouridae), cutthroat eels (Synaphobranchidae), eelpouts (Zoarcidae), and cusk eels (Ophidiidae) are most common. Little is known about the biology of these deepest-living fishes, or the factors that drive their success at hadal depths. Using recent collections from the Mariana Trench, Kermadec Trench, and neighboring abyssal plains, this dissertation investigates the role of trophic ecology, pressure adaptation, and life history in structuring fish communities at the abyssal-hadal boundary. Stomach content and amino acid isotope analyses suggest that suction-feeding predatory fishes like hadal liparids may find an advantage to descending into the trench – where amphipods are abundant. More generalist feeders and scavengers relying on carrion, such as macrourids, might not benefit from this nutritional advantage at hadal depths. Hadal fishes also show specialized adaptation to hydrostatic pressure, as seen in metabolic enzyme activities. Maximum reaction rate of lactate dehydrogenases from hadal liparids increased under pressures of 600 bar, while in shallow-living fishes, this enzyme was pressure-inhibited. These types of pressure adaptation are necessary for fishes to thrive at hadal depths. Intraspecific activities of tricarboxylic acid cycle enzymes, considered proxies of metabolic rate and nutritional condition, increased with depth of capture in hadal snailfishes, further suggesting an advantage to snailfishes living deeper in the trench where food availability may be higher. Analysis of otolith growth zones support an additional hypothesis – snailfishes may be adapted to a seismically active, high-disturbance hadal environment by having relatively short life-spans that are on the order of fifteen

years when compared to other deep-sea fishes. Additional aspects of hadal snailfish biology, including thermal histories, reproduction, swimming kinematics, and buoyancy strategies are explored and discussed. The taxonomic description of a newly-discovered hadal liparid from the Mariana Trench is also included. This study provides insight into the ecology and physiology of deep-dwelling fishes and provides new understanding of adaptations to life in the trenches.

TABLE OF CONTENTS

Acknowledgments iv

Abstract vi

List of Tables ix

List of Figures x

Chapter I 1

Introduction: The hadal liparids

Chapter II 13

Comparative feeding ecology of abyssal and hadal fishes through stomach content and amino acid isotope analysis

Chapter III 49

Metabolic enzyme activities of abyssal and hadal fishes: pressure effects and a re-evaluation of depth-related changes

Chapter IV 82

Life history of abyssal and hadal fishes from otolith growth zones and oxygen isotopes

Chapter V 123

Distribution, composition, and functions of gelatinous tissues in deep-sea fishes

Chapter VI 150

Pseudoliparis swirei: A newly-discovered hadal liparid (Scorpaeniformes: Liparidae) from the Mariana Trench

Chapter VII 177

Conclusions: On the success of the hadal snailfishes

Appendix 196

Supplementary tables and figures

LIST OF TABLES

1.1. Global geographic and bathymetric distribution of hadal liparids....4

1.2. Global collections of hadal liparids by year....6

2.1. Collection information for stomach contents and stable isotope analyses....19

2.2. Hadal liparid prey tables....22

2.3. Prey tables for abyssal species....24

2.4. Isotopic compositions and estimated trophic positions of abyssal and hadal fishes....27

3.1. Collection information for metabolic enzyme activities study....54

3.2. Activities of metabolic enzymes at atmospheric pressure....57

4.1. Estimated age and growth parameters for abyssal and hadal fishes....99

4.2. Samples used in thermal history reconstruction through oxygen isotopes....100

5.1. Composition of gelatinous tissues in deep-sea species....132

5.2. Fishes with gelatinous tissues....134

6.1. Collection details of *Pseudoliparis swirei* from the Mariana Trench....152

6.2. Measurements and counts of *Pseudoliparis swirei*....157

6.3. Ratios of *Pseudoliparis swirei*....158

6.4. Evolutionary divergence between *Pseudoliparis swirei* and close relatives....165

LIST OF FIGURES

1.1. Map of hadal trenches and troughs with depths exceeding 6,500 m 2

1.2. Hadal liparids—*in situ* and fresh photographs and taxonomic drawings 3

1.3. Collection of hadal fishes through baited traps.....5

1.4. Depth distributions of hadal and near-hadal fishes by family 6

2.1. Prey accumulation curves for hadal liparids.....21

2.2. Principal components analysis of hadal liparid and abyssal macrourid diet 26

2.3. $\delta^{15}N$ values of source amino acids by capture depth.....28

2.4. Source amino acid $\delta^{15}N$ values compared to those of bulk tissue 29

3.1. Hadal liparid metabolic enzyme activities by depth of capture.....59

3.2. Lactate dehydrogenase changes in maximum reaction rate at varying pressures.....60

3.3. Malate dehydrogenase changes in maximum reaction rate at varying pressures 61

3.4. Pyruvate kinase changes in maximum reaction rate at varying pressures.....62

3.5. Pyruvate kinase response to pressure with trimethylamine-N-oxide.....63

3.6. Enzyme activities by depth of capture for 67 species of demersal fishes.....64

4.1. Whole and sectioned otoliths of *Careproctus melanurus*.....90

4.2. *Careproctus melanurus* otolith mass and dimensions as a function of body mass 91

4.3. Estimated length-at-age relationships for *Careproctus melanurus* 92

4.4. Whole and sectioned otoliths of hadal liparids.....93

4.5. Hadal liparid otolith dimensions as a function of body mass and standard length.....94

4.6. Estimated length-at-age relationships for hadal liparids.....96

4.7. Estimated length-at-age relationships for abyssal macrourids.....98

4.8. Oxygen isotopic compositions across individual otoliths of abyssal and hadal fishes.....101

4.9. Estimated temperature changes across otolith growth of abyssal and hadal fishes.....102

4.10. Temperature-depth profiles for the Kermadec and Mariana trenches 103

4.11. Estimated temperature of *Careproctus melanurus* and habitat temperature profile.....104

5.1. Gelatinous tissues in deep-sea fishes 125

5.2. Schematic of robotic hadal snailfish model and body shape with gelatinous tissues.....130

5.3. Taxonomic distribution of fishes with gelatinous tissues.....135

6.1. Map of collection locations within the Mariana Trench.....151

6.2. Images of *Pseudoliparis swirei—in situ,* collected specimens, and radiograph.....156

6.3. Lateral view of *Pseudoliparis swirei.* 159

6.4. Ventral view of *Pseudoliparis swirei* and tooth, jaw, and disk structure 160

6.5. Pectoral girdle of *Pseudoliparis swirei*.....161

6.6. Phylogenetic relationships of hadal liparids 164

6.7. Egg sizes and frequencies of *Pseudoliparis swirei*.....166

6.8. Postcoronal pores of freshly-caught *Pseudoliparis swirei*.....168

7.1. Preliminary hadal food web.....180

CHAPTER I

Introduction: The hadal liparids

The hadal zone—deep-sea trenches with depths ranging from 6,000 to 11,000 m—represents 45% of the ocean's depth range but remain one of Earth's least explored habitats. These parts of the ocean take their name from the mythological Greek underworld and are characterized by harsh conditions of high hydrostatic pressures, low temperatures, and perpetual darkness (Bruun, 1957). Most of the hadal zone is made up of subducting trenches, largely located around the Pacific Rim (**Figure 1.1**). Many of the environmental factors experienced by hadal organisms are similar to those on the surrounding abyss and broader deep sea, however, hadal trenches have notably increased hydrostatic pressures, high levels of seismicity, and a distinctly sloping topography relative to other deep-sea habitats. With these environmental differences, there are marked faunal transitions from the abyss to the hadal zone (e.g., Wolff, 1970; Jamieson et al., 2011). The distinct community of hadal fauna includes amphipods, fishes, tanaids, isopods, cumaceans, decapods, echinoderms, nematodes, polychaetes, copepods, molluscs, foraminifera, and cnidarians, at apparently high levels of endemism (Wolff, 1958; Beliaev, 1989; Jamieson et al., 2009a; 2010).

The first fish collected from hadal[1] depths was the ophidiid, *Bassogigas profundismus*, caught in 1901 at 6,035 m in the Mosely Trench by the Princess Alice Expedition (Nielsen, 1964). From the early days of more thorough hadal surveys, however, snailfishes (Liparidae, Scorpaeniformes, **Figure 1.2**) have been among the most commonly caught vertebrates in the hadal environment. On the Danish *HDMS Galathea* expedition, one of two prominent early voyages of hadal research, five individuals of the hadal snailfish *Notoliparis kermadecensis* (formerly *Careproctus kermadecensis*) were caught in the Kermadec Trench in 1952, between depths 6,660–6,770 m, (Nielsen, 1964). Another pioneering hadal expedition aboard the Soviet vessel *RV Vitjaz*, caught the snailfish, *Pseudoliparis amblystomopsis* (then *Careproctus*

[1] Although the official transition from the abyssal to the hadal zone has recently been proposed at 6,500 m (Watling et al., 2013), many of the known faunal changes occur at and around 6,000 m, leading some to prefer this boundary (e.g., Jamieson, 2015).

amblystomopsis), in the Kurile Kamtchatka Trench at 7,230 m in 1955 and in the Japan Trench, at depths as great as 7,579 m in 1957 (Nielsen, 1964). Other hadal and deep-abyssal snailfishes have been seen in the South Sandwich Trench (*Careproctus sandwichensis* at 5,435–5,453 m; Andriashev, 1998) and in the Peru-Chile Trench (Fujii et al., 2010). **Table 1.1** summarizes the known records of liparids in the hadal environment and their depth ranges from the literature and recent trap and baited camera studies. Historical collections of hadal liparids have been few and far between, limiting understanding of the biology and ecology of these fishes, but recent study clearly shows that they are very abundant at hadal depths.

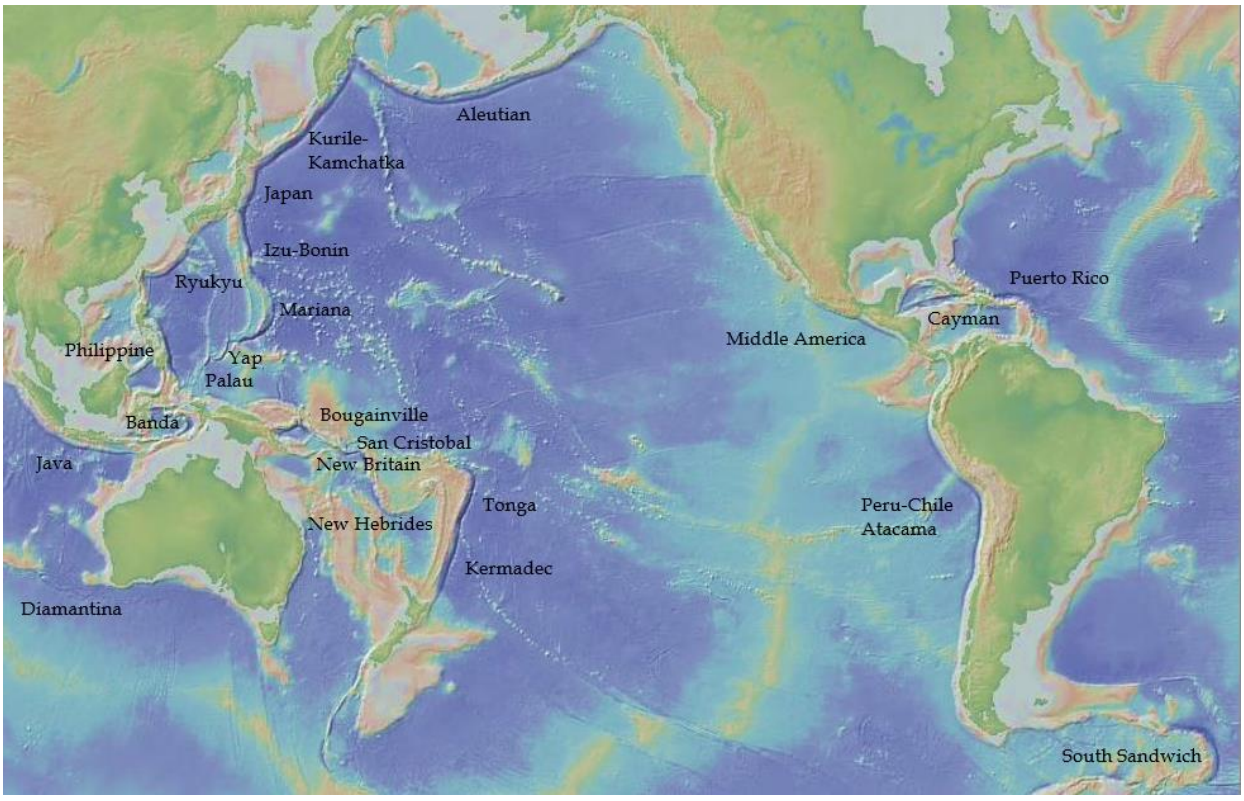

Figure 1.1. Hadal trenches and troughs with depths exceeding 6,500 m (Jamieson, 2011). Map constructed using bathymetry map data from GeoMapApp, Global Multi-Resolution Topography synthesis (Ryan et al., 2009).

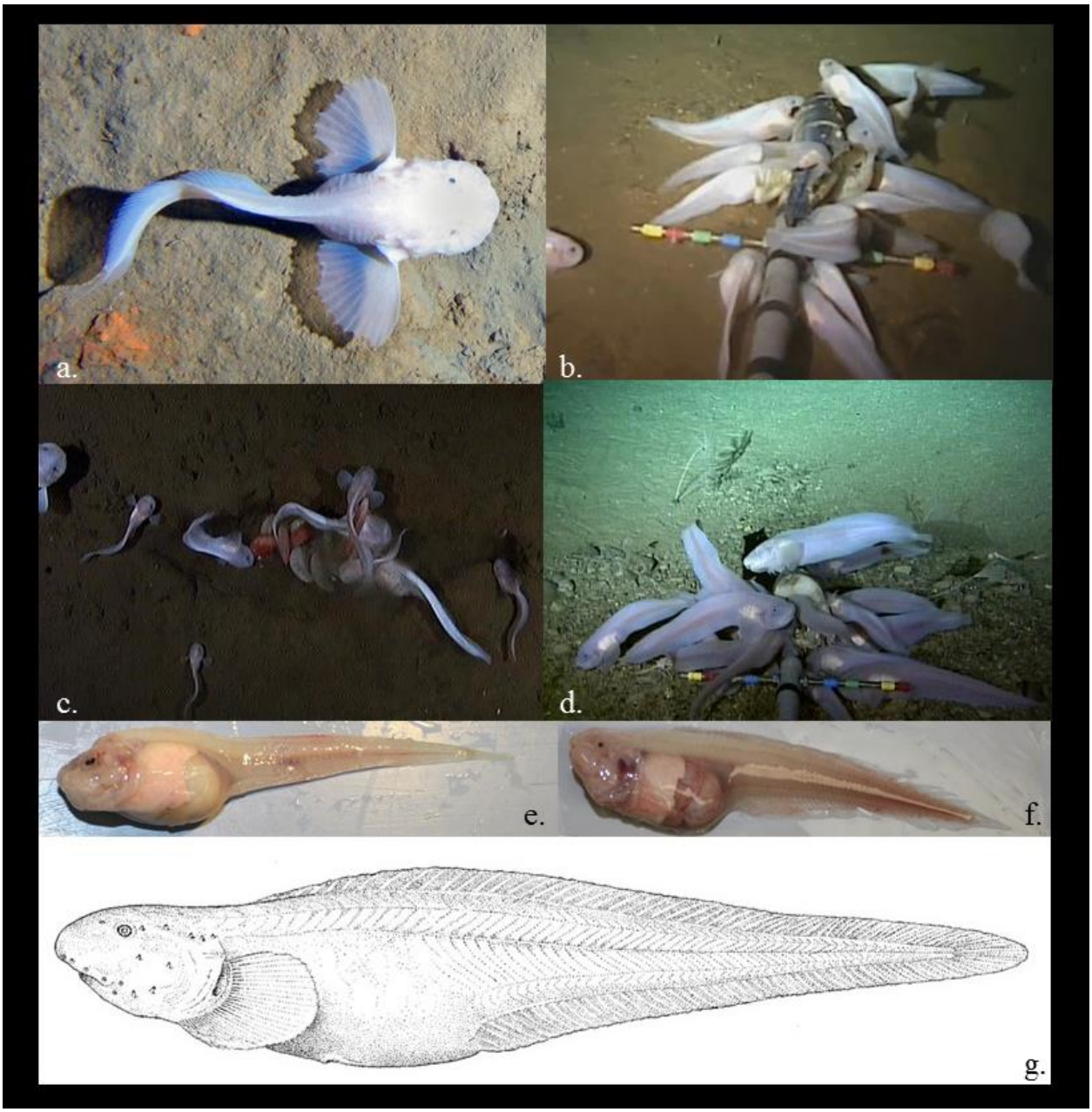

Figure 1.2. Hadal liparids. *In situ* photographs of hadal snailfish, **a)** Peru-Chile Trench, **b)** Mariana Trench (Liparidae sp. nov.), **c)** Japan Trench (*Pseudoliparis belyaevi*), **d)** Kermadec Trench (*Notoliparis kermadecensis*). Photos by Alan Jamieson, University of Aberdeen. Collections of hadal snailfish from the **e)** Mariana (Liparidae sp. nov.) and **f)** Kermadec (*Notoliparis kermadecensis*) trenches, HADES cruises. Photos by Mackenzie Gerringer and Thomas Linley. **g)** Taxonomic drawing of *Notoliparis kermadecensis*, Kermadec Trench (Nielsen, 1964).

Table 1.1. List of the global geographic and bathymetric distribution of known hadal liparids. Includes records of abyssal species near trenches. *Archimede* observation in Puerto Rico Trench is probable, but anecdotal. Depths shown in meters. Undescribed species listed with common names, detailed by Linley et al., 2016.

Trench	Depth	Species	Reference
Japan Trench	7420-7450	*Pseudoliparis amblystomopsis*	Andriashev, 1955
	6380-7587	*Pseudoliparis belyaevi*	Andriashev et al., 1993
Kermadec Trench	5879-7669	*Notoliparis kermadecensis*	Linley et al., 2016
	6456-7560	*Notoliparis stewarti*	Stein, 2016
Kurile-Kamchatka	6156-7587	*Pseudoliparis amblystomopsis*	Andriashev, 1955
Macquarie-Hjort Trench	5400-5410	*Notoliparis macquariensis*	Andriashev, 1978
Mariana Trench	6198-8078	Mariana snailfish	Linley et al., 2016
	8007-8145	Ethereal snailfish	Linley et al., 2016
Peru-Chile Trench	6150	*Notoliparis antonbruuni*	Stein, 2005
	7049	Peru-Chile snailfish	Jamieson, 2012
Puerto Rico Trench	7300	Archimede snailfish	Pérês, 1965
South Orkney Trench	5465-5474	*Notoliparis kurchatovi*	Andriashev, 1975
South Sandwich Trench	5435-5453	*Careproctus sandwichensis*	Andriashev and Stein, 1998

Snailfishes are typically small, tadpole-shaped fishes which live in temperate to cold waters from the intertidal to the hadal environment and from polar systems (Matallanas and Pequeno, 2000) to the subtropics (Chernova et al., 2004). They are one of the most bathymetrically widespread families, and have found notable success at hadal depths (Nielsen, 1964; Jamieson et al., 2009; Linley et al., 2016). There are a number of interesting adaptations known in the liparid family, including an antifreeze protein in the skin of Antarctic species (Evans and Fletcher, 2001; Hobbs and Fletcher, 2013), dermal ossicles that may offer protection with minimum additional weight (Märss et al., 2010), and neutral buoyancy without a swimbladder achieved through decreased skeletal ossification and a subdermal extracellular matrix (Eastman et al., 1994). Comparatively little is known about the family; there are several rare, or at least remote, species of snailfishes, and many species have only recently been described (Johnson, 1969; Andriashev, 1998; Choi et al., 1998; Chernova and Stein, 2002; Stein et al., 2003, 2006; Orr, 2004; Stein, 2005; Chernova, 2006; Knudsen et al., 2007; Chernova and Møller, 2008; Busby and Cartwright, 2009; Kai et al., 2011; Balushkin, 2012; Park et al., 2013; Stein and Drazen, 2014; Tokranov and Orlov, 2014).

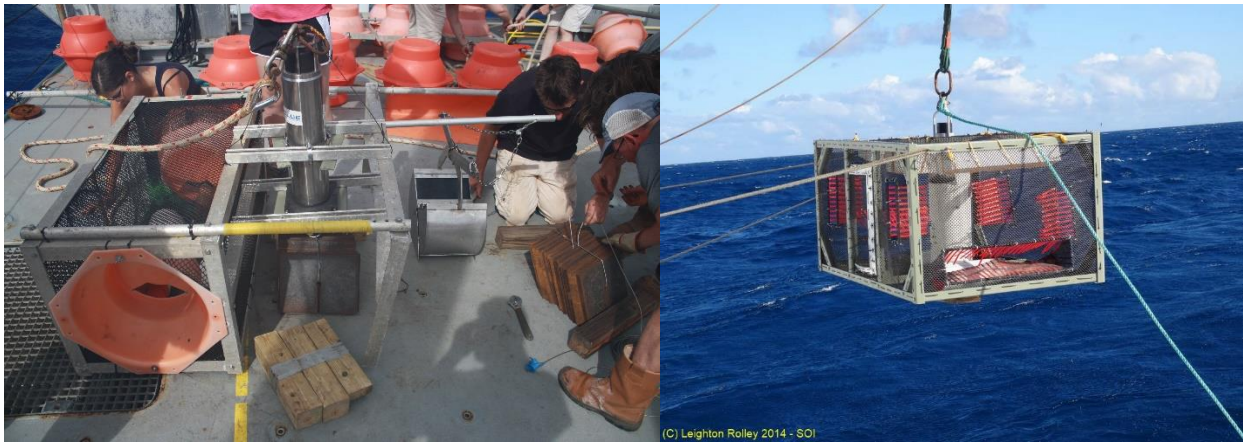

Figure 1.3. Collection of hadal fishes. Baited traps – free vehicles with acoustic releases rated to full-ocean depth. *Left*. Small fish trap and rock grab (University of Aberdeen) being readied for deployment in the Mariana Trench. *Right*. Large fish trap (University of Hawai‘i) above the Kermadec Trench, photo by Leighton Rolley, Schmidt Ocean Institute.

The snailfishes are clearly very successful in hadal trenches, colonizing many of the studied trenches and reaching high abundances there (Fujii, et al., 2010; Linley et al., 2016). Their importance to hadal systems has only been recently realized, largely facilitated by the use of baited traps (**Figure 1.3**) and cameras. The colonization of the deep sea by fishes, and by snailfishes in particular, is understood to be a radiation from shallow waters into the deep (Burke, 1930; Priede and Froese, 2013). Detailed surveys have revealed a noticeable shift in the fish community at the abyssal-hadal boundary, from members of the diverse and abundant cosmopolitan families Macrouridae, Ophidiidae, Synaphobranchidae, and Zoarcidae on the abyssal plains, to the liparids in the hadal zone (**Figure 1.4**). What evolutionary drivers have influenced the success of the snailfish in the trench environment relative to other potential colonizers? This dissertation uses an unprecedented collection from recent cruises to the Kermadec and Mariana trenches (**Table 1.2**) to investigate the biology and ecology of hadal snailfishes and neighboring abyssal fishes to evaluate the reasons for the notable success of liparids in the hadal environment.

Table 1.2. Global collections of hadal liparids by year. Collection year is noted, with depth presented in meters, and number of specimens collected (n) for each species, as of June, 2016. Ships were operated out of the former Soviet Union, Denmark, USA, Japan, and New Zealand. 2011 and 2014 collections include both *Notoliparis kermadecensis* and *N. stewarti*.

Trench	Species	Year	Depth	Ship	n
Kurile-Kamchatka	*Pseudoliparis amblystomopsis*	1953	7230	*Vitjaz*	1
Japan	*Pseudoliparis amblystomopsis*	1955	6156–7579	*Vitjaz*	5
Japan	*Pseudoliparis belyaevi*	1957	7579	*Vitjaz*	1
Kermadec	*Notoliparis kermadecensis*	1952	6660–6770	*Galathea*	5
Peru-Chile	*Notoliparis antonbruuni*	1966	6150	*Anton Bruun*	1
Japan	*Pseudoliparis amblystomopsis*	2009		*Hakuho maru*	2
Kermadec	*Notoliparis spp.*	2011	7002–7050	*Kaharoa*	7
Kermadec	*Notoliparis spp.*	2014	6456–7554	*Thompson*	41
Mariana	Liparidae sp. nov.	2014	6898–7966	*Falkor*	37

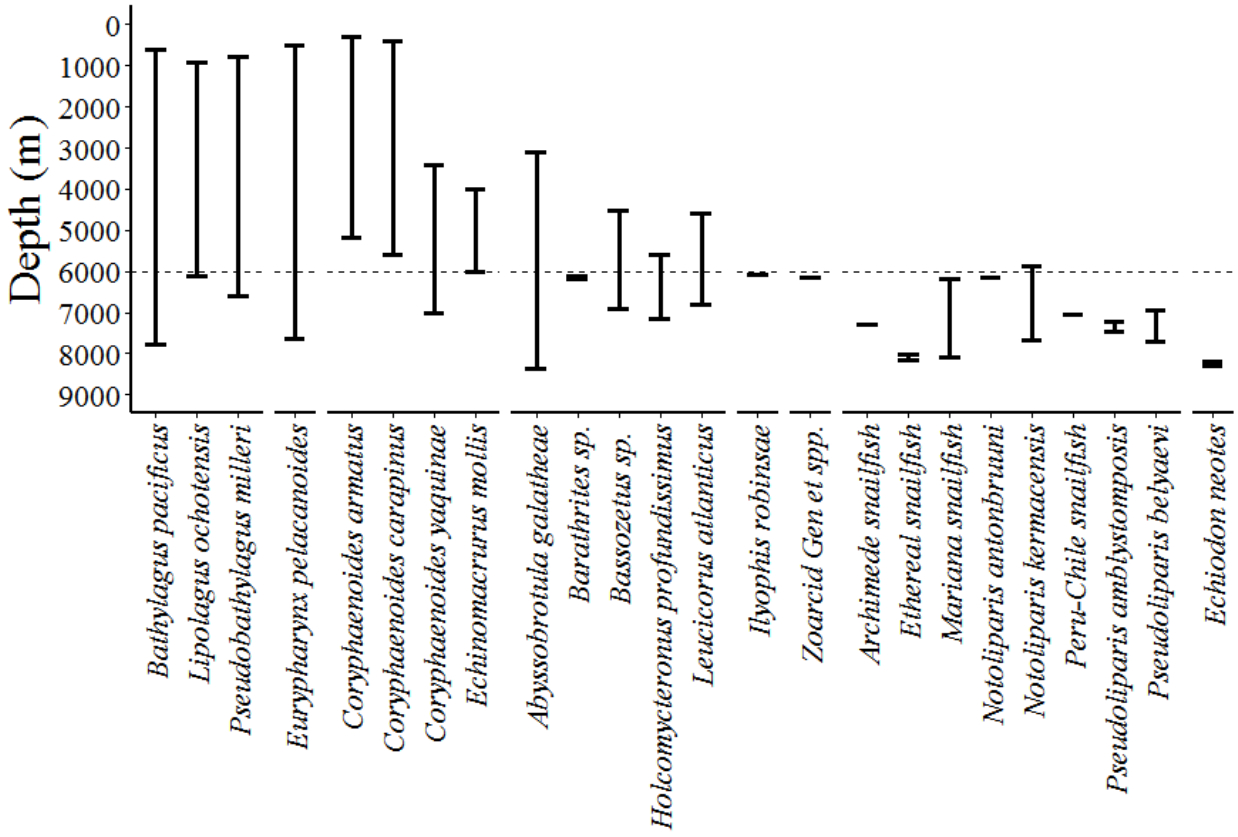

Figure 1.4. Depth distributions of hadal and near-hadal fishes by family. From left to right: Bathylagidae, Eurypharyngidae, Macrouridae, Ophidiidae, Synaphobranchidae, Zoarcidae, Liparidae, Carapidae. 6,000 m abyssal-hadal boundary shown as dotted line. Data from (Linley et al., 2016) and (Jamieson et al., 2009).

The following chapters explore hypotheses that could have contributed to the success of the snailfishes in hadal trenches relative to other families, employing multiple approaches in physiology and ecology. **Chapter II** posits that the trophic ecology of hadal liparids, specifically adaptations to feed on small crustaceans, allows them to take advantage of high amphipod biomass in trenches. Carrion-feeding and piscivorous fishes do not have the same advantage. A corollary to this hypothesis is that for the hadal liparids, individuals living deeper will exhibit better nutritive condition than those at shallower depths, both due to increased amphipod abundance and decreased competition for food, addressed in **Chapter III**. The next chapter also explores the idea that intrinsic pressure adaptations are more pronounced in hadal liparids than in the abyssal fishes, enabling their expansion to greater depths within the trenches. **Chapter IV** suggests that the liparids are shorter-lived than macrourids, which may be adaptive in the high-disturbance hadal environment over evolutionary timescales. Further, the idea that the lack of a planktonic larval stage in hadal liparids might limit dispersal beyond the hadal environment leading to high degrees of endemism is tested using thermal history reconstructions from oxygen isotopic compositions across individual otoliths. Ophidiids and macrourids, which are believed to have a planktonic larval stage, should disperse beyond the trench, leaving little evolutionary mechanism for adapting specifically to the hadal zone. Additional hypotheses tested are that the completely benthic life history of the hadal liparid also allows the trench to serve as a refuge from predation and year-round reproduction in hadal liparids results in increased fitness in the high-disturbance hadal zone. **Chapter V** explores the hypothesis that gelatinous tissue in hadal liparids provides buoyancy under the extreme hydrostatic pressure of the hadal environment, giving them an advantage over deep-sea fish families with gas bladders. **Chapter VI** provides a taxonomic description of a newly discovered species of hadal liparid from the Mariana Trench with morphological and molecular data. Together, these studies provide substantial insights into the biology and ecology of fishes in the hadal zone and the factors driving the success of snailfishes near the ocean's greatest depths.

References

Andriashev, A., 1978. On the third species of the ultra-abyssal genus *Notoliparis* Andr. (Pisces. Liparidae), from the deepwaters of the Macquarie Trench, with some notes on zoogeographic and evolutionary significance of this discovery. Trudy Instituta Okeanologii Akademiia Nauk SSSR 112, 152–161.

Andriashev, A., 1975. A new ultra-abyssal fish, *Notoliparis kurchatovi* gen. et sp. N. (Liparidae) from the South Orkney Trench (Antarctic). Trudy Instituta Okeanologii Akademiia Nauk SSSR 103, 313–319.

Andriashev, A., 1955. A new fish of the snailfish family (Pisces, Liparidae) found at a depth of more than 7 kilometers. Trudy Instituta Okeanologii Akademiia Nauk SSSR 12, 340–344.

Andriashev, A., Stein, D., 1998. Review of the snailfish genus *Careproctus* (Liparidae, Scorpaeniformes) in Antarctic and adjacent waters. Natural History Museum Los Angeles City Scientific Contributions 470.

Andriashev, A.P., Pitruk, D.L., 1993. A review of the ultra-abyssal (hadal) genus *Pseudoliparis* (Scorpaeniformes, Liparidae) with a description of a new species from the Japan Trench. Voprosy ikhtiologii 33, 325–330.

Balushkin, A., 2012. *Volodichthys* gen. nov. new species of the primitive snailfish (Liparidae: Scorpaeniformes) of the southern hemishpere. Description of new species *V. Solovjevae* sp. nov. (Cooperation Sea, the Antarctic). Journal of Ichthyology 52, 1–10. (doi:10.1134/S0032945212010018)

Bruun, A., 1957. General introduction to the reports and list of deep-sea stations. Galathea Report 1, 7–48.

Burke, V., 1930. Revision of fishes of family Liparidae. Bulletin of the United States National Museum. 150, 1–204.

Busby, M., Cartwright, R., 2009. *Paraliparis adustus* and *Paraliparis bullacephalus*: two new snailfish species (Teleostei: Liparidae) from Alaska. Ichthyological Research 56, 245–252. (doi:10.1007/s10228-008-0090-x)

Chernova, N., 2006. New and rare snailfishes (Liparidae, Scorpaeniformes) with the description of four new species from the Southern Hemisphere and tropical east Pacific. Journal of Ichthyology 46, S1–S14. (doi:10.1134/S0032945206100018)

Chernova, N., Møller, P., 2008. A new snailfish, *Paraliparis nigellus* sp. nov. (Scorpaeniformes, Liparidae), from the northern Mid-Atlantic Ridge – with notes on occurrence of *Psednos* in the area. Marine Biology Research 4, 369–375. (doi:10.1080/17451000802017507)

Chernova, N., Stein, D., 2002. Ten new species of *Psednos* (Pisces, Scorpaeniformes: Liparidae) from the Pacific and North Atlantic Oceans. American Society of Ichthyologists and Herpetologists 2002, 755–778.

Chernova, N., Stein, D., Andriashev, A., 2004. Family Liparidae Scopoli 1777. California Academy of Sciences Annotated Checklists Fishes 31.

Choi, Y., Kido, K., Amaoka, K., 1998. Redescription of a snailfish, *Liparis chefuensis*, with comments on its sexual dimorphism and synonymy (Scorpaeniformes: Liparidae. Icthyological Research 45, 314–318.

Eastman, J., Hikida, R., Devries, A., 1994. Buoyancy studies and microscopy of skin and subdermal extracellular matrix of the antarctic snailfish, *Paraliparis devriesi*. Journal of Morphology 220, 85–101. (doi:10.1002/jmor.1052200108)

Evans, R., Fletcher, G., 2001. Isolation and characterization of type I antifreeze proteins from Atlantic snailfish (*Liparis atlanticus*) and dusky snailfish (*Liparis gibbus*). Biochimica et Biophysica Acta 1547, 235–244.

Fujii, T., Jamieson, A., Solan, M., Bagley, P., Priede, I., 2010. A large aggregation of liparids at 7703 meters and a reappraisal of the abundance and diversity of hadal fish. Bioscience 60, 506–515. (doi:10.1525/bio.2010.60.7.6)

Hobbs, R., Fletcher, G., 2013. Epithelial dominant expression of antifreeze proteins in cunner suggests recent entry into a high freeze-risk ecozone. Comparative Biochemistry and Physiology Part A: Molecular & Integrative Physiology 164, 111–8. (doi:10.1016/j.cbpa.2012.10.017)

Jamieson, A., 2011. Ecology of deep oceans: Hadal trenches. Encylcopedia Life Science 1–8. (doi:10.1002/9780470015902.a0023606)

Jamieson, A., 2015. The hadal zone: life in the deepest oceans. Cambridge, United Kingdom.

Jamieson, A., Fujii, T., Solan, M., Matsumoto, A., Bagley, P., Priede, I., 2009. Liparid and macrourid fishes of the hadal zone: *in situ* observations of activity and feeding behaviour. Proceedings of the Royal Society B: Biological Sciences 276, 1037–45. (doi:10.1098/rspb.2008.1670)

Jamieson, A., Kilgallen, N., Rowden, A., Fujii, T., Horton, T., Lörz, A.-N., Kitazawa, K., Priede, I., 2011. Bait-attending fauna of the Kermadec Trench, SW Pacific Ocean: Evidence for an ecotone across the abyssal–hadal transition zone. Deep-Sea Research Part I: Oceanographic Research Papers 58, 49–62. (doi:10.1016/j.dsr.2010.11.003)

Johnson, C., 1969. Contributions ot the biology of the showy snailfish, *Liparis pulchellus*. Copeia 1969, 830–835.

Kai, Y., Ikeguchi, S., Nakabo, T., 2011. A new species of the genus *Careproctus* (Liparidae) from the Sea of Japan. Ichthyological Research 58, 350–354. (doi:10.1007/s10228-011-0241-3)

Knudsen, S., Møller, P., Gravlund, P., 2007. Phylogeny of the snailfishes (Teleostei: Liparidae) based on molecular and morphological data. Molecular Phylogenetics and Evolution 44, 649–66. (doi:10.1016/j.ympev.2007.04.005)

Linley, T.D., Gerringer, M.E., Yancey, P.H., Drazen, J.C., Weinstock, C.L., Jamieson, A.J., 2016. Fishes of the hadal zone including new species, *in situ* observations and depth records of Liparidae. Deep-Sea Research Part I: Oceanographic Research Papers 114, 99–110. (doi:http://dx.doi.org/10.1016/j.dsr.2016.05.003)

Märss, T., Lees, J., Wilson, M., Saat, T., Špilev, H., 2010. The morphology and sculpture of ossicles in the Cyclopteridae and Liparidae (Teleostei) of the Baltic Sea. Estonian Journal of Earch Sciences 59, 263. (doi:10.3176/earth.2010.4.03)

Matallanas, J., Pequeno, G., 2000. A new snailfish species, *Paraliparis orcadensis* sp . nov. (Pisces: Scorpaeniformes) from the Scotia Sea (Southern Ocean). Polar Biology 23, 298–300.

Nielsen, J., 1964. Fishes from depths exceeding 6000 meters. Galathea Report 7, 113–124.

Orr, J., 2004. *Lopholiparis flerxi*: A new genus and species of snailfish (Scorpaeniformes: Liparidae) from the Aleutian Islands, Alaska. American Society of Ichthyologists and Herpetologists 2004, 551–555.

Park, J., Ji, H., Yoon, B., Choi, Y., Ban, T., Kim, J., 2013. First record of a snailfish, *Careproctus colletti* (Scorpaeniformes: Liparidae) from the East Sea, Korea. Korean Journal of Ichthyology 25, 46.

Pérês, J., 1965. *Aperçu sur les résultats de deux plongées effectuées dans le ravin de Puerto-Rico par le bathyscaphe Archimède*. Deep-Sea Research and Oceanographic Abstracts 12, 883–891. (doi:10.1016/0011-7471(65)90811-9)

Priede, I., Froese, R., 2013. Colonization of the deep sea by fishes. Journal of Fish Biology 83, 1528–50. (doi:10.1111/jfb.12265)

Ryan, W., Carbotte, S., Coplan, J., O'Hara, S., Melkonian, A., Arko, R., Weissel, R., Ferrini, V., Goodwillie, A., Nitsche, F., Bonczkowski, J., Zemsky, R., 2009. Global Multi-Resolution Topography synthesis. Geochemistry, Geophysics, Geosystems 10. (doi:10.1029/2008GC002332)

Stein, D., 2005. Descriptions of four new species, redescription of *Paraliparis membranaceus*, and additional data on species of the fish family Liparidae (Pisces, Scorpaeniformes) from the west coast of South America and the Indian Ocean. Zootaxa 1–25.

Stein, D., Bond, C., Misitano, D., 2003. *Liparis adiastolus* (Teleostei, Liparidae): A new snailfish species from the littoral zone of the Northeastern Pacific, and redescription of *Liparis rutteri*. American Society of Ichthyologists and Herpetologists 2003, 818–823.

Stein, D., Drazen, J., 2014. *Paraliparis hawaiiensis*, a new species of snailfish (Scorpaeniformes: Liparidae) and the first described from the Hawaiian Archipelago. Journal of Fish Biology 84, 1519–26. (doi:10.1111/jfb.12377)

Stein, D., Drazen, J., Schlining, K., Barry, J., Kuhnz, L., 2006. Snailfishes of the central California coast: video, photographic and morphological observations. Journal of Fish Biology 69, 970–986. (doi:10.1111/j.1095-8649.2006.01167.x)

Tokranov, A., Orlov, A., 2014. Specific features of distribution, ecology, and dynamics of catches of blotched snailfish *Crystallichthys mirabilis* (Liparidae) in Pacific waters off the northern Kuril Islands and southeastern Kamchatka. Journal of Ichthyology 54, 338–346. (doi:10.1134/S0032945214030151)

Watling, L., Guinotte, J., Clark, M.R., Smith, C.R., 2013. A proposed biogeography of the deep ocean floor. Progress in Oceanography 111, 91–112. (doi:10.1016/j.pocean.2012.11.003)

Wolff, T., 1970. The concept of the hadal or ultra-abyssal fauna. Deep-Sea Research and Oceanographic Abstracts 17, 983–1003. (doi:10.1016/0011-7471(70)90049-5)

CHAPTER II

Comparative feeding ecology of abyssal and hadal fishes through stomach content and amino acid isotope analysis

Abstract

The snailfishes, family Liparidae (Scorpaeniformes), have found notable success in the hadal zone from ~6,000 to 8,200 m, comprising the dominant ichthyofauna in at least five trenches worldwide. Little is known about the biology of these deepest-living fishes, nor the factors that drive their success at hadal depths. Using recent collections from the Mariana Trench, Kermadec Trench, and neighboring abyssal plains, this study investigates the potential role of trophic ecology in structuring fish communities at the abyssal-hadal boundary. Stomach contents were analyzed from two species of hadal snailfishes, *Notoliparis kermadecensis* and a newly-discovered species from the Mariana Trench. Amphipods comprised the majority (Kermadec: 95.2%, Mariana: 97.4% index of relative importance) of stomach contents in both species. Decapod crustaceans, polychaetes (*N. kermadecensis* only), and remains of carrion (squid and fish) were minor dietary components. Diet analyses of abyssal species (families Macrouridae, Ophidiidae, Zoarcidae) collected from near the trenches and the literature are compared to those of the hadal liparids. Stomachs from abyssal fishes also contained amphipods, however macrourids had a higher trophic plasticity with a greater diversity of prey items, including larger proportions of carrion and fish remains; supporting previous findings. Suction-feeding predatory fishes like hadal liparids may find an advantage to descending into the trench—where amphipods are abundant. More generalist feeders and scavengers relying on carrion, such as macrourids, might not benefit from this nutritional advantage at hadal depths. Compound specific isotope analysis of amino acids was used to estimate trophic level of these species (5.3±0.2 *Coryphaenoides armatus*, 5.2±0.2 *C. yaquinae*, 4.6±0.2 *Spectrunculus grandis*, 4.2±0.2 *N. kermadecensis*, 4.4±0.2 Mariana snailfish). Source amino acid $\delta^{15}N$ values were especially high in hadal liparids (8.0±0.3‰ Kermadec, 6.7±0.2‰ Mariana), suggesting a less surface-derived food source than seen in the scavenging abyssal macrourids, *C. armatus* (3.5±0.3‰) and *C. yaquinae* (2.2±0.3‰). These results are compared to bulk muscle tissue isotopic compositions. This study provides the first comprehensive examination

of the feeding ecology of the ocean's deepest-living fishes and informs new understanding of trophic interactions and fish community structure in and near the hadal zone.

Introduction

The hadal zone consists of deep-sea trenches with depths ranging from 6,000 to 11,000 m and houses a distinctly different community than the surrounding abyss with an apparently high level of endemism (Wolff, 1970; Jamieson et al., 2011c). The hadal community includes: amphipods, fishes, tanaids, isopods, cumaceans, decapods, echinoderms, nematodes, polychaetes, copepods, molluscs, foraminifera, and cnidarians (Wolff, 1958; Beliaev, 1989; Jamieson et al., 2009a; 2010). As on the abyssal plains (depths 4,000 – 6,000 m), most of the hadal community is supported by falling carrion and particulate organic matter from the upper ocean (Angel, 1982). The processing of nutrients into the hadal food web is believed to be facilitated by an active heterotrophic psychrophilic and piezophilic microbial community (Zobell, 1952; Yayanos et al., 1981; Kato et al., 1997; Fang et al., 2002; Bartlett, 2003; Nunoura et al. 2015). Although there is evidence for chemosynthetic communities in deep-sea trenches their prevalence and importance in the hadal ecosystem is not yet characterized (Kobayashi et al., 1992; Fujikura et al., 1999; Fujiwara et al., 2001; Ohara et al., 2012). Current understanding of life in the hadal zone comes largely from trawl (Zenkevich and Bogoiavlenskii, 1953; Bruun et al., 1957; Svenska djuphavsexpeditionen, 1957) and free vehicle camera and trap work (Jamieson et al., 2009c, 2009d; Søreide and Jamieson, 2013; Lacey et al., 2016), as well as a few ROV (Momma et al., 2004; Bowen et al., 2008; 2009) and manned submersible operations (Pérês, 1965; Forman, 2009; Gallo, et al., 2015). With the difficulty in observing and sampling this environment, the ecology of hadal organisms and their trophic relationships remain poorly understood.

Video observations, collections, and extrapolation from studies of shallower-living relatives of hadal taxa provide some information about trophic interactions in the hadal zone. *In situ* video collected by free-vehicle landers has allowed a glimpse of the feeding habits of hadal fauna such as: detritus-feeding holothurians (Jamieson et al., 2011b), scavenging isopods (Jamieson et al., 2012), predatory decapods (Jamieson et al., 2009a) and pardaliscid amphipods of the genus *Princaxelia (*Jamieson et al., 2011d), and lysianassoid amphipods, the most well-studied

hadal animals. These amphipods are known to have morphological and chemosensory adaptations to carrion feeding (Dahl, 1979; Kaufmann, 1994; Hargrave et al., 1995; De Broyer et al., 2004) and scavenge and disperse bait rapidly at hadal depths (e.g., Hessler et al., 1978). Previous studies on the feeding ecology of hadal amphipods have found evidence for opportunistic scavenging, and a high degree of trophic flexibility, including adaptations to ingest large amounts of carrion and phytodetritus (Perrone et al., 2003; Blankenship and Levin, 2007; Kobayashi et al., 2012).

Even fewer data exists on the trophic ecology of hadal fishes. Video observations have shown the rapid consumption of bait by fishes such as macrourids at the abyssal-hadal boundary (Jamieson, et al., 2011c). Liparids and ophidiids from the Japan, Kermadec, and Mariana trenches have been observed eating crustaceans (Jamieson et al., 2009b; Fujii et al., 2010; Linley et al., 2017). The present study focuses largely on liparids, a prominent endemic hadal group in at least five trenches (Japan, Kermadec, Kurile-Kamchatka, Mariana, Peru-Chile; Linley et al., 2016). Hadal liparids are small (≤ 30 cm) pink snailfishes that have been found as deep as 8,145 m (Linley et al., 2016). This depth (~8,200 m) is thought to be the lower limit for teleosts due to physiological constraints of pressure adaptation (Yancey et al., 2014). Nielsen (1964) reported stomach contents consisting mostly of amphipods in the liparid *Notoliparis kermadecensis* from the Kermadec Trench. However, the sample size in this description was small. Shallower-living snailfishes in the Kamchatka region are benthic feeders eating mostly crustaceans (Orlov and Tokranov, 2011). Many species of snailfishes from other localities also eat amphipods, which can make up as much as 88.8% of diet by numeric importance (Johnson, 1969; Falk-Petersen et al., 1988; Kobayashi and Hiyama, 1991; Labai et al., 2002; 2003; Glubokov, 2010; Jin, Zhang, and Zue, 2010; Cui et al., 2012).

Studies of the trophic ecology of abyssal species (depths 4,000–6,000 m) are also limited, making comparisons to hadal taxa difficult. Macrourids are thought to have broad generalist diets as determined from stomach contents analysis and stable isotopic composition (e.g., Drazen et al., 2008). Other abyssal species are less well-studied. However, in a recent expedition, the ophidiid *Bassozetus* sp. was observed feeding on amphipods in the Kermadec Trench (Linley et al., 2017). Further details on *in situ* observations and depth distributions of the fish community at the abyssal-hadal boundary are provided by Linley et al. (2017). Based on these studies, we hypothesized that

hadal liparids would have a more specific predatory feeding strategy, while abyssal species such as macrourids might be more generalist opportunistic feeders.

Much of our current understanding of hadal fishes comes from baited trap and camera studies, which create an artificial food-fall. Although this mimics a natural process, it could bias our view of the community's normal feeding ecology. The bait provides a food source for both fishes and their prey, and the interactions observed in this setting may not fully reflect what happens on a routine basis at depth. Further, video observations and stomach contents provide only a brief 'snapshot' view of diet. Multiple approaches are therefore needed to advance the understanding of trophic ecology in the hadal zone.

Stable isotope analysis has been a useful tool in investigating the longer-term feeding ecology of many organisms (e.g., Peterson and Fry, 1987). Traditionally, this involves comparing differences in bulk tissue (generally white muscle) nitrogen isotopic composition, which display an ~2-4‰ ^{15}N enrichment in consumer relative to prey for each increasing trophic level (e.g., Post, 2002). This technique has been used to study four hadal lysianassoid amphipod morphotypes in the Kermadec and Tonga trenches. Bulk $\delta^{15}N$ values in these amphipods ranged from 7.9 to 13.8‰ (Blankenship and Levin, 2007). Interpreting results of nitrogen (and carbon) isotope analysis requires information about the isotopic compositions of organisms at the base of the food web. The isotopic compositions at the base of the hadal food web have not been well-characterized. Therefore, in this study, amino acid compound-specific nitrogen isotope analysis (AA-CSIA, e.g., Popp et al., 2007; Choy et al., 2012) was used to investigate the trophic level of abyssal and hadal fishes. In this newer technique, the $\delta^{15}N$ values of certain "trophic" amino acids, that fractionate with each trophic level (up to ~7‰ relative to source amino acids), are compared to those of "source" amino acids, that maintain relatively consistent $\delta^{15}N$ values throughout the megafaunal food web, to estimate a trophic position (McClelland and Montoya, 2002; Popp et al., 2007; Chikaraishi et al., 2009; Hannides et al., 2009). Source amino acid values are known to change with depth in small, slowly settling particles, with increasing $\delta^{15}N$ values at greater depths (McCarthy et al., 2007; Hannides et al., 2009). Consequently, source amino acid $\delta^{15}N$ values can also provide information about the origin of nitrogen in animal's food.

The aims of this study were three-fold: 1) characterize the diet of the hadal snailfish through stomach contents analysis and compare it to the diets of abyssal species documented in the

literature; 2) compare trophic positions of abyssal and hadal fishes using compound specific isotope analysis of individual amino acids; and 3) explore the role of trophic interactions in structuring fish depth zonation at the abyssal-hadal boundary.

Materials & Methods

Fishes were collected using baited traps on cruises to the Kermadec and Mariana trenches in April-May and November-December of 2014 respectively (**Table 2.1**). Traps, described elsewhere (Linley et al., 2016), were baited with mackerel (in nylon mesh to prevent feeding) and squid. Each captured fish was measured and weighed fresh. Sex was determined visually during dissections at sea. Further information on these collections including site maps can be found in Linley et al. (2016).

Stomach Contents. Stomachs were dissected shipboard, weighed fresh, and preserved in 10% buffered formaldehyde. In the lab, stomachs were weighed whole, then contents were removed and weighed. While whole, each stomach was roughly scored on a fullness scale of 0 to 4, 0 indicating an empty stomach, 1- less than half full, 2- half full, 3- more than half full, and 4- full. Fullness scores included the contribution of digestive mucus. Contents were sorted to discernible taxon and digestive state, a 1 to 4 index; 1- an undigested prey item, 2- some soft parts digested, 3- most soft parts digested with skeleton intact, and 4- items that were very digested, with only a few hard parts remaining. A separate analysis of stomach contents using only items of the higher digestive states was conducted to investigate potential trap effects. If the composition of prey items eaten most recently, when the artificial trap environment was introduced, differed greatly from more highly digested items, this would demonstrate a bias of sampling technique. Prey items of each taxon were grouped by digestive state, counted, weighed, and photographed.

Compositions of stomach contents are presented using four metrics. Percent frequency of occurrence (%F) shows the percentage of stomachs that had a certain prey type present. Percent numerical importance (%N) gives the proportion of a prey group compared to the total number of prey items examined for each species. Percent weight (%W) shows the gravimetric importance of a given prey group in relation to the total weight of all prey. These three indices were also used to

generate an index of relative importance (IRI), which sums the %N and %W multiplied by the %F (Pinkas, 1971). These values were totaled for all items and a %IRI is presented. Further analyses were conducted using the statistical programming platform R (R Core Team, 2013). The nonparametric Kruskal-Wallis test was used for statistical comparisons due to small sample sizes. Cumulative prey curves were generated using the R package vegan (random, 5000 permutations, Oksanen et al., 2016) to investigate sampling thoroughness. A model (Lomolino) was constructed to estimate the maximum number of prey items for each species. Composition of stomach contents between families were compared using analysis of similarities (ANOSIM) in vegan. Principal components analysis (PCA) plots were made in R using the *prcomp* function to investigate differences in prey composition between species (%N). Additional figures were produced using Microsoft Excel and the R package *ggplot2* (Wickam, 2009).

Isotope Analysis. At sea, white muscle samples were collected from the anterior portion of the epaxial muscle and flash frozen in liquid nitrogen. Tissues were stored at -80°C prior to preparation and lyophilized and ground for analysis. Roughly mid-size individuals from representative habitat depths of each species were selected. Bulk muscle tissue nitrogen and carbon isotope analyses were conducted with a mass spectrometer (DeltaXP) coupled with an elemental combustion system (Costech ECS 4010, MAT Conflo IV, ThermoFinnigan). Replicate measurements of individual samples were consistent within 0.12‰ for carbon (range 0.07–0.14‰) and 0.14‰ for nitrogen (range 0–0.21‰). Sample preparation for CSIA-AA followed methods detailed in Hannides et al. (2009) and Choy et al. (2012). The method involves: acid hydrolysis with 6 N HCl, filtration and cation exchange chromatography, esterification of the carboxyl terminus with isopropanol and acetyl chloride, trifluoroacetylation of amine groups with methylene chloride and trifluoroacetyl anhydride, solvent extraction, and redissolvation in ethyl acetate. $\delta^{15}N$ values of individual amino acids were measured using a Delta V Plus mass spectrometer/Trace GC (gas chromatograph) with a GCC III combustion interface. Samples were analyzed in triplicate and measurements normalized to co-injected reference compounds norleucine and aminoadipic acid of known isotopic composition. When coelution of other compounds confounded norleucine and aminoadipic acid values, measurements were regressed against a suite of pure amino acids with known $\delta^{15}N$ values prepared in the same process and analyzed before and after every triplicate

series of sample measurements. Instrumental accuracy averaged 0.4±0.3‰ (range 0.02–1.0‰). Standard deviations of $\delta^{15}N$ values between triplicate runs ranged from 0.02 to 0.9‰ with an average of 0.3±0.2‰ for individual amino acids used in trophic position calculations. All $\delta^{15}N$ values are presented in reference to atmospheric N_2.

Trophic positions were estimated according to the methods described by Chikaraishi et al. (2009) using the following equation, based on the update for fishes by Bradley et al. (2015).

$$\text{Trophic Position} = \frac{\delta^{15}N_{\text{trophicAAs}} - \delta^{15}N_{\text{sourceAAs}} - 3.86}{5.46} + 1$$

Weighted means (by error, e.g., Hayes et al. 1990) of source amino acids (lysine, phenylalanine) are compared to trophic amino acids (alanine, leucine, glutamic acid) as these were the most consistent measurements and according to the recommendations of Bradley et al. (2015). Glycine was excluded from the source amino acid calculations, contrary to the methods of Bradley et al. (2015), due to the co-elution of an unknown compound that could have confounded values. Beta (3.86±0.23) and TDF (trophic discrimination factor, 5.46±0.13) values for this equation were calculated using weighted mean differences between data-derived values of Bradley et al. (2015) considering the omission of glycine.

Results

Table 2.1. Collection Information (n = number of stomachs analyzed, n* = number of stomachs with prey items present). Ranges presented: Depth indicates capture depth. SL: Standard length, measured fresh with fish mass. Sex indicates number of individuals F: female, M: male, J: juvenile. Others were not sexed due to damage. Zoarcidae Gen et spp. includes individuals of the genera *Pachycara* and *Pyrolycus*.

Trench	Species	n	n*	Depth (m)	SL (cm)	Mass (g)	Sex (F, M, J)
Kermadec	*Notoliparis kermadecensis*	38	37	6456–7554	12.9–29	13.6–230	18, 12, 3
	Coryphaenoides armatus	4	2	3569–5112	50.6–78.6	576–1930	1, 2, 0
	Spectrunculus grandis	10	6	3569–3865	26.9–43.9	106–532	0, 3, 5
	Zoarcidae Gen et spp.	3	3	4817–4989	42–46.8	460–660	1, 2, 0
Mariana	Liparidae sp. nov.	29	29	6898–7966	10.5–28.8	8–160	14, 5, 7
	Coryphaenoides yaquinae	1	1	6081	23	40	0, 0, 1

Stomach Contents of Hadal Liparids. Collection information is presented in **Table 2.1** with individual sample details in **Supplementary Table 2.1**. The newly-discovered species of hadal liparid from the Mariana Trench, currently being described, will hereafter be referred to as the Mariana liparid or Mariana snailfish (further details in Linley et al., 2016). Thirty-eight *Notoliparis kermadecensis* stomachs were examined, 37 of which had prey items. Prey was present in all 29 Mariana liparid stomachs examined. Prey accumulation curves, used to evaluate sampling sufficiency, (**Figure 2.1**) showed that the number of prey categories was likely beginning to plateau for both trenches, more so for the Mariana snailfish. A model (Lomolino) estimated asymptotes for these curves at 12.3 prey categories for the *N. kermadecensis* and 8.7 prey categories for the Mariana snailfish.

Large amounts of digestive mucus were present in each stomach. Mucus was not included in prey item weight. Prey items and their composition of total stomach contents by %F, %N, %W, and %IRI are presented in **Table 2.2**. Fish remains include bone, eye lenses, scales, and vertebrae. Crustacean remains include digested exoskeleton pieces that could not be identified to a more specific taxon. Unidentified remains included crustacean or squid eggs found in one Mariana snailfish stomach.

Amphipods were by far the most numerically and gravimetrically important prey item. Every liparid with prey in its stomach had eaten at least one amphipod. As many as 378 amphipods were found in one Kermadec liparid stomach (minimum 1), with as many as 226 in one Mariana liparid stomach (minimum 19). The average number of amphipods found in each stomach was 96.59±71.07 for *N. kermadecensis* and 71.07±52.85 for the Mariana snailfish. Predatory amphipods of the genus *Princaxelia* were also found, albeit infrequently. Lysianassoid amphipods were not identified to higher taxonomic resolution, as morphological classifications are complex and likely in need of revision (Ritchie et al., 2015). Probable morphotypes from these depths in the Mariana and Kermadec trenches include *Bathycallisoma (Scopelocheirus) schellenbergi, Hirondellea dubia,* and *H. gigas* (e.g., France, 1993; Blankenship et al., 2006; Ritchie et al., 2015).

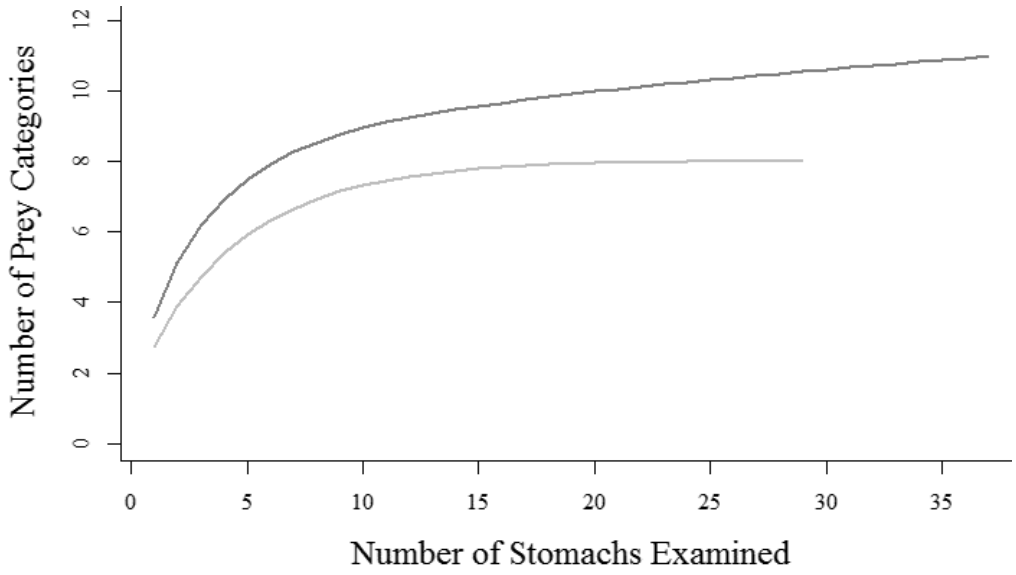

Figure 2.1. Prey accumulation curves for hadal liparids. Includes broad prey categories- brooding amphipods, amphipods with nematode parasites, and *Princaxelia* classified as amphipods. Mariana liparid in light grey, *N. kermadecensis* in black.

Decapod remains were found in the majority of liparid stomachs from both trenches (62.16% of *N. kermadecensis* with food and 58.62% of the Mariana liparid). Decapods had not previously been found in the stomachs of hadal liparids, and snailfish have not yet been seen capturing decapods *in situ*. Most of the decapods were present as highly digested (state 4) remains, though whole individuals up to 8.5 cm total length were found in a few fish.

Polychaete remains (of at least 20 individuals) were found in stomachs of liparids from the Kermadec Trench. Polychaetes are a relatively common, diverse, and characteristic hadal fauna (Kirkegaard, 1956; Jamieson, 2015). These remains are believed to be scale worms of the family *Polynoidae, Pholoidae,* or *Sigalionidae.* Members of the family *Polynoidae* are the most common hadal polychaete (Kirkegaard, 1956; Paterson et al., 2009). Polynoids have recently been imaged in the Kermadec Trench (Jamieson, 2015), and were collected on the same cruise as the liparids in this study (Shank et al. unpublished data), making this the most likely identification. *Sigalionidae* have also been found in trenches, but *Pholoidae* are not known to occur at hadal depths (Paterson et al., 2009). Notably, no polychaetes were found in the Mariana species, although their remains were present in 51.35% of stomachs from *Notoliparis kermadecensis*.

Table 2.2. above) Hadal liparid prey tables for all digestive states. From 37 Kermadec and 29 Mariana liparids with prey remains in their stomachs. Sample size (n) indicates the total number of prey items examined or the total weight of all prey items. **below)** Hadal liparid prey tables showing highly digested items (digestive states 3 and 4) only.

	Kermadec Trench				Mariana Trench			
	%F	**%N**	**%W**	**%IRI**	**%F**	**%N**	**%W**	**%IRI**
Amphipods (Lysianassidae)	100	95.48	84.63	95.73	100	97.26	87.66	87.74
Amphipods (Pardaliscidae)	2.70	0.03	0.40	0.01	3.45	0.05	0.38	0.01
Amphipods with Nematodes	48.65	1.14	0.77	0.49	3.45	0.05	0.00	0.00
Brooding Amphipods	0.00	0.00	0.00	0.00	6.90	0.15	0.19	0.01
Copepods	2.70	0.05	0.37	0.01	0.00	0.00	0.00	0.00
Crustacean Remains	8.11	0.08	0.40	0.02	13.79	0.20	3.19	0.25
Decapods	62.16	0.57	3.31	1.28	58.62	0.83	3.93	1.47
Fish Remains	29.73	1.54	1.97	0.55	20.69	0.68	0.18	0.09
Ostracods	2.70	0.08	0.01	0.00	0.00	0.00	0.00	0.00
Polychaetes	51.35	0.57	5.08	1.54	0.00	0.00	0.00	0.00
Squid	18.92	0.16	2.28	0.25	27.59	0.54	2.51	0.44
Unidentified	21.62	0.30	0.79	0.13	17.24	0.24	1.97	0.20
	n=37	n=3692	117.8 g		n=29	n=2046	110.4 g	

	Kermadec Trench				Mariana Trench			
	%F	**%N**	**%W**	**%IRI**	**%F**	**%N**	**%W**	**%IRI**
Amphipods (Lysianassidae)	91.89	91.81	70.98	89.97	89.66	94.44	75.10	91.43
Amphipods with Nematodes	2.70	0.17	0.01	0.00	3.45	0.14	0.01	0.00
Crustacean Remains	8.11	0.25	1.01	0.06	13.79	0.56	6.89	0.62
Decapods	62.16	1.74	8.42	3.80	58.62	2.36	15.16	6.18
Fish Remains	29.73	3.39	4.17	1.35	20.69	1.94	0.38	0.29
Polychaetes	51.35	1.65	12.83	4.47	0.00	0.00	0.00	0.00
Squid	5.41	0.17	0.64	0.03	3.45	0.14	0.06	0.00
Unidentified	18.92	0.83	1.95	0.32	6.90	0.28	3.43	0.15
	n=37	n=1209	46.3 g		n=29	n=720	51.2 g	

Fish remains were found relatively frequently (29.73% of Kermadec snailfish, 20.69% of Mariana stomachs). Remains included large scales of what appeared to be several species (possibly Melamphaeidae or Bathylagidae or very digested scales of large fishes), portions of eye lens, small vertebrae, and other bones. Some pieces of tissue from bait squid were found in the hadal liparid stomachs (18.42% of *N. kermadecensis* and 10.34% of Mariana snailfish), but other species of squid were also found. Three species were identified from beaks: *Onychoteuthis sp.*, *Walvisteuthis sp.*, and *Magnapinna sp.*, the last a deep-sea benthopelagic squid (Vecchione and Young, 2006).

A small number of other prey items were found, including a few calanoid copepods and ostracods in stomachs of *N. kermadecensis*. Both of these groups have been recorded at hadal depths (Vinogradova, 1962; Jamieson, 2015). Rocks were found in about a third of stomachs from both hadal liparids. Rocks were typically small; likely debris ingested during suction feeding or compacted sediment from digested amphipod guts. Some prey items could not be identified due to advanced digestion. Unidentified material made up a very small portion of the hadal liparid stomach contents (0.12% IRI for *N. kermadecensis,* 0.20% IRI for the Mariana liparid).

Nematode parasites were found in 27.03% (17) of Kermadec liparid stomachs and 13.79% (6) of Mariana liparids. Amphipods with nematode parasites were more common in the Kermadec snailfish (47.37% of stomachs) than in the Mariana snailfish (3.45%). 42 total amphipods with nematodes in *N. kermadecensis* out of 3573 total amphipods were found, with only 1 of 1991 in the Mariana liparid. Details on nematode-parasitized amphipods collected from the Kermadec Trench concurrently with liparids in this study are provided by Leduc and Wilson (2016).

Analysis of prey items in greater digestive states alone (3 and 4) revealed that amphipods still comprised the overwhelming majority of both hadal liparid diets (**Table 2.2b**). Highly digested amphipods were most likely consumed before the traps were deployed (maximum of ~20 hours of bottom time before retrieval). Other prey items such as decapods, fish remains, and polychaetes (*N. kermadecensis* only), appear to be slightly more important dietary components when looking at only highly digested items (**Table 2.2**).

No significant trend was found between percent stomach fullness (mass of stomach content: mass of fish) and depth of capture for either trench. However, there were trends in the number of prey items seen with depth. When standardized to the total mass of the fish, individuals

caught deeper in the Mariana Trench had more prey items in their stomachs (ANOVA, 26 df, F=8.10, p<0.01). In the Kermadec Trench, there was no significant trend (33 df, F=2.74, p=0.108).

Stomach Contents of Abyssal Species. Sample sizes of abyssal fish collections in this study were too small to categorize the complete diets of abyssal species from the Mariana and Kermadec regions (**Table 2.1**). Although stomachs were collected from ten *Spectrunculus grandis*, only six of these had any prey remains present. These remains were all amphipods, in very low numbers (1–6). A few Zoarcidae Gen et spp. stomachs contained amphipods, fish remains, and rocks, however these data are too scant to allow broad conclusions. We found a comparatively diverse collection of prey in *Coryphaenoides armatus*, with contributions from amphipods, fish remains, decapods, polychaetes, and squid (**Table 2.3**). One *Coryphaenoides yaquinae* contained a large number of amphipods, possibly a result of collection location, the individual's small size (juvenile, 23 cm standard length), or the artificial food-fall trap environment. Trematode parasites were found in one *Pachycara sp.* and one *Coryphaenoides armatus* from near the Kermadec Trench.

Table 2.3. Prey tables for abyssal species, including all digestive states. From collection of two *C. armatus*, one *C. yaquinae*, three zoarcids, and six *Spectrunculus grandis* with prey in stomachs.

	Coryphaenoides armatus				*Coryphaenoides yaquinae*			
	%F	**%N**	**%W**	**%IRI**	**%F**	**%N**	**%W**	**%IRI**
Amphipods	50.00	14.29	0.50	7.39	100.00	96.15	76.45	86.30
Crustacean Remains	50.00	0.00	11.65	5.83	0.00	0.00	0.00	0.00
Decapods	50.00	14.29	68.22	41.25	0.00	0.00	0.00	0.00
Fish Remains	50.00	28.57	0.04	14.30	100.00	2.88	2.00	2.44
Polychaete	0.00	0.00	0.00	0.00	100.00	0.96	21.55	11.26
Squid	50.00	14.29	0.11	7.20	0.00	0.00	0.00	0.00
Unidentified	50.00	28.57	19.49	24.03	0.00	0.00	0.00	0.00
	n=2	n=7	27.6 g		n=1	n=104	2.0 g	

	Zoarcidae Gen et spp.				*Spectrunculus grandis*			
	%F	**%N**	**%W**	**%IRI**	**%F**	**%N**	**%W**	**%IRI**
Amphipods	100.00	98.92	96.10	99.16	100.00	100.00	100.00	100.00
Fish Remains	33.33	0.90	0.08	0.16	0.00	0.00	0.00	0.00
	n=3	n=558	32.8 g		n=6	n=16	0.37 g	

For a quantitative comparison of abyssal and hadal fish feeding, we chose the family Macrouridae, a common, often abundant, and relatively well-studied abyssal group, which have traditionally been considered characteristic abyssal species (e.g., Wilson and Waples, 1983). Although we acknowledge that this comparison likely underappreciates the importance of other families in the deep abyssal community, especially ophidiids, (Linley et al., 2017), the paucity of data limits their inclusion in a statistical assessment. Stomach contents data from Drazen et al. (2008) for *C. armatus* and *C. yaquinae* were compared to results from the present study. Small *C. armatus* (≤20 cm pre-anal fin length) were treated as a separate group from larger *C. armatus*, to account for ontogenetic changes in diet. The category crustacean remains include euphausids, mysids, isopods, barnacles, tanaids, and galatheid crabs. The contents of stomachs from abyssal macrourids were significantly different than those of the hadal liparids (ANOSIM, Bray-Curtis dissimilarity, 999 permutations, by %N: $R=0.7916$, $p=0.001$, by %W: $R=0.8749$, $p=0.001$). Although the *C. armatus* and *C. yaquinae* were collected in a different season at a different location, the macrourids that were collected in the present study showed relatively similar results. We therefore believe this to be an appropriate comparison. Principal components analysis revealed that the high abundance of amphipods (high %N), lack of piscivory (low %N of fish remains), and low overall prey diversity in the liparids drove the majority of differences seen in diet between the two groups (**Figure 2.2**). The hadal liparids had low PC1 scores and grouped closely along PC2 whereas the abyssal macrourids had higher PC1 scores and were overall more scattered along both principal axes.

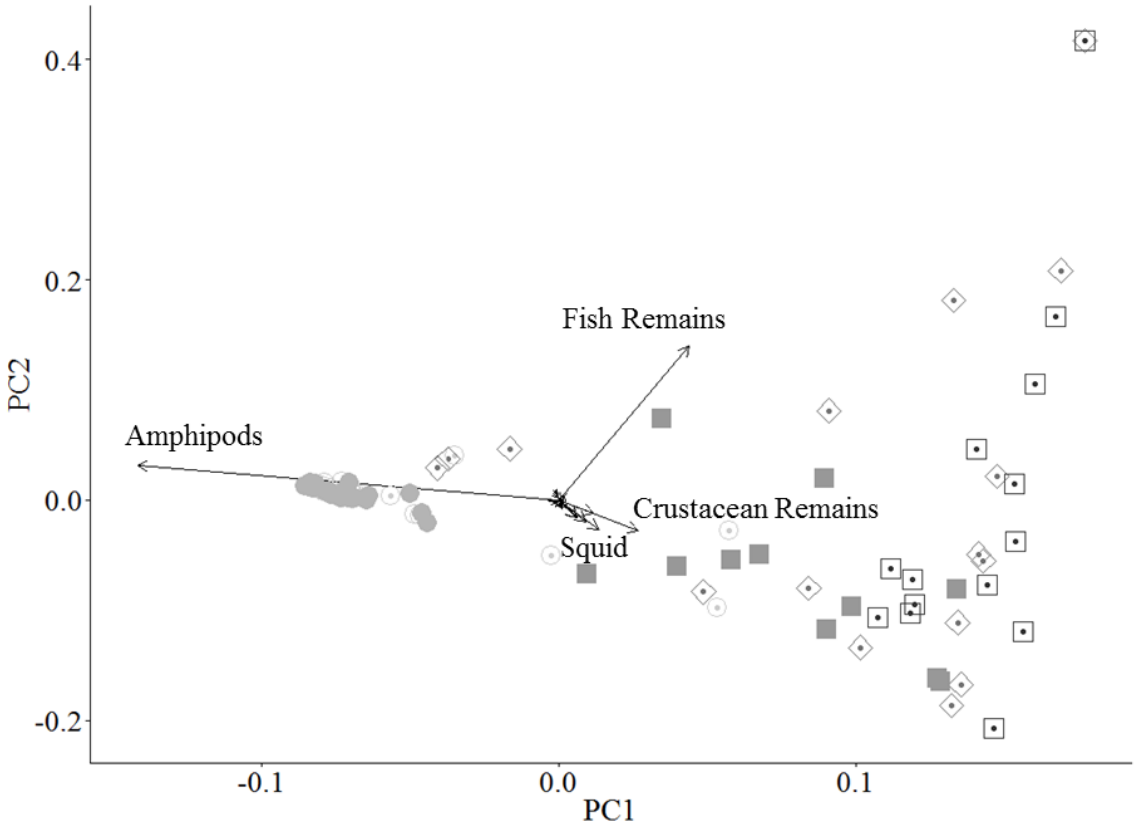

Figure 2.2. Principal components analysis comparing diet composition of hadal liparids and abyssal macrourids. Macrourid data from Drazen et al., 2008. Loadings for most important drivers of differences indicated with labeled black arrows. Comparison based on relative numeric abundance (%N) for each individual (n=15 *C. armatus* large, 16 *C. armatus* small (≤20 cm pre-anal fin length), 11 *C. yaquinae*, 37 *N. kermadecensis*, 29 Mariana liparid). Excludes parasites. *Coryphaenoides armatus* (large - open squares, small – diamonds), *C. yaquinae* (closed squares), *Notoliparis kermadecensis* (open circles), Mariana liparid (closed circles) and *Spectrunculus grandis* (open triangles) shown.

Isotope Analysis. Compound-specific nitrogen isotope analysis of amino acids provided additional information about trophic ecology of these deepest-living fishes. $\delta^{15}N$ values of sixteen individual amino acids were determined for five species (n=3–4). Weighted means of $\delta^{15}N$ values for source amino acids, trophic amino acids, and resulting trophic position estimates are presented in **Table 2.4**. All $\delta^{15}N$ values for measured individual amino acids are available in the supplementary information (**Supplementary Table 2.2**).

Table 2.4. AA-CSIA Results. *C. armatus*, *S. grandis*, and *N. kermadecensis* from the Kermadec Trench, *C. yaquinae* and the Mariana liparid. Depth indicates capture depth (in meters), with individual standard lengths (SL) from fresh measurements. Sample numbers indicate HADES collection information. Standard deviations of weighted means of $\delta^{15}N$ values (‰) for source (lysine, phenylalanine) and trophic (alanine, leucine, glutamic acid) amino acids and trophic positions are presented from three replicate measurements.

Species	Sample #	Depth (m)	SL (cm)	$\delta^{15}N_{sourceAAs}$	$\delta^{15}N_{trophicAAs}$	Trophic Position
C. armatus	100038	3865	50.6	3.96±0.41	30.40±0.19	5.14±0.17
	100363	3601	78.6	3.95±0.36	30.34±0.12	5.13±0.11
	100367	3569	69.0	5.71±0.31	32.26±0.22	5.16±0.18
C. yaquinae	200008	4441	42.6	2.55±0.32	28.69±0.25	5.08±0.20
	200151	5255	30.6	2.80±0.29	28.82±0.20	5.06±0.17
	200152	5255	77.3	3.80±0.17	29.98±0.18	5.09±0.12
S. grandis	100060	4303	40.4	5.47±0.33	27.44±0.23	4.32±0.19
	100377	3569	33.8	5.60±0.46	30.78±0.15	4.90±0.15
	100364	3601	29.0	6.32±0.19	30.51±0.13	4.72±0.11
N. kermadecensis	100175	7515	18.3	8.19±0.50	28.85±0.22	4.08±0.20
	100310	7251	21.0	8.77±0.30	28.89±0.21	3.99±0.17
	100171	7515	18.3	7.29±0.43	29.75±0.19	4.41±0.17
Liparidae sp. nov.	200039	7497	21.0	5.99±0.31	29.81±0.27	4.66±0.20
	200070	7841	17.2	6.78±0.20	29.11±0.35	4.38±0.17
	200033	7495	12.6	5.89±0.33	28.76±0.22	4.48±0.18
	200041	7497	10.5	5.77±0.18	28.15±0.29	4.39±0.15

Weighted means of $\delta^{15}N$ values of source amino acids were significantly different between species (Kruskal-Wallis rank sum test, 4 df, $p=0.01$); higher in hadal species (8.09±0.75‰ Kermadec liparid, 6.11±0.46‰ Mariana liparid) than for abyssal species (4.54±1.01‰ *C. armatus*, 3.05±0.66‰ *C. yaquinae*, 5.79±0.46‰ *S. grandis*; **Figure 2.3**). The ophidiid, *Spectrunculus grandis*, from the Kermadec collection had an intermediate source amino acid value of 5.79±0.46‰ (marginally higher than macrourids, Kruskal-Wallis rank sum test, 1df, $p=0.071$, lower than liparids, $p=0.087$). Source amino acid values were higher in the Kermadec liparid than the Mariana liparid ($p<0.05$). Bulk tissue $\delta^{15}N$ values ranged from 12.3 to 15.5‰ overall, with an average range of 1.1‰ between individuals of the same species (averages: *C. armatus* 13.6±0.8‰; *C. yaquinae* 12.6±0.8‰; Mariana liparid 13.7±0.5‰; *N. kermadecensis* 13.4±0.7‰; *S. grandis* 15.0±0.8‰; **Figure 2.4**).

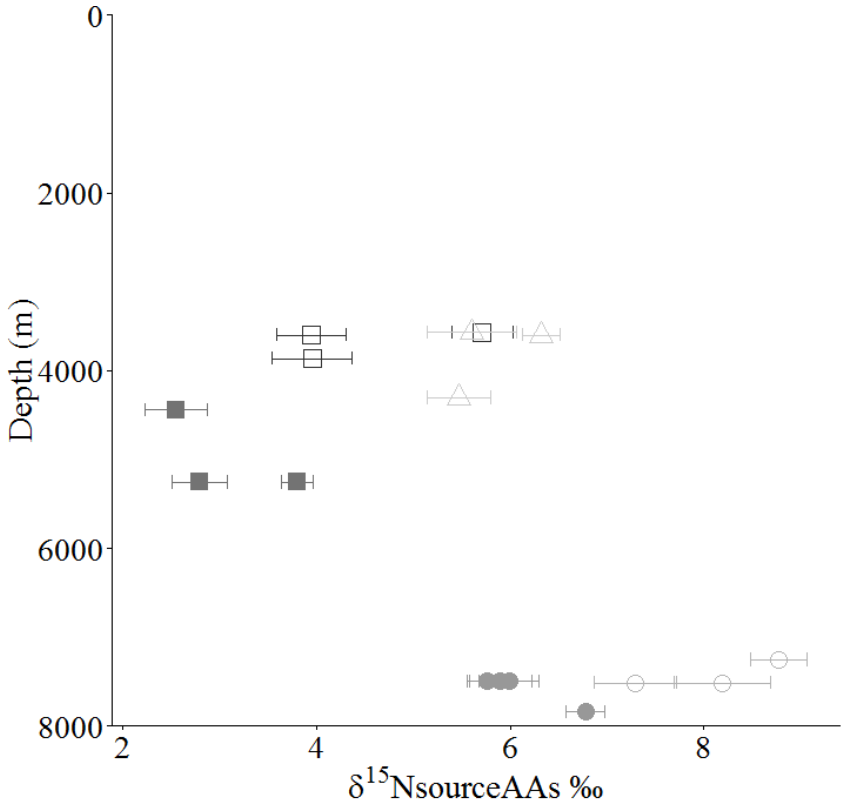

Figure 2.3. $\delta^{15}N$ values (weighted means) of source amino acids (lysine, phenylalanine) by capture depth. Error bars indicate standard deviations between three runs. Capture region and species labeled for each sample group. *Coryphaenoides armatus* (open squares), *C. yaquinae* (closed squares), *Notoliparis kermadecensis* (open circles), Mariana liparid (closed circles) and *Spectrunculus grandis* (open triangles) shown.

Trophic positions (**Table 2.4**) were estimated from the weighted means of $\delta^{15}N$ values of source and trophic amino acids according to Bradley et al. (2015) and were found to be significantly different between families (ANOVA, 4 df, $F=17.41$, $p<0.001$). For hadal liparids, trophic levels were estimated at 4.15±0.22 for *N. kermadecensis* and 4.48±0.13 for the Mariana snailfish. Trophic level estimates were significantly higher for macrourids, 5.14±0.01 for *Coryphaenoides armatus* and 5.08±0.02 for *C. yaquinae*, than for liparids or *S. grandis* (Kruskal-Wallis rank sum test, 1 df, $p<0.05$). The abyssal ophidiid, *Spectrunculus grandis* had an intermediate trophic level (4.65±0.30). No significant difference was found in trophic positions between trenches for liparids ($p=0.16$), suggesting that the species play similar roles in their respective trenches.

Most of the weighted means of source and trophic amino acid $\delta^{15}N$ values were highly consistent between samples of the same species (**Figure 2.3**). Trophic position estimates also varied little within species (**Table 2.4**). The $\delta^{15}N$ values of one *C. armatus* sample (#100367) did not cluster as closely as the other species. While the absolute $\delta^{15}N$ values of this sample differed, the estimated trophic position was very similar to the other two samples.

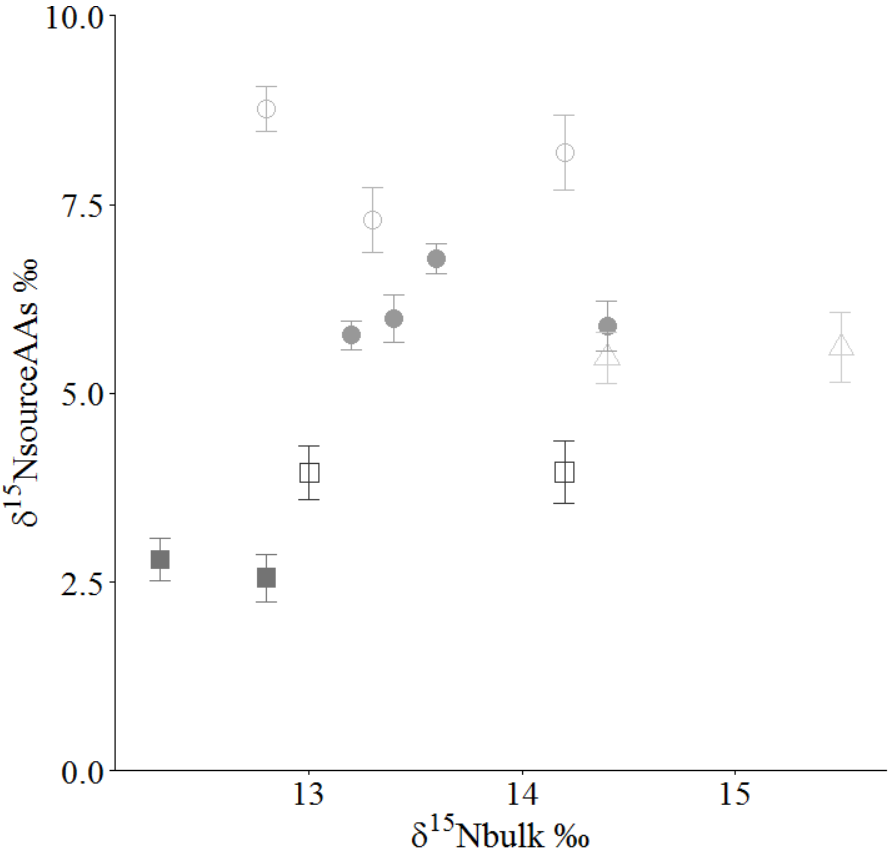

Figure 2.4. Source amino acid $\delta^{15}N$ values (weighted means of lysine and phenylalanine) compared to those of bulk tissue from the same individuals. Error bars indicate standard deviation between triplicate runs. *Coryphaenoides armatus* (open squares), *C. yaquinae* (closed squares), *Notoliparis kermadecensis* (open circles), Mariana liparid (closed circles) and *Spectrunculus grandis* (open triangles) shown.

Discussion

Stomach Contents. We describe the feeding habits of two hadal snailfishes from the Mariana Trench and Kermadec Trench. Both snailfishes seem to be predatory. Amphipods were the most abundant prey items in stomach contents of both species. This study is the first to document that hadal liparids also feed on decapods and polychaetes. The finding of decapods, large predatory amphipods (*Princaxelia*), and a few other large lysianassoid amphipods (up to 7.6 cm in size) in the diet of hadal snailfishes suggests that liparids can catch fast-swimming animals and are the top predators known in both trenches. The hadal liparids from both trenches have a highly developed and strongly muscularized pharyngeal jaw apparatus to facilitate processing of large, live prey (Gerringer and Linley, unpublished data). Polychaetes were present in stomachs of *Notoliparis kermadecensis* from the Kermadec Trench although they were not found in the Mariana liparid. It is possible that they are not common and/or not present at hadal depths in the Mariana Trench, that they are present but not eaten by liparids, or that they are present and eaten but missed in this collection. The published literature conflicts on whether or not these polychaetes have been collected from the Mariana Trench (Kirkegaard, 1956; Paterson et al., 2009; Gallo et al., 2015; Jamieson, 2015).

Some fish remains and squid beaks were found in stomachs of both hadal liparid species, however, we do not believe squid and fish are captured as live prey. Fish and squid remains found in this study appeared to be from species not known from the hadal zone, further suggesting that these fishes were consumed as carrion. The relative sizes of the squid and the snailfishes also indicate that these remains were ingested after dying. The morphology of the hadal liparid jaw, with small palatine teeth, also makes it unlikely that hadal snailfishes are catching live fish prey (Nielsen, 1964). Many of the squid and fish remains were found surrounded by, even thoroughly embedded with, large numbers of amphipods. The hadal snailfishes were likely targeting swarms of amphipods that were feeding on squid or fish remains. This behavior has been seen several times in video observations by Linley et al. (2017), who also suggest that ingestion of carrion is relatively infrequent and probably incidental in hadal liparids.

Prey accumulation curves suggest that our sampling effort likely captured much of the diversity of the diet of the Mariana Trench liparids. However, our limited number of specimens

probably prevented us from describing the complete diet of the Kermadec Trench liparids. Trap effects have not confounded the overall trends described in this study. Amphipods also made up the majority of highly digested prey items. High proportions of amphipods were also found in both the *N. kermadecensis* holotype (10 amphipods) and paratype (16 amphipods) collected by trawl (not by trap) on the *Galathea* expedition (Nielsen, 1964).

Amphipod abundance increases with depth in the hadal zone (Jamieson, 2015), suggesting a potential advantage to predatory fishes descending into the trench. The increase in number of prey items with depth of capture in the diet of the Mariana liparid could suggest that in the Mariana Trench amphipods were increasingly abundant or available with increasing depth. It is possible that the Mariana amphipod distributions or availability contribute to the relatively deeper distribution of the Mariana liparid (Linley et al., 2016), but greater sample sizes across the full depth range of these species are needed before firm conclusions can be reached.

Our principal components analysis of stomach content composition supports the hypothesis that there are indeed differences in feeding habits between the abyssal macrourids and hadal liparids. According to stomach contents analysis, hadal liparids are more selective predators, clustering tightly in the principal components analysis. The high degree of scatter in the macrourid data show that these abyssal species have varied generalist diets and rely heavily on carrion and squid (Drazen et al 2008). The few macrourid individuals available for stomach contents analysis in this study support this trend. With limited numbers of species and individuals available, we were not able to fully characterize the diets of abyssal species for comparison to the hadal community.

Fortunately, a few existing studies allow for qualitative comparison of hadal fish feeding ecology to that of other abyssal families. Crustacean, gastropod, polychaete, and detritus remains were observed in radiographs of three specimens of *S. grandis* (Uiblein et al., 2008). A more detailed stomach contents analysis of *S. grandis* (n=9, 2000–2500 m collection depth), found a mixed diet (actinozoans, polychaetes, amphipods, tanaids, mysids, euphausids, decapods, cephalopods, echinoderms, chateognaths, and fish fragments), with the largest contributions from epibenthic fauna (Mauchline and Gordon, 1984). Very few studies exist on the feeding ecology of zoarcids (e.g., Ferry, 1997), which have representative species at upper hadal depths (Linley et al., 2016). One deep-sea zoarcid, *Lycodes atlanticus*, was found to rely on benthic invertebrates, with a diet of sponges, polychaetes, gastropods, pycnogonids, ostracods, isopods, amphipods, and

ophiuroids (n=34, 723–2251 m collection depth, Sedberry and Musick, 1978). There are other abyssal fish taxa that reach near-hadal depths that could have potentially colonized trenches. One such group are the Chlorophthalmoids (Order Aulopiformes), including the deep-sea tripodfishes, Ipnopidae. *Bathypterois longipes, B. grallator,* and *B. phenax* stomach contents were found to contain mostly crustaceans (copepods, amphipods, decapods, ostracods, and mysids, collection depths 1239–5345 m) suggesting that these are epibenthic crustacean feeders (Crabtree et al., 1991). Other members of this order are believed to rely on the benthic food web, with polychaetes, bivalves, and copepods making up the majority of their stomach contents (*Ipnops murrayi*, n=43, 1239–4539 m collection depths, Crabtree et al., 1991). These results suggest a potentially higher diversity of diet components than seen in hadal liparids. It is possible that these abyssal species with less-specialized feeding have had less selective pressure to descend far into hadal trenches.

Investigations of synaphobranchid eel diet showed carrion to be of significant importance, while amphipods did not contribute (Merrett and Domanski, 1985; Jones and Breen, 2014). This tendency towards scavenging is supported by a functional morphology analysis of *Synaphobranchus brevidorsalis* and *Ilyophis brunneus* (Eagderi, et al., 2016), shallower representatives of abyssal genera. Synaphobranchids at abyssal depths are thought to rely on a diet of largely dead or dying pelagic species and have been shown to wait for larger scavengers to tear carrion, making it more accessible (Jamieson et al., 2011a). While benthic biomass of small crustaceans such as amphipods may increase in the hadal zone, the occurrence of large carrion falls would not be a function of depth (Linley et al., 2017). Perhaps this fact and the lack of large scavengers such as sharks have resulted in little selective pressure for these eels to colonize the hadal zone. Future study on abyssal ophidiids and zoarcids, and other deep abyssal taxa (Synaphobranchidae, Ipnopidae) will be needed to fully characterize this relationship.

Isotope Analysis. The $\delta^{15}N$ values of source amino acids can be used to trace origins of nutrient input to the hadal zone. This input can be thought of in two major pathways; first—sinking particles that slowly descend to hadal depths and organic material that accumulates through downslope transport due to trench topography and seismic activity, and second—organisms that rapidly sink after death in overlying waters. Both sources ultimately come from the euphotic zone, however processing times and mechanisms are distinct for each. This has important implications

for the isotopic compositions of source amino acids from the two pathways. Large carrion falls will sink quickly, carrying with them the isotopic compositions of the feeding depth of the carrion. We can therefore consider input from carrion as derived from the euphotic zone with source amino acid $\delta^{15}N$ values that are comparatively low representing the primary producers at the base of the food web (Hannides et al., 2009). Lower source amino acid $\delta^{15}N$ values in the macrourids are consistent with a more upper ocean-derived food source, with larger input of fast-sinking carrion. These lower values support the reliance on fast-sinking carrion found previously (Drazen et al., 2008). Conversely, small particles will be reprocessed as they sink, becoming increasingly enriched in ^{15}N with depth through the multiple microbial trophic interactions that occur throughout this long descent (Hannides et al., 2013). Those organisms that are more closely tied to the benthic food web (that consume detritivores or their primary and secondary predators) will have higher source amino acid $\delta^{15}N$ values reflecting that relationship. Particles that have followed the slow sinking pathway become the primary base of the benthic food web, although this is not always the case if there are significant inputs of rapidly sinking larger particles (e.g., after a spring bloom) which could have lower source amino acid $\delta^{15}N$ values (McCarthy et al., 2007). The liparids with higher weighted mean source amino acid $\delta^{15}N$ values appear more directly connected to the benthic hadal food web, where nutrient input is primarily sinking particles.

The ophidiid, *S. grandis*, had higher $\delta^{15}N$ values in source amino acids relative to the abyssal macrourid, *C. armatus*, collected from a similar depth in the same region, suggesting a less surface-derived food source. It is therefore likely that *S. grandis* is more closely dependent on the benthic food web, supported by the few stomach contents data available in the present study and in the literature (Mauchline and Gordon, 1984; Uiblein et al., 2008). The source amino acid values may be lower than in the liparids because *S. grandis* occasionally feeds on carrion, as seen in some video observations (Janßen et al., 2000; Henriques et al., 2002; Kemp et al., 2006; Cousins et al., 2013b). Source amino acid $\delta^{15}N$ values from *N. kermadecensis* collected from the Kermadec Trench were slightly higher than those of the Mariana Trench liparid. The $\delta^{15}N$ values of the isotopic baseline may therefore be higher in waters overlying the Kermadec Trench. This could be a result of differences in sources of nitrate (with different $\delta^{15}N$ values) to waters in these environments, the extent of nitrate utilization by phytoplankton in these regions (Waser et al.,

1998; Sigman et al., 2009), or nitrogen fixation dominating the nitrogen source of phytoplankton (Montoya et al., 2002; Hannides et al., 2009).

Our results also suggest that conclusions from bulk tissue N isotope measurements should be drawn cautiously for hadal organisms. It is well documented that shifts in source amino acid isotope values can strongly influence the interpretation of bulk tissue $\delta^{15}N$ values (e.g., Hannides et al. 2009; Choy et al., 2015; Nielsen et al., 2015). In our study, fishes with the highest bulk tissue $\delta^{15}N$ values (*N. kermadecensis*, Mariana liparid; **Figure 2.4**) did not have the highest trophic positions, highlighting the limitations of drawing conclusions from bulk tissue alone. Amino acid specific analyses show that the higher bulk tissue $\delta^{15}N$ values in hadal liparids are due to high values in the 'isotopic baseline,' rather than trophic position alone. These results further demonstrate the value of the compound-specific method for isotope measurements of individual amino acid, particularly in systems like hadal trenches, where the base of the food web is extremely difficult to determine and therefore is poorly characterized.

This study provides the first trophic position estimates for fishes from the hadal zone. Based on trophic position (~4) and stomach contents, liparids are likely the top predators below the abyssal-hadal boundary. Our results suggest that hadal amphipods are at approximately trophic level three, which follows previous analysis, although there is a large degree of variation in amphipod diet (Blankenship and Levin, 2007). The trophic level of liparids is also relatively high, partially due to input from predatory crustaceans. High trophic levels in macrourids support previous findings that documented macrourid reliance on small fishes and squid, as well as large carrion falls (Drazen et al., 2008). The higher source amino acid value in one *C. armatus* could suggest a smaller contribution of upper-ocean carrion for that individual.

Fishes in the Hadal Food Web. Our findings on the feeding ecology of hadal fishes contribute to a new understanding of trophic interactions in the deepest seas. Where present (e.g., Kermadec, Mariana, Japan, Peru-Chile trenches), hadal snailfishes are the top known predators of the upper hadal zone. These fishes suction feed on mainly amphipods, though they also catch predatory crustaceans such as decapods and *Princaxelia* amphipods. Some hadal liparids will also eat polychaetes. Hadal amphipods are known to have extremely diverse prey, including carrion, urochordates, ascidians, salps, diatoms, detritus, polychaetes, and copepods (Blankenship and

Levin, 2007) and are even known to cannibalize one another in an artificial trap environment (Ingram and Hessler, 1983). The amphipods obviously make up an important part of the hadal food web, (Blankenship and Levin, 2007) and clearly are the most important prey of hadal snailfishes.

We are a long way from a complete understanding of the energetic pathways at work in the hadal zone. Deep-sea trenches are still relatively unexplored, and undiscovered species and interactions probably outnumber the known. Our understanding of the hadal community is heavily biased by gear type, as the difficulties and high costs of sampling at such high hydrostatic pressures favor the use of free-vehicle cameras and traps and the study of bait-attending fauna (e.g., Jamieson et al., 2011c). Even if we had a thorough understanding of hadal community structure, construction of a hadal food web is not straightforward. We found evidence for variation in trophic interactions between trenches, such as a higher prey diversity in liparids from the Kermadec Trench as compared to those in the Mariana Trench. A common hypothesis for inter-trench variability is that productivity of surface waters overlying the trench will affect the community below. The extent of this relationship and the effects of downslope funneling and organic matter accumulation due to trench topography have yet to be fully characterized (e.g., Itou et al., 2000; Ichino et al., 2015). Further, the depth-related changes in community structure, present in most groups, mean that trophic interactions at 6,000 m are likely different than those at 9,000 m in the same trench. This has been demonstrated in some hadal amphipods (Blankenship and Levin, 2007), but likely spans to other taxa as well. For example, the probable lack of fishes below ~8,200 m (Yancey, et al., 2014) would of course lead to a very different food web in the lower reaches of the trench than that seen in the upper hadal zone. More investigation of these trophic relationships and on processes in the environments overlying hadal trenches will be needed to understand the hadal food web and the role of trenches in global biogeochemical cycling.

Conclusions

This study provides the first in depth investigation of the trophic ecology of fish species in the hadal zone, using multiple approaches. Hadal liparids are clearly predatory, relying heavily on amphipods as a food source, as seen in stomach contents analysis. This is supported by video

observations of hadal liparids *in situ*, which showed high numbers of predatory feeding events in hadal liparids (Fujii et al., 2010; Jamieson et al., 2009b; Linley et al., 2016). High $\delta^{15}N$ values of source amino acids also suggest that hadal liparids are closely tied to the benthic food web. Macrourids from the abyss near the Kermadec and Mariana trenches displayed a high degree of trophic plasticity (stomach contents analysis diversity, in agreement with previous findings), a close linkage to the pelagic food web (lower $\delta^{15}N$ values of source amino acids), and a high trophic level of >5, further suggesting the importance of both carrion and live fish and squid to their diet. Although more research is needed on other abyssal groups (Ophidiidae, Zoarcidae, Synaphobranchidae) our results demonstrate differences in feeding strategy between characteristic abyssal species (Family Macrouridae) and dominant endemic hadal species (Family Liparidae).

Trophic interactions may be important evolutionary drivers of depth zonation patterns in abyssal and hadal fishes. At the upper edges of the trench, the hadal fish community resembles that found on the abyssal plain, with macrourids, ophidiids, zoarcids, and synaphobranchids. From depths around 6,500–8,200 m, in a number of trenches, however, the fish fauna seems to shift to a dominance by the family Liparidae (Jamieson et al., 2011c; Linley et al., 2016). While scavenging and piscivorous fishes do not extend far into the hadal zone, suction-feeding predatory fishes are dominant. This community shift at the upper edges of the trench may, in part, relate to a difference in trophic strategy. The increased amphipod biomass in the hadal zone compared to the abyss may provide little benefit for macrourids and synaphobranchids to descend to hadal depths, but large advantage for suction-feeding fishes such as liparids. This may be one of the reasons why liparids are so notably successful in many hadal trenches.

Contributors

Gerringer, M.E.[1], Popp, B.N.[2], Linley, T.D.[3], Jamieson, A.J.[3], Drazen, J.C.[1]

[1]Department of Oceanography, University of Hawai‘i at Mānoa, Honolulu, Hawaii 96822, USA.
[2]Department of Geology and Geophysics, University of Hawai‘i at Mānoa, Honolulu, Hawaii 96822, USA.

[3]School of Marine Science and Technology, Ridley Building, Newcastle University, Newcastle Upon Tyne, UK. NE1 7RU.

AJJ, TDL, MEG, and JCD collected specimens. MEG and JCD analyzed stomach contents. MEG and BNP conducted and interpreted isotope analyses. All authors contributed to the writing and editing of the manuscript and the discussion of ideas therein.

This study appears in *Deep-Sea Research Part I: Oceanographic Research Papers*
Volume 121, pages 110-120.
(doi: 10.1016/j.dsr.2017.01.003)

Acknowledgments

The authors would like to extend their sincere gratitude to the captains and crews of the *R/Vs Thompson* and *Falkor*. We thank Iris Altima (University of Hawai‘i) for assistance identifying polychaetes and crustacean remains, Richard Young (University of Hawai‘i) for his contribution to squid beak identification, Matteo Ichino (University of Southampton), Paul Yancey, and Chloe Weinstock (Whitman College), and the other HADES cruise participants for collection and dissection help at sea, and Natalie Wallsgrove and Cassie Lyons (University of Hawaii) for assistance with isotope analyses. M. Gerringer thanks the National Science Foundation Graduate Research Fellowships Program for their support. We are grateful for funding from the National Science Foundation (OCE #1130712) and Schmidt Ocean Institute.

References

Angel, M.V., 1982. Ocean trench conservation. The Environmentalist 2 (1-2), 1–17. (doi:10.1007/BF02340472)

Bartlett, D., 2003. Microbial life in the trenches. Marine Technoloogy Society Journal 43 (5), 128–131. (doi:10.4031/MTSJ.43.5.5)

Beliaev, G., 1989. Deep-Sea Ocean Trenches and their Fauna. USSR Academy of Sciences. Translation: Brueggeman, P.L., Scripps Institution of Oceanography Library.

Blankenship, L., Levin, L., 2007. Extreme food webs: Foraging strategies and diets of scavenging amphipods from the ocean's deepest 5 kilometers. Limnology and Oceanography 52, 1685–1697. (doi:10.4319/lo.2007.52.4.1685)

Blankenship, L., Yayanos, A., Cadien, D., Levin, L., 2006. Vertical zonation patterns of scavenging amphipods from the hadal zone of the Tonga and Kermadec Trenches. Deep-Sea Research Part I: Oceanographic Research Papers 53, 48–61. (doi:10.1016/j.dsr.2005.09.006)

Bowen, a. D., Yoerger, D.R., Taylor, C., McCabe, R., Howland, J., Gomez-Ibanez, D., Kinsey, J.C., Heintz, M., McDonald, G., Peters, D.B., Bailey, J., Bors, E., Shank, T., Whitcomb, L.L., Martin, S.C., Webster, S.E., Jakuba, M.V., Fletcher, B., Young, C., Buescher, J., Fryer, P., Hulme, S., 2009. Field trials of the Nereus hybrid underwater robotic vehicle in the challenger deep of the Mariana Trench. Ocean. 2009, MTS/IEEE Biloxi – Marine Technology for Our Future Global and Local Challenges.

Bowen, A., Yoerger, D., Taylor, C., Mccabe, R., Howland, J., Gomez-ibanez, D., Kinsey, J., Heintz, M., Mcdonald, G., Peters, D., Fletcher, B., Young, C., Buescher, J., Whitcomb, L., Martin, S., Webster, S., Jakuba, M., 2008. The Nereus hybrid underwater robotic vehicle for global ocean science operations to 11,000m depth. OCEANS 1–10. (doi:10.1109/OCEANS.2008.5151993)

Bradley, C.J., Wallsgrove, N.J., Choy, C.A., Drazen, J.C., Hetherington, E.D., Hoen, D.K., Popp, B.N., 2015. Trophic position estimates of marine teleosts using amino acid compound specific isotopic analysis. Limnology and Oceanography Methods 13, 476–493. (doi:10.1002/lom3.10041)

Bruun, A., Greve, S., Mielche, H., Spaerck, R., 1957. The Galathea Deep Sea Expedition. AIBS Bulletin, 7(3), 38. (doi:10.2307/1292343)

Chikaraishi, Y., Ogaw, N., Ohkouchi, N., 2009. Compound-specific nitrogen isotope analysis of amino acids: Implications of aquatic food web studies. Geochimica et Cosmochimica Acta 73, A219–A219.

Choy, C., Davison, P., Drazen, J., Flynn, A., Gier, E., Hoffman, J., McClain-Counts, J., Miller, T., Popp, B., Ross, S., Sutton, T., 2012. Global trophic position comparison of two dominant mesopelagic fish families (Myctophidae, Stomiidae) using amino acid nitrogen isotopic analyses. PLoS One 7, e50133. (doi:10.1371/journal.pone.0050133)

Choy, C.A., Popp, B.N., Hannides, C.C.S., Drazen, J.C., 2015. Trophic structure and food resources of epipelagic and mesopelagic fishes in the North Pacific Subtropical Gyre ecosystem inferred from nitrogen isotopic compositions. Limnology and Oceanography 60 (4), 1156–1171. (doi:10.1002/lno.10085)

Churchill, D.A., Heithaus, M.R., Grubbs, R.D., 2015. Effects of lipid and urea extraction on δ15N values of deep-sea sharks and hagfish: Can mathematical correction factors be generated? Deep-Sea Research Part II: Topical Studies in Oceanography 115, 103–108. (doi:10.1016/j.dsr2.2014.12.013)

Cousins, N.J., Linley, T.D., Jamieson, A.J., Bagley, P.M., Blades, H., Box, T., Chambers, R., Ford, A., Shields, M. A., Priede, I.G., 2013. Bathyal demersal fishes of Charlie-Gibbs Fracture Zone region (49-54°N) of the Mid-Atlantic Ridge: II. Baited camera lander observations. Deep-Sea Research Part II: Topical Studies in Oceanography 98, 397–406. (doi:10.1016/j.dsr2.2013.08.002)

Crabtree, R.E., Carter, J., Musick, J.A., 1991. The comparative feeding ecology of temperate and tropical deep-sea fishes from the western North Atlantic. Deep-Sea Research Part A: Oceanographic Research Papers 38(10), 1277–1298. (doi:10.1016/0198-0149(91)90027-D)

Cui, X., Grebmeier, J., Cooper, L., 2012. Feeding ecology of dominant groundfish in the northern Bering Sea. Polar Biology 35, 1407–1419. (doi:10.1007/s00300-012-1180-9)

Dahl, E., 1979. Deep-sea carrion feeding amphipods: evolutionary patterns in niche adaptation deep-sea carrion feeding amphipods: evolutionary patterns in niche adaptation. Oikos 33(2), 167–175. (doi:10.2307/3543994)

DeBroyer, C., Nyssen, F., Dauby, P., 2004. The crustacean scavenger guild in Antarctic shelf, bathyal and abyssal communities. Deep-Sea Research Part II: Topical Studies in Oceanography 51, 1733–1752. (doi:10.1016/j.dsr2.2004.06.032)

Drazen, J., Popp, B., Choy, C., Clemente, T., De Forest, L., Smith, K.J., 2008. Bypassing the abyssal benthic food web: Macrourid diet in the eastern North Pacific inferred from stomach content and stable isotopes analyses. Limnology and Oceanography 53, 2644–2654. (doi:10.4319/lo.2008.53.6.2644)

Eagderi, E., Christiaens, J., Boone, M., Jacobs, P., Adriaens, D., 2016. Functional morphology of the feeding apparatus in *Simenchelys parasitica* (Simenchelyinae: Synaphobranchidae), an alleged parasitic eel. Copeia 104(2), 421–439. (doi:10.1643/CI-I5-329)

Falk-Petersen, I., Frivoll, V., Gulliksen, B., Haug, T., Vader, W., 1988. Age/size relations and food of two snailfishes, *Liparis gibbus* and *Careproctus reinhardii* (Teleostei, Liparididae) from Spitsbergen coastal waters. Polar Biology 8, 353–358. (doi:10.1007/BF00442026)

Fang, J., Barcelona, M., Abrajano, T., Nogi, Y., Kato, C., 2002. Isotopic composition of fatty acids of extremely piezophilic bacteria from the Mariana Trench at 11,000 m. Marine Chemistry 80, 1–9. (doi:10.1016/S0304-4203(02)00069-5)

Ferry, L., Food habits of the two-line eelpout (*Bothrocara brunneum*: Zoarcidae) at two deep-sea sites in the eastern North Pacific. Deep-Sea Research Part I: Oceanographic Research Papers 44(3), 521–531. (doi:10.1016/S0967-0637(96)00120-3)

Fisher, R., 1954. On the sounding of trenches. Deep-Sea Research 2(1), 48–58. (doi:10.1016/0146-6313(54)90056-8)

Forman, W., 2009. From Beebe and Barton to Piccard and Trieste. Marine Technology Society Journal 43, 27–36. (doi:10.4031/MTSJ.43.5.14)

France, S., 1993. Geographic variation among three isolated populations of the hadal amphipod *Hirondellea gigas* (Crustacea: Amphipoda: Lysianassoidea). Marine Ecology Progress Series 92, 277–287. (doi:10.3354/meps092277)

Fujii, T., Jamieson, A., Solan, M., Bagley, P., Priede, I., 2010. A large aggregation of liparids at 7703 meters and a reappraisal of the abundance and diversity of hadal fish. Bioscience 60, 506–515. (doi:10.1525/bio.2010.60.7.6)

Fujikura, K., Kojima, S., Tamaki, K., Maki, Y., Hunt, J., Okutani, T., 1999. The deepest chemosynthesis-based community yet discovered from the hadal zone, 7326 m deep, in the Japan Trench. Marine Ecology Progress Series 190, 17–26. (doi:10.3354/meps190017)

Fujiwara, Y., Kato, C., Masui, N., Fujikura, K., Kojima, S., 2001. Dual symbiosis in the cold-seep thyasirid clam *Maorithyas hadalis* from the hadal zone in the Japan Trench, western Pacific. Marine Ecology Progress Series 214, 151–159. (doi:10.3354/meps214151)

Gallo, N.D., Cameron, J., Hardy, K., Fryer, P., Bartlett, D.H., Levin, L.A., 2015. Submersible- and lander-observed community patterns in the Mariana and New Britain trenches: Influence of productivity and depth on epibenthic and scavenging communities. Deep-Sea Research Part I: Oceanographic Research Papers 99, 119–133. (doi:10.1016/j.dsr.2014.12.012)

Glubokov, A., 2010. The data on *Careproctus furcellus* and *C. rastrinus* (Liparidae) from the Olyutorskii Gulf of the Bering Sea: Size composition, indices of organs, and diet. Journal of Ichthyology 50, 52–64. (doi:10.1134/S0032945210010078)

Hannides, C.C.S., Popp, B.N., Landry, M.R., Graham, B.S., 2009. Quantification of zooplankton trophic position in the North Pacific Subtropical Gyre using stable nitrogen isotopes. Water Research 54(1), 50–61. (doi:10.4319/lo.2009.54.1.0050)

Hannides, C.C.S., Popp, B.N., Choy, C.A., Drazen, J.C., 2013. Midwater zooplankton and suspended particle dynamics in the North Pacific Subtropical Gyre: A stable isotope perspective. Limnology and Oceanography 58(6), 1931–1946. (doi:10.4319/lo.2013.58.6.1931)

Hargrave, B.T., Phillips, G.A., Prouse, N.J., Cranford, P.J., 1995. Rapid digestion and assimilation of bait by the deep-sea amphipod *Eurythenes gryllus*. Deep-Sea Research Part I: Oceanographic Research Papers 42, 1905–1921. (doi:10.1016/0967-0637(95)00080-1)

Hayes, J.M., Freeman, K.H., Hoham, C.H., Popp, B.N., 1990. Compound-specific isotopic analyses, a novel tool for reconstruction of ancient biogeochemical processes. Organic Geochemistry 16, 1115–1128. (doi: 10.1016/0146-6380(90)90147-R)

Henriques, C., Priede, I., Bagley, P., 2002. Baited camera observations of deep-sea demersal fishes of the northeast Atlantic Ocean at 15–28 N off West Africa. Marine Biology 141, 307–314. (doi:10.1007/s00227-002-0833-6)

Hessler, R., Ingram, C., Yayanos, A., Burnett, B., 1978. Scavenging amphipods from the floor of the Philippine Trench. Deep-Sea Research 25(11), 1029–1047. (doi:10.1016/0146-6291(78)90585-4)

Ichino, M.C., Clark, M.R., Drazen, J.C., Jamieson, A., Jones, D.O.B., Martin, A.P., Rowden, A.A., Shank, T.M., Yancey, P.H., Ruhl, H.A., 2015. The distribution of benthic biomass in hadal trenches : A modelling approach to investigate the effect of vertical and lateral organic matter transport to the seafloor. Deep-Sea Research Part I: Oceanographic Research Papers 100, 21–33. (doi:10.1016/j.dsr.2015.01.010)

Itou, M., Matsumura, I., Noroki, S., 2000. A large flux of particulate matter in the deep Japan Trench observed just after the 1994 Sanriku-Oki earthquake. Deep-Sea Research Part I: Oceanographic Research Papers 47, 1987–1998. (doi:10.1016/s0967-0637(00)00012-1)

Ingram, C., Hessler, R., 1983. Distribution and behavior of scavenging amphipods from the central North Pacific. Deep-Sea Research Part A: Oceanographic Research Papers 30, 683–706. (doi:10.1016/0198-0149(83)90017-1)

Jamieson, A., 2015. The hadal zone: life in the deepest oceans. Cambridge, United Kingdom. (doi:10.1017/CBO9781139061384)

Jamieson, A., Fujii, T., Bagley, P., Priede, I., 2011a. Scavenging interactions between the arrow tooth eel *Synaphobranchus kaupii* and the Portuguese dogfish *Centroscymnus coelolepis*. Journal of Fish Biology 79, 205–16. (doi:10.1111/j.1095-8649.2011.03014.x)

Jamieson, A., Fujii, T., Mayor, D., Solan, M., Priede, I., 2010. Hadal trenches: the ecology of the deepest places on Earth. Trends in Ecology and Evolution 25, 190–7. (doi:10.1016/j.tree.2009.09.009)

Jamieson, A., Fujii, T., Priede, I., 2012. Locomotory activity and feeding strategy of the hadal munnopsid isopod *Rectisura* cf. *herculea* (Crustacea: Asellota) in the Japan Trench. Journal of Experimental Biology 215, 3010–7. (doi:10.1242/jeb.067025)

Jamieson, A., Fujii, T., Solan, M., Matsumoto, A., Bagley, P., Priede, I., 2009a. First findings of decapod crustacea in the hadal zone. Deep-Sea Research Part I: Oceanographic Research Papers 56, 641–647. (doi:10.1016/j.dsr.2008.11.003)

Jamieson, A., Fujii, T., Solan, M., Matsumoto, A., Bagley, P., Priede, I., 2009b. Liparid and macrourid fishes of the hadal zone: *in situ* observations of activity and feeding behaviour. Proceedings of the Royal Society B: Biological Sciences 276, 1037–45. (doi:10.1098/rspb.2008.1670)

Jamieson, A., Fujii, T., Solan, M., Priede, I., 2009c. HADEEP: Free-falling landers to the deepest places on Earth. Marine Technology Society Journal 43, 151–160. (doi:10.4031/MTSJ.43.5.17)

Jamieson, A., Gebruk, A., Fujii, T., Solan, M., 2011b. Functional effects of the hadal sea cucumber *Elpidia atakama* (Echinodermata: Holothuroidea, Elasipodida) reflect small-scale patterns of resource availability. Marine Biology 158, 2695–2703. (doi:10.1007/s00227-011-1767-7)

Jamieson, A., Kilgallen, N., Rowden, A., Fujii, T., Horton, T., Lörz, A.-N., Kitazawa, K., Priede, I., 2011c. Bait-attending fauna of the Kermadec Trench, SW Pacific Ocean: Evidence for an ecotone across the abyssal–hadal transition zone. Deep-Sea Research Part I: Oceanographic Research Papers 58, 49–62. (doi:10.1016/j.dsr.2010.11.003)

Jamieson, A., Lörz, A.-N., Fujii, T., Priede, I., 2011d. *In situ* observations of trophic behaviour and locomotion of *Princaxelia* amphipods (Crustacea: Pardaliscidae) at hadal depths in four West Pacific Trenches. Journal of the Marine Biological Association of the United Kingdom 92, 1–8. (doi:10.1017/S0025315411000452)

Jamieson, A., Solan, M., Fujii, T., 2009d. Imaging deep-sea life beyond the abyssal zone. Sea Technology.

Janßen, F., Treude, T., Witte, U., 2000. Scavenger assemblages under differing trophic conditions: a case study in the deep Arabian Sea. Deep-Sea Research Part II: Topical Studies in Oceanography 47, 2999–3026. (doi:10.1016/s0967-0645(00)00056-4)

Jin, X., Zhang, B., Xue, Y., 2010. The response of the diets of four carnivorous fishes to variations in the Yellow Sea ecosystem. Deep-Sea Research Part II: Topical Studies in Oceanography 57, 996–1000. (doi:10.1016/j.dsr2.2010.02.001)

Johnson, C., 1969. Contributions ot the biology of the showy snailfish, *Liparis pulchellus*. Copeia 1969, 830–835. (doi:10.2307/1441806)

Jones, M., Breen, B., 2014. Role of scavenging in a synaphobranchid eel (*Diastobranchus capensis*, Barnard, 1923), from northeastern Chatham Rise, New Zealand. Deep-Sea Research Part I: Oceanographic Research Papers 85, 118–123. (doi:10.1016/j.dsr.2013.12.006)

Kato, C., Li, L., Tamaoka, J., Horikoshi, K., 1997. Molecular analyses of the sediment of the 11,000-m deep Mariana Trench. Extremophiles 1, 117–23. (doi:10.1007/s007920050024)

Kaufmann, R., 1994. Structure and function of chemoreceptors in scavenging lysianassoid amphipods. Journal of Crustacean Biology 14, 54–71. (doi:10.1163/193724094X00470)

Kemp, K.M., Jamieson, A.J., Bagley, P.M., McGrath, H., Bailey, D.M., Collins, M.A., Priede, I.G., 2006. Consumption of large bathyal food fall, a six-month study in the NE Atlantic. Marine Ecology Progress Series 310, 65–76. (doi:10.3354/Meps310065)

Kirkegaard, J., 1956. Benthic polychaeta from depths exceeding 6000 meters. Galathea Report 2, 63–78.

Kobayashi, H., Hatada, Y., Tsubouchi, T., Nagahama, T., Takami, H., 2012. The hadal amphipod *Hirondellea gigas* possessing a unique cellulase for digesting wooden debris buried in the deepest seafloor. PLoS One 7, e42727. (doi:10.1371/journal.pone.0042727)

Kobayashi, K., Ashi, J., Boulegue, J., Cambray, H., Chamot-Rooke, N., Fujimoto, H., Furuta, T., Iiyama, J., Koizumi, T., Mitsuzawa, K., Monma, H., Murayama, M., Naka, J., Nakanishi, M., Ogawa, Y., Otsuka, K., Okada, M., Oshida, A., Shima, N., Soh, W., Takeuchi, A., Watanabe, M., Yamagata, T., 1992. Deep-tow survey in the KAIKO-Nankai cold seepage areas. Earth and Planetary Science Letters 109, 347–354.

Kobayashi, T., Hiyama, S., 1991. Distribution, abundance, and food habits of the snailfish *Liparis tanakai* in the Suo Sea, Seto Inland Sea. Japanese Journal of Ichthyology 38, 207–210.

Labai, V., Poltev, Y., Mukhametov, I., 2003. Feeding of the snailfish *Careproctus* cf . *cyclocephalus* in Pacific Waters of the Northern Kuril Islands. Russian Journal of Marine Biology 29, 104–109.

Labai, V., Poltev, Y., Mukhametov, I., 2002. Feeding of the Snailfish *Careproctus roseofuscus* in Pacific Waters of the Northern Kuril Islands and Southeastern Kamchatka. Russian Journal of Marine Biology 28, 252–258.

Lacey, N.C., Rowden, A.A., Clarke, M., Kilgallen, N.M., Linley, T., Mayor, D.J., Jamieson, A.J., 2016. Community structure and diversity of scavenging amphipods from bathyal to hadal depths in three South Pacific trenches. Deep-Sea Research Part I: Oceanographic Research Papers 111, 121–137. (doi:10.1016/j.dsr.2016.02.014)

Leduc, D., Wilson, J., 2016. Benthimermithid nematode parasites of the amphipod *Hirondellea dubia* in the Kermadec Trench. Parasitology Research 115(4), 1675–1682. (doi:10.1007/s00436-016-4907-7)

Linley, T.D., Gerringer, M.E., Yancey, P.H., Drazen, J.C., Weinstock, C.L., Jamieson, A.J., 2016. Fishes of the hadal zone including new species, *in situ* observations and depth records of Liparidae. Deep-Sea Research Part I: Oceanographic Research Papers 114, 99–110. (doi:10.1016/j.dsr.2016.05.003)

Linely, T.D., Stewart, A.L., McMillan, P.J., Clark, M.R., Gerringer, M.E., Drazen, J.C., Fujii, T., Jamieson, A.J., Bait attending fishes of the abyssal zone and hadal boundary: community structure, functional groups and species distribution in the Kermadec, New Hebrides and Mariana trenches. Deep-Sea Research Part I: Oceanographic Research Papers 121, 38–53. (doi:10.1016/j.dsr.2016.12.009)

Mauchline, J., Gordon, J.D.M., 1984. Occurrence and feeding of berycomorphid and percomorphid teleost fish in the Rockall Trough. ICES Journal of Marine Science 41(3), 239–247. (doi:10.1093/icesjms/41.3.239)

McCarthy, M.D., Benner, R., Lee, C., Fogel, M.L., 2007. Amino acid nitrogen isotopic fractionation patterns as indicators of heterotrophy in plankton, particulate, and dissolved organic matter. Geochimica et Cosmochimica Acta 71, 4727–4744. (doi:10.1016/j.gca.2007.06.0-61)

McClelland, J.W., Montoya, J.P., 2002. Trophic relationships and the nitrogen isotopic composition of amino acids in plankton. Ecology 83, 2173–2180. (doi:10.2307/3072049)

Merrett, N., Domanski, P., 1985. Observations on the ecology of deep-sea bottom-living fishes collected off Northwest Africa: II. The Moroccan Slope (27–34 N), with special reference to *Synaphobranchus kaupi*. Biological Oceanography 3, 349–399. (doi:10.1016/0079-6611(80)90002-6)

Montoya, J.P., Carpenter, E.J., Capone, D.G., 2002. Nitrogen fixation and nitrogen isotope abundances in zooplankton of the oligotrophic North Atlantic. Limnology and Oceanograrphy 47(6), 1617–1628. (doi:10.4319/lo.2002.47.6.1617)

Momma, H., Watanabe, M., Hashimoto, K., Tashiro, S., 2004. Loss of the Full Ocean Depth ROV Kaiko - Part 1 : ROV Kaiko - A Review. Proceedings of the Fourteenth International Offshore and Polar Engineering Conference 1, 880653.

Nielsen, J., 1964. Fishes from depths exceeding 6000 meters. Galathea Report 7, 113–124.

Nielsen, J.M., Popp, B.N., Winder, M., 2015. Meta-analysis of amino acid stable nitrogen isotope ratios for estimating trophic position in marine organisms. Oecologia 178, 631–642. (doi:10.1007/s00442-015-3305-7)

Nunoura, T., Takaki, Y., Hirai, M., Shimamura, S., Makabe, A., Koide, O., 2015. Hadal biosphere: Insight into the microbial ecosystem in the deepest ocean on Earth. Proceedings of the National Academy of Sciences 112(11), E1230–E1236. (doi:10.1073/pnas.1421816112)

Ohara, Y., Reagan, M.K., Fujikura, K., Watanabe, H., Michibayashi, K., Ishii, T., Stern, R.J., Pujana, I., Martinez, F., Girard, G., Ribeiro, J., Brounce, M., Komori, N., Kino, M., 2012. A serpentinite-hosted ecosystem in the Southern Mariana Forearc. Proceedings of the National Academy of Sciences 109, 2831–2835. (doi:10.1073/pnas.1112005109)

Oksanen, J., Blanchet, F., Kind, R., Legendre, P., Minchin, P., O'Hara, R., Simpson, G., Solymos, P., Stevens, H., Wagner, H., 2016. vegan: Community Ecology Package.

Orlov, A., Tokranov, A., 2011. Some rare and insufficiently studied snailfish (Liparidae, Scorpaeniformes, Pisces) in the Pacific Waters off the Northern Kuril Islands and Southeastern Kamchatka, Russia. ISRN Zoology 2011, 1–12. (doi:10.5402/2011/341640)

Paterson, G.L.J., Glover, A.G., Barrio Froján, C.R.S., Whitaker, A., Budaeva, N., Chimonides, J., Doner, S., 2009. A census of abyssal polychaetes. Deep-Sea Research Part II: Topical Studies in Oceanography 56, 1739–1746. (doi:10.1016/j.dsr2.2009.05.018)

Pérês, J., 1965. *Aperçu sur les résultats de deux plongées effectuées dans le ravin de Puerto-Rico par le bathyscaphe Archimède.* Deep-Sea Research and Oceanographic Abstracts 12, 883–891. (doi:10.1016/0011-7471(65)90811-9)

Perrone, F.M.F., Croce, N. Della, Dell, A., Della Croce, N., Dell'anno, A., 2003. Biochemical composition and trophic strategies of the amphipod *Eurythenes gryllus* at hadal depths (Atacama Trench, South Pacific). Chemistry and Ecology 19, 441–449. (doi:10.1080/0275754031000095723)

Peterson, B., Fry, B., 1987. Stable isotopes in ecosystem studies. Annual Reviews of Ecology, Evolution, and Systematics 18, 293–320. (doi:10.1146/annurev.es.18.110187.001453)

Pinkas, L., 1971. Food habits of albacore, bluefin tuna, and bonito in California waters, Fish Bulletin 152. Sacramento State of California, Department of Fish and Game, Sacramento.

Popp, B., Graham, B., Olson, R., Hannides, C., Lott, M., López-ibarra, G., Galván-magaña, F., Fry, B., 2007. Insight into the trophic ecology of yellowfin tuna, *Thunnus albacares*, from compound-specific nitrogen isotope analysis of proteinaceous amino acids, in: Stable Isotopes as Indicators of Ecological Change. 173–190. (doi:10.1016/S1936-7961(07)01012-3)

Post, D., 2002. Using stable isotopes to estimate trophic position: Models, methods, and assumptions. Ecology 83, 703–718. (doi:10.2307/3071875)

R Core Team, 2013. R: A language and environment for statistical computing. R Foundation for Statistical Computing, Vienna, Austria. http://www.R-project.org/.

Ritchie, H., Jamieson, A. J., Piertney, S.B., 2015. Phylogenetic relationships among hadal amphipods of the Superfamily Lysianassoidea: Implications for taxonomy and biogeography. Deep-Sea Research Part I: Oceanographic Research Papers 105, 119–131. (doi:10.1016/j.dsr.2015.08.014)

Sedberry, G., Musick J., 1978. Feeding strategies of some demersal fishes of the continental slope and rise off the Mid-Atlantic coast of the USA. Marine Biology 44(4), 357–375. (doi:10.1007/BF00390900)

Sigman, D. M., Karsh, K. L., Casciotti, K. L., 2009. Ocean process tracers: Nitrogen isotopes in the ocean, in: Steele, J. H., Turekian, K. K., Thorpe, S. A. (Eds.), Encyclopedia of Ocean Sciences. Academic Press, London, pp. 4138–4153.

Søreide, F., Jamieson, A., 2013. Ultradeep-sea exploration in the Puerto Rico Trench. OCEANS – Bergen, 2013 MTS/IEEE. 1–4. (doi:10.1109/OCEANS-Bergen.2013.6607944)

Svenska djuphavsexpeditionen, 1957. Reports of the Swedish Deep-Sea Expedition, 1947-1948.

Uiblein, F., Nielsen, J.G., Møller, P.R., 2008. Systematics of the ophidiid genus *Spectrunculus* (Teleostei: Ophidiiformes) with resurrection of *S. crassus*. Copeia 2008, 542–551. (doi:10.1643/CI-07-027)

Vecchione, M., Young, R., 2006. The squid family Magnapinnidae (Mollusca: Cephalopoda) in the Atlantic Ocean, with a description of a new species. Proceedings of the Biological Society of Washington 119, 365–372. (doi:10.2988/0006-324X(2006)119[365:TSFMMC]2.0.CO;2)

Vinogradova, N., 1962. Vertical zonation in the distribution of deep-sea benthic fauna in the ocean. Deep-Sea Research 8, 245–250. (doi:10.1016/0146-6313(61)90025-9)

Waser, N. A. D., Harrison, P. J., Nielsen, B., Calvert, S. E., Turpin, D. H., 1998. Nitrogen isotope fractionation during the uptake and assimilation of nitrate, nitrite, ammonium, and urea by a marine diatom. Limnology and Oceanography 43(2), 215–224. (doi:10.4319/lo.1998.43.2.0215)

Wickam, H., 2009. ggplot2: elegant graphics for data analysis. Springer-Verlag New York.

Wilson, R., Waples, R., 1983. Distribution, morphology, and biochemical genetics of *Coryphaenoides armatus* and *C. yaquinae* (Pisces: Macrouridae) in the central and eastern North Pacific. Deep-Sea Research Part A: Oceanographic Research Papers 30, 1127–1145. (doi:10.1016/0198-0149(83)90092-4)

Wolff, T., 1970. The concept of the hadal or ultra-abyssal fauna. Deep-Sea Research and Oceanographic Abstracts 17, 983–1003. (doi:10.1016/0011-7471(70)90049-5)

Wolff, T., 1958. The hadal community, an introduction. Deep-Sea Research 6, 95–124. (doi:10.1016/0146-6313(59)90063-2)

Yancey, P., Gerringer, M., Drazen, J., Rowden, A., Jamieson, A., 2014. Marine fish may be biochemically constrained from inhabiting the deepest ocean depths. Proceedings of the National Academy of Sciences U. S. A. 111, 4461–5. (doi:10.1073/pnas.1322003111)

Yayanos, A., Dietz, A., Van Boxtel, R., 1981. Obligately barophilic bacterium from the Mariana trench. Proceedings of the National Academy of Sciences U. S. A. 78, 5212–5215. (doi:10.1073/pnas.78.8.5212)

Zenkevich, I., Bogoiavlenskii, A., 1953. Detailed oceanographic research in the region of the Kurile-Kamchatka Deep in May-June 1953. Trudy Instituta Okeanologii Akademiia Nauk 16, 24–46.

Zobell, C., 1952. Bacterial life at the bottom of the Philippine Trench. Science 115(2993), 507–508. (doi:10.1126/science.115.2993.507)

CHAPTER III

Metabolic enzyme activities of abyssal and hadal fishes: pressure effects and a re-evaluation of depth-related changes

Abstract

Metabolic enzyme activities of muscle tissue have been useful and widely-applied indicators of whole animal metabolic rate, particularly in inaccessible systems such as the deep sea. Previous studies have been conducted at atmospheric pressure, regardless of organism habitat depth. However, maximum reaction rates of some of these enzymes are pressure dependent, complicating the use of metabolic enzyme activities as proxies of metabolic rates. Here, we show pressure-related rate (V_{max}) changes in lactate and malate dehydrogenase (LDH, MDH) and pyruvate kinase (PK) in six fish species (2 hadal, 2 abyssal, 2 shallow). LDH V_{max} decreased with pressure for the two shallow species, but, in contrast to previous findings, it increased for the four deep species, suggesting evolutionary changes in LDH reaction volumes. MDH V_{max} increased with pressure in all species (up to 51±10 % at 600 bar), including the tide pool snailfish, *Liparis florae* (activity increase at 600 bar 44±9 %), suggesting an inherent negative volume change of the reaction. PK was inhibited by pressure in all species tested, including the hadal liparids (up to 34±3% at 600 bar), suggesting a positive volume change during the reaction. The addition of 400 mM TMAO counteracted this inhibition at both 0.5 and 2.0 mM ADP concentrations for the hadal liparid, *Notoliparis kermadecensis*. We revisit depth-related trends in metabolic enzyme activities according to these pressure-related rate changes and new data from seven abyssal and hadal species from the Kermadec and Mariana trenches. Results show that pressure-related rate changes are another variable to be considered in the use of enzyme activities as proxies for metabolic rate, in addition to factors such as temperature and body mass, with abyssal and hadal species. With the pressure effects taken into consideration, metabolic enzyme activities can still be useful proxies for species living at greater habitat depths. Intraspecific increases in activities of tricarboxylic acid cycle enzymes with depth of capture, independent of body mass, in two hadal snailfishes suggest improved nutritional condition for individuals deeper in the hadal zone, likely related to food availability. These new data demonstrate previously unknown pressure effects on enzyme reaction

rates and inform the discussion of factors controlling metabolic rate in the deep sea, including the visual interactions hypothesis and extend published trends to the planet's deepest-living fishes.

Introduction

Certain citric acid cycle and glycolysis enzymes have been commonly used as proxies for whole-animal metabolic rate and activity (Childress and Somero, 1979; Sullivan and Smith, 1982; Dickson et al., 1993; Vetter and Lynn, 1997; Hickey and Clements, 2003; Dahlhoff, 2004; Friedman et al., 2012; Torres et al., 2012; Ombres et al., 2011; Condon et al., 2012; Drazen et al., 2015; Saavedra et al., 2015). This technique has been particularly valuable in deep-sea systems, due to the logistical constraints of traditional measurements of metabolic rate, such as the monitoring of oxygen consumption, although a few of these data exist at great depths (e.g., Smith et al., 1978; Hughes et al., 2011; Drazen and Yeh, 2012). Four major metabolic enzyme activities (maximum reaction rate, V_{max}) are typically used to estimate metabolic rate—lactate dehydrogenase (LDH), pyruvate kinase (PK), citrate synthase (CS), and malate dehydrogenase (MDH). LDH, which catalyzes the conversion of lactate to pyruvic acid in glycolysis, and PK, which catalyzes an ATP-yielding step in glycolysis, are used as proxies to indicate burst locomotory capability and anaerobic capacity (Childress and Somero, 1979; Dahlhoff, 2004). The activities of the tricarboxylic acid (TCA) cycle enzymes, CS and MDH, are applied as indicators of routine metabolic rate and aerobic activity (Somero and Childress, 1980; Childress and Thuesen, 1992; Thuesen and Childress, 1993).

The most common use of enzyme activities in deep-sea animals has been to evaluate changes in metabolism with depth (e.g., Childress and Somero, 1979; Sullivan and Somero, 1980; Siebenaller et al., 1982). Many taxa such as pelagic cephalopods, shrimps, and fishes, as well as benthic fishes, show declines in both measured respiration rates and metabolic enzyme activities in white and red muscle (e.g., Childress and Thuesen, 1992; Thuesen and Childress, 1993; Drazen et al., 2015). These declines are hypothesized to reflect a decrease in metabolic rate, which has been attributed to a reduction in food supply with depth (Smith et al., 1978; Siebenaller and Yancey, 1984) and/or reduced predator-prey interaction distances with declining light levels, known as the visual interactions hypothesis (Childress, 1995; Seibel and Drazen, 2007). The latter

hypothesis suggests that in dark environments, where interaction distances are short, there is limited selective pressure for high locomotory capacities, explaining the declines in metabolic activities with depth that are not otherwise accounted for by temperature and body mass. This hypothesis was recently supported by an analysis of 61 species of benthic and benthopelagic fishes ranging from 50 to 3180 m depth, using a standardized methodology of measuring metabolic enzyme activities (Drazen et al., 2015).

Conclusions of these studies rely on the assumptions not only that metabolic enzyme activities are indeed indicators of metabolic rate, but also that rates of these metabolic enzymes at atmospheric hydrostatic pressure reflect those at *in situ* pressures. However, the effects of pressure on enzyme catalysis can be non-linear and complex (reviewed by Mozhaev et al., 1996), calling into question the assumption that maximum reaction rates would not change with pressure. Half-saturation constants (K_m) for NADH of A_4-lactate dehydrogenase (originally termed M_4), which catalyzes the conversion of pyruvate to lactate to convert NADH to NAD^+ in glycolysis, have been shown in a number of deep-sea fish species to be either insensitive or less sensitive to pressure than orthologs from shallow species (Siebenaller and Somero, 1979; Somero and Siebenaller, 1979; Siebenaller, 1984; Dahlhoff et al., 1990). A similar insensitivity was discovered in other important metabolic enzymes of deep-sea fishes—MDH (Dahlhoff and Somero, 1991) and phosphofructokinase (PFK; Moon et al., 1971a). These types of studies have suggested that pressure insensitivity in deep-sea species comes at the cost of a reduced catalytic efficiency (Somero and Siebenaller, 1979; Hennessey and Siebenaller, 1985). Enzyme concentration can be increased to offset the effects of lower catalytic efficiencies (capacity adaptations), so tissue-specific maximum reaction rate (V_{max}) has not been hypothesized to change with pressure in fishes. However, at least 25 enzymes are known to exhibit increased maximum activity under pressure. Most of these have been isolated from piezophilic microbes (Eisenmenger and Reyes-De-Corcuera, 2009; Luong and Winter, 2015), but at least one animal enzyme has this property: a cellulase from the hadal amphipod *Hirondellea gigas* reportedly increased activity at 100 MPa (their habitat pressure in the Mariana Trench) relative to atmospheric pressure (Kobayashi et al., 2012).

In other contrasting studies, other enzymes appear to lack intrinsic pressure adaptations or are only partially adapted, and so may require protection from pressure by factors extrinsic to the

protein, i.e., other cellular molecules. For example, K_m of ADP (but not V_{max}) for PK in both shallow and deep-sea fish and anemones was found to be equally, and greatly, inhibited by pressure, such that higher ADP concentrations than in routine assay buffers are needed to achieve V_{max} (Yancey et al., 2001, 2004). However, in the presence of the osmolyte trimethylamine oxide (TMAO)—which is high in the deep-sea animals from which PK was tested (Kelly and Yancey 1999)—K_m of ADP was largely restored under pressure. TMAO was designated a 'piezolyte' ('pressure solute') for this property (Martin et al. 2002), which arises from TMAO's enhancing effects on water structure (reviewed by Yancey and Siebenaller 2015). Unlike PK, LDHs appear to rely on both intrinsic and extrinsic adaptations. As noted earlier, K_m of NADH for LDH from many deep-sea fishes is more resistant to pressure than for shallow orthologs, but is still somewhat sensitive. However, full counteraction of this residual pressure inhibition was found with TMAO at *in situ* concentrations (Gillett et al. 1997; Yancey et al. 2004). Despite these and findings for other taxa, the effects of pressure on enzyme maximum reaction rates (as opposed to K_m) have been considered negligible in studies of metabolic rate. Moreover, enzyme kinetic responses to pressure in fishes at *in situ* habitat pressures greater than 40 MPa have not been explored.

To inform the discussion of metabolic rate declines with depth, we use recent collections from the Mariana and Kermadec trenches to extend the published depth range of metabolic enzyme activities for fishes from ~3,000 to almost 8,000 m (*in situ* pressure ~80 MPa), approaching the likely depth limit for bony fishes (Yancey et al., 2014; Linley et al., 2016). The inclusion of hadal species in this analysis also allows the exploration of two additional factors that may affect metabolic rates besides light levels, namely (as noted earlier) food availability as well as hydrostatic pressure. In terms of food supply, although the deep sea is generally considered a food-limited environment, the topographies of hadal trenches are hypothesized to facilitate the accumulation of organic matter (George and Higgins, 1979; Danovaro et al., 2003; Jamieson et al., 2011; Ichino et al., 2015). This is comparable to submarine canyons, which channel organic material, resulting in high faunal abundance, biomass and diversity (e.g., De Leo et al., 2010). In subducting trenches, downslope transport is enhanced by seismic activity and internal tides, resulting in the deposition of material into the trench (Itou et al., 2000; Oguri et al., 2013; Turnewitsch et al., 2014). The depositional characteristic of the hadal zone likely allows trenches to support higher biomass than the surrounding abyss (Wolff, 1970; Beliaev, 1989; Jamieson et

al., 2010), as seen in increased amphipod (Jamieson, 2015) and meiofaunal (Danovaro et al., 2002; Itoh et al., 2011) abundances with depth and high rates of sediment-community oxygen consumption (Glud et al., 2013; Wenzhöfer et al., 2016). This increased food availability may be a strong evolutionary driver to inhabit greater depths for a number of animals, particularly for the amphipod-feeding hadal snailfishes (Linley et al. 2017; Gerringer et al., 2017; **Chapter II**). According to previous analyses, neither food availability nor pressure is expected to affect metabolic rate in the deep sea interspecifically (reviewed by Seibel and Drazen, 2007). The hadal zone offers an ideal site to explore the effects of both of these factors using a standardized protocol.

Here, we investigate pressure-related rate changes in three metabolic enzymes from deep- and shallow-adapted fishes. We then apply the pressure-related rate changes in metabolic enzyme activities to published and new results measured at atmospheric pressure, allowing a re-evaluation of the depth trends for metabolic proxies. This study extends a large existing dataset of metabolic enzyme activities to much greater depths with new data on abyssal and hadal species and elucidates depth-related trends in metabolic rate in fishes in light of pressure-related changes in maximum enzyme reaction rates.

Materials & Methods

Sample Collection. Abyssal and hadal fishes were collected by free-vehicle trap baited with mackerel near and from the Kermadec (Apr–May, 2014) and Mariana trenches (Nov–Dec, 2014). Further details on collection sites and traps are provided by Linley et al. (2016). *Liparis florae*, the tidepool snailfish, was collected from Puget Sound near Friday Harbor, WA by trawl and hand net (July, 2014). A shallower-living (550 m) cold adapted species was also included, *Paraliparis devriesi* Andriashev 1980 collected by trawl from Antarctica (Andvord Bay, FjordEco Cruise), where it lives at a habitat temperature of ~ -1°C, comparable to the hadal environment. Whole fish were kept on ice or in a cold room and processed as quickly as possible. White muscle samples were dissected from the anterior portion of the epaxial muscle. Red muscle and gelatinous tissues were carefully avoided. Tissues were frozen immediately in liquid nitrogen and stored at -80°C prior to analysis in the lab.

Enzyme Activities at Atmospheric Pressure. For comparison to published studies, maximum activities of four metabolic enzymes—citrate synthase (CS), lactate dehydrogenase (LDH), malate dehydrogenase (MDH) and pyruvate kinase (PK)—were measured using a standard unpressurized spectrophotometric method described by Condon et al. (2012) and Drazen et al. (2015), updated from Srere (1969) and Yancey and Somero (1978). Assays were conducted on white muscle homogenates ground in 10 mM tris(hydrozymethyl)aminomethane hydrochloride (Tris-HCl) buffer (pH 7.55 at 10°C) at a ratio of 1:10. Two tissue samples from each fish were assayed in duplicate. Although habitat temperature for these species is colder (down to -1.0°C), assays were conducted at 10°C to allow for comparison to published values (e.g., Drazen et al., 2015). Chemicals for all assays were sourced from Sigma-Aldrich. Collection information for the samples analyzed at atmospheric pressure are presented in **Table 3.1.**

Table 3.1. Collection information. Standard lengths and mass are taken from fresh fish. N indicates the number of individuals with measured CS, LDH, MDH, and PK activities. Sex indicates the number of male, female, and immature individuals. Others not sexed due to damage. Sex was determined visually.

Species	Location	Depth (m)	n	SL (cm)	Mass (g)	Sex
Liparidae						
Liparis florae	Puget Sound	~1–30	5	8.2–14.6	6.7–35.3	0, 0, 0
Liparidae sp. nov.	Mariana	6961–7929	16	13.7–26	8–160	4, 8, 2
Notoliparis kermadecensis	Kermadec	6500–7500	20	13.9–31.5	26–230	5, 11, 1
Paraliparis devriesi	Andvord Bay	550	3	~12–18	-	-
Macrouridae						
Coryphaenoides armatus	Kermadec	3500–4000	4	51.9–84.6	576–3130	2, 0, 0
Coryphaenoides yaquinae	Kermadec	5000	1	70.5	1344	0, 0, 0
Coryphaenoides yaquinae	Mariana	4441–6081	4	23.8–78.4	40–2200	0, 2, 2
Ophidiidae						
Spectrunculus grandis	Kermadec	3500–4000	5	29–73.8	106–2128	0, 1, 4
Synaphobranchidae						
Diastobranchus capensis	Kermadec	1500	1	91	608	0, 1, 0
Zoarcidae						
Pachycara sp.	Kermadec	5000	2	44.2–47.4	460–660	1, 0, 0

Enzyme Activities as a Function of Hydrostatic Pressure. In addition to standard unpressurized assays, enzymes from 6 species (all Liparidae and Macrouridae in **Table 3.1**) were tested under

pressure. White muscle samples (~0.1 g) were homogenized in a 1 ml buffer of 50 mM Tris-HCl, 1 mM ethylenediaminetetraacetic acid (EDTA), and 1 mM dithiothreitol (DTT) (pH=7.5 at 5°C). Homogenates were centrifuged for 10 minutes at 2,000 x g at 4°C. All chemicals were sourced from Sigma-Aldrich (St. Louis, MO, USA). To minimize variation due to pipetting error and slightly differing amounts of enzyme in different parts of the tissue, pressures were varied incrementally on one proceeding reaction. Before each pressure test, an atmospheric pressure check determined that the reaction maintained a linear rate over the time of the assay. All pressure assays were conducted at 5°C. Individual samples used for experiments were randomly selected.

A stainless-steel cuvette chamber (Mustafa et al., 1971) was used for pressure assays with a Jasco V550 UV/Vis spectrophotometer (Easton, MD, USA). Cell volume was 5 ml, though all reactions were added to 5.1 ml to prevent any air in the chamber. To minimize condensation on the cell windows, trays of desiccant (silica gel) and a steady stream of nitrogen gas were added to the closed chamber. Each assay lasted 300 seconds. To minimize error from mixing effects, only data from the last 250 seconds were used. After 100 seconds at atmospheric pressure, pressure was increased to 200 bar by hand pump for 50 seconds, then 400 and 600 bar. The pressure was then released back to 1 bar to measure enzyme recovery for the final 50 seconds. Reaction rates were determined from the last 40 seconds of slope at each pressure and converted to units of activity (µmoles of substrate converted to product per minute) per g wet weight of tissue. The cell was rinsed and aspirated once with isopropyl alcohol and twice with distilled water between assays.

Lactate dehydrogenase (LDH) activities were measured as follows. The reaction buffer, 80 mM Tris-HCl (pH=7.55 at 5°C), was added to the cell in the spectrophotometer first. 150 µM nicotinamide adenine dinucleotide (NADH) was then added to determine initial absorbance. Enough homogenate (between 3 and 10 µl) was added to achieve a linear reaction rate for 300 seconds. Finally, 512 µl of 40 mM sodium pyruvate was added to start the reaction. The chamber was closed and sealed quickly and the extinction of NADH measured. Final concentrations of NADH and pyruvate were 0.15 mM and 4 mM. To measure pyruvate kinase activity, a buffer of 80 mM Tris-HCl, 100 mM potassium chloride (KCl), 10 mM magnesium sulfate ($MgSO_4$), and 0.1 mM fructose-1,6-biphosphate was added to the chamber. 512 µl of 150 µM NADH was added, followed by 5 µl rabbit LDH (Type II, ammonium sulfate suspension, 800–1200 units/mg protein), the homogenate (5–15 µl for linear rate) and 100 mM phosphoenolpyruvic acid (PEP). The

reaction was initiated by the addition of 512 µl 20 mM adenosine diphosphate (ADP). Final concentrations of NADH, PEP, and ADP were 0.15 mM, 1.0 mM, and 2.0 mM respectively. Malate dehydrogenase assays were run in an 80 mM Tris buffer with 150 µM NADH. Homogenate was added (4–5 microliters to achieve linear reaction rate across 300 seconds). Reaction was initiated with mixing of 0.5 mM oxaloacetic acid. Final concentrations of NADH and oxaloacetate were 0.15 mM and 0.05 mM.

The increase in pressure results in a slight expansion of the cuvette as the windows of the cell seat in their rubber O-rings, increasing the path length across which the extinction of NADH is measured. A blank with buffer and NADH solution was measured at each pressure and the slight increase in absorbance was recorded and subtracted as a correction factor: 1.18, 2.26, and 3.35% for 200, 400, and 600 bar, respectively.

To investigate pressure-related changes in reaction rate in the presence of the osmolyte TMAO, the pyruvate kinase assay was selected for the hadal snailfish, *Notoliparis kermadecensis*. Protocol followed that listed above, with the addition of 400 mM TMAO, levels found in these fish (Yancey et al., 2014). Assays were conducted with 0.5 mM and 2.0 mM ADP levels, and activities measured at 1 bar and high pressure (655 bar).

Re-evaluation of Depth Trends. Atmospheric pressure results were compared to activities at *in situ* pressures found using the same collection. For families that were tested under pressure (Macrouridae, Liparidae), atmospheric pressure enzyme activities were adjusted to reflect the percent reaction rate changes seen at *in situ* pressure. Results were compared to depth trends shown in the literature using the same method of enzyme analysis (Drazen et al., 2015).

Statistics. Trends with body mass and depth were investigated using generalized linear models (GLM) constructed based on the log-link function, assuming normal distributions in the statistical programming platform, R (R Core Development Team, 2015). Normal quantile-quantile plots and plots of residuals were examined to check these assumptions. Best-fit GLM models were chosen according to lowest Akaike Information Criteria. Figures were constructed using the R package ggplot2 (Wickam, 2009).

Results

Enzyme Activities at Atmospheric Pressure. Results of four metabolic enzyme activities for nine species are presented in **Table 3.2**. LDH and PK were significantly correlated (linear model, R^2=0.63, F(1, 65)=105.6, p<0.001), as were MDH and CS (R^2=0.82, F(1, 65)=5.81, p=0.019), validating activity results. Family was a significant predictor of activity for all enzymes (ANOVA, LDH: F(4, 62)=11.99, p<0.001; PK: F(4, 62)=25.54, p<0.001; MDH: F(4, 62)=5.34, p<0.001; CS: F(4, 62)=6.60, p<0.001). Post hoc testing (Tukey HSD multiple comparisons of means, 95% confidence interval) revealed LDH activity was lowest in liparids, compared to macrourids (p<0.01), ophidiids (p<0.001), synaphobranchids (p<0.01), and zoarcids (p<0.05). PK activities were also lowest in liparids, relative to macrourids (p<0.01), ophidiids (p<0.01), synaphobranchids (p<0.001), and zoarcids (p<0.001). Citrate synthase activity was significantly higher in liparids than in macrourids (p<0.01) and ophidiids (p<0.01). Activity of MDH in liparids was lower than in macrourids (p<0.05), but higher than in ophidiids (p<0.05).

Table 3.2. Atmospheric pressure activities of four metabolic enzymes. Errors are presented as standard deviations. Activities are presented in Units per gram tissue wet weight. Capture location indicated: K, Kermadec and M, Mariana trench regions.

	CS	LDH	MDH	PK
Liparidae				
Liparis florae	1.46±0.50	34.40±7.79	32.44±5.71	20.40±2.98
Liparidae sp. nov. (M)	1.05±0.44	40.18±16.71	22.00±6.16	21.82±6.68
Notoliparis kermadecensis	1.16±0.78	21.97±8.08	17.82±6.99	16.15±2.82
Macrouridae				
Coryphaenoides armatus	0.39±0.27	62.93±11.24	38.69±8.19	31.13±5.83
Coryphaenoides yaquinae (K)	0.37	83.65	19.7	26.3
Coryphaenoides yaquinae (M)	0.55±0.18	31.60±4.51	22.03±3.48	22.02±11.25
Ophidiidae				
Spectrunculus grandis	0.29±0.09	66.51±24.16	9.25±2.20	30.16±4.51
Synaphobranchidae				
Diastobranchus capensis	0.34	96.03	21.01	54.3
Zoarcidae				
Pachycara sp.	0.49±0.37	73.55±5.24	18.92±5.42	50.31±14.56

No significant trends were found between mass and enzyme activity across all families, however, there were some intraspecific trends with body mass. Larger individuals had significantly lower citrate synthase activities in hadal liparids (log-transformed linear model, *N. kermadecensis* R^2=0.23, F(1, 17)=4.97, p<0.05; Mariana liparid R^2=0.55, F(1, 14)=17.28, p<0.001) and abyssal macrourids (*C. yaquinae* R^2=0.86, F(1, 3)=18.17, p<0.05; *C. armatus* R^2=0.34, F(1, 2)=1.05, p<0.05). LDH activity was higher in larger *C. yaquinae* individuals (R^2=0.81, F(1, 3)=13.03, p<0.05). In larger individuals of the hadal liparid, *N. kermadecensis*, MDH activities were significantly higher (R^2=0.41, F(1, 17)=11.91, p<0.01). PK did not vary significantly with body mass for any species tested. Sample sizes for *Diastobranchus capensis* and *Pachycara sp.* were not large enough to test mass effects.

At atmospheric pressure, enzyme activities for hadal liparids were largely similar to shallower-living counterparts from this study and published results from Drazen et al. (2015), with a few differences. Lactate dehydrogenase activities were significantly different only between *N. kermadecensis* and the Mariana liparid, the latter being higher (post-hoc Tukey HSD, 95% confidence interval, p<0.001). *L. florae* had significantly higher MDH than *C. melanurus* (from Drazen et al., 2015; p<0.01), *N. kermadecensis* (p<0.001), and the Mariana liparid (p<0.05). PK activity was higher in *L. florae* than in *C. melanurus* (Drazen et al., 2015; p<0.01), the Mariana liparid (p<0.05), and *N. kermadecensis* (p<0.001). Citrate synthase activity did not vary significantly across all liparid species (ANOVA, F(5, 44)=0.47, p=0.794).

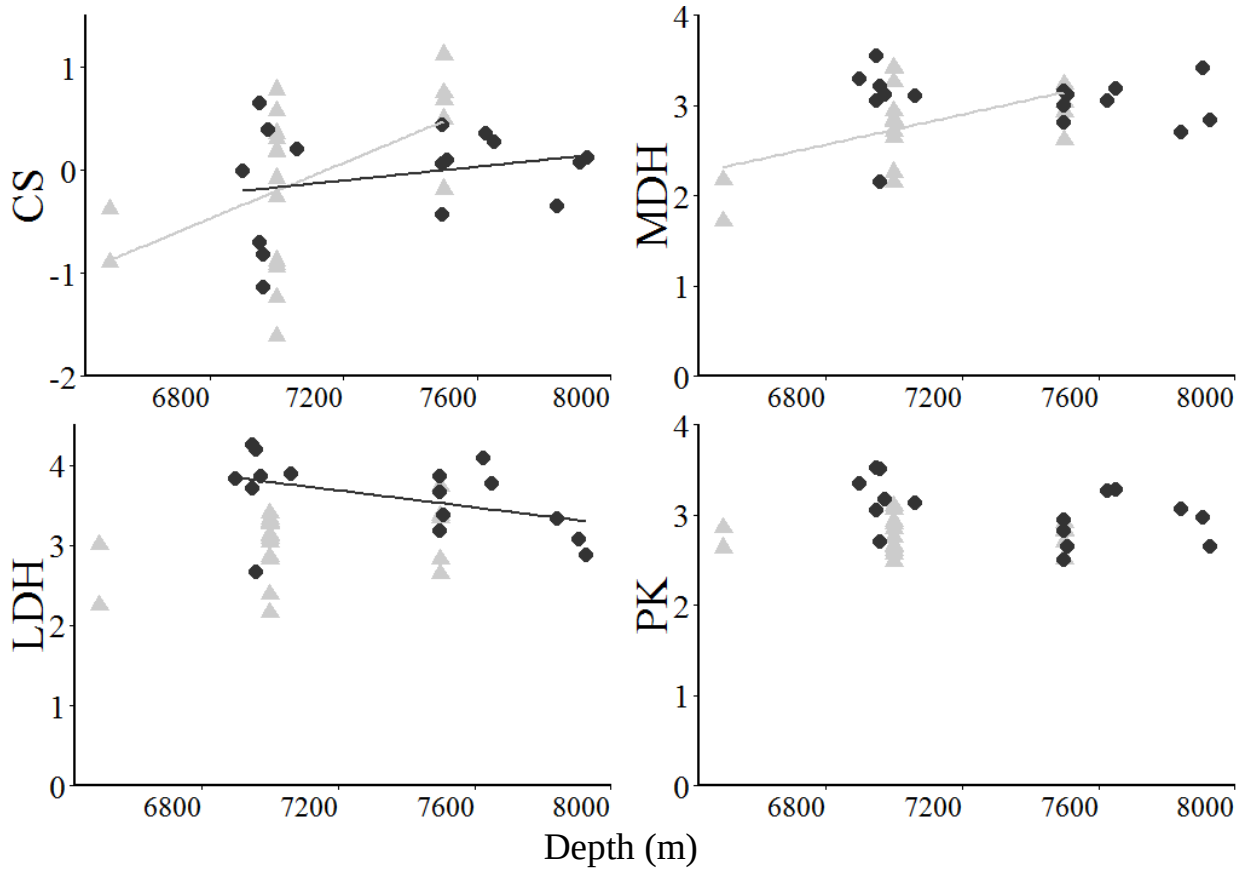

Figure 3.1. Hadal liparid enzyme activities at atmospheric pressure (log-transformed, U/g wet mass) by depth of capture (m). Linear regressions are shown for significant depth relationships from GLMs that included mass effects, Mariana liparid (M) in black circles *Notoliparis kermadecensis* (K) in grey triangles (R^2 values CS: M=0.015, CS: K=0.339, MDH: K=0.204, LDH: M=0.235).

In the Mariana liparid, CS activities increased intraspecifically with depth of capture independent of body mass, and LDH decreased, while other intraspecific relationships between enzyme activity and depth were not significant (**Figure 3.1**; GLM, depth, mass, interaction, 15 df, LDH: t=-2.50, -1.86, 1.85, p<0.05, =0.088, 0.088; MDH: t=-1.06, -0.73, 0.67, p=0.308, 0.481, 0.516; CS: t=-2.61, -2.77, 2.54, p<0.05, 0.05, 0.05; PK: depth, mass t=-1.45, -0.01, p=0.170, 0.992). For *N. kermadecensis*, LDH and PK showed no significant depth effects, while CS and MDH increased with depth of capture (GLM, depth, mass, 18 df, LDH: t=1.78, -0.31, p=0.095, 0.758; MDH: t=2.68, -3.57, p<0.05, 0.01; CS: t=2.69, -2.16; p<0.05, 0.05; PK: t=-0.17, -1.69, p=0.870, 0.111).

Enzyme Activities as a Function of Pressure. Changes in maximum reaction rate, V_{max}, with pressure were seen in all three enzymes. In the case of lactate dehydrogenase (LDH), abyssal and hadal species showed enhanced activity under pressure, while shallow-adapted species were inhibited by pressure (ANOVA, *C. armatus* $F(5, 37)=7.52$, $p<0.001$; *C. yaquinae* $F(5, 24)=3.28$, $p<0.05$; *N. kermadecensis* $F(5, 31)=4.74$, $p<0.01$; Mariana liparid not statistically significant $F(5, 10)=1.63$, $p=0.24$; *L. florae* $F(4, 15)=10.47$, $p<0.001$; *P. devriesi* $F(4, 22)=9.76$, $p<0.001$). Maximum activities seemed to occur near habitat pressures for all species (**Figure 3.2**).

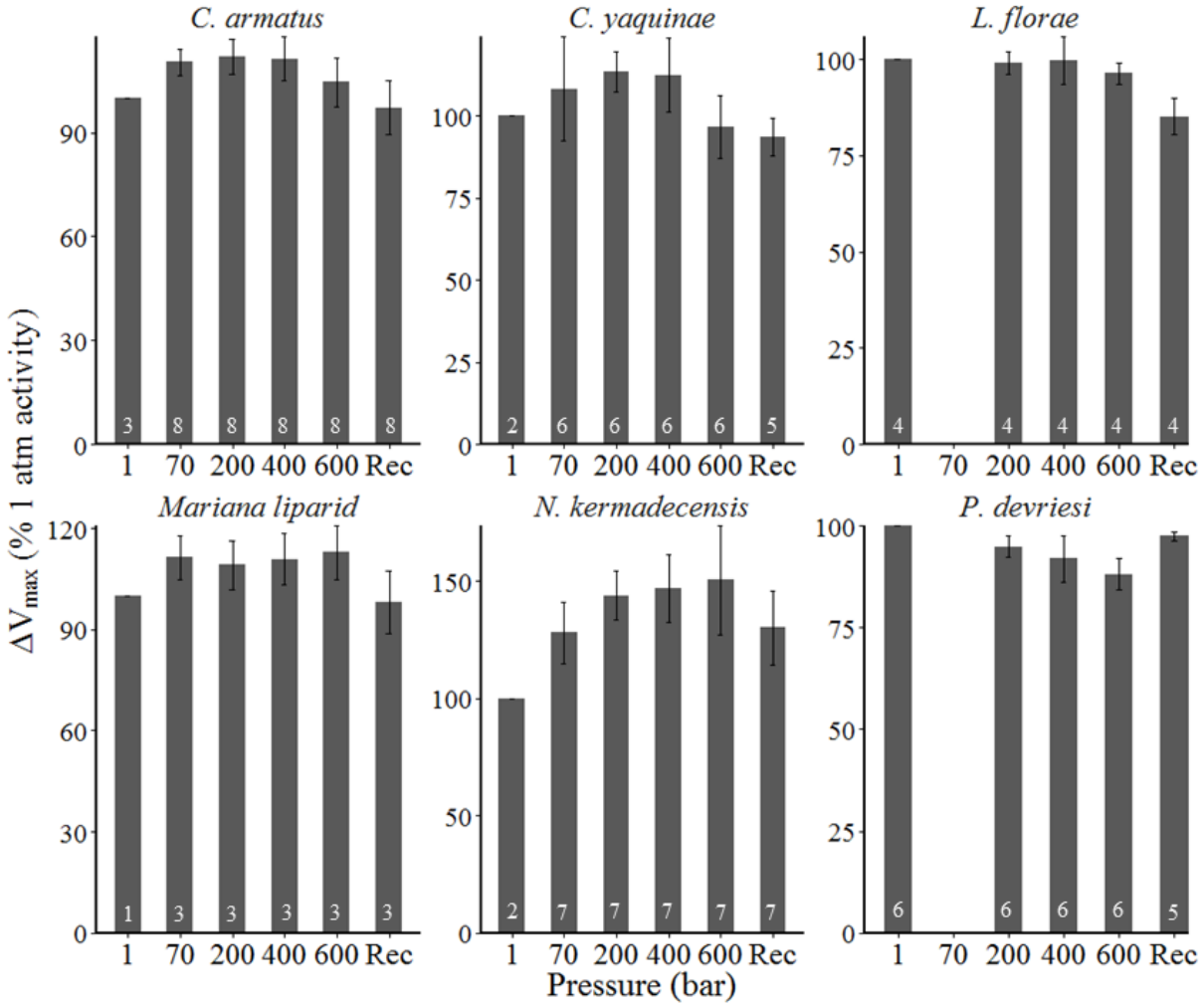

Figure 3.2. Lactate Dehydrogenase change in V_{max} at varying pressures. Shown in percent of activity at atmospheric pressure for each assay. Results from repeat assays (n values included at the base of each bar) of one individual per species. Error bars show standard deviations between assays. Recovery (Rec) shows rate after return to atmospheric pressure after pressure trials.

Malate dehydrogenase (MDH) showed increased activity with pressure for all species (**Figure 3.3**). This pressure activation from atmospheric pressure rates were statistically significant for all species tested, except *C. armatus* (ANOVA, *L. florae* $F(3, 29)=13.57$, $p<0.001$; *C. armatus* $F(3, 34)=0.53$, $p=0.66$; *N. kermadecensis* $F(3, 15)=24.57$; $p<0.001$; *P. devriesi* $F(3, 20)=3.50$, $p<0.05$; *C. yaquinae* $F(3, 31)=3.54$, $p<0.05$; Mariana liparid $F(3, 35)=9.79$, $p<0.001$). Some species, particularly *C. armatus*, showed more scatter in repeat assays than others.

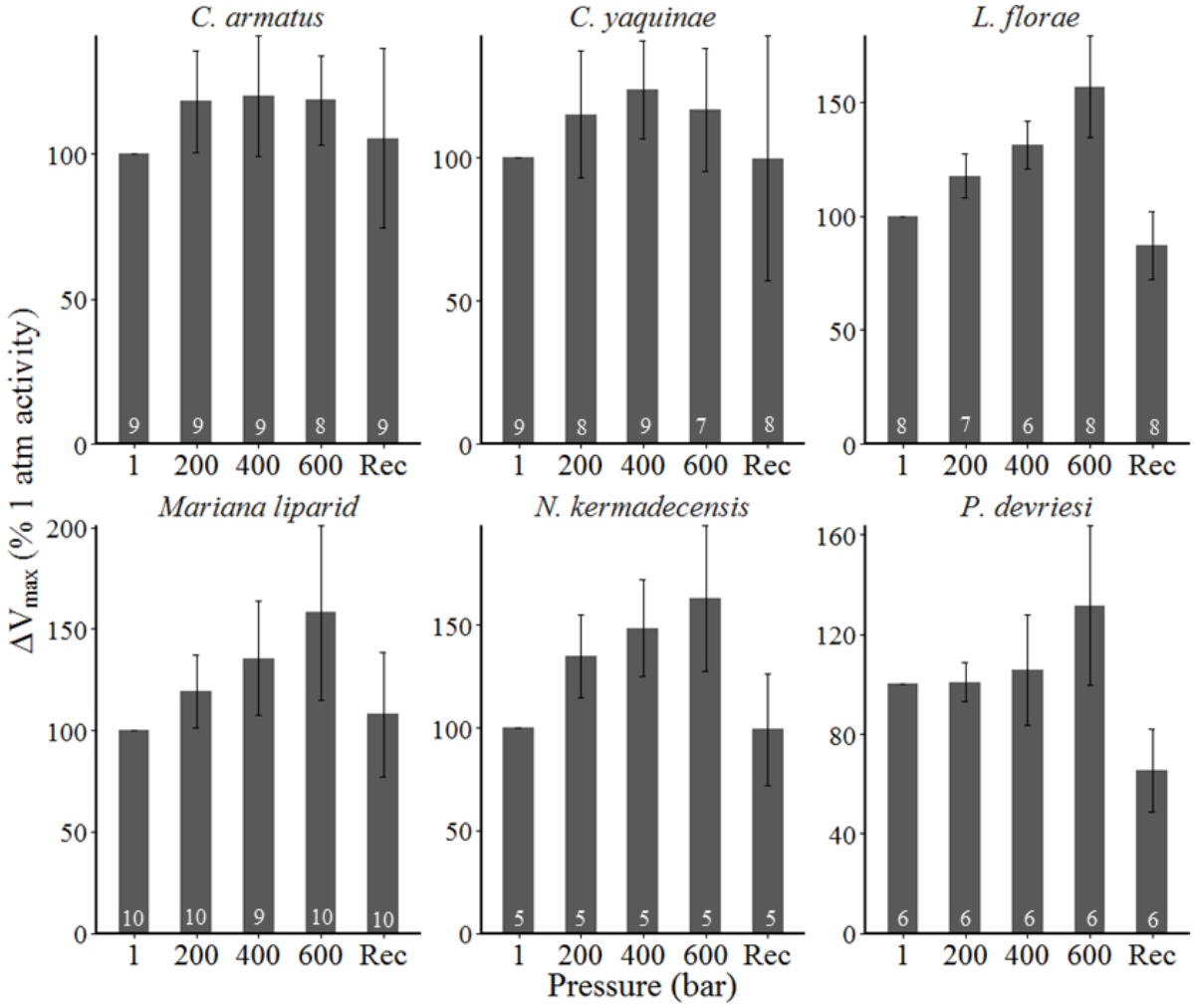

Figure 3.3. Malate Dehydrogenase change in V_{max} at varying pressures. Shown in percent of activity at atmospheric pressure for each assay. Results from repeat assays (n values included at the base of each bar) of one individual per species (n=2 for Mariana Trench liparid). Recovery (Rec) shows rate after return to atmospheric pressure after pressure trials.

Pyruvate kinase was inhibited by pressure in all species, from shallow to hadal (**Figure 3.4**), statistically significantly for *C. armatus* (ANOVA, $F(4, 17)=18.34$, $p<0.001$), *C. yaquinae* ($F(4, 20)=12.98$, $p<0.001$), *N. kermadecensis* ($F(4, 28)=4.38$, $p<0.01$) and the Mariana liparid ($F(4, 20)=14.22$, $p<0.001$), and near significantly for *L. florae* ($F(4, 18)=2.72$, $p=0.062$). Recovery after decompression was highly variable for all enzymes and were omitted from statistical tests. All recovery rates were likely confounded by uneven changes in system optics with the release of pressure.

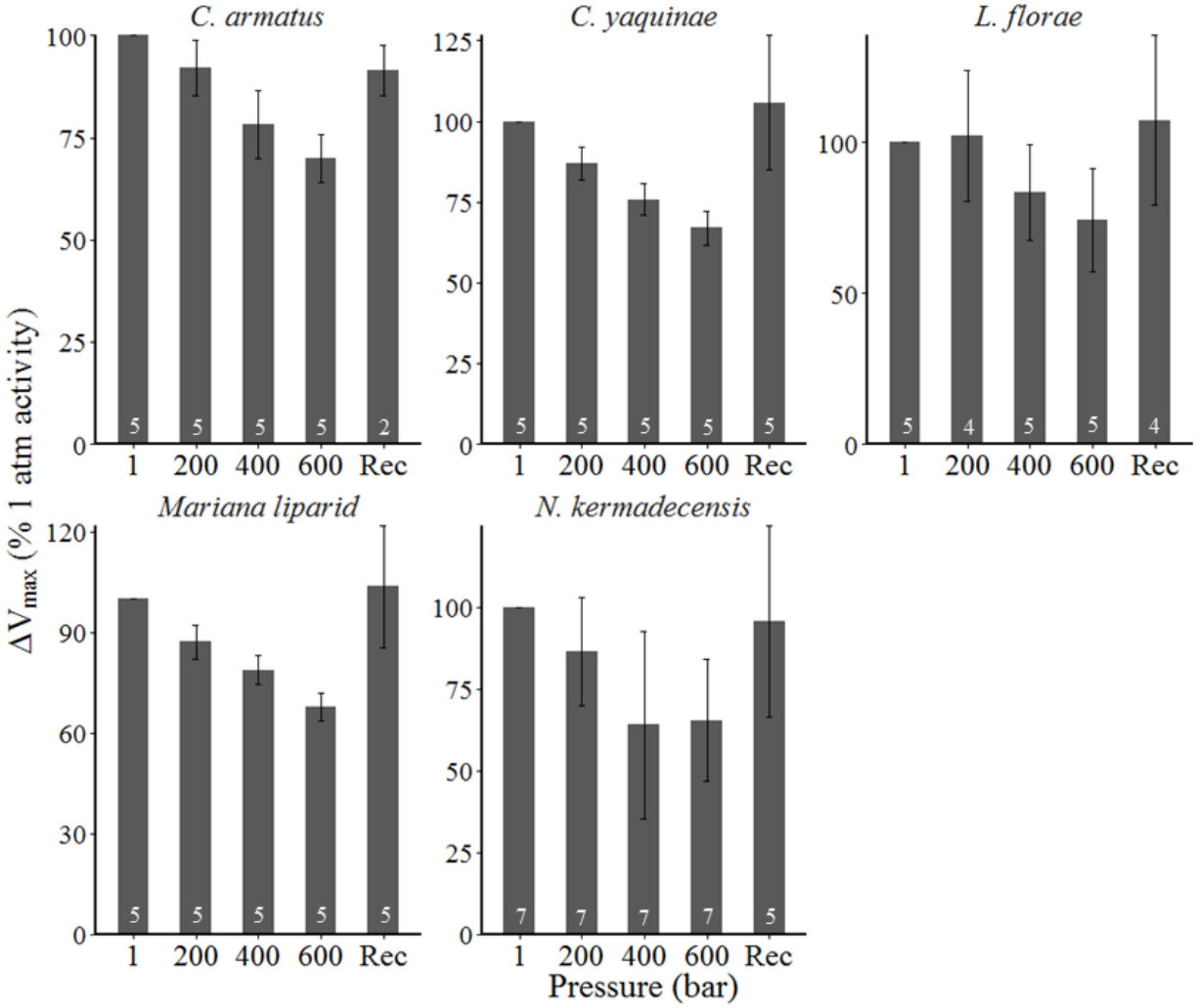

Figure 3.4. Pyruvate Kinase change in V_{max} at varying pressures. Shown in percent of activity at atmospheric pressure for each assay. Results from repeat assays (n values included at the base of each bar) of one individual per species. Recovery (Rec) shows rate after return to atmospheric pressure after trials.

The addition of TMAO counteracted this pressure-inhibition of pyruvate kinase, dramatically restoring the activity of pyruvate kinase at both a low and high ADP concentration (**Figure 3.5**). TMAO had no effect on activity (V_{max}) at atmospheric pressure at high substrate concentrations but did increase activity at subsaturating levels (0.5 mM ADP).

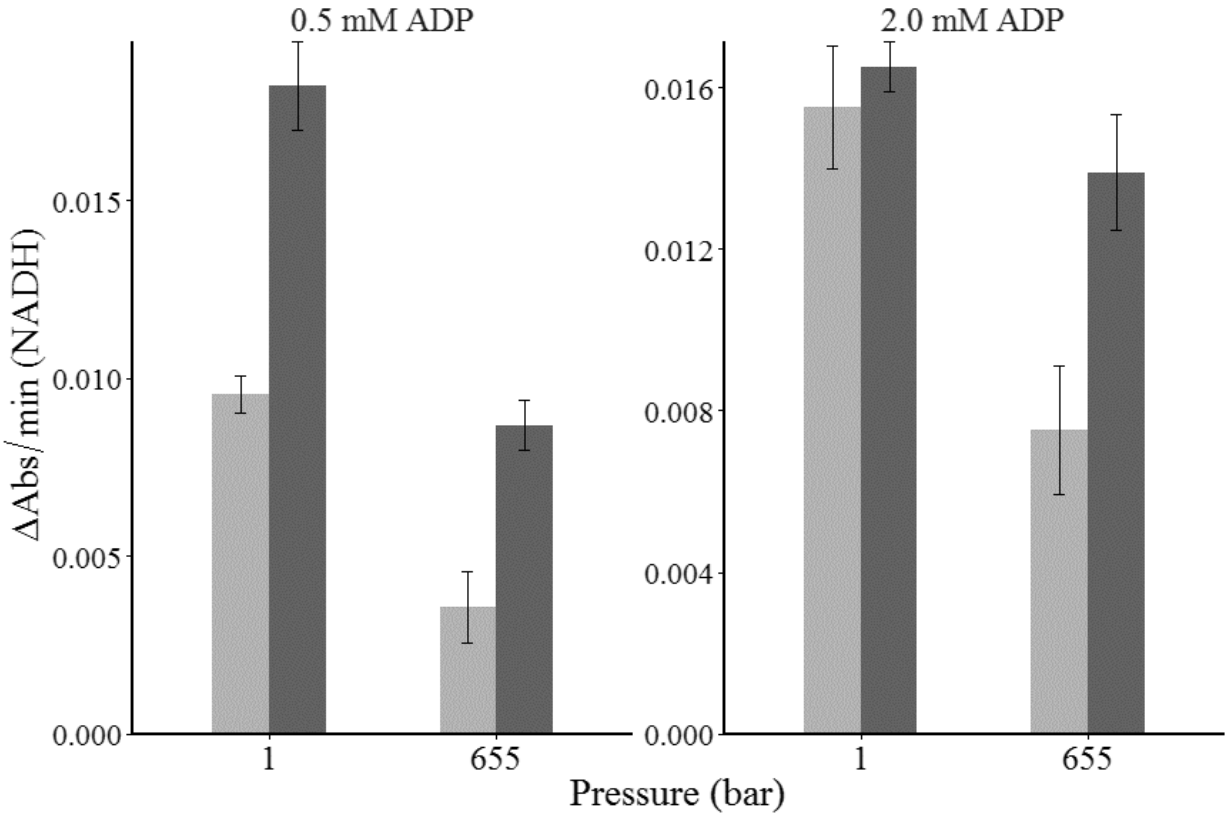

Figure 3.5. Pyruvate Kinase response to pressure with TMAO. At two concentrations of ADP. Assay with addition of 400 mM TMAO in dark grey, control pressure response in light grey. Data for *N. kermadecensis* (n=4 for 0.5mM ADP, n=3 for 2.0mM ADP). TMAO effect on activity was significant for each treatment (Mann-Whitney-Wilcoxon test; $p<0.05$), except at 1 bar and 2 mM ADP ($p=0.35$).

Depth and Pressure Trends. Figure 3.6 shows how the enzyme activities of species studied here compare to the trends shown by Drazen et al. (2015) by depth and how incorporation of the rate changes due to *in situ* pressure (results from above) would alter the Drazen et al. (2015) results. Both citrate synthase and malate dehydrogenase activities were higher than expected according to the Drazen et al. (2015) regression. LDH and PK were somewhat higher than the regression from shallower-living species predicted. Increased activities of LDH at *in situ* pressures increased this

difference slightly. PK activities at *in situ* pressures were similar to the regression prediction, although these did not take into account the TMAO effect, which counteracts pressure inhibition of the enzyme, but only at subsaturating ADP concentrations.

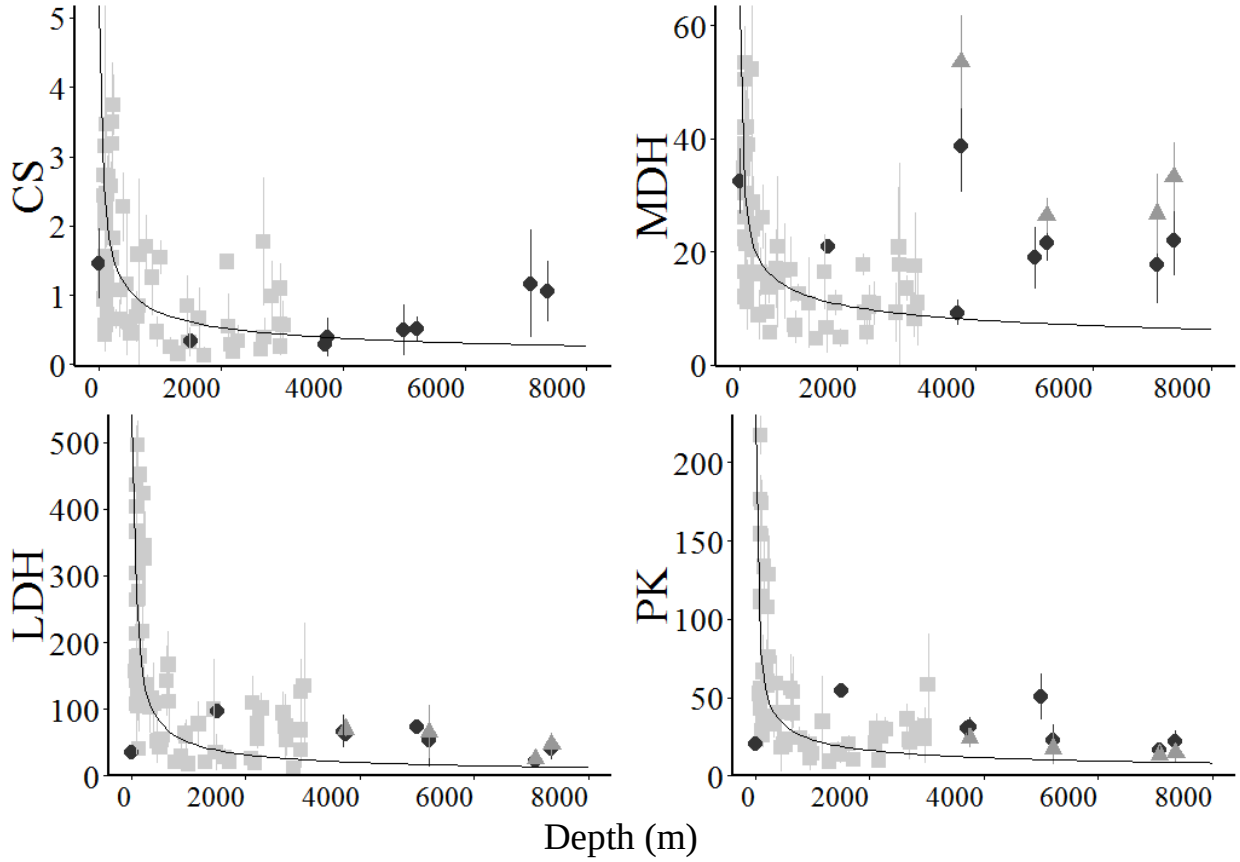

Figure 3.6. Average enzyme activity (U/g wet mass) by average depth of capture (m) for 67 species of demersal fishes. Present study 1 atm results (dark grey circles), Drazen et al., 2015 1 atm (light grey squares), and expected activities at *in situ* pressures for study species (triangles) shown. Error bars show standard deviation between individuals (n=1–20). Models of depth-related declines in activities for benthopelagic species from Drazen et al., 2015 shown in black curves. Pressure effects on CS not tested.

Discussion

Deep-sea species are known to display enzymic pressure adaptation. This has been understood as a maintenance of functional stability under increasing pressure, through the pressure-insensitivity of K_m (Siebenaller and Somero, 1979; Somero and Siebenaller, 1979;

Siebenaller, 1984; Dahlhoff et al., 1990). This insensitivity has been hypothesized to come at the cost of reduced catalytic efficiencies, based on experiments of LDH, MDH, and PK. Previous work focused mainly on half-saturation constant, K_m, responses, while maximum reaction rate, V_{max}, was not hypothesized to change with pressure at the level of the tissue because of species' ability to increase enzyme concentration. Further, previous work focused on shallower-living (<1000 m) deep-sea species and as a result, pressure typically was not modified during V_{max} experiments.

Contrary to previous assumptions, we found pressure-related changes in V_{max} per gram of tissue for three enzymes, with LDH maximized at habitat pressure, MDH showing pressure activation in all tested species, and PK consistently pressure-inhibited. For V_{max} to change in these assays as a function of pressure, one of two things must be changing—either the K_m value or the catalytic efficiency. Although pressure related changes in K_m value are well known (e.g., Siebenaller, 1984), the present assays were conducted at high substrate concentrations that would not have been rate limiting. Therefore, catalytic efficiencies likely change with pressure—in both directions—depending upon volume changes in the reaction. These results show that macromolecular evolution (stabilization of K_m) has not completely resulted in stability of V_{max}. According to Le Chatelier's principle, reactions with net positive volume change are inhibited by pressure, whereas reactions which have reduced volume in the products are favored with pressure (e.g., Somero, 1992; Macdonald, 1997). Our results suggest negative volume changes for lactate dehydrogenase in the abyssal and hadal species tested, as well as for malate dehydrogenase in all species. This dramatic increase in activity with pressure has not, to our knowledge, been previously shown in MDH. There are studies of MDHs capable of adaptation to extreme temperature conditions, such as one that remains active (90%) even after it is boiled for six hours (Gharib et al., 2016). The pressure-enhancement effects may be more pronounced than those seen in LDH due to the dimeric, rather than tetrameric, nature of the enzyme.

Pressure-related changes in V_{max} may not have been addressed in earlier work for a number of reasons. Changes in K_m with pressure are perhaps a more intuitive indicator of macromolecular sensitivity to pressure than maximum reaction rates. It was believed that LDHs of deep-sea species were inefficient in catalysis compared to cold-adapted shallow species (Somero and Siebenaller, 1979). However, that conclusion came from catalytic efficiencies measured at atmospheric pressure. Understanding enzymic adaptation in deep-sea fishes as a tradeoff between catalytic

efficiency and pressure sensitivity is incomplete when the reduced catalytic efficiency of LDH is only the case at low pressures. Given these new data, this paradigm should be reconsidered. Another study that concluded low catalytic efficiencies of LDH in deep-sea fishes was based on pressure incubations of LDH for an hour in pressure vessels. After decompression, activity was measured at atmospheric pressure (Hennessey and Siebenaller, 1985). When measuring the progress of one reaction, we found that recovery of LDH after pressurization was extremely variable, and often the enzyme did not recover. By measuring V_{max} at atmospheric pressure after an incubation, Hennessey and Siebenaller (1985) explored decompression survivability, missing the pressure-activation and change in catalytic efficiency of LDH in these deep-sea fishes. Another previous experiment found that maximum catalytic rate of LDH in *Coryphaenoides* is pressure insensitive until about 800 bar, when it becomes inhibited (Moon et al., 1971b). We measured reaction rates on one reaction, with a step-wise increase in pressure and with more replicates and greater precision than the spectrophotometer technology allowed at the time of that experiment, where variability or rapid pressurization may have masked the pressure activation. Also, in shallower-living (bathyal) deep-sea species, this pressure-activation effect may be small. The hadal fishes add a more dramatic example to this trend, displaying a nearly 50% increase in maximum catalytic rate at habitat pressure.

Since the three enzymes showed very different responses in maximum reaction rate to changing pressures, this suggests that these results are not due to system artifacts such as changes in optics with pressure. We note that even when using a sensitive spectrophotometer and measuring changes over one reaction, results were variable. Some of this variability may have stemmed from tissue degradation. For example, the Mariana liparid showed high variability compared to *N. kermadecensis*, perhaps because it was retrieved through warm surface waters (>25ºC) before trap recovery, although every effort was made to minimize recovery time and samples were dissected on ice and frozen immediately in liquid nitrogen. Further, the early studies on pressure activities of enzymes from deep-sea fish found that phosphofructokinase from abyssal *Coryphaenoides* reaches peak maximum reaction rate near 300 bar (Moon et al., 1971c). The authors noted that this is a low-activity, unstable enzyme that is very susceptible to degradation and decompression, and this finding seems to have remained unexplored.

In previous studies, metabolic enzyme activities have been useful and widely-applied indicators of metabolic rate and condition (reviewed by Dahlhoff, 2004). Studies have shown depth-related declines in enzyme activity (LDH, PK, MDH, CS) from surface waters to depths over 3000 m in benthic and benthopelagic species (e.g., Drazen, et al., 2015). As noted earlier, results were interpreted as a decline in metabolic rate due to decreasing predator-prey interaction distances with decreasing light availability (visual interactions hypothesis), while older studies attributed such declines to reduced food supply (reviewed by Childress, 1995). Again, assays have traditionally been conducted only at atmospheric pressure however, our studies show that for abyssal and hadal species, maximum reaction rates (V_{max}) of three of these enzymes (LDH, PK, and MDH) are pressure-dependent, suggesting that pressure-related changes in maximum reaction rate may alter interpretations of these depth-related trends in metabolic rate. This is a complicated issue, as the degree to which results at atmospheric pressure differ from *in situ* pressure rates may depend on the enzyme, TMAO effects, and the habitat depth of the fish. To begin to address this, we compared our atmospheric pressure activity results to those presented by Drazen et al. (2015, same experimental method) and applied estimates of how these activities would change at *in situ* pressure for the four abyssal and hadal species tested in this study (**Figure 3.6**).

Results of enzyme activities for nine species measured at atmospheric pressure are comparable to those measured in previous studies. *C. armatus* activities were similar to those measured off California (Drazen et al., 2015), although MDH values were significantly higher in the present study, perhaps anomalously high according to the depth trends presented in **Figure 3.6**. In another macrourid, *C. yaquinae*, LDH and PK activities were lower than in *C. armatus*, perhaps reflecting differences in trophic strategy (Drazen et al., 2008). *Spectrunculus grandis* activities were near identical to those from near California (Drazen et al., 2015), measured using the same experimental method. *D. capensis* activities were largely similar to activities for *Synaphobranchus kaupii*, another deep-sea eel from the North Atlantic (235–3,200 m), with the exception of PK, which was significantly higher in our study (Bailey et al., 2005). With a sample size of one, however, it would be imprudent to infer too much from this difference. As seen in other studies, glycolytic enzymes were lower in liparids than in macrourids, ophidiids, synaphobranchids, and zoarcids, suggesting lower burst locomotory capability. Large differences in body mass between these families might also explain some of these differences (e.g., Childress and Somero, 1990).

Despite pressure-related changes in activity reported here, atmospheric pressure activity results are still useful as proxies for intraspecific variations in metabolic rate, as we found in hadal liparids. Citrate synthase values increased with depth of capture in hadal liparids from the Kermadec and Mariana trenches, independently of body mass. This trend may have been weaker for the Mariana liparid due to lack of shallower hadal collections (nearer to 6,000 m). Resource availability is hypothesized to be higher in hadal systems, due to a funneling of organic matter into the steep topography of the trench (e.g., George and Higgins, 1979; Danovaro et al., 2003; Itoh et al., 2011; Ichino et al., 2015). Laboratory controlled studies showed intraspecific increases in metabolic enzyme activity in fishes that were better fed (Yang and Somero, 1993; Dutil et al., 1998; Martínez et al., 2003; Ombres et al., 2011). The results of this study indicate higher metabolic rate and/or better nutritional condition with depth. An increase in number of prey items per gram of fish with depth of capture in the Mariana liparids (Gerringer et al., 2017; **Chapter II**) and a higher abundance of liparids within the trench than at the upper edges (Linley et al., 2016) may support what the citrate synthase results suggest—an increase in nutritive condition with depth. Few interspecific differences were seen between the two groups, though LDH activity was significantly higher in the liparid from the Mariana than in *Notoliparis kermadecensis* from the Kermadec, maybe reflecting greater competition for food under the oligotrophic Mariana surface waters (Longhurst et al., 1995; Watling et al., 2013).

The decline in enzyme activity with depth appears to hold true overall, despite being somewhat tempered by pressure effects. With these new data included, the glycolytic enzymes, PK and LDH show the most significant declines, suggesting a lower burst locomotory potential in deep-sea species. Although PK showed significant pressure-inhibition of maximum reaction rate for all species tested (**Figure 3.4**), the addition of the counteracting osmolyte TMAO in a hadal liparid restored reaction rates to those seen at atmospheric pressure (**Figure 3.5**). It is probable, then, that the rate reductions presented in **Figure 3.6**, which do not take into account this restoration of activity with added TMAO, do not reflect *in situ* activity for pyruvate kinase. CS and MDH activities are higher than the Drazen et al. (2015) models predicted, particularly at hadal depths, perhaps due to increased food availability, as discussed above. These additional data extend the depth range of previous studies by over 4000 m. Earlier conclusions that there are depth-related declines in enzyme activity still hold. Most of these changes occur over the first thousand

meters, where pressure effects as observed here would be minimal, and the decline with depth is of a much greater magnitude than the pressure inhibition or activation observed. The initial decline is likely based on light levels as stated by the visual interactions hypothesis (Childress, 1995), while at abyssal and hadal depths, food availability may play a greater role.

Enzyme activities are already known to be approximate, imperfect, proxies for metabolic rate. Overall, pressure-related rate changes are merely another variable to be considered in the use of enzyme activities as proxies for metabolic rate, adding to an already long list of factors including temperature, body mass (Childress and Somero, 1990; Burness et al., 1999; Martínez et al., 2000; Sullivan and Somero, 1983, present results), locomotory and feeding strategies, phylogeny, nutritional condition, mitochondrial density and specific activity (Moyes et al., 1992), age (Singh and Kanugo, 1969), tissue storage (Nilsson and Ekstrand, 1993), and citrate concentration (for MDH; Gelpi et al., 1992), that can confound results and make interpretations difficult (e.g., Gibb and Dickson, 2002). Pressure effects should be considered when comparing species across large habitat pressure ranges. For example, in our atmospheric results, the significantly higher MDH values in *L. florae* are likely an example of pressure confounding effects. At *in situ* pressures, both hadal liparid activities were significantly higher, up to 150% of the activity at atmospheric pressure. Swimming speeds in *L. florae* and the hadal liparids are comparable when standardized for temperature (Gerringer and Linley, unpublished data). When using LDH activity as a proxy, previous studies may have underestimated burst capacity for deep-adapted species living at or below ~4000 m by up to 50%. This could provide some explanation for studies that have found higher than expected swimming performance in deep-sea fish species (e.g., Bailey et al., 2003; Bailey et al., 2005).

Our results further highlight the interplay of extrinsic and intrinsic adaptation. Pyruvate kinase was most susceptible to pressure, with reduced activity seen in all species. For enzymes like pyruvate kinase, the stabilizing effects of extrinsic adaptations may be particularly important. The piezolyte TMAO is known to stabilize proteins under high pressure due to the interaction with the water molecules in solution (e.g., Sarma and Paul, 2013), and TMAO is known to increase with depth in fishes and other taxa as an extrinsic pressure adaptation (Kelly and Yancey, 1999; Linley et al., 2016; Yancey et al., 2014). Yancey et al. (2001; 2004) found significant decreases in K_m of PK from *Antimora microlepis* (bathyal morid cod), as well as from an abyssal sea anemone

and from rabbit muscle, with the addition of 250-300 mM TMAO offsetting some or all of the inhibitory increases by pressure. The saturation of the pyruvate kinase mechanism could require something like TMAO to repel water from the active site of the reaction. In the present study, we found that TMAO considerably counteracted the inhibition of pyruvate kinase activity under pressure, suggesting that, while some enzymes such as LDH may be intrinsically adapted to function under high pressure, others may need extrinsic adaptation, such as stabilizing cosolutes.

Pressure-related changes in metabolic enzyme activities at abyssal and hadal depths re-open an old question: Does hydrostatic pressure affect whole animal metabolic rates? Although previous studies have suggested that it does not (Seibel and Drazen, 2007), this may need to be reconsidered for abyssal and hadal organisms. On a biomolecular level, the effects of temperature and pressure are similar, with low temperatures and high pressures having comparable effects (reviewed by Somero, 1992). For example, in lipid membrane fluidity, a pressure increase of 1000 atm is thought to be similar to a temperature decrease of 13–21°C (Somero, 1992). This comparison is oversimplified; however, volume changes, whether from changes in temperature or changes in pressure, will affect reaction rates. New models are seeking to quantify and predict these effects (Chen and Makhatadze, 2017). The effects of temperature on metabolic rate are accepted. For most of life on Earth, the effects of pressure on metabolic rate may be negligible; however, at extremely high pressures, such as on the abyssal plain and in hadal trenches or the deep subsurface biosphere, pressure effects may be significant. This may have implications for models such as the metabolic theory of ecology, which seeks to explain biological processes and patterns through temperature and body size (Brown et al., 2004), or the growing degree day, which standardizes time to temperature (e.g., Neuheimer and Taggart, 2007). Perhaps future work considering organisms that live at high pressures will require an additional component in metabolic models, something of a degree-day-bar, to consider the biological effects of high hydrostatic pressures.

Acknowledgments

The authors thank the captains and crews of the *R/V Thompson* and *R/V Falkor*. We are also grateful for the help of Thomas Linley (University of Aberdeen), Alan Jamieson (University of Aberdeen), Matteo Ichino (University of Southampton), Chloe Weinstock (Whitman College), and the participants of National Science Foundation's (NSF) HADES Program cruises, who assisted with collection and processing of fish samples at sea. Thanks to Matt Tietbohl and Stacy Farina for their help with *L. florae* collection and dissection, Craig Smith and Amanda Ziegler (University of Hawai'i) for *P. devriesi* collection, Erik Thuesen (The Evergreen State College), Suzanne Maroney (The Evergreen State College), and Tim Machonkin (Whitman College) for laboratory assistance, and Anna Downing (Whitman College) and Telissa Wilson (The Evergreen State College) for help running pressure assays. Funding for this research was provided by the National Science Foundation (NSF-OCE 1130494, 1130712, and 0727135, NSF-PLR 1443680) and Schmidt Ocean Institute. M. Gerringer is grateful for the support of the National Science Foundation's Graduate Research Fellowships Program.

Contributors

Gerringer, M.E.[1], Drazen, J.C.[1], Yancey, P.H.[2]

[1]Department of Oceanography, University of Hawai'i at Mānoa, Honolulu, HI 96822, USA.
[2]Biology Department, Whitman College, WA 99362, USA.

MEG, JCD, and PHY collected samples. MEG ran atmospheric pressure assays. MEG and PHY conducted assays using the pressure system. All authors contributed to the writing and editing of the manuscript.

References

Bailey, D., Bagley, P., Jamieson, A., Collins, M., Priede, I., 2003. *In situ* investigation of burst swimming and muscle performance in the deep-sea fish *Antimora rostrata* (Günther, 1878). Journal of Experimental Marine Biology and Ecology 286, 295–311. (doi:10.1016/S0022-0981(02)00534-8)

Bailey, D., Genard, B., Collins, M., Rees, J., Unsworth, S., Battle, E., Bagley, P., Jamieson, A., Priede, I., 2005. High swimming and metabolic activity in the deep-sea eel *Synaphobranchus kaupii* revealed by integrated *in situ* and *in vitro* measurements. Physiology and Biochemical Zoology 78, 335–46. (doi:10.1086/430042)

Beliaev, G., 1989. Deep-Sea Ocean Trenches and their Fauna.

Brindley, A. a., Pickersgill, R.W., Partridge, J.C., Dunstan, D.J., Hunt, D.M., Warren, M.J., 2008. Enzyme sequence and its relationship to hyperbaric stability of artificial and natural fish lactate dehydrogenases. PLoS One 3. (doi:10.1371/journal.pone.0002042)

Brown, J., Gillooly, J., Allen, A., Savage, V., West, B., 2004. Toward a metabolic theory of ecology. Ecology 85, 1771–1789. (doi:10.1890/03-9000)

Burness, G., Leary, S., Hochachka, P., Moyes, C., 1999. Allometric scaling of RNA, DNA, and enzyme levels: an intraspecific study. American Journal of Physiology 277, R1164.

Chen, C.R., Makhatadze, G.I., 2017. Molecular determinant of the effects of hydrostatic pressure on protein folding stability. Nature Communications 8, 1–9. (doi:10.1038/ncomms14561)

Childress, J., 1995. Are there physiological and biochemical adaptations of metabolism in deep-sea animals? Trends in Ecology and Evolution 10, 30–6. (doi:10.1016/S0169-5347(00)88957-0)

Childress, J., Somero, G., 1990. Metabolic Scaling: A new perspective based on scaling of glycolytic enzyme activities. American Zoologist 30, 161–173. (doi:10.1093/icb/30.1.161)

Childress, J., Somero, G., 1979. Depth-related enzymic activities in muscle, brain and heart of deep-living pelagic marine teleosts. International Journal on Life in Oceans and Coastal Waters 52, 273–283. (doi:10.1007/BF00398141)

Childress, J.J., Thuesen, E. V, 1992. Metabolic potential of deep-sea animals: Regional and global scales. Deep-Sea Food Chains and the Global Carbon Cycle 217–236. (doi:10.1007/978-94-011-2452-2_13)

Condon, N., Friedman, J., Drazen, J., 2012. Metabolic enzyme activities in shallow- and deep-water chondrichthyans: implications for metabolic and locomotor capacity. Marine Biology 159, 1713–1731. (doi:10.1007/s00227-012-1960-3)

Dahlhoff, E., 2004. Biochemical indicators of stress and metabolism: applications for marine ecological studies. Annual Review of Physiology 66, 183–207. (doi:10.1146/annurev.physiol.66.032102.114509)

Dahlhoff, E., Schneidemann, S., Somero, G., 1990. Pressure-temperature interactions on M4-lactate dehydrogenases from hydrothermal vent fishes: Evidence for adaptation to elevated temperatures by the Zoarcid *Thermarces andersoni*, but not by the Bythitid, *Bythites hollisi*. Biological Bulletin 179, 134–139. (doi:10.2307/1541747)

Dahlhoff, E., Somero, G., 1991. Pressure and temperature adaptation of cytosolic malate-dehydrogenases of shallow-living and deep-living marine-invertebrates—evidence for high body temperatures in hydrothermal vent animals. Journal of Experimental Biology 159, 473–487.

Danovaro, R., Della Croce, N., Dell'Anno, A., Pusceddu, A., 2003. A depocenter of organic matter at 7800 m depth in the SE Pacific Ocean. Deep-Sea Research Part I: Oceanographic Research Papers 50, 1411–1420. (doi:10.1016/j.dsr.2003.07.001)

Danovaro, R., Gambi, C., Della Croce, N., 2002. Meiofauna hotspot in the Atacama Trench, eastern South Pacific Ocean. Deep-Sea Research Part I: Oceanographic Research Papers 49, 843–857. (doi:10.1016/S0967-0637(01)00084-X)

De Leo, F., Smith, C., Rowden, A., Bowden, D., Clark, M., 2010. Submarine canyons: hotspots of benthic biomass and productivity in the deep sea. Proceedings of the Royal Society B: Biological Sciences 277, 2783–92. (doi:10.1098/rspb.2010.0462)

Dickson, K., Gregorio, M., Gruber, S., Loefler, K., Tran, M., Terrell, C., 1993. Biochemical indices of aerobic and anaerobic capacity in muscle tissues of California elasmobranch fishes differing in typical activity level. International Journal on Life in Oceans and Coastal Waters 117, 185–193. (doi:10.1007/BF00345662)

Drazen, J., Yeh, J., 2012. Respiration of four species of deep-sea demersal fishes measured *in situ* in the eastern North Pacific. Deep-Sea Research Part I: Oceanographic Research Papers 60, 1–6. (doi:10.1016/j.dsr.2011.09.007)

Drazen, J.C., Friedman, J.R., Condon, N.E., Aus, E.J., Gerringer, M.E., Keller, A. A., Elizabeth Clarke, M., 2015. Enzyme activities of demersal fishes from the shelf to the abyssal plain. Deep-Sea Research Part I: Oceanographic Research Papers 100, 117–126. (doi:10.1016/j.dsr.2015.02.013)

Dutil, J., Lambert, Y., Guderley, H., Blier, P.U., Pelletier, D., Desroches, M., 1998. Nucleic acids and enzymes in Atlantic cod (*Gadus morhua*) differing in condition and growth rate trajectories. Canadian Journal of Fisheries and Aquatic Sciences 55, 788–795. (doi:10.1139/f97-294)

Eisenmenger, M.J., Reyes-De-Corcuera, J.I., 2009. High pressure enhancement of enzymes: A review. Enzyme and Microbial Technology 45, 331–347. (doi:10.1016/j.enzmictec.2009.08.001)

Friedman, J., Condon, N., Drazen, J., 2012. Gill surface area and metabolic enzyme activities of demersal fishes associated with the oxygen minimum zone off California. Limnology and Oceanography 57, 1701–1710. (doi:10.4319/lo.2012.57.6.1701)

Gelpi, J., Dordal, A., Mazo, A., Cortes, A., 1992. Kinetic studies of the regulation of mitochondrial malate dehydrogenase by citrate. Biochemical Journal 283, 289–297. (doi:10.1042/bj2830289)

George, R., Higgins, R., 1979. Eutrophic hadal benthic community in the Puerto Rico Trench. Ambio Special Reports 51–58.

Gerringer, M.E., Popp, B.N., Linley, T.D., Jamieson, A.J., Drazen, J.C., 2017. Comparative feeding ecology of abyssal and hadal fishes through stomach content and amino acid isotope analysis. Deep-Sea Research Part I: Oceanographic Research Papers 121, 110–120. (doi:10.1016/j.dsr.2017.01.003)

Gharib, G., Rashid, N., Bashir, Q., Afza, A., 2016. Pcal _ 1699, an extremely thermostable malate dehydrogenase from hyperthermophilic archaeon *Pyrobaculum calidifontis*. Extremophiles 20, 57–67. (doi:10.1007/s00792-015-0797-3)

Gibb, A., Dickson, K., 2002. Functional morphology and biochemical indices of performance: Is there a correlation between metabolic enzyme activity and swimming performance? Integrative and Comparative Biology 42, 199–207. (doi:10.1093/icb/42.2.199)

Glud, R., Wenzhöfer, F., Middelboe, M., Oguri, K., Turnewitsch, R., Canfield, D., Kitazato, H., 2013. High rates of microbial carbon turnover in sediments in the deepest oceanic trench on Earth. Nature Geoscience 6, 284–288. (doi:10.1038/NGEO1773)

Hennessey, J., Siebenaller, J., 1985. Pressure inactivation of tetrameric lactate dehydrogenase homologues of confamilial deep-living fishes. Biochemical, Systems, and Environmental Physiology 155, 647–652. (doi:10.1007/BF00694577)

Hickey, A., Clements, K., 2003. Key metabolic enzymes and muscle structure in triplefin fishes (Tripterygiidae): a phylogenetic comparison. Journal of Comparative Physiology B 173, 113–23. (doi:10.1007/s00360-002-0313-9)

Hughes, S., Ruhl, H., Hawkins, L., Hauton, C., Boorman, B., Billett, D., 2011. Deep-sea echinoderm oxygen consumption rates and an interclass comparison of metabolic rates in Asteroidea, Crinoidea, Echinoidea, Holothuroidea and Ophiuroidea. Journal of Experimental Biology 214, 2512–21. (doi:10.1242/jeb.055954)

Ichino, M.C., Clark, M.R., Drazen, J.C., Jamieson, A., Jones, D.O.B., Martin, A.P., Rowden, A.A., Shank, T.M., Yancey, P.H., Ruhl, H.A., 2015. The distribution of benthic biomass in hadal trenches: A modelling approach to investigate the effect of vertical and lateral organic matter transport to the sea floor. Deep-Sea Research Part I: Oceanographic Research Papers 100, 21–33. (doi:10.1016/j.dsr.2015.01.010)

Itoh, M., Kawamura, K., Kitahashi, T., Kojima, S., Katagiri, H., Shimanaga, M., 2011. Bathymetric patterns of meiofaunal abundance and biomass associated with the Kuril and Ryukyu trenches, western North Pacific Ocean. Deep-Sea Research Part I: Oceanographic Research Papers 58, 86–97. (doi:10.1016/j.dsr.2010.12.004)

Itou, M., Matsumura, I., Noriki, S., 2000. A large flux of particulate matter in the deep Japan Trench observed just after the 1994 Sanriku-Oki earthquake. Deep-Sea Research Part I: Oceanographic Research Papers 47, 1987–1998. (doi:10.1016/S0967-0637(00)00012-1)

Jamieson, A.J., 2015. The hadal zone: life in the deepest oceans. Cambridge, United Kingdom.

Jamieson, A., Fujii, T., Mayor, D., Solan, M., Priede, I., 2010. Hadal trenches: the ecology of the deepest places on Earth. Trends in Ecology and Evolution 25, 190–7. (doi:10.1016/j.tree.2009.09.009)

Jamieson, A., Kilgallen, N., Rowden, A., Fujii, T., Horton, T., Lörz, A.-N., Kitazawa, K., Priede, I., 2011. Bait-attending fauna of the Kermadec Trench, SW Pacific Ocean: Evidence for an ecotone across the abyssal–hadal transition zone. Deep-Sea Research Part I: Oceanographic Research Papers 58, 49–62. (doi:10.1016/j.dsr.2010.11.003)

Kobayashi, H., Hatada, Y., Tsubouchi, T., Nagahama, T., Takami, H., 2012. The hadal amphipod *Hirondellea gigas* possessing a unique cellulase for digesting wooden debris buried in the deepest seafloor. PLoS One 7, e42727. (doi:10.1371/journal.pone.0042727)

Linley, T.D., Gerringer, M.E., Yancey, P.H., Drazen, J.C., Weinstock, C.L., Jamieson, A.J., 2016. Fishes of the hadal zone including new species, *in situ* observations and depth records of Liparidae. Deep-Sea Research Part I: Oceanographic Research Papers 114, 99–110. (doi:http://dx.doi.org/10.1016/j.dsr.2016.05.003)

Linley, T.D., Steward, A.L., McMillan, P.J., Clark, M.R., Gerringer, M.E., Drazen, J.C., Fujii, T., Jamieson, A.J., 2017. Bait-attending fishes of the abyssal zone and hadal boundary: Community structure, functional groups and species distribution in the Kermadec, New Hebrides, and Mariana trenches. Deep-Sea Research Part I: Oceanographic Research Papers 121, 38–53. (doi:10.1016/j.dsr.2016.12.009)

Longhurst, A., Sathyendranath, S., Platt, T., Caverhill, C., 1995. An estimate of global primary production in the ocean from satellite radiometer data. Journal of Plankton Research 17, 1245–1271. (doi:10.1093/plankt/17.6.1245)

Luong, T.Q., Winter, R., 2015. Combined pressure and cosolvent effects on enzyme activity—a high-pressure stopped-flow kinetic study on α-chymotrypsin. Physical Chemistry Chemical Physics 17(35), 23273–8. (doi:10.1039/C5CP03529E)

Macdonald, A., 1997. Hydrostatic pressure as an environmental factor in life processes. Comparative Biochemistry and Physiology 116, 291–297. (doi:10.1016/S0300-9629(96)00354-4)

Martínez, M., Dutil, J.D., Guderley, H., 2000. Longitudinal and allometric variation in indicators of muscle metabolic capacities in atlantic cod (*Gadus morrhua*). Journal of Experimental Zoology 287, 38–45. (doi:10.1002/1097-010X(20000615)287:1<38::AID-JEZ5>3.0.CO;2-V)

Martínez, M., Guderley, H., Dutil, J.-D., Winger, P.D., He, P., Walsh, S.J., 2003. Condition, prolonged swimming performance and muscle metabolic capacities of cod *Gadus morhua*. Journal of Experimental Biology 206, 503–511. (doi:10.1242/jeb.00098)

Moon, T.W., Mustafa, T., Hochachka, P.W., 1971a. The adaptation of enzymes to pressure part II: A comparison of muscle pyruvate kinases from surface and mid water fishes with the homologous enzyme from an off shore benthic species. American Zoologist 11, 491–502. (doi:10.1093/icb/11.3.491)

Moon, T.W., Mustafa, T., Hochachka, P.W., 1971b. Effects of hydrostatic pressure on catalysis by different lactate dehydrogenase isozymes from tissues of an abyssal fish. American Zoologist 11, 473–478. (doi:10.1093/icb/11.3.473)

Moon, T.W., Mustafa, T., Hochachka, P.W., 1971c. Effects of hydrostatic pressure on catalysis by epaxial muscle phosphofructokinase from an abyssal fish. American Zoologist 11, 467–471. (doi:10.1093/icb/11.3.467)

Moyes, C., Mathieu-Costello, O., Brill, R., Hochachka, P., 1992. Mitochondrial metabolism of cardiac and skeletal muscles from a fast (*Katsuwonus pelamis*) and a slow (*Cyprinus carpio*) fish. Canadian Journal of Zoology 70, 1246–1253. (doi:10.1139/z92-172)

Mozhaev, V. V, Heremans, K., Frank, J., Masson, P., Balny, C., 1996. High pressure effects on protein structure and function. Proteins 24, 81–91. (doi:10.1002/(SICI)1097-0134(199601)24:1<81::AID-PROT6>3.0.CO;2-R)

Mustafa, T., Moon, T.W., Hochachka, P.W., 1971. Effects of pressure and temperature on the catalytic and regulatory properties of muscle pyruvate kinase from an off-shore benthic fish. American Zoologist 11, 451–466. (doi:10.1093/icb/11.3.451)

Neuheimer, A., Taggart, C., 2007. The growing degree-day and fish size-at-age: the overlooked metric. Canadian Journal of Fisheries and Aquatic Science 64, 375–385. (doi:10.1139/f07-003)

Nilsson, K., Ekstrand, B., 1993. The effect of storage on ice and various freezing treatments on enzyme leakage in muscle tissue of rainbow trout (*Oncorhynchus mykiss*). Zeitschrift für Lebensmittel-Untersuchung und -Forschung. 197, 3–7. (doi:10.1007/BF01202691)

Oguri, K., Kawamura, K., Sakaguchi, A., Toyofuku, T., Kasaya, T., Murayama, M., Fujikura, K., Glud, R., Kitazato, H., 2013. Hadal disturbance in the Japan Trench induced by the 2011 Tohoku-Oki earthquake. Scientific Reports 3, 1915. (doi:10.1038/srep01915)

Ombres, E., Donnelly, J., Clarke, M., Harms, J., Torres, J., 2011. Aerobic and anaerobic enzyme assays in Southern California Rockfish: Proxies for physiological and ecological data. Journal of Experimental Marine Biology and Ecology 399, 201–207. (doi:10.1016/j.jembe.2010.11.007)

Pequeux, A., 1980. Effects of high pressure on ion transport and osmoregulation, in: Ali, M.A. Mohamed A., Montréal, U. (Eds.), Environmental Physiology of Fishes. New York: Plenum Press, New York.

Saavedra, L.M., Quiñones, R.A., Gonzalez-Saldía, R.R., Niklitschek, E.J., 2015. Aerobic and anaerobic enzymatic activity of orange roughy (*Hoplostethus atlanticus*) and alfonsino (*Beryx splendens*) from the Juan Fernandez seamounts area. Fish Physiology and Biochemistry 42(3), 869–82. (doi:10.1007/s10695-015-0181-3)

Seibel, B., Drazen, J., 2007. The rate of metabolism in marine animals: environmental constraints, ecological demands and energetic opportunities. Philosophical Transactions of the Royal Society B 362, 2061–78. (doi:10.1098/rstb.2007.2101)

Siebenaller, J., Somero, G., 1979. Pressure-adaptive differences in the binding and catalytic properties of muscle-type (M_4) lactate dehydrogenases of shallow- and deep-living marine fishes. Journal of Comparative Physiology 129, 295–300. (doi:10.1007/BF00686984)

Siebenaller, J., Somero, G., Haedrich, R., 1982. Biochemical characteristics of macrourid fishes differing in their depths of distribution. Biological Bulletin 163, 240–249. (doi:10.2307/1541512)

Siebenaller, J., Yancey, P., 1984. Protein composition of white skeletal muscle from mesopelagic fishes having different water and protein contents. International Journal on Life in Oceans and Coastal Waters 78, 129–137. (doi:10.1007/BF00394692)

Siebenaller, J.F., 1984. Structural comparison of lactate dehydrogenase homologs differing in sensitivity to hydrostatic pressure. Biochimica et Biophysica Acta 786, 161. (doi:10.1016/0167-4838(84)90085-2)

Singh, S., Kanugo, M., 1969. Alterations in lactate dehydrogenase of the brain, heart, skeletal muscle, and liver of rats of various ages. Journal of Biochemistry 243, 4526–4529.

Smith, K.L., White, G.A., Laver, M.B., Haugsness, J.A., 1978. Nutrient exchange and oxygen consumption by deep-sea benthic communities: Preliminary *in situ* measurements. Limnology and Oceanography 23, 997–1005. (doi:10.4319/Io.1978.23.5.0997)

Somero, G., 1992. Adaptations to high hydrostatic pressure. Annual Reviews in Physiology 54, 557–577. (doi:10.1146/annurev.ph.54.030192.003013)

Somero, G., Childress, J., 1980. A violation of the metabolism-size scaling paradigm: Activities of glycolytic enzymes in muscle increase in larger-size fish. Physiological Zoology 53, 322–337. (doi:10.1086/physzool.53.3.30155794)

Somero, G.N., Siebenaller, J.F., 1979. Inefficient lactate dehydrogenases of deep-sea fishes. Nature 282, 100. (doi:10.1038/282100a0)

Srere, P., 1969. Citrate synthase:[EC 4.1.3.7. Citrate oxaloacetate-lyase (CoA-acetylating)]: [EC 4.1.3.7. Citrate oxaloacetate-lyase (CoA-acetylating)]. Methods in Enzymology 13, 3–11. (doi:10.1016/0076-6879(69)13005-0)

Sullivan, K., Somero, G., 1980. Enzyme activities of fish skeletal muscle and brain as influenced by depth of occurrence and habits of feeding and locomotion. International Journal on Life in Oceans and Coastal Waters 60, 91–99. (doi:10.1007/BF00389152)

Sullivan, K.M., Smith, K.L., 1982. Energetics of sablefish, *Anoplopoma fimbria*, under laboratory conditions. Canadian Journal of Fisheries and Aquatic Sciences 39, 1012–1020. (doi:10.1139/f82-136)

Sullivan, K.M., Somero, G.N., 1983. Size- and diet-related variations in enzymic activity and tissue composition in the sablefish, *Anoplopoma fimbria*. Biological Bulletin 164, 315–326. (doi:10.2307/1541147)

R Core Development Team, 2015. R: A Language and Environment for Statistical Computing. R Found. Stat. Comput. Vienna, Au.

Thuesen, E., Childress, J., 1993. Metabolic rates, enzyme activities, and chemical compositions of some deep-sea pelagic worms, particularly *Nectonemertes mirabilis* (Nemertea). Deep-Sea Research Part I: Oceanographic Research Papers 40, 937–951. (doi:10.1016/0967-0637(93)90082-E)

Torres, J., Grigsby, M., Clarke, M., 2012. Aerobic and anaerobic metabolism in oxygen minimum layer fishes: the role of alcohol dehydrogenase. Journal of Experimental Biology 215, 1905–14. (doi:10.1242/jeb.060236)

Turnewitsch, R., Falahat, S., Stehlikova, J., Oguri, K., Glud, R.N., Middelboe, M., Kitazato, H., Wenzhöfer, F., Ando, K., Fujio, S., Yanagimoto, D., 2014. Recent sediment dynamics in hadal trenches: Evidence for the influence of higher-frequency (tidal, near-inertial) fluid dynamics. Deep-Sea Research Part I: Oceanographic Research Papers 90, 125–138. (doi:10.1016/j.dsr.2014.05.005)

Vetter, R., Lynn, E., 1997. Bathymetric demography, enzyme activity patterns, and bioenergetics of deep-living scorpaenid fishes (genera *Sebastes* and *Sebastolobus*): paradigms revisited. Marine Ecology Progress Series 155, 173–188. (doi:10.3354/meps155173)

Watling, L., Guinotte, J., Clark, M.R., Smith, C.R., 2013. A proposed biogeography of the deep ocean floor. Progress in Oceanography 111, 91–112. (doi:10.1016/j.pocean.2012.11.003)

Wenzhöfer, F., Oguri, K., Middelboe, M., Turnewitsch, R., Toyofuku, T., Kitazato, H., Glud, R.N., 2016. Benthic carbon mineralization in hadal trenches: Assessment by *in situ* O_2 microprofile measurements. Deep-Sea Research Part I: Oceanographic Research Papers 116, 276–286. (doi:10.1016/j.dsr.2016.08.013)

Wickam, H., 2009. ggplot2: elegant graphics for data analysis.

Wolff, T., 1970. The concept of the hadal or ultra-abyssal fauna. Deep-Sea Research and Oceanographic Abstracts 17, 983–1003. (doi:10.1016/0011-7471(70)90049-5)

Yancey, P., Fyfe-Johnson, A., Kelly, R., Walker, V., Aunon, M., 2001. Trimethylamine oxide counteracts effects of hydrostatic pressure on proteins of deep-sea teleosts. Journal of Experimental Zoology 289, 172–176. (doi:10.1002/1097-010X(20010215)289:3<172::AID-JEZ3>3.0.CO;2-J)

Yancey, P., Gerringer, M., Drazen, J., Rowden, A., Jamieson, A., 2014. Marine fish may be biochemically constrained from inhabiting the deepest ocean depths. Proceedings of the National Academy of Sciences U. S. A. 111, 4461–5. (doi:10.1073/pnas.1322003111)

Yancey, P., Somero, G., 1978. Temperature dependence of intracellular pH: Its role in the conservation of pyruvate apparent K_m values of vertebrate lactate dehydrogenases. Journal of Comparative Physiology 125, 129–134. (doi:10.1007/BF00686748)

Yancey, P.H., Rhea, M.D., Kemp, K.M., Bailey, D.M., 2004. Trimethylamine oxide, betaine and other osmolytes in deep-sea animals: Depth trends and effects on enzymes under hydrostatic pressure. Cellular and Molecular Biology 50, 371–376.

Yang, T., Somero, G., 1993. Effects of feeding and food deprivation on oxygen consumption, muscle protein concentration and activities of energy metabolism enzymes in muscle and brain of shallow-living (*Scorpaena guttata*) and deep-living (*Sebastolobus alascanus*) scorpaenid fishes. Journal of Experimental Biology 181, 213–232.

CHAPTER IV

Life history of abyssal and hadal fishes from otolith growth zones and oxygen isotope

Abstract

Hadal trenches are isolated habitats that cover the greatest ocean depths (6,500–11,000 m) and are believed to host high levels of endemism across multiple taxa. A group of apparent hadal endemics is within the snailfishes (Liparidae), found in at least five geographically separated trenches. Little is known about their biology, let alone the reasons for their success at hadal depths around the world. This study investigated the life history of hadal liparids using sagittal otoliths of two species from the Kermadec (*Notoliparis kermadecensis*) and Mariana trenches (Liparidae sp. nov.) in comparison to successful abyssal macrourids found at the abyssal-hadal transition zone. Otoliths for each species revealed alternating opaque and translucent growth zones that could be quantified in medial sections. Assuming these annuli represent annual growth, ages were estimated for the two hadal liparid species to be from 5 to 16 years old. These estimates were compared to the shallower-living snailfish *Careproctus melanurus*, which were older than described in previous studies, expanding the potential maximum age for the liparid family to near 25 years. Age estimates for abyssal macrourids ranged from 8 to 29 years for *Coryphaenoides armatus* and 6 to 16 years old for *C. yaquinae*. In addition, $^{18}O/^{16}O$ ratios ($\delta^{18}O$) were measured across the otolith using an ion microprobe to investigate the thermal history of the three liparids, and two macrourids. Changes in $\delta^{18}O$ values were observed across the otoliths of *C. melanurus*, *C. armatus*, and both hadal liparids, the latter of which may represent a change of >5°C in habitat temperature through ontogeny. The results indicated there is a pelagic larval stage for the hadal liparids that rises to a depth above 1000 m, followed by a return to the hadal environment as these liparids grow. This result was unexpected for the hadal liparids given their isolated environment and large eggs. This study presents a first look at the life history of some of the deepest-living fishes though otolith analyses.

Introduction

Hadal trenches cover the greatest ocean depths (6,500–11,000 m) and have a distinct fauna from the surrounding deep-sea environment with high apparent levels of endemism (Wolff, 1959; Beliaev, 1989; Jamieson, 2015). A characteristic and charismatic endemic group known as the snailfishes (Family Liparidae) are prominent members of the hadal community in at least five widely-distributed trenches (Japan, Kermadec, Kurile-Kamchatka, Mariana, and Peru-Chile; Nielsen, 1964; Jamieson et al., 2009; Fujii et al., 2010; Linley et al., 2016). These hadal fishes are notably different from common abyssal species that border the hadal zone in both form and functional role. Hadal liparids have small, translucent bodies and appear to be specialized predators (Linley et al., 2017; Gerringer et al., 2017; **Chapter II**). In contrast, characteristic abyssal species such as macrourids have dark coloring and opaque tissues and are generalized benthopelagic predators and scavengers (e.g., Drazen et al. 2008). Observations of large aggregations of these snailfishes that are similar in form, at similar depths, and yet widely dispersed geographically in the seemingly isolated hadal systems, frames the question—why are liparids so successful in the hadal zone?

A recent and unprecedented collection of otoliths (small aragonitic ear bones; Degens et al., 1969) from hadal snailfishes provided an opportunity to investigate the life history of the deepest dwelling fishes. Otoliths have long been used in fish ecology for age estimation because they usually form annual growth rings (Jackson 2007). Age, growth, and longevity are traditionally estimated using whole or sectioned otoliths where putative annual growth zones are counted (e.g., Williams and Bedford, 1974). This technique has been applied to fishes from habitats as deep as ~3,900 meters (Wilson, 1988). Some otolith age estimates indicate that deep dwelling fishes may live longer than shallow living congeners and have raised the question of whether the trend can be applied to similar circumstances and species in the deep sea (Cailliet et al., 2001). Although the simple older-deeper dichotomy has been called into question, the idea remains (Drazen and Haedrich, 2012). The factors driving depth-related longevity are complicated and may be related to phylogeny, temperature, pressure, oxidative stress, and food availability, among other factors (Cailliet et al., 2001; Drazen and Haedrich, 2012).

In this study, two main life history hypotheses that may factor into the success of liparids near the greatest ocean depths are investigated. First, hadal liparids may be suited to the high-disturbance environment of hadal trenches, which are located primarily at subduction zones, due to shorter lifespans than groups living on the abyssal plain. Due to the small size of the hadal liparid otoliths (<1 mm) and the general paucity of data on snailfish age and growth (Falk-Petersen et al., 1988; Orlov and Tokranov, 2011), otoliths of a shallower, common deep-sea liparid *Careproctus melanurus* were investigated. These larger snailfish otoliths allowed the development of a sectioning and age estimation protocol for the family before conducting age estimation on the rare hadal otolith collection. To provide additional context and test whether the deeper-older trend applies in other fish orders, we examined growth patterns in *Coryphaenoides armatus* and *C. yaquinae*, which are common deep-abyssal and upper-hadal species (e.g., Linley et al., 2017).

The second hypothesis is that hadal snailfishes do not have a long-range dispersal mechanism that transports larvae out of the trench. Macrourids and many other deep-sea fishes have numerous small eggs and pelagic larvae, some of which occur in the epipelagic (Stein, 1980; Merrett and Haedrich, 1997; Busby, 2005). In contrast, members of the Liparidae are known to brood, and to have very large eggs (Stein, 1980) and in some cases, have complex developmental strategies; most notably carcinophyly, whereby they deposit eggs in the gills of lithodid crabs (Yau et al., 2000; Poltev and Steksova, 2010), and even spawn in crab traps (Poltev and Steksova, 2010). In addition, based on the relatively low number of large eggs found in *Notoliparis kermadecensis* (Nielsen, 1964), we expected that larvae and juveniles of snailfishes would remain localized in the trench environment to increase survivorship. These factors of low fecundity, high parental investment, and an apparent lack of pelagic life history stages may have allowed for the radiation of the group into the hadal zone.

Otolith microchemistry provides an opportunity to test both hypotheses regarding early life history. In addition to their value in age estimation, otoliths can incorporate chemical signatures from the environment that provide clues to their life history (Campana and Neilson, 1985; Campana and Thorrold, 2001; Trueman et al., 2012). By comparing how chemical signatures change through the growth of the otolith, it is possible to determine if the fish experienced environmental temperature changes over its lifespan, even with low sample sizes (Trueman et al., 2013). In the case of hadal and abyssal fishes, this is a valuable source of information, because

direct observations of these fishes are brief, opportunistic, and historically rare. As otoliths grow in a sequence of deposited rings, their chemical composition reflects the nature of the environment at time of deposition (Kalish, 1991; 1989). Oxygen isotope ratios in the otoliths change as a function of temperature, allowing thermal history reconstruction (e.g., Kozdon et al., 2011; 2013; Olson et al., 2012; Befus, 2016). Thus, the ratios of $^{18}O/^{16}O$ can be used to calculate habitat temperatures across a fish's life (Thorrold et al., 1997), to within 1°C precision at a 95% probability level (Høie et al., 2004). Generally, lower $\delta^{18}O$ values indicate higher temperatures at the time of deposition, due to thermodynamic effects on isotope fractionation. Changes across an otolith are often indicative of an ontogenetic vertical migration or shallow-living planktonic larval stage, and this technique has been used to determine the thermal histories of a number of deep-sea species including slickheads (Shiao et al., 2016), rattails (Lin et al., 2012), cusk eels (Chang et al., 2015), and cutthroat eels (Shiao et al., 2014).

This study aimed to 1) estimate age in hadal snailfishes and abyssal macrourids by counting otolith growth zones; 2) construct ontogenetic temperature profiles to investigate life history through oxygen isotope analysis along the growth axis of otoliths for each species; and 3) discuss the role of life history and growth in driving community structure and endemism in fishes of the hadal zone. We provide a first look at the life history of some of the planet's deepest-living fishes to inform discussions of hadal endemism and depth-related trends in growth and longevity.

Materials & Methods

Otoliths from three liparid and two macrourid species were investigated for age and growth. Sagittal otoliths were extracted from 38 *Notoliparis kermadecensis* specimens collected in April-May of 2014 and from 28 specimens of a new liparid species from the Mariana Trench, collected in November-December of 2014. The new species is currently being described and is hereafter referred to as the Mariana liparid. Sampling and collection details for both trench locations are provided elsewhere (Linley et al., 2016). Extracted otoliths were initially placed in 75% ethanol and later cleaned and air-dried for storage in 2 mL cryovials. An age estimation protocol for hadal liparids was developed using a confamilial reference species that has more massive otoliths, *Careproctus melanurus*. The 29 *Careproctus melanurus* specimens were collected in the Southern

California Bight by trawl in 2013–2015 (**Supplementary Table 4.1**). Fish were frozen whole at sea and otoliths were extracted after thawing in the laboratory. *Careproctus melanurus* otoliths were washed in 50% bleach solution to remove remaining tissue, rinsed in deionized water, and then dried. Age estimates for two abyssal macrourids, *Coryphaenoides armatus* and *C. yaquinae*, were made from archived otoliths collected from Station M in 1995–1998 (collection details in Drazen, 2002). Total fish mass and standard length were measured at sea on freshly collected specimens for the hadal collections. For the abyssal macrourids, total fish mass was measured in the lab for frozen specimens, and total, head, and pre-anal fin lengths were measured at sea. Sex was determined macroscopically. Hadal otoliths were weighed in the lab using a microbalance (±0.0001 mg precision). Otolith dimensions were measured using fine scale calipers (0.01 mm). Length and width were digitally measured for the hadal liparid otoliths using ImageJ (Schneider et al., 2012).

Age Estimation. The *C. melanurus* otoliths were first polished in the medial plane sulcus-side down by hand. The polished side was mounted on glass slides with resin (Cytoseal 60, Richard-Allan Scientific). The resin cured overnight and the other side of the otolith was polished using an Isomet lapping wheel (SBT, Model 900) with 600-grit wet-dry carbide paper (Buehler). The end result revealed growth ring structure across a medial section. Fine polishing was done by hand as needed with diamond lapping film. Success with this approach led to use of the method for the hadal specimens. For the much smaller hadal liparid otoliths, polishing was done in a similar manner to reveal a medial section, but polishing was performed entirely by hand on a smooth glass panel using 6 and 9 µm diamond lapping film (Buehler). Otoliths from *Coryphaenoides armatus* and *C. yaquinae* were cut in the transverse plane to 0.6 mm sections using an Isomet low-speed saw (Buehler), then mounted and polished using the lapping wheel method described above. Otolith sections were aged by two readers (Gerringer, Andrews) and initial estimates were based on various interpretations of the concentric growth zone structure. Refined criteria were determined based on well-defined sections for each species and an examination of length-at-age relationships (irregular patterns pointed to alternative counting criteria). The counting protocol for both abyssal macrourids here followed that detailed by Andrews et al. (1999a) for *Coryphaenoides acrolepis*. Although the importance of age estimate validation is recognized (e.g., Campana, 2001),

none of the currently available methods for validation were practical for these species and the counts presented here were assumed to be annual (Morales-Nin and Panfili, 2005).

Thermal History Reconstruction. Otoliths were cleaned in methanol and cast in epoxy (Epoxicure, Buehler, Lake Bluff, IL, USA) in stainless steel bullets (liparids) and aluminum rings (macrourids). These were heated to 80°C to remove excess moisture and desiccated in a vacuum chamber for ~30 seconds before curing at 50°C overnight. Samples were polished to reveal the core using a series of grinding papers and diamond lapping films (Buehler 240, 400, 600 grit; 15, 9, 6, 3, 1, and 0.5 μm). Polished sections were sonicated in methanol, dried, and carbon coated (~250 Å, Cressington Carbon Coater, 208carbon, Watford, UK), then inspected visually with optical microscopy and scanning electron microscopy (SEM; JEOL JSM-5900LV, USA). Oxygen-isotope compositions across the otolith were measured using an ion microprobe (Cameca ims-1280, University of Hawai‘i at Mānoa, W.M. Keck Research Laboratory). For each measurement, the carbon coat was removed with the application of a 2.5 nA Cs^+ primary ion beam, rastered over a 25 x 25 μm^2 area for 120 seconds presputtering. For data collection, the raster size was reduced to 15 x 15 μm^2. Each measurement consisted of 30 cycles with 10 seconds' integration time per cycle. The automatic beam centering routine was applied. A normal incidence electron flood gun was used for charge compensation in an analyzed area. The two oxygen ions, $^{16}O^-$ and $^{18}O^-$, were measured in multicollection mode using two Faraday cups with 10^{10} and 10^{11} ohm registers, respectively. The magnetic field was regulated using a nuclear magnetic resonance controller. Mass resolving power was ~2,000, enough to discriminate interference ions. Carbonate reference materials (University of Wisconsin Calcite, UWC 1 and UWC 3) were used to determine instrumental isotope fractionation corrections. Although the otoliths are probably aragonite, a different polymorph, the difference in oxygen isotope measurements between calcite and aragonite is likely small (Matta et al., 2013) and no correction was applied in the present study. Data are reported as δ values in parts per thousand (permil; ‰) relative to Vienna Standard Mean Ocean Water (VSMOW):

$$\delta^{18}O = (((^{18}O/^{16}O)_{sample}/(^{18}O/^{16}O)_{VSMOW})-1)*1000$$

Reproducibilities (2σ) in calcite reference material measurements were 0.15‰) for UWC 1 and 0.15 to 0.17‰ for UWC 3. Measurement errors are given as 2σ and reflect both the measurement precision (2 standard error) for each analysis and the reproducibility (2 standard deviation) of standard measurements on the analysis day. Measurement spots were then inspected via SEM to ensure quality of the reading. Measurements taken on rough surfaces or those with large visible cracks were discarded and those with potential small scratches were noted. Values were measured relative to VSMOW (Vienna standard mean ocean water), and then converted to VPDB (Vienna Pee Dee Belemnite) based on true ratios. These converted values are compared to those yielded by the Coplen et al. (1983) equation (below) that has usually been employed with this technique (e.g., Høie et al., 2004).

$$\delta^{18}O_{VSMOW} = 1.03091 \cdot \delta^{18}O_{VPDB} + 30.91‰ \qquad \text{(Coplen et al., 1983)}$$

$$\alpha = \frac{\delta^{18}O_{otolith} + 1000}{\delta^{18}O_{seawater} + 1000}$$

$$1000 \ln \alpha = 16.75 \left(\frac{1000}{T}\right) - 27.09 \qquad \text{(Høie et al., 2004)}$$

Habitat temperatures were calculated from $\delta^{18}O$ values (‰ vs. VPDB) according to the equations presented by Høie et al. (2004) and reproduced above. Temperature (*T*) was calculated in Kelvin and was converted to °C. Local data on habitat temperatures at collection depth were recorded by free-vehicle lander for the abyssal and hadal species (described Linley et al., 2016) and by CTD at the collection site for *C. melanurus*. Temperature profiles for *C. melanurus* were extracted from the World Ocean Database (WOD; Boyer et al., 2013; Locarnini et al., 2013) for locations within 0.1 degree of capture site in May and October from two CTD casts (WOD unique ID numbers 8531355 and 8531681). Due to the lack of environmental data at deep abyssal and hadal depths, $\delta^{18}O$ values of seawater were calculated according to the outermost measurements taken from each otolith, which were presumed to reflect the known capture temperature. This manner of calibrating temperature estimates is generally considered accurate to within ±1°C (Thorrold et al., 1997; Høie et al., 2004). Based on instrumental reproducibility of UWC 1 and UWC 3 measurements and

within-sample measurement variation, temperature error (2σ) in the dataset was between ±0.8 and ±2.5°C (mean ±1.6°C).

Data analyses for both age estimation and thermal history reconstruction were conducted using the statistical programming platform R (R Core Development Team, 2015) and figures were generated using the package *ggplot2* (Wickam, 2009). Tentative von Bertalanffy growth functions were fitted to length-at-age data using the package *fishmethods* (Nelson, 2016), considering the recommendations of Pardo et al. (2013) anchored at zero due to there being few juveniles and limited sample sizes in the collections.

Results

Age Estimation: *Careproctus melanurus.* Twenty-nine *C. melanurus* specimens spanned 11.8 to 21.8 cm standard length and body masses from 8.1 to 139.5 grams (**Supplementary Table 4.1**). There were eighteen female, six male, and five unsexed individuals collected from depths of 340–841 m. Otolith mass was between 1.352 and 6.240 mg and dimensions were 1.65–2.72 mm in length, 1.98–3.14 mm in width, and 0.6–1.1 mm in height (otoliths shown in **Figure 4.1**).

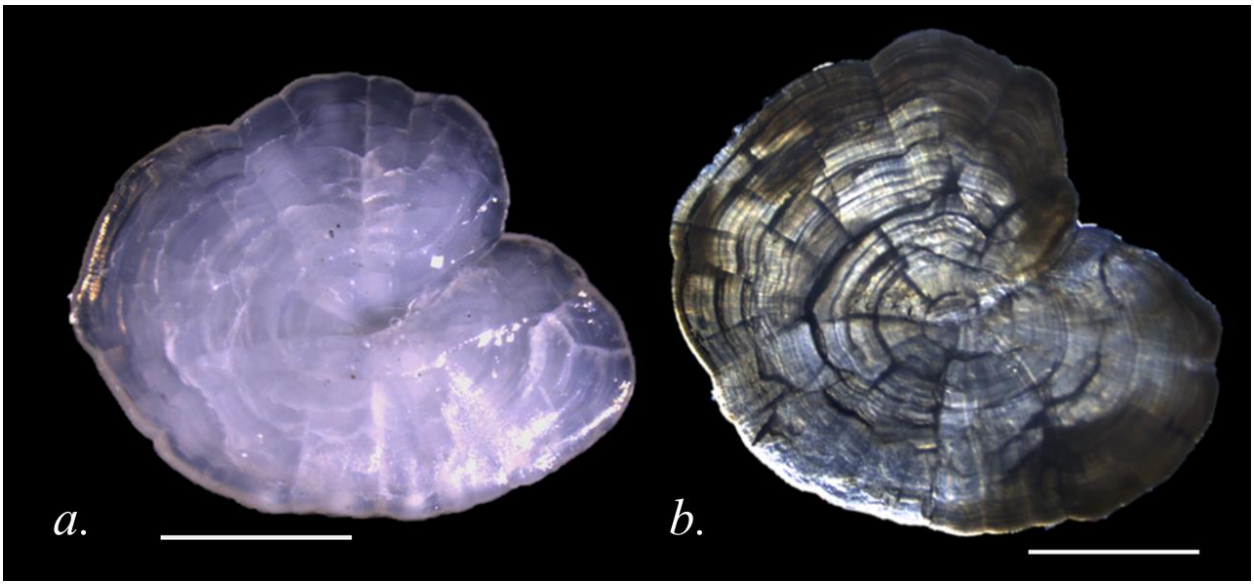

Figure 4.1. Two views of *C. melanurus* otoliths that provide details on the growth structure for this species. ***a*)** Whole *C. melanurus* sagittal otolith viewed in reflected light (sample 379#5). ***b*)** Otolith thin section (medial plane), viewed with transmitted light (sample 340#1) with an estimated age of ~24 years for subjective enumeration of annuli. Scale bars 1 mm.

There were no significant differences between left and right otoliths within individuals for mass (Welch two-sample t-test, t_{55}=-0.190, p=0.850), length (t_{52}=0.663, p=0.510), width (t_{52}=0.615, p=0.541), or height (t_{50}=-0.468, p=0.642). All metrics (mass, length, width, height) correlated significantly with standard length (ANOVA, $F_{1,27}$=25.7, p<0.001; $F_{1,27}$=15.3, p<0.001; $F_{1,27}$=8.6, p<0.01; $F_{1,27}$=20.4, p<0.001) and body mass ($F_{1,27}$=27.1, p<0.001; $F_{1,27}$=20.4, p<0.001; $F_{1,27}$=14.6, p<0.001; $F_{1,27}$=19.5, p<0.001), with otolith mass having the strongest slope (**Figure 4.2**). Age estimates for *C. melanurus* were between 9 and 24 years assuming opaque zones represent annual growth rings (**Figure 4.3**).

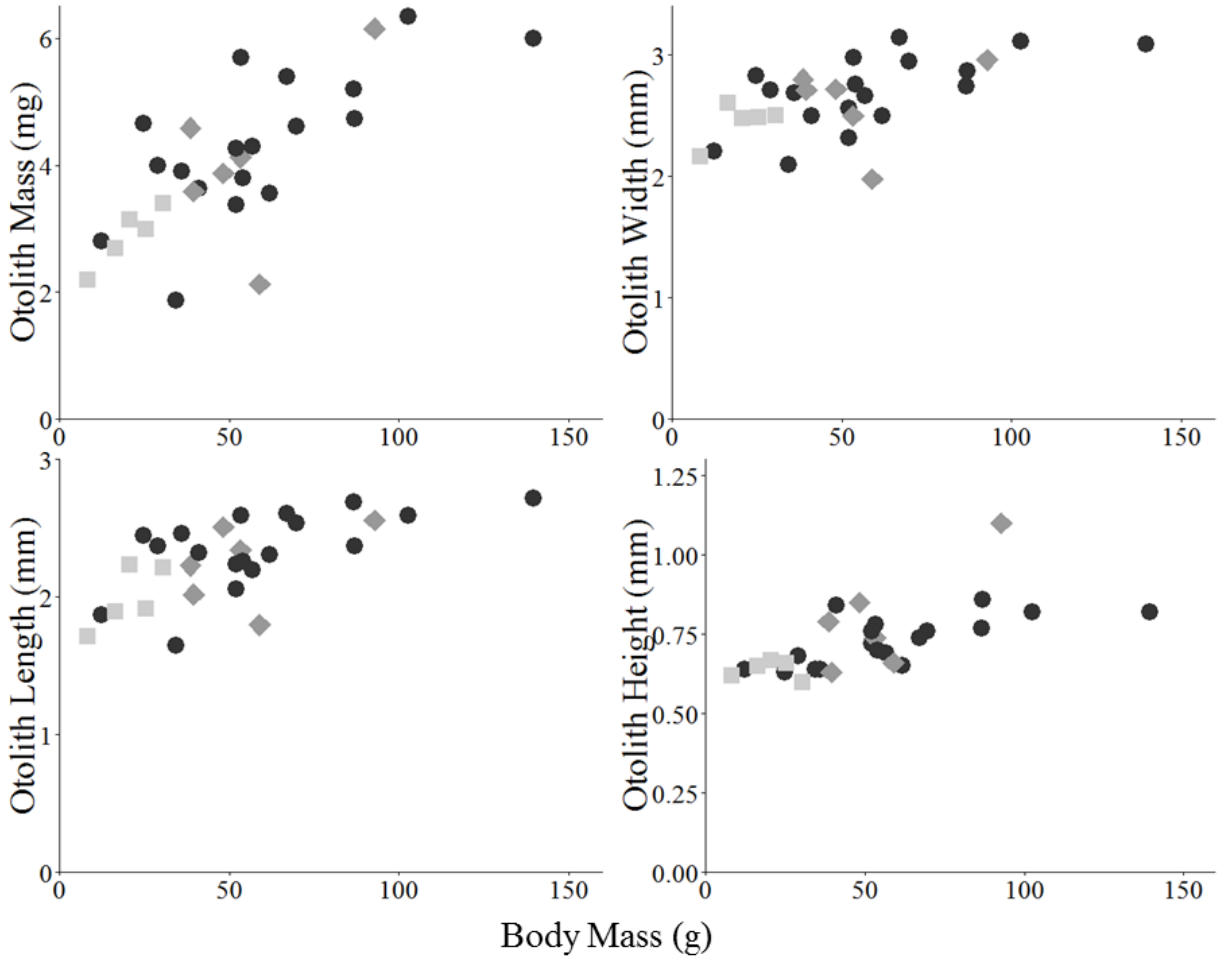

Figure 4.2. *Careproctus melanurus* otolith mass and dimensions as a function of fish body mass (g). Females (circles), males (diamonds), and juveniles (squares). Mass plots show results from the left otolith, other figures are based on one randomly selected otolith from each individual (n=29).

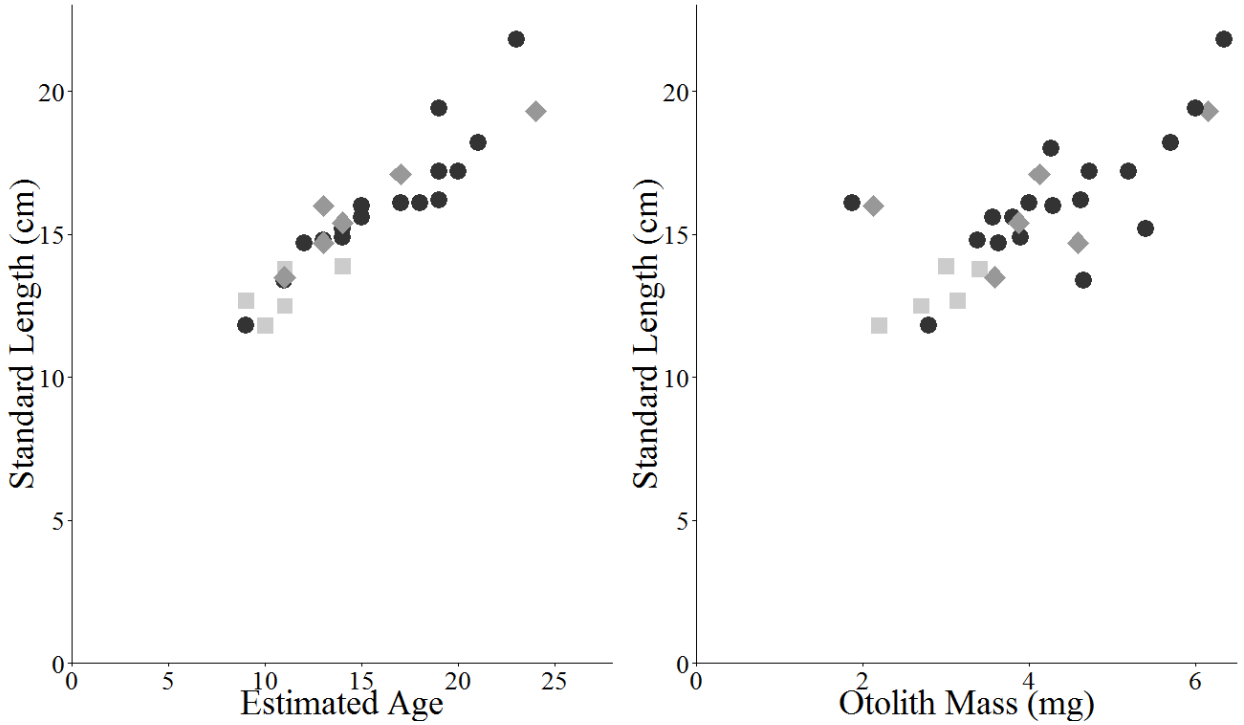

Figure 4.3. ***a)*** Length-at-age relationships for *C. melanurus* (n=29). Results from females shown with circles, males with diamonds, and immature individuals with squares. Estimated age (years) based on otolith growth zones. ***b)*** Length as a function of otolith mass for *C. melanurus* (n=29) for comparison.

Age Estimation: Hadal liparids. Standard lengths of the 28 Mariana liparid individuals used for age estimation ranged from 10.5–28.8 cm. Individual body mass ranged from 8 to 160 g, from capture depths 6,914–7,966 m. Thirteen of these were females, five males, seven juveniles, and three unsexed. Otoliths (**Figure 4.4**) of this species weighed from 0.3050 to 1.4460 mg, were between 0.827 and 1.547 mm in length, 0.688 to 1.265 mm in width, and 0.35 to 0.59 mm in height.

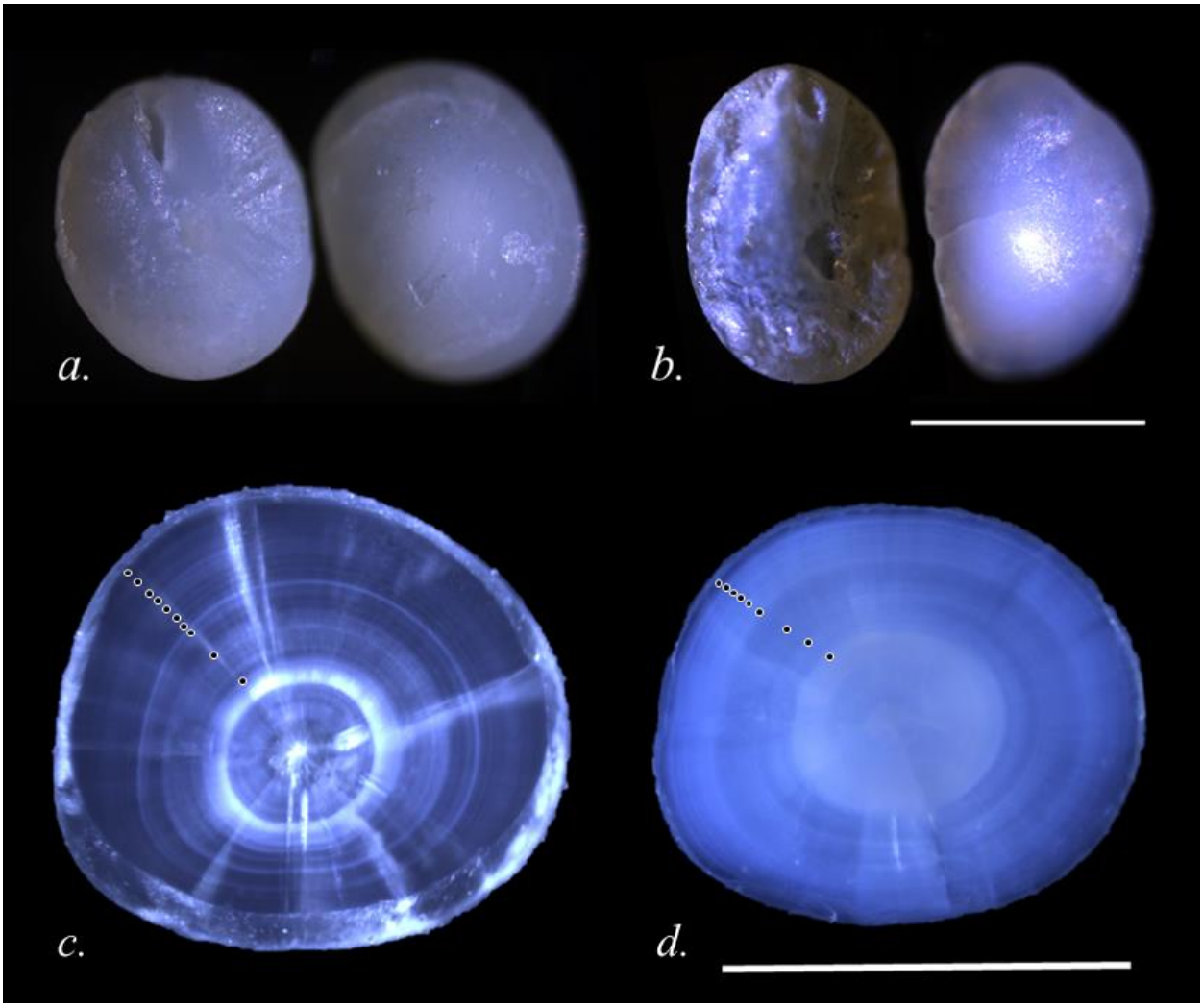

Figure 4.4. Hadal liparid otoliths. ***a)*** *N. kermadecensis*, sample 100326, whole. ***b)*** Mariana liparid, sample 200021, whole. ***c)*** *N. kermadecensis*, sample 100219, thin section, estimated age: 10 years. ***d)*** Mariana liparid, sample 200134, thin section, estimated age: 9 years. Counted zones are marked. Scale bars 1 mm.

In the 38 *Notoliparis kermadecensis* collected from the Kermadec Trench, depths 6,456–7,554 m, standard lengths were between 12.9 and 29.0 cm, and body mass ranged from 20 to 230 g. There were 19 females, 12 males, three juveniles, and four unsexed individuals. *Notoliparis kermadecensis* otolith mass was 0.3766–2.0050 mg, length was 0.879–1.539 mm, width was 0.671–1.311 mm, and height was 0.40–0.80 mm. Further collection details and individual results for all liparids can be found in **Supplementary Table 4.1**.

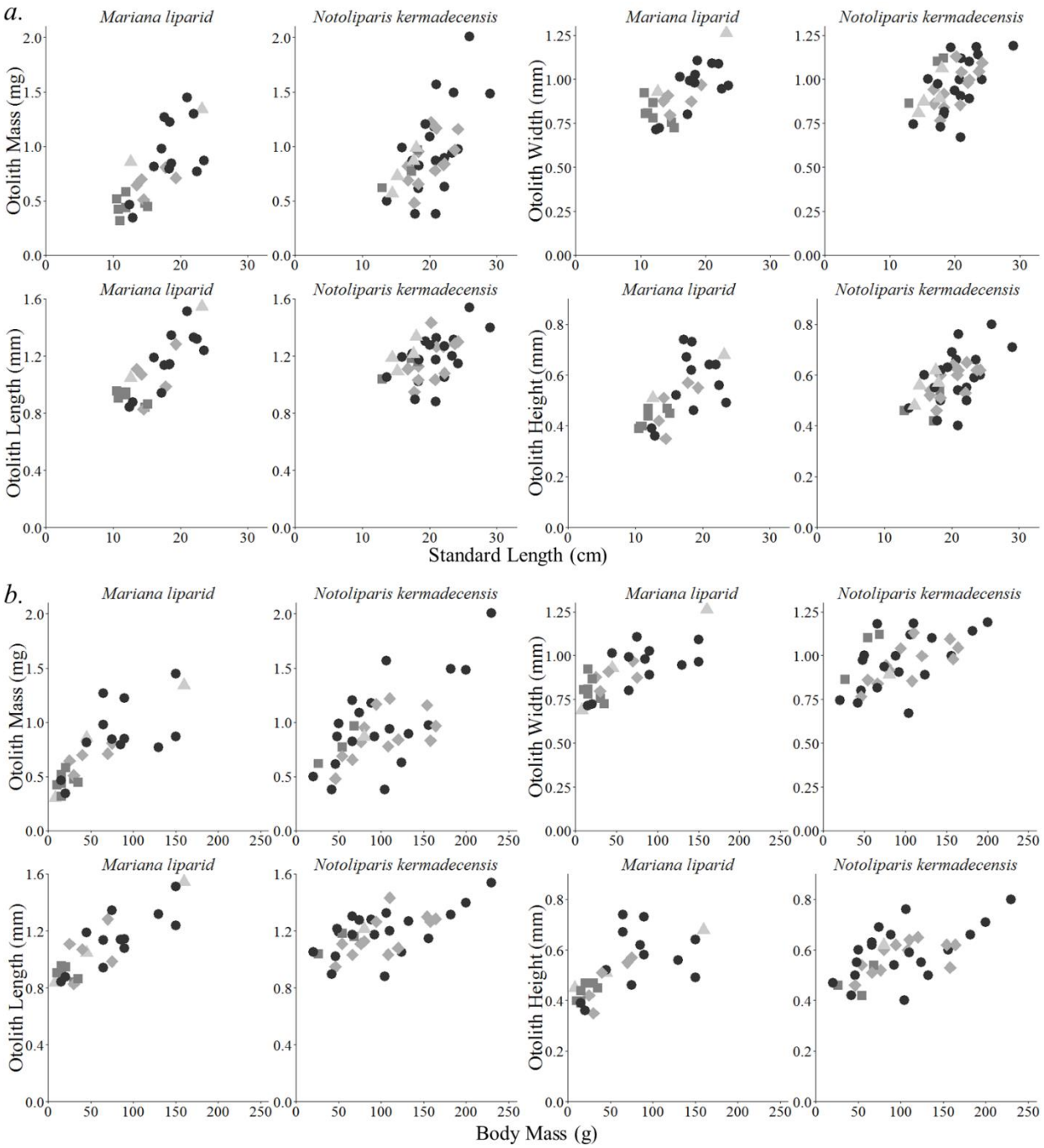

Figure 4.5. Otolith mass, width, length, and height by standard length (***a***), and total body mass (***b***). Females (circles), males (diamonds), juveniles (squares), and unknown sex (triangles). Width and length measured from photographs using ImageJ, height measured with calipers by hand, all from one randomly selected otolith from 28 individuals of the Mariana liparid and 38 *N. kermadecensis*.

All metrics (otolith mass, length, width, and height) increased significantly with both standard length and body mass for both hadal liparid species (ANOVA – standard length: Mariana liparid $F_{1,25}$=19.9, p<0.001; $F_{1,25}$=22.3, p<0.001; $F_{1,25}$=12.9, p<0.01; $F_{1,25}$=16.6, p<0.001; *N. kermadecensis* $F_{1,36}$=21.5, p<0.001; $F_{1,36}$=11.2, p<0.01; $F_{1,36}$=18.8, p<0.001; $F_{1,36}$=18.3, p<0.001; body mass: Mariana liparid $F_{1,25}$=44.0, p<0.001; $F_{1,25}$=62.9, p<0.001; $F_{1,25}$=32.2, p<0.001; $F_{1,25}$=20.8, p<0.001; *N. kermadecensis* $F_{1,33}$=26.0, p<0.001; $F_{1,33}$=19.0, p<0.001; $F_{1,33}$=19.5, p<0.001; $F_{1,33}$=17.7, p<0.001; **Figure 4.5**). Measurements between otoliths of individual fishes were not significantly different in mass, length, width, or height for either the Mariana liparid (Welch two-sample t-test, t_{49}=-0.107, p=0.854; t_{52}=-0.107, p=0.915; t_{51}=-0.241, p=0.811; t_{51}=-0.127, p=0.899) or *N. kermadecensis* (t_{69}=0.124, p=0.901; t_{70}=-0.864, p=0.390; t_{70}=0.315, p=0.754; t_{70}=-0.093, p=0.926). Assuming opaque zones represent annual growth, ages for these specimens were estimated to be 5 to 12 years old for the Mariana liparid and 6 to 15 years old for *N. kermadecensis* (**Figure 4.6**).

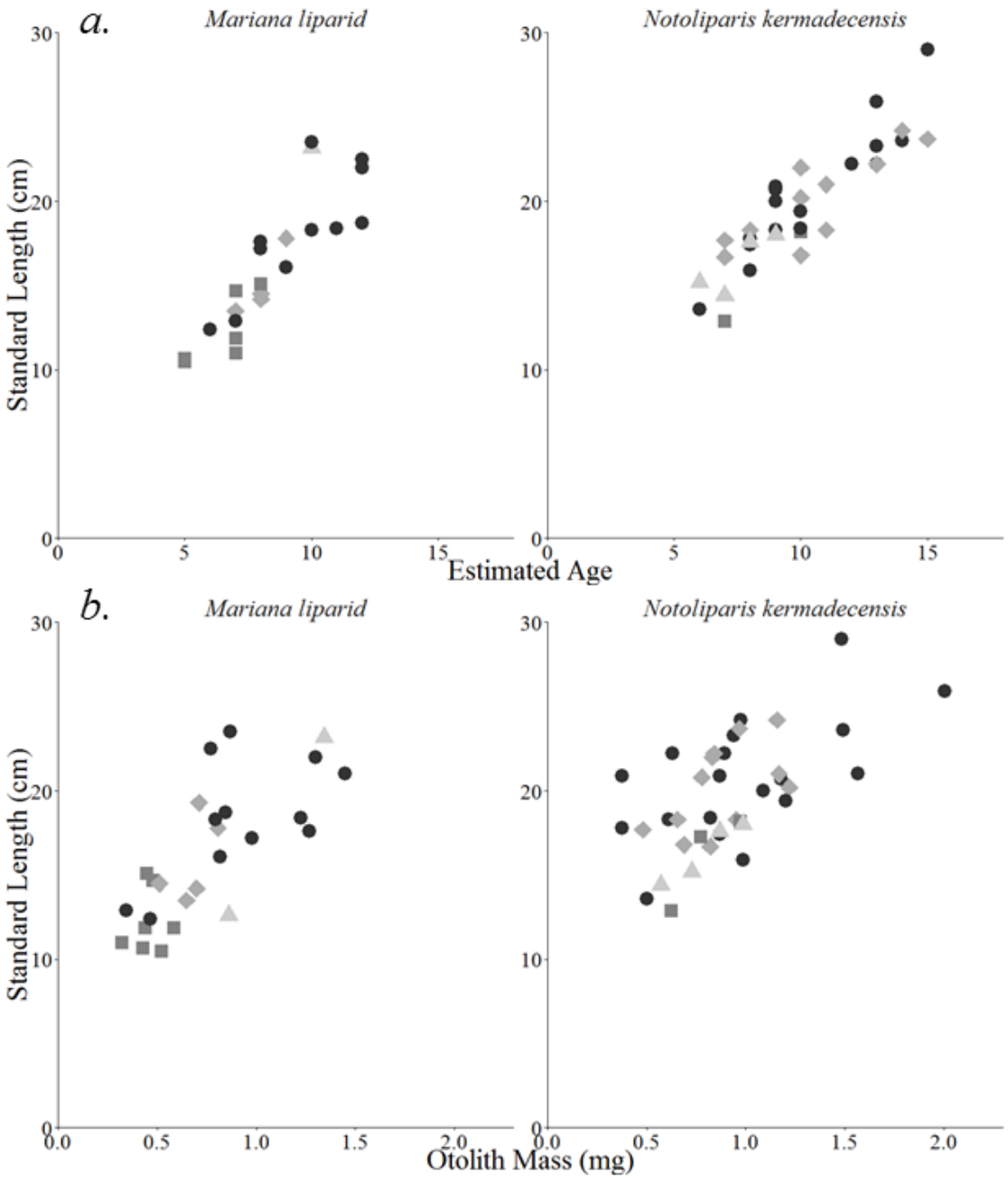

Figure 4.6. ***a)*** Length-at-age relationships for two hadal snailfishes, the Mariana liparid (n=23) and *N. kermadecensis* (n=34). Females (circles), males (diamonds), juveniles (squares), and unknown sex (triangles). Estimated age (in years) assuming opaque rings represent annual growth zones. ***b)*** Standard length as a function of otolith mass (mg) for comparison.

Age Estimation: Abyssal Macrourids. Otoliths from 114 *Coryphaenoides armatus* were sectioned for age estimation. Individuals ranged in total length from 44.0 to 93.5 cm and had body masses between 300 and 3760 g. Macrourid tails are often lost or broken, making growth relationships difficult to analyze, therefore head lengths (range 7.25 to 15.38 cm) were used for length-at-age comparisons here. There were 31 females, 74 males, and nine of unknown sex. Otoliths weighed between 0.0362 and 0.1503 g, were 1.00–2.30 mm in height, 3.60–6.30 mm in width, and 3.50–7.35 mm in length. Forty-four *Coryphaenoides yaquinae* individuals were analyzed, with total lengths ranging from 34.7 to 65.0 cm, weighing 179 to 1107 g. Head lengths were between 7.4 and 12.0 cm. Of these, 40 were identified as female, two as male, and two of unknown sex. Otoliths of *C. yaquinae* ranged in mass from 0.0246 to 0.0858 g, in height from 1.20 to 1.90 mm, in width from 3.60 to 5.70 mm, and in length from 3.30 to 5.70 mm. Collection details, specimen measurements, and individual age estimates for both macrourids are available in **Supplementary Table 4.2**.

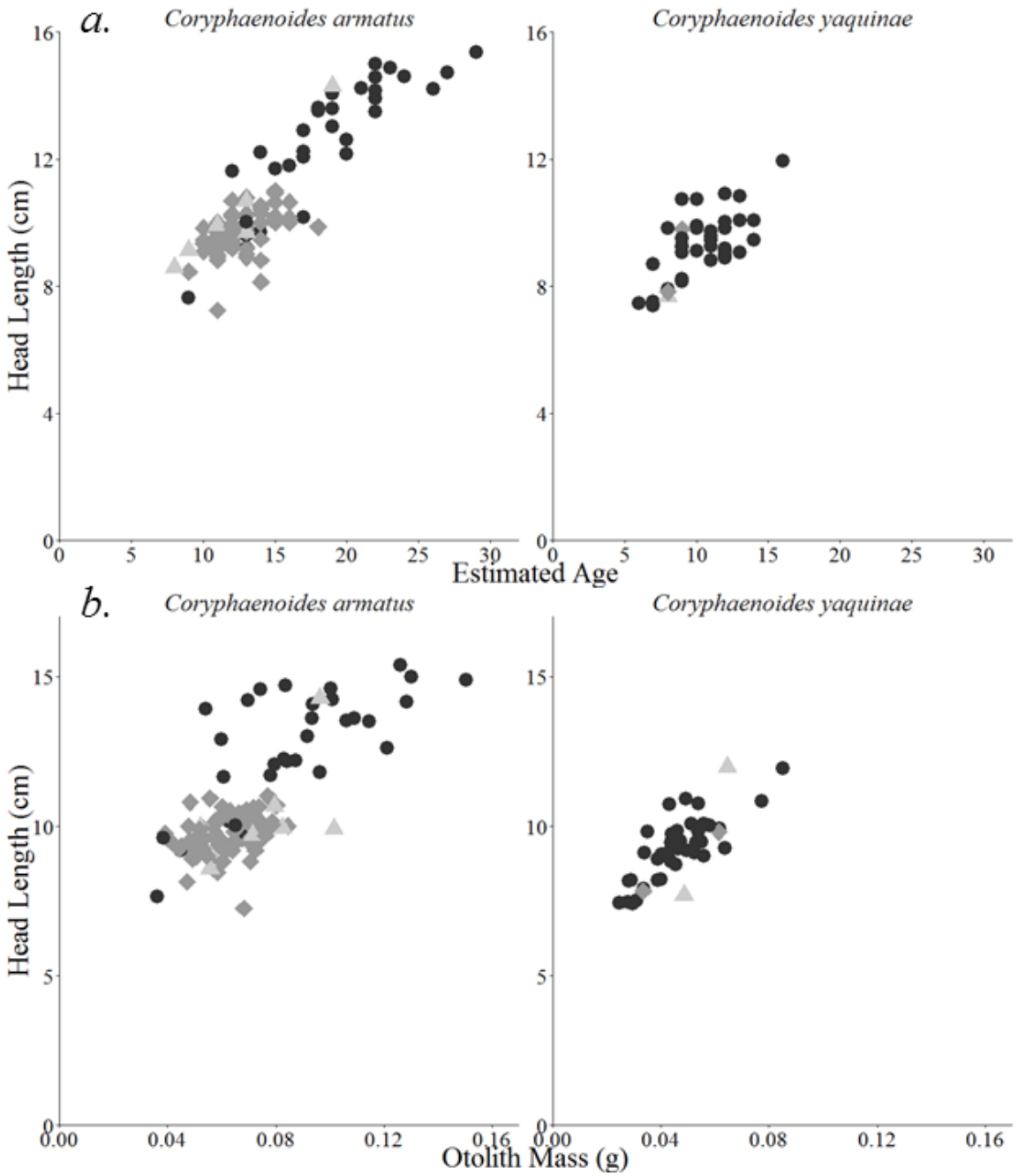

Figure 4.7. ***a)*** Length-at-age relationships for two abyssal macrourids, *Coryphaenoides armatus* (n=107) and *C. yaquinae* (n=42). Females (circles), males (diamonds), and unknown sex (triangles). Estimated age (in years) assuming opaque rings represent annual growth zones. ***b)*** Head length as a function of otolith mass (g) for comparison.

Left and right otoliths did not vary significantly in mass (Welch two-sample t-test: *C. armatus* t_{224}=-0.964, p=0.336; *C. yaquinae* t_{85}=-0.383, p=0.703), length (*C. armatus* t_{224}=-0.413, p=0.680; *C. yaquinae* t_{84}=-0.324, p=0.747), width (*C. armatus* t_{223}=-1.434, p=0.153; *C. yaquinae* t_{84}=-0.045, p=0.965), or height (*C. armatus* t_{220}=-0.667, p=0.506; *C. yaquinae* t_{85}=-0.706, p=0.482). Otolith mass, length, width, and height all increased significantly with head length (ANOVA: *C. armatus* $F_{1,110}$=134.3, p<0.001; $F_{1,110}$=44.9, p<0.001; $F_{1,109}$=64.9, p<0.001; $F_{1,110}$=64.5, p<0.001; *C. yaquinae* $F_{1,42}$=63.3, p<0.001; $F_{1,42}$=25.8, p<0.001; $F_{1,42}$=60.1, p<0.001; $F_{1,42}$=33.8, p<0.001) and body mass (*C. armatus* $F_{1,109}$=129.4, p<0.001; $F_{1,109}$=47.0, p<0.001; $F_{1,108}$=61.1, p<0.001; $F_{1,109}$=75.6, p<0.001; *C. yaquinae* $F_{1,41}$=66.7, p<0.001; $F_{1,41}$=18.1, p<0.001; $F_{1,41}$=43.9, p<0.001; $F_{1,41}$=42.2, p<0.001) in both *C. armatus* and *C. yaquinae*. Age estimates for *Coryphaenoides armatus* in this collection ranged from 8 to 29 years old. Otoliths from *Coryphaenoides yaquinae* had fewer annuli, with ages estimated from 6 to 16 years old (**Figure 4.7**). Growth parameters for all study species are presented in **Table 4.1**.

Table 4.1. Tentative growth parameters and age estimates for liparids and macrourids. Lengths (cm) are standard length for liparids and head length for macrourids. Number of otoliths used in age estimation (n) shown. Growth coefficient (*k*), maximum length (L_{inf}), number of iterations to convergence (i), and residual sums of squares (RS) for von Bertalanffy growth function models are presented. Growth function fitted based on head length for macrourids, standard length for liparids.

Species	n	Length (cm)	Body Mass (g)	Age Estimates	L_{inf} (cm)	*k*	RS	i
Coryphaenoides armatus	107	7.3–15.4	300–3760	8–29	18.3	0.062	81.3	7
Coryphaenoides yaquinae	42	7.4–12.0	179–1107	6–16	11.1	0.181	23.5	3
Careproctus melanurus	29	11.8–21.8	8–140	9–24	22.9	0.079	22.8	6
Notoliparis kermadecensis	38	12.9–29.0	20–230	6–15	34.7	0.086	91.4	5
Mariana liparid	28	10.5–28.8	8–160	5–12	75.9	0.029	84.8	15

Thermal History Reconstruction. For all samples tested (**Table 4.2**), $\delta^{18}O$ values ranged from 28.8 to 33.8‰ relative to VSMOW. Errors (2σ) of individual point measurements ranged from ±0.18 to ±0.54‰ (mean 0.35‰) vs. VSMOW. The highest values were found in the deeper-living species (**Figure 4.8**). Significant increases in $\delta^{18}O$ values (corresponding to decreases in habitat temperature) with increasing distance from the core were found for *C. armatus* (ANOVA,

($F_{1,8}$=23.2, p<0.05), *N. kermadecensis* ($F_{1,4}$=18.2, p<0.05), and nearly significant increases were found for the Mariana liparid ($F_{1,4}$=5.9, p=0.073). *C. melanurus* $\delta^{18}O$ values also varied across the otolith, being lower in the first or second annuli than at the core, and then increasing toward the outer rings. No significant change across the otolith was found for *C. yaquinae* ($F_{1,8}$=0.1, p=0.705). $\delta^{18}O$ values at points on different sides of the otolith and at similar distances from the core were consistent (**Figure 4.8**). Images of the otolith surface using scanning electron microscopy revealed some measurement points on roughly polished surfaces (triangles in **Figure 4.8**). Based on previous laboratory observations, these values may be expected to be significantly higher (up to 4‰) than the true sample values (Kita et al., 2009). Conversions to VPDB are shown using the true ratios. We found no significant differences between this method and conversion via the Coplen et al. equation (1983; Welch two-sample t-test, t_{142}=0.041, p=0.968).

Table 4.2. Samples used for thermal history reconstruction. Depth in meters and SL is standard length in centimeters. Number of points measured along otolith were taken in two opposing transects. Mean temperature over the capture depths is listed with ranges in the text. $\delta^{18}O$ values (‰ vs. VSMOW) for seawater estimated based on outermost measurement and capture temperature.

Species	**Location**	**Depth**	**°C**	**$\delta^{18}O_{sw}$**	**SL**	**Sex**	**Sample ID**	**Points**
Careproctus melanurus	California	834	5.1	-3.80	18.0	female	841#1	8
Coryphaenoides armatus	Kermadec Trench	3865	1.2	-1.74	50.3	male	100038	10
Coryphaenoides yaquinae	Mariana Trench	5255	1.5	-1.52	77.3	female	200152	10
Mariana liparid	Mariana Trench	7841	1.8	-0.86	11.9	juvenile	200072	6
Notoliparis kermadecensis	Kermadec Trench	7515	1.3	-1.34	18.3	male	100171	6

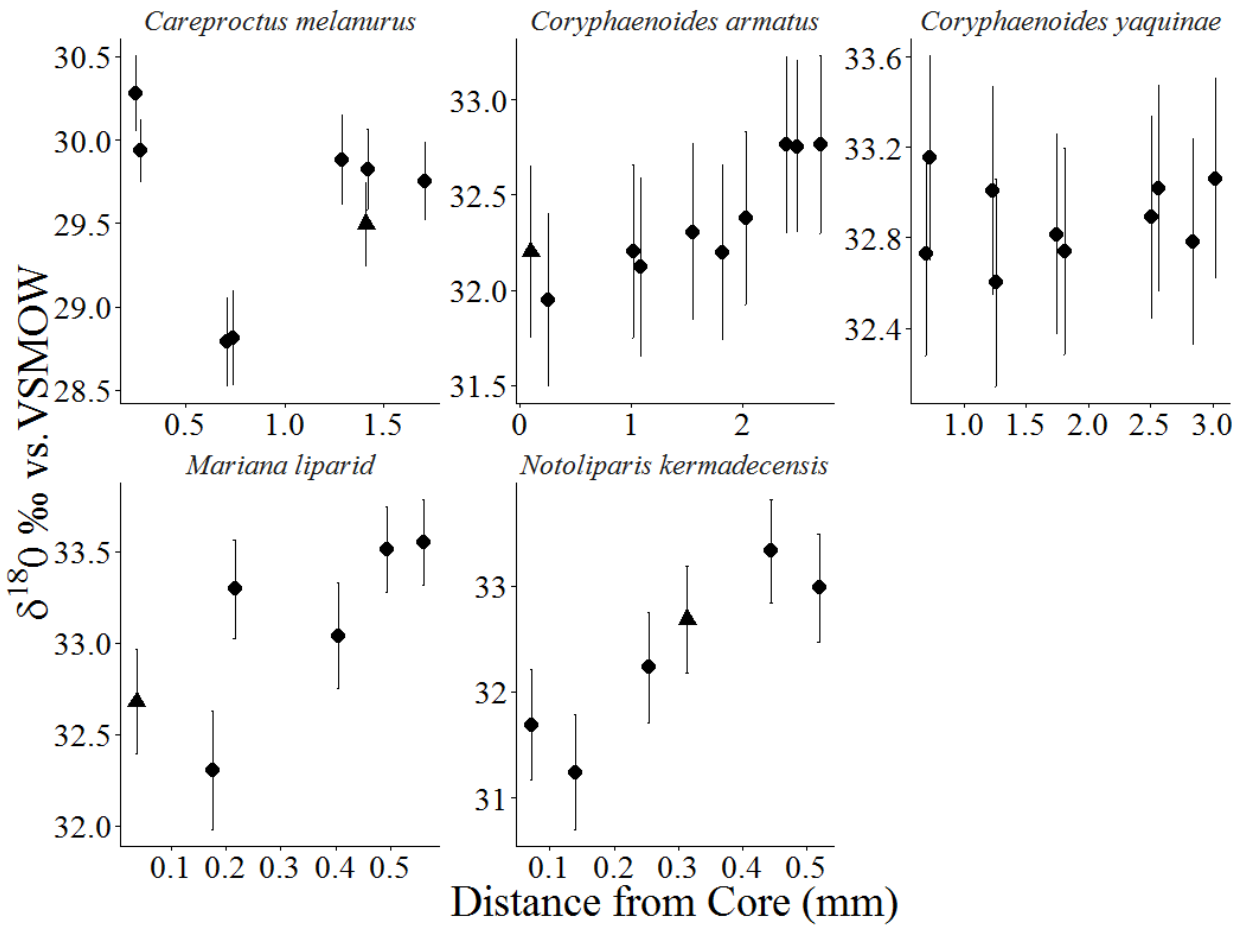

Figure 4.8. Measurements of $\delta^{18}O$ values (‰ vs. VSMOW) across individual otoliths by species. Triangles indicate measurements that may have scratches based on SEM inspection. Error bars indicate 2σ. Distance measured from center of the otolith core.

For calibration of the Mariana liparid $\delta^{18}O$ measurements, we used habitat temperature measured *in situ* and the $\delta^{18}O$ value at the outer otolith edge to solve for the $\delta^{18}O$ of seawater. Habitat temperature for adults ranged from 1.7 to 1.9°C (mean 1.8°C) based on temperature-depth data and specimen collection depth (6,914–7,966 m, Jamieson and Linley, unpublished data; 13,787 temperature measurements over 14 deployments greater than 6,914 m). The mean temperature of 1.8°C, and the outer edge $\delta^{18}O$ values (**Figure 4.8**), gave a $\delta^{18}O$ value of -0.86‰ for seawater. Using this value for the thermal reconstruction, the corresponding habitat temperature at the innermost (otolith core) measurement was estimated to be ~6°C (**Figure 4.9**). This finding suggests a larval phase depth shallower than 1,000 m (~430–920 m) in overlying waters. The Kermadec

liparid, *Notoliparis kermadecensis*, was collected from depths between 6,456 and 7,554 m, with a temperature range of 1.2–1.3°C (mean 1.3°C; 3,929 measurements over 5 deployments, July 2007). Based on the outermost $\delta^{18}O$ value in the otoliths, this would correspond to a $\delta^{18}O$ value of seawater of approximately -1.34‰. Habitat temperature estimates from the core measurements were calculated to be as warm as 8°C (**Figure 4.9**). This indicates the larval phase was at depths between ~450 and 930 m in overlying waters (**Figure 4.10**).

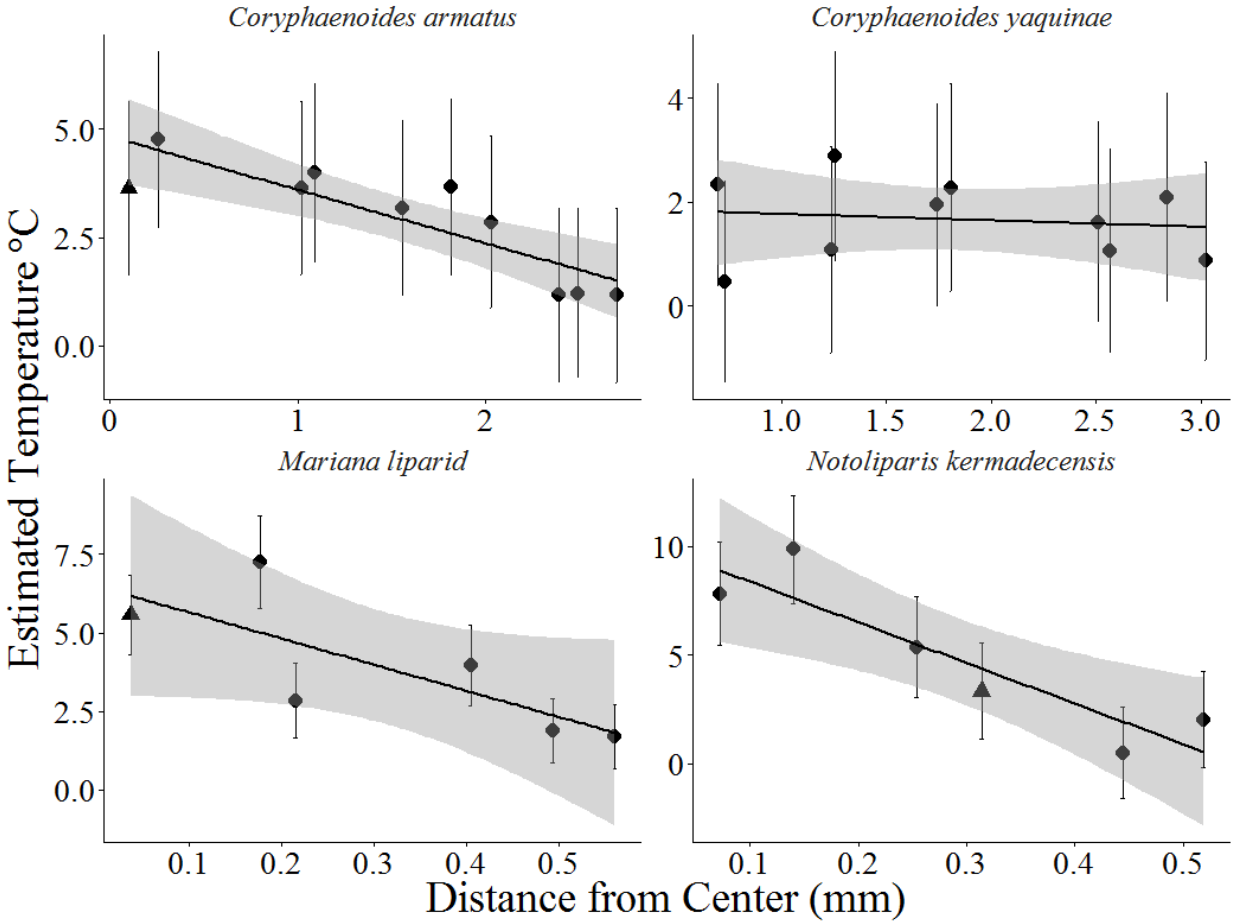

Figure 4.9. Estimated temperature changes across the otoliths of the abyssal and hadal fishes of this study. Calculated $\delta^{18}O$ for seawater at collection locations was used to calibrate the measured $\delta^{18}O$ values through the otolith transects to determine water temperature through ontogeny (Høie et al., 2004). Triangles indicate measurements with potential scratches seen in SEM. Linear fits with 95% confidence intervals shown in gray.

The abyssal grenadier specimens provided contrasting results (**Figure 4.8**). The *C. yaquinae* specimen was collected from 5,255 m at a location near the Mariana Trench. Mean habitat temperature from this individual was estimated to be 1.5°C (1.4–1.5°C) for a depth range of 5,000–5,500 m (4,380 CTD measurements over 22 deployments). Hence, the calibrated $\delta^{18}O$ value of seawater was estimated to be -1.52‰. Habitat temperature varied little across the otolith and represented depths below 2,000 m. The *C. armatus* specimen was from the abyssal plains near the Kermadec Trench from a depth of 3,865 m with temperature range of 1.0 to 1.6°C (mean 1.2°C, depths 3,500–4,500 m, 2,119 temperature measurements over nine deployments, in 2007 and 2014). The calibrated $\delta^{18}O$ value of seawater was -1.74‰, which led to habitat temperatures ranging from 1 to 4°C across the otolith. This suggests a change in habitat and a larval phase at depths deeper than 1,000 m, but above the bottom.

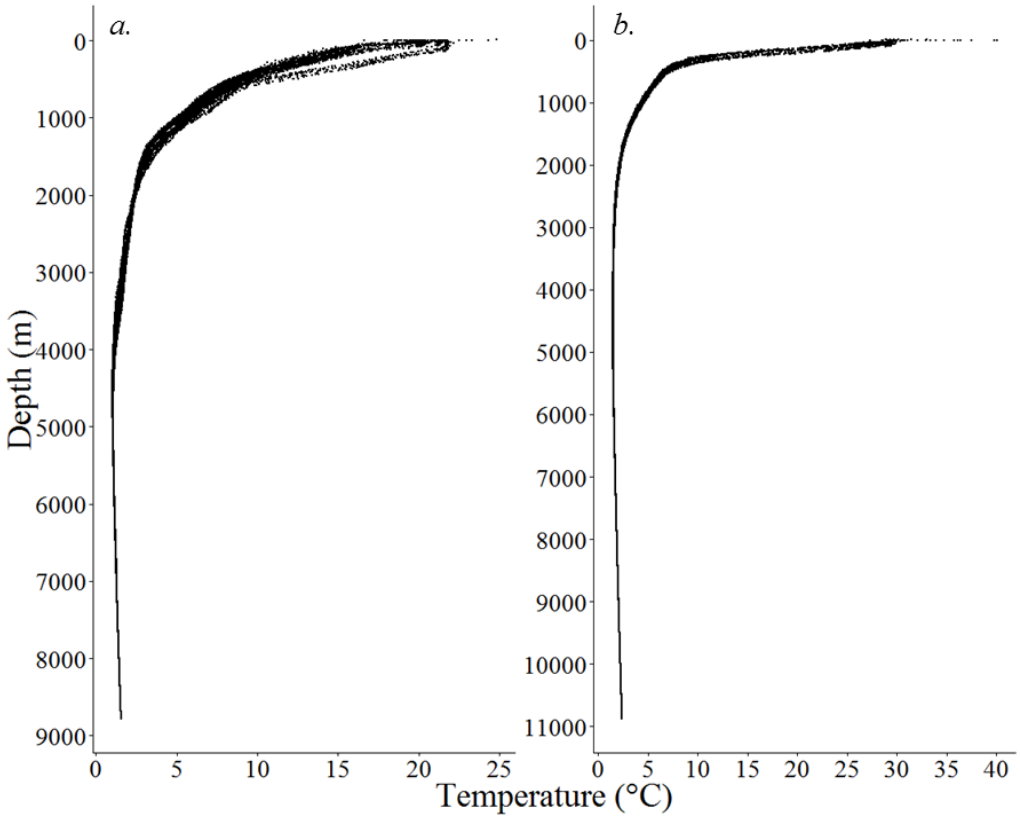

Figure 4.10. Temperature-depth profiles for locations near the collections sites within the Kermadec Trench (left) and Mariana Trench (right) trenches (Unpublished data, A. Jamieson and T. Linley, deployment details provided by Linley et al., 2017). Profiles are based on 35,535 measurements over 13 deployments for the Kermadec Trench and 60,627 measurements over 24 deployments for the Mariana Trench (2007–2014).

The collection depth for the *C. melanurus* specimen was 834 m with a corresponding habitat temperature of 5.09°C. The calibrated $\delta^{18}O$ value of seawater was -3.80‰. Measurements across the otolith provided evidence that habitat temperature increased to approximately ~9°C, and then returned to ~5°C. This suggests a pelagic larval phase to depths of 125 to 300 m, prior to the juveniles and adults subsequently settling at greater depths (**Figure 4.11**).

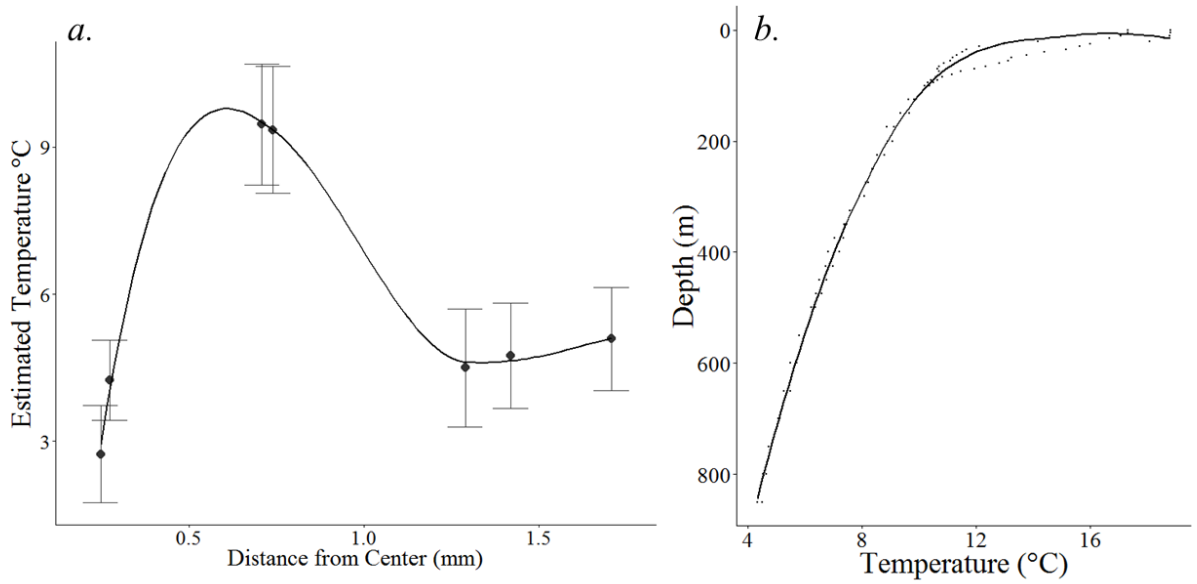

Figure 4.11. ***a)*** Estimated temperature changes across the otolith of an adult *Careproctus melanurus* (sample 841#1). Calculated $\delta^{18}O$ for seawater at collection locations was used to calibrate the measured $\delta^{18}O$ values through the otolith transects to determine water temperature through ontogeny (Høie et al., 2004). ***b)*** Temperature profile for *Careproctus melanurus* collection site. Data extracted from WOD. Profile constructed from 88 measurements in May and October.

Discussion

Information on the age, growth, and longevity of snailfishes is lacking as few studies have been pursued for members of this family. One study that used whole otoliths to estimate the age of *Liparis gibbus* and *Careproctus reinhardti* from off Spitsbergen in the Arctic Ocean led to maximum ages of 6 and 7 years, respectively (Falk-Petersen et al., 1988). The study mentions that the annuli were easy to read. However, it must be considered that sectioned otoliths regularly reveal more growth zone structure not visible in whole otoliths. These finer rings are often annual,

reflecting seasonal changes in nutrient inputs, and lead to much greater estimates of age (e.g., Beamish 1979; Andrews et al., 2002). In our collection, the difference between what was visible in the whole versus sectioned *C. melanurus* otoliths was dramatic (**Figure 4.1**). Otolith sectioning was necessary for age estimation of the smaller liparids used in this study. Maximum age estimates of 10 to 13 years for the family in general, including previous estimates for *C. melanurus* from the northwestern Pacific Ocean, were based on counting growth zones using the break-and-burn method (Orlov and Tokranov, 2011). Our results suggest that snailfishes in general may be longer-lived, with estimates on the order of twenty years. This discrepancy warrants further investigation, including the use of validation techniques.

The small sample size and narrow specimen length range prevented a reasonable fit of the von Bertalanffy growth function for our study species, especially given the lack of very small/young fish (Horn et al., 2010), except as an exploratory tool. In addition, length at maturity for *C. melanurus* remains unknown (Stein, 1980) and precludes an estimate of age at maturity. However, if the length of each species tends to plateau with increasing otolith mass, we can conclude that fish approaching maximum size were sampled and that estimates of age may represent maximum age for the species. For *C. melanurus*, growth zones were well defined in the medial sections. Our tentatively fitted von Bertalanffy function suggested a maximum standard length of near 23 cm, near the maximum size from this collection. Subjectivity in age estimation was greatest in the earliest growth because of what appear to be checks (non-annual marks) with spacing that was inconsistent with asymptotic growth. Edge effects were also a problem for the more recent growth. Assuming some degree of accuracy in the estimates here, *C. melanurus* may approach maximum size in ~15–20 years, with a longevity on the order of 25 years (**Figure 4.3**). In addition, the low slope for the increase in size with age for the youngest fish studied implies either early overcounting or a low growth coefficient (k). An anchored von Bertalanffy growth function yielded a k value of 0.079 for *C. melanurus*, similar to that found in other upper slope-dwelling fishes (Drazen and Haedrich, 2012).

This study provides the first age estimates for the planet's deepest-living fishes based on otolith growth zones. Age estimates for the Mariana liparid were as high as 12 years, and up to 15 years old for *Notoliparis kermadecensis* from the Kermadec Trench. Although sample sizes for liparids in this study were low for a comprehensive quantification of age and growth, similarities

between the otolith mass to standard length, and estimated ages to standard length relationships (**Figure 4.6**), provide evidence for consistency in the age estimation protocol. These estimates are much less than may have been predicted according to the older-deeper trend seen in other studies (Cailliet et al., 2001), although as more age estimation work has been done on a variety of deep-sea commercial and bycatch species, a high variability in ages at depth has emerged (e.g., Andrews et al., 1999a, 2009, 2012; Horn et al, 2012; Tracey et al., 2016). The relatively low ages and moderate growth are concordant with the growing recognition that food supply in trenches may be higher than the surrounding abyss due to accumulation of organic matter through topographic funneling (George and Higgins, 1979; Danovaro et al., 2002; Itoh et al., 2011; Ichino et al., 2015). The low ages are also consistent with the hypothesis that liparids are adapted to a higher-disturbance environment than the abyssal plain. The growth coefficient (*k)* for *Notoliparis kermadecensis* was slightly higher than that found for *C. melanurus*, at 0.086 and 0.079 respectively, although the sample size for the Mariana liparid was too small for reasonable growth parameters for comparison. Additionally, increased longevity and slower rates to maturity may not be advantageous in the hadal environment. Hadal subduction zones are highly susceptible to disturbance (Itou et al., 2000; Oguri et al., 2013) compared to the surrounding abyss, which is generally considered a comparatively stable environment. Seismic activity can cause turbidity flows, which can greatly impact species distributions (Fisher and Raitt, 1962; Richardson et al., 1995; Danovaro et al., 2002). Snailfish may be adapted to the hadal environment by having faster growth, with less time to reproductive maturity.

Many more age estimates exist for the macrourid fishes (reviewed by Swan and Gordon, 2001), allowing a framework for discussion of the deeper-older trends. Another rattail in the same genus, *Coryphaenoides acrolepis* was validated to reach ages of least 56 years based on $^{210}Pb/^{226}Ra$ dating, with growth zone age estimates as high as 73 years (Andrews et al., 1999a). Using a similar counting protocol developed by that study, the present maximum age estimates were 29 and 16 years for *C. armatus* and *C. yaquinae*, respectively. Neither length-at-age curve for these species reached a plateau, therefore it is possible that maximum ages for both macrourids can be greater than found in this collection given sampling adequacy. While longevity for *C. armatus* and *C. yaquinae* does not appear to be on the order of 100 years, as may have been expected from the deeper-older hypothesis, sampling adequacy and age reading need further investigation.

Gadiformes such as the macrourids have been shown to be longer-lived with depth of occurrence in the first thousand meters (Drazen and Haedrich, 2012). However, this trend does not seem to continue linearly to abyssal and shallow-hadal depths. Therefore, that it is unlikely that longevity in deep-sea fishes is governed exclusively by temperature or hydrostatic pressure.

Given the available data, age at maturity may be less than ten years for both hadal snailfish species. Standard length at maturity was approximately 13–15 cm for the Mariana liparid and near 13–17 cm for *N. kermadecensis*. While we found clear relationships between size, age, and otolith mass, it could be inaccurate to estimate age from only the otolith mass, as has been found for other species (e.g., Pilling et al., 2003). Two-stage otolith-mass growth relationships are not uncommon in deep-sea species, whereby the otolith-mass growth rate slows with age, often related to the onset of spawning (and close banding representing a 'transition zone') such as for orange roughy *Hoplostethus atlanticus* (e.g., Smith et al., 1995; Francis and Horn, 1997; Tracey and Horn, 1999) and splitnose rockfish *Sebastes diploproa* (Bennett et al., 1982). Alternatively, for a number of oreo species, the transition zone appears to be related to a change from pelagic to demersal habitat (James et al., 1988; Stewart et al., 1995). These fish have much greater longevity than estimated for hadal liparids, hence the shift in growth pattern may not be as obvious in the hadal snailfishes. However, there did seem to be a shift to finer ring structure indicating a slowing of growth at three to four years for the hadal liparids (**Figure 4.4**). For *Coryphaenoides armatus*, this shift usually occurred near five years, and close to three years for *Coryphaenoides yaquinae*. Based on this visible change in the otolith growth pattern, age at maturity may occur relatively early for both hadal liparids and abyssal macrourids.

There are certain limitations to the age estimation method employed here that must be acknowledged. It is well known that annual growth rings require validation (e.g., Campana, 2001; Cailliet and Andrews 2008). It is possible that some growth zones represent sub-annual increment structure from unknown environmental signals, such as smaller-scale seasonal changes or stochastic food fall events (e.g., Brothers et al., 1976; Hüssy et al., 2010; Pannella, 1980). The list of potential age validation techniques (e.g., Campana, 2001) becomes much shorter in deep-sea systems (discussed Mace et al., 1990; Andrews et al., 1999a). Ship time, sampling equipment, and depth issues make a mark/recapture study impractical for hadal fishes. Most other methods are also challenging for various reasons. One of the more feasible methods is an analysis of growth in

the outer most ring collected in different seasons (Gordon and Swan, 1996), but this would require extended temporal sampling opportunities that are not currently available in hadal environments. Validation by radiometric dating has been applied to some deep-sea fishes (Andrews et al., 1999a, 2009), but the amount of material required and the necessity of pooling individuals of similar age precludes this kind of analysis (Andrews et al., 1999b). Only about one hundred hadal liparids have been collected in the fifty years since their discovery (Andriashev, 1955; Nielsen, 1964; Andriyashev et al., 1993; Stein, 2005; Linley et al., 2016), hence this amount of material is not available. Despite these limitations, the development of a protocol based on a shallower-living liparid species provided some credence to the estimates. Furthermore, the known seasonality in the deep sea (e.g., Lampitt, 1985; Lutz et al., 2007; Rowe, 2013; Morales-Nin and Panfili, 2005), presumably even at hadal depths, provides at least a conceptual framework for the formation of annual growth zones. With the present lack of a feasible validation method for hadal snailfishes, we must consider these age estimates as preliminary and note their uncertainty.

Oxygen isotopic compositions across the otolith were used to investigate changes in habitat temperature. For *Careproctus melanurus* we found clear changes (1.5‰) that corresponded to a 5°C increase within the first few years of growth (~3–4 years), followed by a return to cooler temperatures later in life. This likely reflects an early life history stage that moves upward in the water column, settles to the bottom on the upper slope, which is followed by an ontogenetic downslope migration with increasing size and age. This may not be an unusual circumstance for benthic or benthopelagic species of the continental slope—Pacific grenadier have been collected just below the thermocline and the smallest individuals are collected only on the upper slope (A.H. Andrews, personal communication; Matsui et al., 1991). Changes in isotopic composition across the abyssal macrourid otoliths were far less pronounced or absent. There may have been a slight decrease in habitat temperature throughout growth for *Coryphaenoides armatus*, but no change was observed for *C. yaquinae*. These findings may indicate that the vertical migration of larvae before settling back to the bottom is well below the thermocline. A shallow juvenile phase discovered using oxygen isotope analysis of *Coryphaenoides rupestris* otoliths (Longmore et al., 2011), but this does not seem to be the case for these deepest-dwelling congeners and abyssal macrourid larvae have not been located.

Given the temperature-depth profiles collected for *C. armatus* in the Kermadec Trench, an individual collected near 4,000 m with a habitat temperature of 1–2°C, likely had a larval stage close to 1,000 m depth, perhaps accounting for their elusiveness, and also matching a deep downslope migration of juveniles from middle slope to greater abyssal depths (Collins et al., 2005). Results from the hadal liparid isotopic analyses were surprising, with significant increases in $\delta^{18}O$ values across the otolith for both species. These changes could reflect an up to eight-degree change in habitat temperature, which would place larvae at a surprising depth of shallower than 1,000 m, thousands of meters above the adult populations, which appear endemic to their respective trench systems. According to the size of the opaque growth zones, the largest temperature changes for both species seem to be in the first two years of life. Depth differences in various life history stages of deep-sea fishes revealed by isotope analysis are not uncommon, such as reported for bluenose (*Hyperoglyphe antarctica*) off New Zealand by Horn et al. (2010), orange roughy off Ireland (Shephard et al., 2007), and the jellynose fish (*Ateleopus japonicus* and *Ijimaia dofleini*) near Taiwan (Shiao et al., 2017), but the depth differences between pelagic and demersal stages of the hadal liparids suggested here far exceed those of other species.

The estimation of $\delta^{18}O$ values for seawater, given limited environmental data on the deep-sea systems, is approximate and not directly measured as in other studies that have applied this method (e.g., Thorrold et al., 1997). The similarities of estimated $\delta^{18}O$ values of seawater between the sites and in different species provides some support for the validity of the method. Further, slight changes in water mass salinity are not expected to change isotopic fractionation patterns substantially (Fowler et al., 1995; Elsdon and Gillanders, 2002). Thus, it is likely that changes in $\delta^{18}O$ values across the otolith indeed reflect changes in habitat temperature. The measurement of organic material, rather than the aragonitic portion of the otolith, can cause significant differences in measured isotopic values (e.g., Grønkjær et al., 2013); however, these differences are usually ~5‰ (vs. VPDB) below expected values and relatively easy to identify as outliers (Shiao et al., 2014). The fact that changes in the present study followed a consistent trend and were highly reproducible within the spot measurements of the same annulus on a corresponding side of the otolith provides support for measurement precision. Although the absolute temperatures reported are approximate, the change in isotopic composition across the otolith should reflect relative ontogenetic change in habitat temperature.

The ion microprobe results contradict what may be expected from the extremely large eggs (up to 9.4 mm in the newly discovered Mariana liparid) and low fecundities found in the hadal liparids (**Chapter VI**; Nielsen, 1964), which both suggest the possibility of parental care and a benthic larval stage. Gravid females of *Notoliparis kermadecensis* were caught in the Kermadec Trench in both April and November, suggesting continuous or at least a sub-annual periodicity to reproduction (present study collection, HADEEP). An alternative explanation for the temperature increase across the otolith would be that the fish originated in a location deeper in the trench, at warmer temperatures due to the effects of adiabatic heating (Bryden, 1973). If the snailfishes spawned deeper in the trench and moved to the upper trench slopes as they grew, they would undergo a temperature decrease of almost 1°C as they matured (**Figure 4.10**). Such a change is much less than our results suggest based on temperature predictions (Høie et al., 2004), although it is possible that the equation is overly sensitive to changes in delta values. Pressure effects on oxygen isotope fractionation would, however, not be significant until pressures tenfold higher than those seen at hadal depths (Clayton et al., 1975; Polyakov and Kharlashina, 1994) and so pressure effects can be eliminated from further consideration.

Conclusions

This study provides the first age estimates for fishes from hadal depths. Age estimates from counting opaque growth zones in sagittal otoliths suggested that hadal liparids do not fit the deeper-older trend seen for shallower-living fishes (e.g., Cailliet et al., 2001). The reason for their moderate growth rates and relatively young ages could be adaptations to the greater food levels in this seismically active, high disturbance environment of the hadal zone. Results from ^{18}O measurements across the otolith suggest that hadal snailfishes have a shallower pelagic larval stage. This contradicts expectations that a benthic life history could allow them to benefit from the absence of predators at hadal depths and could account for high levels of hadal endemism. Limited dispersal may not have confined liparids to the hadal environment. The success of the snailfishes in the hadal zone may be related to other factors, such as trophic ecology and pressure adaptation.

Acknowledgements

We thank the captains and crews of the RVs *Thompson*, *Falkor*, *New Horizon*, and *Sproul*, and FVs *Noah's Ark* and *Last Straw*. We would like to extend our gratitude to the participants of the Hadal Ecosystems Studies Program and the Summer 2014 Northwest Fishery Science Center (NWFSC) groundfish trawl survey for their contributions to fish collection, to A. Orlov and A. Tokranov for consultation on *Careproctus* age estimation, and to Bob Humphries and the NOAA PIFSC for use of facilities. Funding was provided by the National Science Foundation (OCE #1130712 to J.C. Drazen and OCE#89-22620 and OCE #92-17334 to K.L. Smith), UC Ship Funds, and by Schmidt Ocean Institute (cruise K141109). This material is based upon work supported by the National Science Foundation Graduate Research Fellowship under Grant No. DGE-1144086 to N. Gallo. Any opinions, findings, and conclusions, or recommendations expressed in this material are those of the authors and do not necessarily reflect the views of the National Science Foundation. M. Gerringer is grateful for the support of the National Science Foundation Graduate Research Fellowships Program.

Contributors

Gerringer, M.E.[1], Andrews, A.H.[2], Huss, G.R.[3], Nagashima, K.[3], Gallo, N.D.[4], Clark, M.R.[5], Linley, T.D.[6], Jamieson, A.J.[6], Drazen, J.C.[1]

[1]Department of Oceanography, University of Hawai'i at Mānoa, Honolulu, HI 96822, USA.
[2]NOAA Fisheries, Pacific Islands Fisheries Science Center, Honolulu, HI 96818, USA.
[3]Hawai'i Institute of Geophysics and Planetology, University of Hawai'i at Mānoa, Honolulu, HI 96822, USA.
[4]Scripps Institution of Oceanography, University of California San Diego, La Jolla, CA 92093, USA.
[5]National Institute of Water and Atmospheric Research, Wellington, New Zealand.
[6]School of Marine Science and Technology, Newcastle University, Newcastle Upon Tyne, UK. NE1 7RU.

JCD, AJJ, TDL, and MEG collected abyssal and hadal fish specimens. NDG collected *Careproctus melanurus* samples. MEG and AHA developed the sectioning protocols and estimated ages. MEG, GRH, and KN conducted oxygen isotope analyses. All authors contributed to the discussion and interpretation of the ideas presented and the writing and editing of the manuscript.

References

Andrews, A., Cailliet, G., Coale, K., 1999a. Age and growth of the Pacific grenadier (*Coryphaenoides acrolepis*) with age estimate validation using an improved radiometric ageing technique. Canadian Journal of Fisheries and Aquatic Sciences 56, 1339–1350. (doi:10.1139/f99-054)

Andrews, A., Coale, K., Nowicki, J., Lundstrom, C., Palacz, Z., Burton, E., Cailliet, G., 1999b. Application of an ion-exchange separation technique and thermal ionization mass spectrometry to ^{226}Ra determination in otoliths for radiometric age determination of long-lived fishes. Canadian Journal of Fisheries and Aquatic Sciences 56, 1329–1338. (doi:10.1139/f99-053)

Andrews A.H., Cailliet, G.M., Coale, K.H., Munk, K.M., Mahoney, M.M., O'Connel, V.M., 2002. Radiometric age validation of the yelloweye rockfish (*Sebastes ruberrimus*) from southeastern Alaska. Marine and Freshwater Research 53, 139–146. (doi:10.1071/MF01126)

Andrews A.H., Tracey D.M., Dunn M.R. (2009) Lead–radium dating of orange roughy (*Hoplostethus atlanticus*): validation of a centenarian life span. Canadian Journal of Fisheries and Aquatic Sciences 66, 1130–1140. (doi:10.1139/F09-059)

Andrews, A. H., DeMartini, E. E., Brodziak, J., Nichols, J. S., Humphreys, R. L., 2012. A long-lived life history for a tropical, deep-water snapper (*Pristipomoides filamentosus*): bomb radiocarbon and lead–radium dating as extensions of daily increment analyses in otoliths. Canadian Journal of Fisheries and Aquatic Sciences 69, 1850–1869. (doi:10.1139/f2012-109)

Andriashev, A., 1955. A new fish of the snailfish family (Pisces, Liparidae) found at a depth of more than 7 kilometers. Trudy Instututa Okeanologii 12, 340–344.

Andriyashev, A.P., Pitruk, D.L., Andriashev, A., Pitruk, D.L., Andriyashev, A.P., Pitruk, D.L., 1993. A review of the ultra-abyssal (hadal) genus *Pseudoliparis* (Scorpaeniformes, Liparidae) with a description of a new species from the Japan Trench. Voprosy ikhtiologii 33, 325–330.

Beamish, R., 1979. New information on the longevity of Pacific ocean perch (*Sebastes alutus*). Journal of the Fisheries Research Board of Canada 36, 1395–1400. (doi:10.1139/f79-199)

Befus, K.S., 2016. Crystallization kinetics of rhyolitic melts using oxygen isotope ratios. Geophysical Research Letters 43, 592–599. (doi:10.1002/2015GL067288.Received)

Beliaev, G.M., 1989. Deep-Sea Ocean Trenches and their Fauna. Nauka Publishing House, Moscow, USSR.

Bennett, J.T., Boehlert, G.W., Turekian, K.K., 1982. Confirmation of longevity in *Sebastes diploproa* (Pisces: Scorpaenidae) from $^{210}Pb/^{226}Ra$ measurements in otoliths. Marine Biology 71, 209–215. (doi:10.1007/BF00394632)

Boyer, T.P., Antonov, J.I., Baranova, O.K., Coleman, C., Garcia, H.E., Grodsky, A., Johnson, D.R., Locarnini, R.A., Mishonov, A. V, Brien, T.D.O., Paver, C.R., Reagan, J.R., Seidov, D., Smolyar, I. V, Zweng, M.M., Sullivan, K.D., 2013. World Ocean Database 2013. (doi:10.7289/V5NZ85MT)

Brothers, E., Mathews, C., Lasker, R., 1976. Daily growth increments in otoliths from larval and adult fishes. Fisheries Bulletin 74.

Busby, M.S., 2005. An unusual macrourid larva (Gadiformes) from San Juan Island, Washington, USA. Ichthyological Research, 52(1), 86–89. (doi:10.1007/s10228-004-0255-1)

Bryden, H.L., 1973. New polynomials for thermal expansion, adiabatic temperature gradient, and potential temperature of sea water. Deep-Sea Research and Oceanographic Abstracts 20, 401–408. (doi:10.1016/0011-7471(73)90063-6)

Cailliet, G.M., Andrews, A.H. 2008. Age-validated longevity of fishes: Its importance for sustainable fisheries. In: Fisheries for global welfare and environment. Eds: K. Tsukamoto, Kawamura, Takeuchi, T.T., Beard, Jr., T.D., Kaiser, M.J. 5th World Fisheries Congress 2008, TERRAPUB, Tokyo, Japan. pp. 103–120.

Cailliet, G., Andrews, A., Burton, E., Watters, D., Kline, D., Ferry-Graham, L., 2001. Age determination and validation studies of marine fishes: do deep-dwellers live longer? Experimental Gerontology 36, 739–764. (doi:10.1016/S0531-5565(00)00239-4)

Campana, S., 2001. Accuracy, precision, and quality control in age determination, including a review of the use and abuse of age validation methods. Journal of Fish Biology 59, 197–242. (doi:10.1006/jfbi.2001.1668)

Campana, S., Neilson, J., 1985. Microstructure of fish otoliths. Canadian Journal of Fisheries and Aquatic Sciences 42, 1014–1032. (doi:10.1139/f85-127)

Campana, S., Thorrold, S., 2001. Otoliths, increments, and elements: keys to a comprehensive understanding of fish populations? Canadian Journal of Fisheries and Aquatic Sciences 58, 30–38. (doi:10.1139/f00-177)

CARE, Committee of Age Reading Experts, 2006. Manual on Generalized Age Determination.

Chang, N.N., Liu, E.Y., Liao, Y.C., Shiao, J.C., 2015. Vertical habitat shift of viviparous and oviparous deep-sea cusk eels revealed by otolith microstructure and stable-isotope composition. Journal of Fish Biology 86, 845–853. (doi:10.1111/jfb.12605)

Clayton, R.N., Goldsmith, J.R., Karel, K.J., Mayeda, T.K., Robert C., N., 1975. Limits on the effect of pressure on isotopic fractionation. Geochimica et Cosmochimica Acta 39, 1197–1201. (doi:10.1016/0016-7037(75)90062-9)

Coplen, T.B., Kendall, C., Hopple, J., 1983. Comparison of stable isotope reference samples. Nature 302, 236. (doi:10.1038/302236a0)

Danovaro, R., Gambi, C., Della Croce, N., 2002. Meiofauna hotspot in the Atacama Trench, eastern South Pacific Ocean. Deep-Sea Research Part I: Oceanographic Research Papers 49, 843–857. (doi:10.1016/S0967-0637(01)00084-X)

Degens, E., Deuser, W., Haedrich, R., 1969. Molecular structure and composition of fish otoliths. International Journal on Life in Oceans and Coastal Waters 2, 105–113. (doi:10.1007/BF00347005)

Drazen, J.C., 2002. A seasonal analysis of the nutritional condition of deep-sea macrourid fishes in the north-east Pacific. Journal of Fish Biology, 60(5), 1280-1295. (doi:10.1006/jfbi.2002.1943)

Drazen, J.C., Popp, B.N., Choy, C.A., Clemente, T., De Forest, L., Smith, K.L., 2008. Bypassing the abyssal benthic food web: Macrourid diet in the eastern North Pacific inferred from stomach content and stable isotopes analyses. Limnology and Oceanography 53(6), 2644–2654. (doi:10.4319/lo.2008.53.6.2644)

Drazen, J., Haedrich, R., 2012. A continuum of life histories in deep-sea demersal fishes. Deep-Sea Research Part I: Oceanographic Research Papers 61, 34–42. (doi:10.1016/j.dsr.2011.11.002)

Elsdon, T.S., Gillanders, B.M., 2002. Interactive effects of temperature and salinity on otolith chemistry: challenges for determining environmental histories of fish. Canadian Journal of Fisheries and Aquatic Sciences 59, 1796–1808. (doi:10.1139/f02-154)

Falk-Petersen, I., Frivoli, V., Gulliksen, B., Haug, T., Vader, W., 1988. Age/size relations and food of two snailfishes, *Liparis gibbus* and *Careproctus reinhardii* (Teleostei, Liparididae) from Spitsbergen coastal waters. Polar Biology 8, 353–358. (doi:10.1007/BF00442026)

Fisher, R., Raitt, R., 1962. Topography and structure of the Peru-Chile Trench. Deep-Sea Research 9, 423–443. (doi:10.1016/0011-7471(62)90094-3)

Fowler, A., Campana, S., Thorrold, S., Jones, C., 1995. Experimental assessment of the effect of temperature and salinity on elemental composition of otoliths using solution-based ICPMS. Canadian Journal of Fisheries and Aquatic Sciences 52, 1421–1430. (doi:10.1139/f95-137)

Francis, R.I.C.C., Horn, P.L. 1997. Transition zone in otoliths of orange roughy (*Hoplostethus atlanticus*) and its relationship to the onset of maturity. Marine Biology 129, 681. (doi:10.1007/s002270050211)

Fujii, T., Jamieson, A., Solan, M., Bagley, P., Priede, I., 2010. A large aggregation of liparids at 7703 meters and a reappraisal of the abundance and diversity of hadal fish. Bioscience 60, 506–515. (doi:10.1525/bio.2010.60.7.6)

George, R., Higgins, R., 1979. Eutrophic hadal benthic community in the Puerto Rico Trench. Ambio Special Reports 51–58.

Gerringer, M.E., Popp, B.N., Linley, T.D., Jamieson, A.J., Drazen, J.C., 2017. Comparative feeding ecology of abyssal and hadal fishes through stomach content and amino acid isotope analysis. Deep-Sea Research Part I: Oceanographic Research Papers 121, 110–120. (doi:10.1016/j.dsr.2017.01.003)

Gordon, J., Swan, S., 1996. Validation of age readings from otoliths of juvenile roundnose grenadier, *Coryphaenoides rupestris*, a deep-water macrourid fish. Journal of Fish Biology 49, 289–297. (doi:10.1111/j.1095-8649.1996.tb06082.x)

Grønkjær, P., Pedersen, J., Ankjærø, T., Kjeldsen, H., Heinemeier, J., Steingrund, P., Nielsen, J., Christensen, J., 2013. Stable N and C isotopes in the organic matrix of fish otoliths: validation of a new approach for studying spatial and temporal changes in the trophic structure of aquatic ecosystems. Canadian Journal of Fisheries and Aquatic Sciences 146, 143–146. (doi:10.1139/cjfas-2012-0386)

Høie, H., Otterlei, E., Folkvord, A., 2004. Temperature-dependent fractionation of stable oxygen isotopes in otoliths of juvenile cod (*Gadus morhua*). ICES Journal of Marine Science 61, 243–251. (doi:10.1016/j.icesjms.2003.11.006)

Horn P.L., Neil H.L., Paul L.J., Marriott P., 2010. Age validation and growth of bluenose *Hyperoglyphe antarctica* using the bomb chronometer method of radiocarbon ageing. Journal of Fish Biology 77, 1552–1563. (doi:10.1111/j.1095-8649.2010.02787.x)

Horn, P.L., Tracey, D.M., Clark, M.R., 1998. Between area differences in age and length at first maturity of orange roughy (*Hoplostethus atlanticus*). Marine Biology 132, 187–194. (doi:10.1007/s002270050385)

Horn, P.L., Neil, H.L., Paul, L. J., McMillan, P. J., 2012. Age verification, growth, and life history of rubyfish *Plagiogeneion rubiginosum.* New Zealand Journal of Marine and Freshwater Research. 46, 353–368. (doi:10.1080/00288330.2012.676052)

Hüssy, K., Hinrichsen, H.-H., Fey, D., Walther, Y., Velasco, A., 2010. The use of otolith microstructure to estimate age in adult Atlantic cod *Gadus morhua*. Journal of Fish Biology 76, 1640–54. (doi:10.1111/j.1095-8649.2010.02602.x)

Ichino, M.C., Clark, M.R., Drazen, J.C., Jamieson, A., Jones, D.O.B., Martin, A.P., Rowden, A.A., Shank, T.M., Yancey, P.H., Ruhl, H.A., 2015. The distribution of benthic biomass in hadal trenches: A modelling approach to investigate the effect of vertical and lateral organic matter transport to the sea floor. Deep-Sea Research Part I: Oceanographic Research Papers 100, 21–33. (doi:10.1016/j.dsr.2015.01.010)

Itoh, M., Kawamura, K., Kitahashi, T., Kojima, S., Katagiri, H., Shimanaga, M., 2011. Bathymetric patterns of meiofaunal abundance and biomass associated with the Kuril and Ryukyu trenches, western North Pacific Ocean. Deep-Sea Research Part I: Oceanographic Research Papers 58, 86–97. (doi:10.1016/j.dsr.2010.12.004)

Itou, M., Matsumura, I., Noriki, S., 2000. A large flux of particulate matter in the deep Japan Trench observed just after the 1994 Sanriku-Oki earthquake. Deep-Sea Research Part I: Oceanographic Research Papers 47, 1987–1998. (doi:10.1016/S0967-0637(00)00012-1)

Jackson, J.R., 2007. Earliest references to age determination of fishes and their early application to the study of fisheries. Fisheries. 32(7), 321–328. (doi:10.1577/1548-8446(2007)32[321:ERTADO]2.0.CO;2)

James, G.D., Inada, T., Nakamura, I., 1988. Revision of the oreosomatid fishes (family Oreosomatidae) from the southern oceans, with a description of a new species. New Zealand Journal of Zoology 15, 291–326. (doi:10.1080/03014223.1988.10422620)

Jamieson, A.J., 2015. The hadal zone: life in the deepest oceans. Cambridge, United Kingdom.

Jamieson, A., Fujii, T., Solan, M., Matsumoto, A., Bagley, P., Priede, I., 2009. Liparid and macrourid fishes of the hadal zone: *in situ* observations of activity and feeding behaviour. Proceedings of the Royal Society B: Biological Sciences 276, 1037–45. (doi:10.1098/rspb.2008.1670)

Kalish, J., 1991. ^{13}C and ^{18}O isotopic disequilibria in fish otoliths: metabolic and kinetic effects. Marine Ecology Progress Series 75, 191–203. (doi:10.3354/meps075191)

Kalish, J., 1989. Otolith microchemistry: validation of the effects of physiology, age, and environment on otolith composition. Journal of Experimental Marine Biology and Ecology 132, 151–178. (doi:10.1016/0022-0981(89)90126-3)

Kita, N.T., Ushikubo, T., Fu, B., Valley, J.W., 2009. High precision SIMS oxygen isotope analysis and the effect of sample topography. Chemical Geology 264, 43–57. (doi:10.1016/j.chemgeo.2009.02.012)

Kozdon, R., Kelly, D.C., Kita, N.T., Fournelle, J.H., Valley, J.W., 2011. Planktonic foraminiferal oxygen isotope analysis by ion microprobe technique suggests warm tropical sea surface temperatures during the Early Paleogene. Paleoceanography 26, 1–17. (doi:10.1029/2010PA002056)

Kozdon, R., Kelly, D.C., Kitajima, K., Strickland, A., Fournelle, J.H., Valley, J.W., 2013. *In situ* $\delta^{18}O$ and Mg/Ca analyses of diagenetic and planktic foraminiferal calcite preserved in a deep-sea record of the Paleocene-Eocene thermal maximum. Paleoceanography 28, 517–528. (doi:10.1002/palo.20048)

Lampitt, R.S., 1985. Evidence for the seasonal deposition of detritus to the deep-sea floor and its subsequent resuspension. Deep-Sea Research Part A: Oceanographic Research Papers 32, 885–897. (doi:10.1016/0198-0149(85)90034-2)

Lin, H., Shiao, J., Chen, Y., Iizuka, Y., 2012. Ontogenetic vertical migration of grenadiers revealed by otolith microstructures and stable isotopic composition. Deep-Sea Research Part I: Oceanographic Research Papers 61, 123–130. (doi:10.1016/j.dsr.2011.12.005)

Linley, T.D., Gerringer, M.E., Yancey, P.H., Drazen, J.C., Weinstock, C.L., Jamieson, A.J., 2016. Fishes of the hadal zone including new species, *in situ* observations and depth records of Liparidae. Deep-Sea Research Part I: Oceanographic Research Papers 114, 99–110. (doi:http://dx.doi.org/10.1016/j.dsr.2016.05.003)

Linley, T.D., Stewart, A.L., McMillan, P.J., Clark, M.R., Gerringer, M.E., Drazen, J.C., Fujii, T., Jamieson, A.J., 2017. Bait attending fishes of the abyssal zone and hadal boundary: Community structure, functional groups and species distribution in the Kermadec, New Hebrides and Mariana trenches. Deep-Sea Research Part I: Oceanographic Research Papers 121, 38–53. (doi:10.1016/j.dsr.2016.12.009)

Locarnini, R., Mishonov, A., Antonov, J., Boyer, T., Garcia, H., Baranova, O., Zweng, M., Paver, C., Reagan, J., Johnson, D., Hamilton, M., Seidov, D., 2013. World Ocean Atlas 2013, Volume 1: Temperature. NOAA Atlas 73, 40 pp.

Longmore, C., Trueman, C.N., Neat, F., O'Gorman, E.J., Milton, J.A., Mariana, S., 2011. Otolith geochemistry indicates life-long spatial populaiton structuring in deep-sea fish, *Coryphaenoides rupestris*. Marine Ecology Progress Series 435, 209–224. (doi:10.3354/meps09197)

Lutz, M.J., Caldeira, K., Dunbar, R.B., Behrenfeld, M.J., 2007. Seasonal rhythms of net primary production and particulate organic carbon flux to depth describe the efficiency of biological pump in the global ocean. Journal of Geophysical Research: Oceans 112, C10011. (doi:10.1029/2006JC003706)

Mace, P.M., Fenaughty, J.M., Coburn, R.P., Doonan, I.J., Mace, P.M., Fenaughty, J.M., Coburn, R.P., Doonan, I.J., Mace, P.M., Fenaughty, J.M., Coburn, R.P., Doonan, I., 1990. Growth and productivity of orange roughy (*Hoplostethus atlanticus*) on the north Chatham Rise. New Zealand Journal of Marine and Freshwater Research 24, 105–119. (doi:10.1080/00288330.1990.9516406)

Matsui, T., Kato, S., Smith, S., 1991. Biology and potential use of pacific grenadier, *Coryphaenoides acrolepis*, off California. Marine Fisheries Review 52(3), 1–17.

Matta, M.E., Orland, I.J., Ushikubo, T., Helser, T.E., Black, B.A., Valley, J.W., 2013. Otolith oxygen isotopes measured by high-precision secondary ion mass spectrometry reflect life history of yellowfin sole (*Limanda apsera*). Rapid Communications in Mass Spectrometry 27(6), 691–699. (doi:10.1002/rcm.6502)

Mead, G., Bertelsen, E., Cohen, D., 1964. Reproduction among deep-sea fishes. Deep-Sea Research 11, 569–596. (doi:10.1016/0011-7471(64)90003-8)

Merrett, N.R., Haedrich, R.L., 1997. Deep-sea demersal fish and fisheries. Chapman & Hall, London, 282 p.

Morales-Nin, B., Panfili, J., 2005. Seasonality in the deep sea and tropics revisited: what can otoliths tell us? Marine and Freshwater Research, 56(5), 585–598. (doi:10.1071/MF04150)

Nelson, G.A., 2016. Fishmethods: Fishery Science Methods and Models in R.

Nielsen, J., 1964. Fishes from depths exceeding 6000 meters. Galathea Rep. 7, 113–124.

Oguri, K., Kawamura, K., Sakaguchi, A., Toyofuku, T., Kasaya, T., Murayama, M., Fujikura, K., Glud, R., Kitazato, H., 2013. Hadal disturbance in the Japan Trench induced by the 2011 Tohoku-Oki earthquake. Scientific Reports 3, 1915. (doi:10.1038/srep01915)

Olson, I.C., Kozdon, R., Valley, J.W., Gilbert, P.U.P.A., 2012. Mollusk shell nacre ultrastructure correlates with environmental temperature and pressure. Journal of the American Chemical Society 134, 7351–7358. (doi:10.1021/ja210808s)

Orlov, A., Tokranov, A., 2011. Some rare and insufficiently studied snailfish (Liparidae, Scorpaeniformes, Pisces) in the Pacific Waters off the Northern Kuril Islands and Southeastern Kamchatka, Russia. ISRN Zoology 2011, 1–12. (doi:10.5402/2011/341640)

Pannella, G., 1980. Growth patterns in fish sagittae. Plenum Press, New York, NY, United States.

Pardo, S.A., Cooper, A.B., Dulvy, N.K., 2013. Avoiding fishy growth curves. Methods in Ecology and Evolution 4(4), 353–360. (doi:10.111/2041-210x.12020)

Pilling, G., Grandcourt, E., Kirkwood, G., 2003. The utility of otolith weight as a predictor of age in the emperor *Lethrinus mahsena* and other tropical fish species. Fisheries Research 60, 493–506. (doi:10.1016/S0165-7836(02)00087-5)

Poltev, Y., Steksova, V., 2010. Cases of spawn occurrence of fishes of the genus *Squaloliparis* (Osteichthyes: Liparidae) in crab traps in waters of southeastern Sakhalin. Russian Journal of Marine Biology 36, 316–319. (doi:10.1134/S1063074010040115)

Polyakov, V.B., Kharlashina, N.N., 1994. Effect of pressure on equilibrium isotopic fractionation. Geochimica et Cosmochimica Acta 58, 4739–4750. (doi:10.1016/0016-7037(94)90204-6)

Richardson, M., Briggs, K., Bowles, F., Tletjent, J., 1995. A depauperate bentbic assemblage from the nutrient-poor sediments of the Puerto Rico Trench. Deep-Sea Research Part I: Oceanographic Research Papers 42, 351–364. (doi:10.1016/0967-0637(95)00007-S)

Rowe, G., 2013. Seasonality in deep-sea food webs—A tribute to the early works of Paul Tyler. Deep-Sea Research Part II: Topical Studies in Oceanography 92, 9–17. (doi:10.1016/j.dsr2.2013.01.025)

Schneider, C.A., Rasband, W.S., Eliceiri, K.W., 2012. NIH Image to ImageJ: 25 years of image analysis. Nature Methods 9, 671–675. (doi:10.1038/nmeth.2089)

Shephard S., Trueman C., Rickaby R., Rogan E., 2007. Juvenile life history of NE Atlantic orange roughy from otolith stable isotopes. Deep-Sea Research Part I: Oceanographic Research Papers 54, 1221–1230. (doi:10.1016/j.dsr.2007.05.007)

Shiao, J., Itoh, S., Yurimoto, H., Iizuka, Y., Liao, Y., 2014. Oxygen isotopic distribution along the otolith growth axis by secondary ion mass spectrometry: Applications for studying ontogenetic change in the depth inhabited by deep-sea fishes. Deep-Sea Research Part I: Oceanographic Research Papers 84, 50–58. (doi:10.1016/j.dsr.2013.10.006)

Shiao, J.C., Liu, E.Y., Sui, T.D., 2016. Up-and-down shift in residence depth of slickheads (Alepocephalidae) revealed by otolith stable oxygen isotopic composition. Journal of Fish Biology 88(3), 1265–1272. (doi:10.1111/jfb.12904)

Shiao, J.C., Sui, T.D., Chang, N.N., Chang, C.W., 2017. Remarkable vertical shift in residence depth links pelagic larval and demersal adult jellynose fish. Deep-Sea Research Part I: Oceanographic Research Papers 121, 160–168. (doi:10.1016/j.dsr.2017.01.011)

Smith, D.C., Fenton, G.E., Robertson, S.G., Short, S.E., 1995. Age determination and growth of orange roughy (*Hoplostethus atlanticus*): a comparison of annulus counts with radiometric ageing. Canadian Journal of Fisheries and Aquatic Sciences 52, 391–401. (doi:10.1139/f95-041)

Stein, D., 2005. Descriptions of four new species, redescription of *Paraliparis membranaceus*, and additional data on species of the fish family Liparidae (Pisces, Scorpaeniformes) from the west coast of South America and the Indian Ocean. Zootaxa 1–25. (doi:10.11646/zootaxa.1019.1.1)

Stein, D., 1980. Aspects of reproduction of liparid fishes from the continental slope and abyssal plain off oregon, with notes on growth. Copeia 1980, 687–699.

Stewart, B.D., Fenton, G.E., Smith, D.C., Short, S.E., 1995. Validation of otolith-increment age estimates for a deepwater fish species, the warty oreo *Allocyttus verrucosus*, by radiometric analysis. Marine Biology 123, 29–38. (doi:10.1007/BF00350320)

Swan, S.C., Gordon, J.D.M., 2001. A review of age estimation in macrourid fishes with new data on age validation of juveniles. Fisheries Research 51, 177–195. (doi:10.1016;/S0165-7836(01)00244-2)

R Core Development Team, 2015. R: A Language and Environment for Statistical Computing. R Found. Stat. Comput. Vienna, Au.

Thorrold, S., Campana, S., Jones, C., Swart, P., 1997. Factors determining ^{13}C and ^{18}O fractionation in aragonitic otoliths of marine fish. Geochimica et Cosmochimica Acta 61, 2909–2919.

Tracey, D.M., Horn, P.L., 1999. Background and review of ageing of orange roughy (*Hoplostethus atlanticus*) from New Zealand and elsewhere. New Zealand Journal of Marine Freshwater Research. 33, 67–86. (doi:10.1080/00288330.1999.9516868)

Trueman, C.N., Mackenzie, K.M., Palmer, M.R., 2012. Identifying migrations in marine fishes through stable-isotope analysis. Journal of Fish Biology 81, 826–847. (doi:10.1111/j.1095-8649.2012.03361.x)

Trueman, C., Rickaby, R., Shephard, S., 2013. Thermal, trophic and metabolic life histories of inaccessible fishes revealed from stable-isotope analyses: a case study using orange roughy *Hoplostethus atlanticus*. Journal of Fish Biology 83, 1613–1636. (doi:10.1111/jfb.12267)

Wickam, H., 2009. ggplot2: elegant graphics for data analysis.

Williams, T., Bedford, B., 1974. The use of otoliths for age determination, in: Bagenal, T.B. (Ed.), Ageing of Fish. Unwin Brothers, Old Woking, England, pp. 114–123.

Wilson, R., 1988. Analysis of growth zones and microstructure in otoliths of two macrourids from the North Pacific abyss. Environmental Biology of Fishes 21, 251–261. (doi:10.1007/BF00000374)

Wolff, T., 1959. The hadal community, an introduction. Deep-Sea Research 6, 95–124. (doi:10.1016/0146-6313(59)90063-2)

Yau, C., Collins, M., Everson, I., 2000. Commensalism between a liparid fish (*Careproctus* sp.) and stone crabs (Lithodidae) photographed *in situ* using a baited camera. Journal of the Marine Biological Association of the United Kingdom 80, 379–380. (doi:10.1017/S0025315499002052)

CHAPTER V

Distribution, composition, and functions of gelatinous tissues in deep-sea fishes

Abstract

Many deep-sea fishes have a gelatinous layer, or subdermal extracellular matrix, below the skin or around the spine. We document the distribution of gelatinous tissues across fish families (~200 species in ten orders), then review and investigate their composition and function. Gelatinous tissues from nine species were analysed for water content (96.53±1.78%), ionic composition, osmolality, protein (0.39±0.23%), lipid (0.69±0.56%), and carbohydrate (0.61±0.28%). Results suggest that gelatinous tissues are mostly extracellular fluid, which may allow animals to grow inexpensively. Further, almost all gelatinous tissues floated in cold seawater, thus may contribute to buoyancy through low density in some species. We also propose a new hypothesis: gelatinous tissues, which are inexpensive to grow, may sometimes provide a method to increase swimming efficiency by fairing the transition from trunk to tail. Such a layer is particularly prominent in hadal snailfishes (Liparidae); therefore, a robotic snailfish model was designed and constructed to analyse the influence of gelatinous tissues on locomotory performance. The model swam faster with a water layer, functionally representing gelatinous tissue, around the tail than without. Results suggest that the tissues may, in addition to providing buoyancy and low-cost growth, aid deep-sea fish locomotion.

Introduction

In some species of fishes, a distinct watery tissue layer is present, usually between the skin and muscle or between muscle bundles (**Figure 5.1**). It has long been known that fishes in the superorder Elopomorpha (Anguilliformes, Albuliformes, Elopiformes, and Saccopharyngiformes) have larvae called leptocephali in which most of the body consists of an acellular gelatinous matrix providing structural support in the absence of a vertebral column and transparency for camouflage (e.g., Pfeiler, 1999; Miller, 2009). The first known scientific record of these tissues in a fully adult

fish comes from the Challenger Report description of the gelatinous blind cusk eel *Aphyonus gelatinosus*, in which the 'anterior half of the skin forms a large loose bag which, during life, is probably filled and distended with mucus' (Günther, 1887). Gelatinous tissue is even a defining character in the genus *Careproctus* of the family Liparidae (snailfish), which 'best illustrates the production of pseudotissue which envelops the body and fins just beneath the skin' (Burke, 1930). The literature sometimes refers to these tissues as the subdermal extracellular matrix, or SECM (e.g., Eastman et al., 1994; Ozaka et al., 2009). More recently, such tissues have been found in species of hadal snailfish in the Kermadec and Mariana trenches. In a freshly collected fish, the layer of clear gelatinous tissue is prominent (**Figure 5.1a**), though as the skin is lacerated, this tissue leaks out and melts away. It is largely concentrated just behind the abdominal cavity, with a thin layer around the tail.

Although these gelatinous tissues have been noted in several species and can compose up to a third of the mass of a fish (Eastman et al., 1994), they have not been compared across families and their functions remain unresolved. In addition to structural support and transparency, one possible role proposed for gelatinous larval fishes (e.g., Marliave and Peden, 1989) and some deep-sea invertebrates (e.g., Mitra and Zaman, 2016) is to allow growth to large size at low metabolic cost. This hypothesis may apply to adult fishes as well. One study investigated the potential antifreeze function of the gelatinous tissues in an Antarctic fish, but found no evidence to suggest a role in cold-tolerance (Jung et al., 1995). Eastman et al. (1994) found free nerve endings present within the gelatinous tissues of *Paraliparis devriesi*. It was hypothesized that these may serve as mechanoreceptors in three Antarctic liparids, allowing the fish to detect displacement of the gelatinous layer during movement (Eastman and Lannoo, 1998; Lannoo et al., 2009). The potential sensory role of gelatinous tissues, however, is proposed to be secondary to another function—buoyancy.

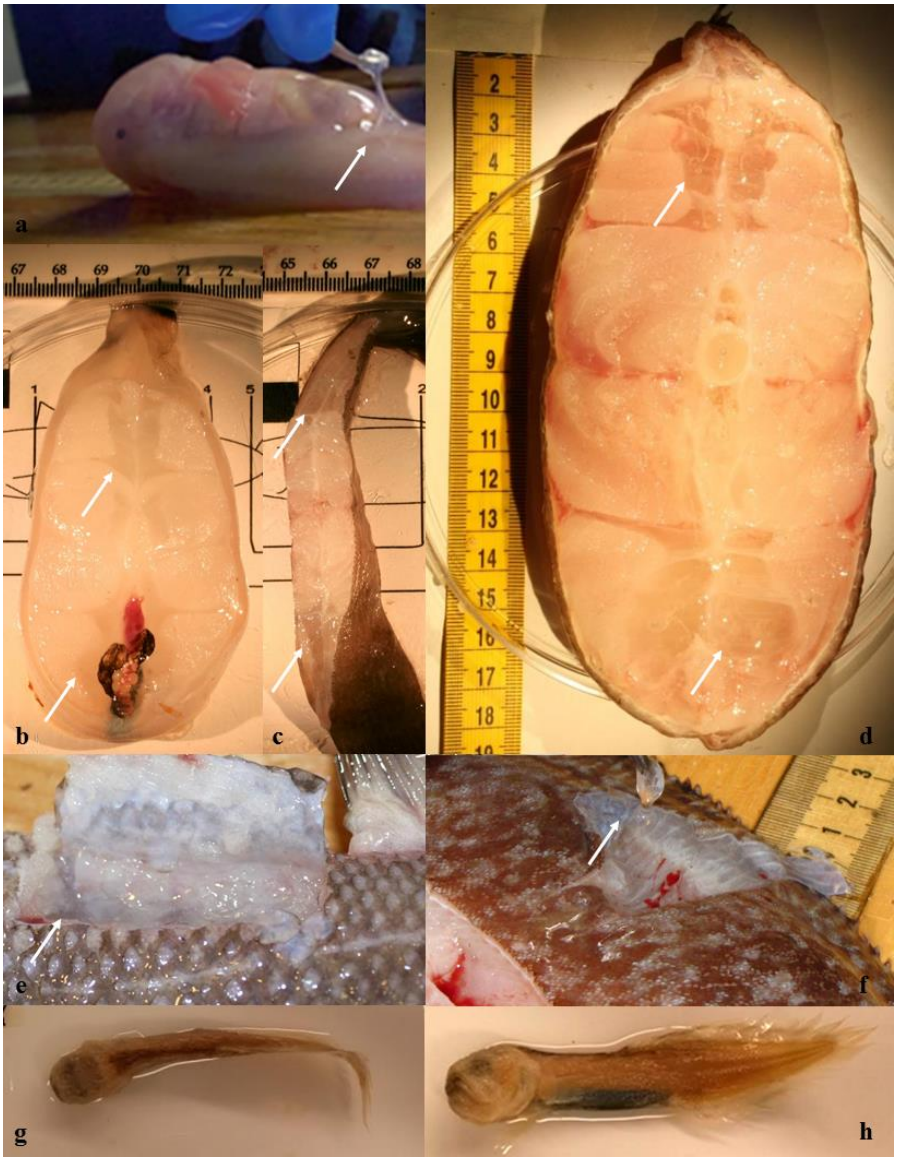

Figure 5.1. Gelatinous Tissues. Arrows point to gelatinous tissue layers. a) *Notoliparis kermadecensis*, family Liparidae, hadal snailfish. Gelatinous tissues prominent directly below skin, concentrated around posterior of cavity and along tail. *Photo by J. Reed. Image courtesy of the HADES Program, NSF, NOAA OER, (© WHOI).* b - d) Cross-sections of fishes showing gelatinous tissues bundles. b) Twoline eelpout, *Bothracara brunneum*, family Zoarcidae. c) Deep-sea sole, *Embassichthys bathybius*, family Pleuronectidae. *Photos by J. Friedman.* d) Giant cusk eel, *Spectrunculus grandis*, family Ophidiidae. *Photo by P. Yancey.* e) Gelatinous tissues between muscle bands in *Coryphaenoides yaquinae*, family Macrouridae. *Photo by M. Gerringer.* f) *E. bathybius* gelatinous tissues. *Photo by P. Yancey.* g/h) Preserved *Barathronus* sp., family Aphyonidae (SIO 92-109). In life, body is surrounded with gelatinous tissues. With tissues gone, body is thin and flat. Dorsal (g) and lateral (h) views. *Photos by M. Gerringer.*

Gelatinous layers have been described in a number of mid-water fishes, leading to the hypothesis that they are an adaptation for buoyancy, first introduced by Denton and Marshall (1958) and expanded by Davenport and Kjorsvik (1986) and Yancey et al. (1989). In all but the deepest-living teleost fishes, internal ion concentrations and osmolalities are lower than seawater. For example, extracellular fluids of typical shallow teleosts have about 170 mM NaCl and lesser amounts of other ions, yielding an osmolality of 350–400 mosmoles/kg (e.g., Prosser et al., 1970). In comparison, average seawater has roughly 500 mM NaCl plus other ions yielding about 1000–1100 mosmoles/kg. Thus, extracellular fluid, including that in gelatinous tissues, with very little non-lipid organic material will be less dense than seawater (unlike many tissues such as muscle, bone, and cartilage). In addition, some gelatinous tissues in midwater fishes have even lower ion concentrations than other body fluids, further increasing buoyancy (Yancey et al., 1989). The buoyancy hypothesis was further supported by Eastman et al. (1994) in a study of gelatinous tissues in the Antarctic snailfish, *Paraliparis devriesi*, which are believed to achieve neutral buoyancy through decreased bone ossification and the presence of this layer. These low-density tissues and fluids would be adaptive under the high hydrostatic pressures of the deep sea, where the inflation of a swimbladder becomes increasingly difficult (Scholander, 1954).

References to the presence and function of gelatinous tissues have often been speculative and passing. Here, we analyse compositions of these tissues in selected species, evaluate the proposed buoyancy function, synthesize and review references to gelatinous tissues, investigate depth-related trends in the presence of these tissues, and introduce a new hypothesis: gelatinous tissues may be an adaptive method of changing body shape at low growth cost, acting as a fairing material to increase locomotor performance.

Materials & Methods

Proximate Chemistry and Buoyancy Tests. *Samples.* Fishes were collected by trawl from Monterey Bay in April and October 2009 and by baited trap in the Kermadec Trench in 2011 and 2014. Collection information for gelatinous tissues analysed in this study is presented in **Supplementary Table 5.1**. *Buoyancy.* Fresh pieces of gelatinous and white muscle tissues were placed about halfway down in a graduated cylinder or glass jar filled with seawater at 2–5°C

shortly after capture, and sink or rise times (to travel 6 cm) were measured. *Water Content.* Gelatinous tissues were dried at 60°C for three days and remaining dry mass was compared to original wet tissues mass. *Osmotic Pressure.* A vapour pressure osmometer, Wescor 5500, was used in the laboratory for most species, and at sea for *N. kermadecensis*, to determine sample osmolality. Samples were homogenized with a small pestle in a microfuge tube, then centrifuged at 2,000 x g for 30 minutes at 4°C. 10 µL of the resulting supernatant was measured with an osmometer. The 290 mmol/kg and 1000 mmol/kg standards were checked periodically to confirm accurate calibration. *Sample Preparation.* A section of frozen gelatinous tissues, clear of white muscle, was cut and weighed to obtain about 0.1 g, with a precision of 0.0001 g. The section was ground in 7% perchloric acid (PCA) or 70% ethanol, added at 9 times the tissues mass, to precipitate proteins. The sample was refrigerated overnight, then centrifuged for 20 minutes at 15,500 x g at 4ºC. The supernatant, transferred to a new tube, was used for inorganic ion and organic osmolyte analyses, while the pellet was used for protein analysis. When ethanol was used to homogenize tissues, the supernatant was evaporated and the remaining powder dissolved in distilled water. The supernatants in PCA were titrated with 2 M KOH to pH 6.5–7.5. The resulting precipitate was centrifuged and the supernatant removed to a new tube. The PCA method was not used for ion analysis because of the required addition of potassium. *Protein.* Protein content was determined with the Bicinchoninic Acid (BCA) Protein Assay (Smith et al., 1985). Bovine serum albumin was used as a standard. *Lipids.* Lipid contents were analysed using the Bligh and Dyer (1959) extraction and colorimetric determination of content with the sulfuric acid charring method of Marsh and Weinstein (1966) with triolein as a standard. *Carbohydrates.* Carbohydrate analysis was conducted using phenol and sulfuric acid (Dubois et al., 1956), with D-glucose as a standard, measured in a spectrophotometer (Beckman Coulter DU 730) at 480 nm. *Ions.* Sodium and potassium contents were analysed by atomic absorption (PerkinElmer AAnalyst 400) in 10 µL aliquots of the PCA homogenates dissolved in 10 mL of purified water. All results are presented as average ± standard deviation.

Taxonomic Distribution. Records of gelatinous tissues in fishes were collected in an extensive literature search. Recent unpublished findings from coastal to hadal surveys are also presented. Anecdotally, these tissues were thought to be more common in deeper-living fishes. To test this,

common depth ranges of fishes with gelatinous tissues were taken from FishBase (Froese and Pauly, 2015). The effects of phylogenetic relationships can confound interpretation of this type of analysis, as closely related species become a kind of pseudoreplicate (Felsenstein, 1985). To account for this potential error, and to clarify the distribution of gelatinous tissues across families, a phylogenetic tree was constructed using mitochondrial cytochrome oxidase subunit I (COI) gene sequences extracted from GenBank (Benson et al., 2009). Available sequences were selected from families with gelatinous tissues across representative depth ranges. A set of commonly sequenced fishes with available habitat depths was included for comparison. Sequences were aligned with the tool Multiple Sequence Comparison by Log-Expectation (MUSCLE, Edgar, 2004; McWilliam et al., 2013), a tree generated through Randomized Axelerated Maximum Likelihood (RAxML) using a bootstrap method with 1000 iterations (Stamatakis, 2014), both through the CIPRES (Cyberinfrastructure for Phylogenetic Research) Science Gateway (Miller et al., 2010). The tree was visualized through the Interactive Tree of Life (iTOL v3, Letunic and Bork, 2006). Statistical analyses were conducted in the programming platform R (R Core Development Team, 2015). Generalised linear models (GLM) using minimum and maximum depths, and the median of each depth range were fitted using the Gaussian family. Models were selected through optimization of Akaike Information Criteria (AIC).

Alteration of Body Shape. Few studies have investigated locomotion in deep-sea fishes (e.g., Bailey et al., 2003; Collins et al., 1999; Kenaley et al., 2014; Luck and Pietsch, 2008), largely due to the difficulty of direct experimentation. To test the effect of body shape change with gelatinous tissues, a robotic model was designed after the Kermadec Trench snailfish, *Notoliparis kermadecensis*. This technique has become a valuable tool to investigate swimming biomechanics in a number of shallow-living fishes (e.g., Lauder et al., 2012; Leftwich et al., 2012; Tangorra et al., 2011) and is well-suited to deep-sea species that cannot easily be brought into a laboratory setting. The plastic (PLA) body and fins were 3D printed (ORION HB #58744) based on a model constructed from a photogrammetry recreation of freshly captured specimens collected on the HADES (HADal Ecosystems Studies) Cruise in April and May of 2014 (Model: MeshMixer, Slicing: Cura, 3D Printing: Repetier Host). The swim test was programmed onto an Arduino Nano microcontroller. Tail beat frequency (0.5 beats per second) was chosen to match that found through

video analysis of the hadal snailfish, *Pseudoliparis belyaevi*, filmed *in situ* in the Japan Trench (described in Fujii et al., 2010). The robot was powered by a 9V battery with constant cycle-averaged power and swam using a Servo motor connected to two piano wires that oscillated the tail region back and forth (**Figure 5.2**). To simulate white muscle, a silicone rubber mould was cast for the tail. Two ~ten-second swim trials for the submerged, neutrally buoyant robot were conducted with both empty and full tail 'skin.' Water represented the gelatinous tissues, to isolate the shape effect from changes due to tail stiffness. In some species, such as the cusk eel *Spectrunculus grandis*, it is unlikely that the gelatinous tissue flows freely as water in our model would. However, in the liparids, morphological analyses suggest that gelatinous layers are displaced during movement (Eastman and Lannoo, 1998; Lannoo et al. 2009). This is also suggested by *in situ* video of hadal snailfishes swimming, which show the gelatinous tissues rippling under the skin, making water below the skin, rather than gelatine, an appropriate analogue. Swim trials were filmed and body lengths per second and tail beat amplitude were compared between trials (with the same tail beat frequency and power) using ImageJ (Schneider et al., 2012).

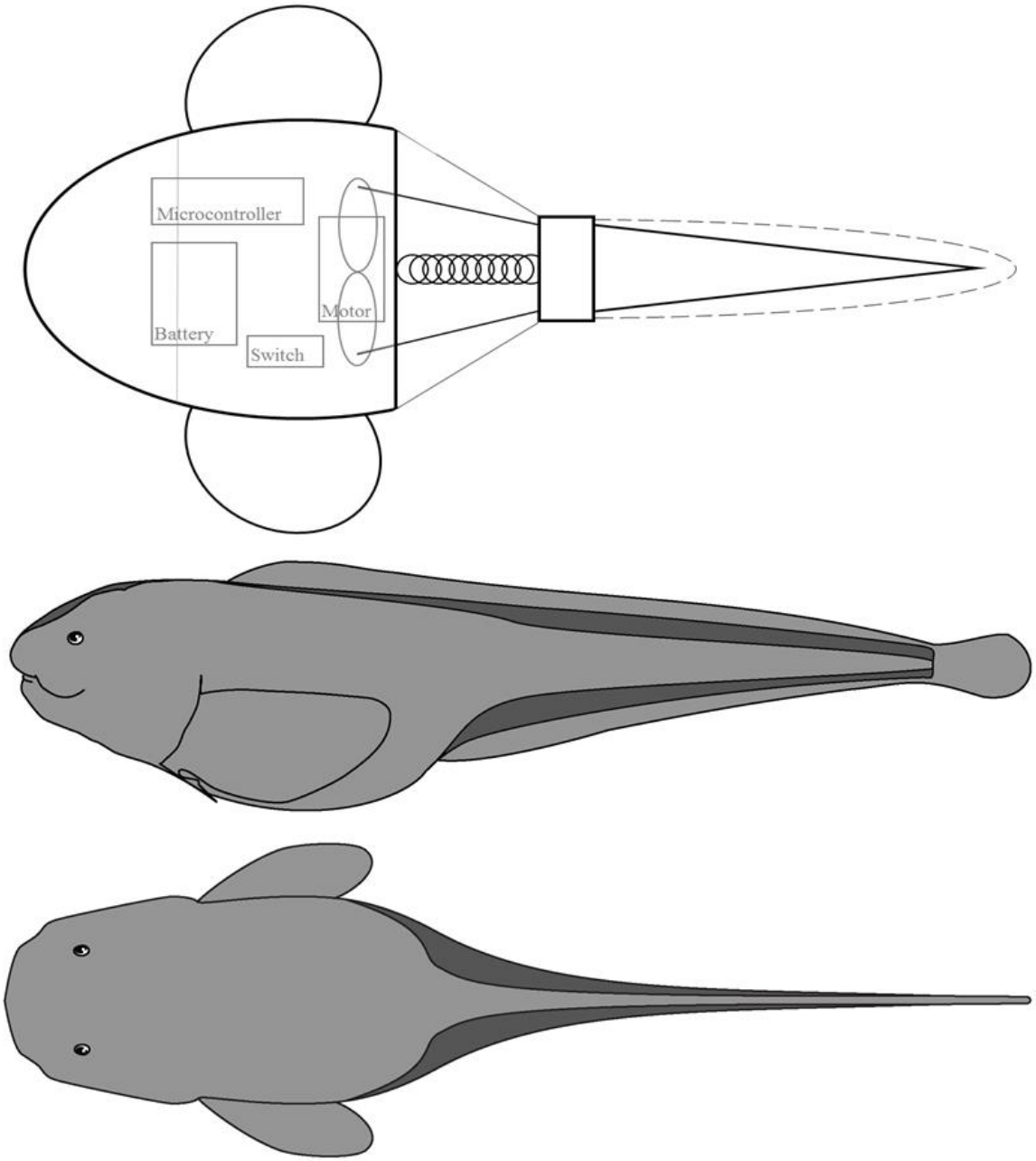

Figure 5.2. above) Schematic of robotic hadal snailfish model. Microcontroller (Arduino Nano), Motor (Tower Pro TM, Micro Servo 9g, SG90), Battery (Duracell, 9V). Tail muscle is a cast silicone rubber (Ecoflex R 00-10) with a volume-adjustable skin (latex condom, Trojan Magnum). Additional materials used include hot glue, a spring, piano wire, a bottle cap, marine epoxy, electrical tape, and miscellaneous hardware as ballast. Dotted line indicates outer skin, kept empty in trials with no gelatinous tissue analogue. below) Hadal liparid body shape with gelatinous tissues in dark grey. Dorsal and anal fin rays connect to epaxial and hypaxial muscle tissue while gelatinous tissues surround. *Drawing by T. Linley.*

Results

Buoyancy and Proximate Chemistry. In shipboard buoyancy experiments, gelatinous tissues from most species floated in seawater, the only exception being tissues from *N. kermadecensis*, which appeared to be neutrally buoyant (did not rise or sink in the cylinder). When placed in cold (2°C) seawater, a whole hadal snailfish sank very slowly, tail first. Float rates were collected for gelatinous tissues from five species. Tissues travelled 6 cm upwards in 2.96±0.26 seconds (*B. brunneum*, n=4), 2.53±0.86 seconds (*E. bathybius*, n=9), 3.55±0.60 seconds (*M. pacificus*, n=3), 1.16±0.31 seconds (*P. karenae*, n=3), and 3.71±0.80 seconds (*S. grandis* 2000 m, n=4).

Analyses of nine species (common depths 750–7500 m) revealed that tissues were primarily water (96.5±1.8%) with minor amounts of other constituents (**Table 5.1**). Protein, carbohydrate, and lipid contents were low (0.39±0.23, 0.61±0.28, and 0.69±0.57, respectively). Sodium contents were much higher than potassium contents (Na: K ratio from 18 to 38; Welch two-sample t-test, $p \leq 0.0001$), as is typical of extra- but not intracellular fluids. Sodium contents also trended higher with depth (157 mmol/kg at 1000 m to 362 at 7000 m) both inter- and intraspecifically (e.g., *S. grandis*, 205 mmol/kg at 2000 vs 318 mmol/kg at 4149 m). Most tissues had similar potassium contents (6.5–12.8 mmol/kg), though higher in the deepest fish, *N. kermadecensis* (14.4±0.7 mmol/kg). Osmolalities, in mosmoles/kg, were measured in gelatinous tissues of six species. Values ranged from 311–385 in four species from 1000–2000 m, and were higher in the two deeper species analysed, most notably *N. kermadecensis* at 945 mosmoles/kg.

Table 5.1. Proximate chemistry of gelatinous tissues in representative species. Numbers in parentheses indicate sample size for each analysis. Capture depth in meters. Sodium, potassium given in mmol/kg wet mass, and osmolality in mosmol/kg. *B. brunneum* osmolality value from sample collected at 2000 m.

Species	Capture Depth	Potassium	Sodium	Na/K	% Water	% Protein	% Carb	% Lipid	Osmolality
Careproctus melanurus	750–1000	8.47±0.82 (3)	157±30.4 (3)	18.5	98.4±0.26 (3)	0.21±0.22 (3)	0.99 (1)	0.2 (1)	
Careproctus cypselurus	1000	8.51 (1)	158 (1)	18.6	97.9 (1)	0.23 (1)	0.51 (1)	0.15 (1)	
Embassichthys bathybius	1000	7.24±2.5 (4)	187±23.8 (4)	25.9	97.0±1.32 (4)	0.25±0.09 (4)	0.51±0.19 (4)	1.58±1.77 (3)	377±16.2 (3)
Microstomus pacificus	1000	8.33±3.24 (3)	188±5.27 (3)	22.5	96.4±1.24 (3)	1.1±1.15 (3)	0.54±0.2 (3)	0.97±0.73 (3)	312 (1)
Bothrocara brunneum	1000–2000	9.23±1.24 (2)	196±7.42 (2)	21.2	97.6±0.84 (3)	0.37±0.03 (3)	0.58 (1)	0.28±0.19 (2)	385 (1)
Spectrunculus grandis	2000	12.8 (1)	205 (1)	16.0	96.5 (1)	0.63 (1)	1.25 (1)		355 (1)
Pachycara karenae	3000	6.54±0.47 (3)	195±14.5 (3)	29.9	95.8±1.13 (3)	0.65±0.28 (3)	0.38 (1)	1.31±0.12 (2)	467 (1)
Spectrunculus grandis.	4149	8.31 (1)	318 (1)	38.3					
Pyrolycus sp.	4817	8.20 (1)	284 (1)	34.6					
Notoliparis kermadecensis	7000–7500	14.4±0.72 (3)	362±38.4 (3)	28.4	93.1±0.55 (3)	0.65±0.09 (3)			945±78.7 (5)

Taxonomic Distribution. Fish species with gelatinous tissues were found in ten orders, thirteen families, and approximately 200 species, presented in **Table 5.2**. References to 'gelatinous tissues' or 'subdermal extracellular matrix' were included in these results. Fishes in the family Aphyonidae (recently absorbed into the Bythitidae; Møller et al., 2016) are described, for example: 'skin loose, transparent and gelatinous' (Nielsen et al., 1999). Images of freshly caught fish confirm that this refers to the gelatinous tissues. Other occurrences of gelatinous tissues have been seen and verified by the authors in recent captures. We note that the gelatinous tissues are present in many, but not all, species of the snailfish genus *Paraliparis*. Additional species of the genus *Lycodapus* may contain gelatinous tissues as well, though this has not been confirmed (Marliave and Peden, 1989). Depth ranges for species with gelatinous tissues are presented in **Table 5.2**. Median depths of occurrence ranged from approximately 300 to 7400 m (mean approximately 1800 m). Most species with records of gelatinous tissues typically live around or below 1000 m depth and include both benthic and pelagic species.

For phylogenetic comparisons and more robust testing of this depth trend, a selection of common depths of occurrence were collected from FishBase for 117 species, 17 of which are known to have gelatinous tissues (**Supplementary Table 5.2**). Generalized linear models showed fishes with gelatinous tissues to have significantly deeper min, mid, and maximum depths ($t=2.40$, $p<0.05$; $t=3.01$, $p<0.01$; $t=2.95$, $p<0.01$; 117 df) across all species, a finding confirmed by a non-parametric Kruskal-Wallis rank sum test (mid and max depths, $p\leq0.01$, $p=0.001$) across all species. This was also a significant trend within families (e.g., Gadiformes, min: $t=6.70$, $p<0.005$, mid: $t=4.75$, $p<0.005$, max: $t=3.20$, $p<0.01$, 27 df; Pleuronectiformes, mid: $t=3.0$, $p<0.01$, max: $t=3.1$, $p<0.01$, 16 df). Phylogenetic relationships between these species are presented in **Figure 5.3**, generated through alignment of mitochondrial COI sequences of 111 species, 17 with gelatinous tissues, available from GenBank. Sequence accession numbers are included in the supplemental information. Species with gelatinous tissues were present across multiple clades, and represent the deeper-living species within clades (further illustrated in **Supplementary Figure 5.1**).

Table 5.2. Fishes with gelatinous tissues, from literature and current capture data. Reference indicates the publication that describes the gelatinous tissues. Larval fishes with gelatinous tissues not included. [1]Anderson and Hubbs, 1981; [2]Anderson, 1994; [3]Anderson, 2012; [4]Andriashev and Pitruk, 1993; [5]Andriashev and Stein 1998; [6]Andriashev, 1998; [7]Bianchi et al., 1999; [8]Busby and Cartwright, 2009; [9]Chen, 2002; [10]Chernova, 2001; [11]Chernova and Møller, 2008; [12]Davenport and Kjorsvik, 1986; [13]Denton and Marshall, 1958; [14]Eastman et al., 1994; [15]Endo and Okamura, 1992; [16]Federov et al., 2003; [17]Friedman et al., 2012; [18]Fujii et al., 2010; [19]Hart, 1973; [20]Jamieson, et al. 2009; [21]Kai et al., 2011; [22]Knudsen and Møller, 2008; [23]Lannoo et al., 2009; [24]Linley et al., 2016; [25]Masuda et al. 1984; [26]Nielsen, 1986; [27]Nielsen, 1990; [28]Nielsen, 1998; [29]Nielsen et al., 1999; [30]Ozaka et al., 2009; [31]Parin et al., 2002; [32]Peden, 1979; [33]Pietsch, 1986; [34]Present Study; [35]Russian Academy of Sciences, 2000; [36]Shinohara et al., 1994; [37]Stein et al., 2001; [38]Stein, 2005; [39]Vetter et al., 1994; [40]Yancey et al., 1989. *Those species formerly classified as family Aphyonidae (Møller et al., 2016). **Pelagic fish, maximum depth greatly overestimated (Fujii et al., 2010). Note that some, but not all species of the genus *Paraliparis* have gelatinous tissues. Depth ranges presented in metres.

Order	Family	Genus or Species	Depth Range	Reference
Ateleopodiformes	Ateleopodidae	*Ateleopus japonicus*	140–600[9]	30
Gadiformes	Macrouridae	*Coryphaenoides yaquinae*	3400–6945[15, 20]	34
Lophiiformes	Melanocetidae	*Melanocetus johnsonii*	100–1500[33]	34
Ophidiiformes	Bythitidae	23 species*	2000–6000[28]	29
	Ophidiidae	*Apagesoma delosommatus*	2487–4150[29]	29
		Apagesoma edentatum	5082–8082[29]	29
		Barathrites iris	? –5285[26]	34
		Spectrunculus grandis	800–4300[7]	34
Osmeriformes	Bathylagidae	*Bathylagus pacificus*	772–7700**[35]	40
		Pseudobathylagus milleri	772–6600**[36]	40
Perciformes	Zoarcidae	*Bothrocara brunneum*	129–2570[16]	34
		Derepodichthys alepidotus	1000–2904[2]	1
		Lycodapus mandibularis	100–1370[19]	32
		Pachycara karenae	2780–3100[3]	34
Pleuronectiformes	Pleuronectidae	*Embassichthys bathybius*	41–1800[35]	39
		Microstomus pacificus	10–1370[35]	17
Saccopharyngiformes	Eurypharyngidae	*Eurypharynx pelecanoides*	1200–1400[25]	13
Scorpaeniformes	Cyclopteridae	*Cyclopterus lumpus*	0–868[31]	12
	Liparidae	*Careproctus*, 119 species	6–>5000[6]	5, 21, 22
		Lipariscus nanus	0–910[35]	38
		Nectoliparis pelagicus	557–3383[16]	38
		Notoliparis,4 species	5879–7669[24]	34
		Paraliparis, 26 species	233–2150[8, 11]	8, 11, 14, 23, 37
		Psednos balushkini	914–917[37]	37
		Psednos gelatinosus	0–650[10]	10
		Psednos nataliae	1100–1120[37]	37
		Pseudoliparis, 2 species	6945–7703[18]	4
Stomiiformes	Stomiidae	*Chauliodus macouni*	25–4390[27]	40
		Chauliodus sloani	494–100[36]	13
		Tactostoma macropus	30–2000[36]	40

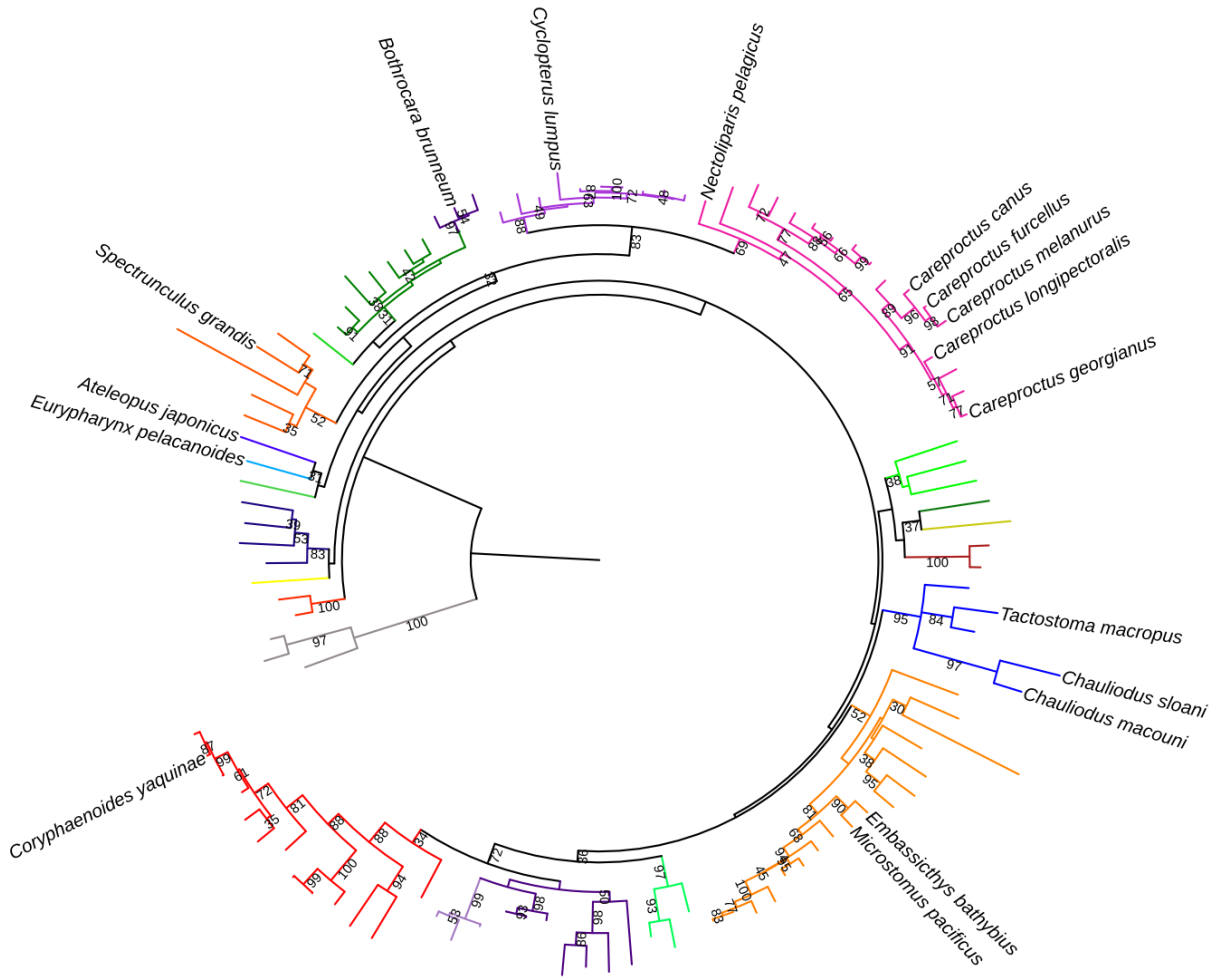

Figure 5.3. Phylogenetic relationships of a selection of species with gelatinous tissues. Based on mitochondrial COI gene sequences. Sequence accession numbers and depths included in supplemental information. Species with gelatinous tissues are labelled. Bootstrap confidence levels above 30% for the phylogeny are displayed. Stomiidae artificially grouped according to the phylogeny by Kenaley et al. (2013) based on alternative loci. Pleuronectidae and Paralichthyidae grouped (orange). Families are coloured, from root to tip: Myxinidae (outgroup, in gray), Bathylagidae (orange), Balistidae (yellow), Myctophidae (blue), Trichiuridae (green), Eurypharyngidae (light blue), Ateleopodidae (purple), Ophidiidae (orange), Hexagrammidae (light green), Stichaeidae (green), Zoarcidae (purple), Cyclopteridae (light purple), Liparidae (pink), Gobiidae (light green), Engraulidae (green), Callionymidae (yellow), Lophiidae (red), Stomiidae (blue), Paralichthyidae (orange), Pleuronectidae (orange), Serranidae (green), Moridae (purple), Gadidae (light purple), Macrouridae (red).

Alteration of Body Shape. Gelatinous tissues change the body shape of the hadal liparid, as illustrated in **Figure 5.2**. Intuitively, this changes the drag profile around the animal. In all swim trials, the robotic model performed significantly better with the gelatinous tissue analogue (0.074±0.007 body lengths per second) than without (0.022±0.007) with constant cycle-averaged power provided at a constant tail beat frequency of 0.5 beats per second (Welch two-sample t-test, $p=0.019$). Tail beat amplitude was 16.1±0.3% of body length and did not vary significantly between treatments ($p>0.05$).

Discussion

Distribution and Composition. Proximate chemical analysis of gelatinous tissues in nine benthic and benthopelagic species showed high water content and low protein, lipid, and carbohydrate content in comparison to white muscle (86.3±2.7% for 7 species with gelatinous tissues; Drazen et al., 2015). Our average for water content (96.5%) is consistent with previous studies of gelatinous tissues, which found 93.3% water in *Cyclopterus lumpus* (Davenport and Kjorsvik 1986), 96% in *Bathylagus pacificus* (Yancey et al., 1989), and 97% in *Paraliparis devriesi* (Eastman et al. 1994). Osmolality increases with depth, in part due to higher extracellular sodium and in part because of organic osmolytes (especially trimethylamine oxide, TMAO) that increase with depth to combat the negative effects of high hydrostatic pressure (Yancey et al., 2014; Linley et al., 2016). In concert with the ionic concentrations and osmolalities of these tissues, these data suggest that the layers are of similar compositions and are mainly extracellular fluid. The high seawater content of gelatinous tissues makes them inexpensive to produce in bulk.

We found support for the hypothesis that gelatinous tissues in fishes are a characteristically deep-sea phenomenon. Phylogenetic relationships were a potential concern; especially as there are certain genera where gelatinous tissues are more common—e.g., *Aphyonus, Careproctus, Paraliparis*. The method of Felsenstein (1985) for investigating trends without confounding influence of phylogeny is designed for use with continuous variables, but has been met with criticism for categorical variables (e.g., Maddison and FitzJohn, 2014). Considering these concerns, we investigated depth trends within clades. The results hold true within multiple orders: gelatinous tissues appear more often in deeper-living species. Although our phylogeny is based on

one locus and a limited number of sequences, it clearly illustrates the broad taxonomic distribution of gelatinous tissues. The fact that the gelatinous tissues are present across ten orders supports multiple evolutions of the tissues in deep-water species. In our limited phylogeny, we found evidence for at least eight potential evolutions of the tissues. In other phylogenies, supported by multiple loci and large numbers of sequences, gelatinous tissues are still present in species across many clades, from basal to highly derived (Near et al., 2013; Betancur-R. et al., 2013).

Although we were thorough in our literature searches and covered a broad depth range in our surveys, it is likely that the list presented in **Table 5.2** is not exhaustive. Often, the tissue has leaked away shortly after capture or during preservation, and it is not always recorded in taxonomic descriptions or it is regarded as unimportant. This study reveals how common and multi-functional gelatinous tissues may be, and we suggest that future studies should note its presence.

Gelatinous Tissues as a Buoyancy Mechanism. In our investigation, most gelatinous tissues did float in shipboard tests, suggesting that buoyancy is indeed a main function of these tissues, in agreement with most previous findings (Davenport and Kjorsvik 1986, Yancey et al., 1989). The one exception was the deepest fish tested, *N. kermadecensis* (hadal snailfish), which also had a significantly higher potassium content and lower percent water than other species (**Table 5.2**), indicating more intracellular components than in other species. These buoyancy and composition results suggest that the gelatinous tissue is not positively buoyant in that species. It is possible that testing at atmospheric pressure may have biased these results since these fish were collected from considerably greater depths than the other species. Observations of the swimming behaviour of these fish *in situ* suggests that the entire fish is slightly negatively buoyant, settling to the seabed when active swimming ceases. This swimming behaviour has been observed in multiple hadal trench liparids (*Notoliparis kermadecensis*, *Pseudoliparis amblystomopsis*, Liparidae sp. nov. Mariana Trench). These fishes do not have swim bladders, and the gelatinous tissues, even if not positively buoyant, would have lower density than most other tissues (e.g., bone, muscle), so may help reduce overall body density and thus rate of sinking, as previously suggested for *Chauliodus sloani,* a pelagic viperfish species that also has gelatinous tissue that is not positively buoyant (Denton and Marshall, 1958). Additionally, the gelatinous subdermal extracellular matrix is often found in fishes with aglomerular kidneys and lacking gas bladders, such as *Ateleopus japonicus*,

which may serve to reduce whole-animal density (Ozaka et al., 2009). However, the correlation between the aglomerular kidney and gelatinous tissues remains to be fully explored.

As noted earlier, previous work on mesopelagic fishes revealed lower ion concentrations in gelatinous tissue compared to blood (Yancey et al., 1989). Our osmolality values hint at a similar pattern for gelatinous tissue because they are well below osmolalities of blood and muscle of other fish species from comparable depths. Muscle osmolalities at 1000 m have been reported at ~400 (cf. gelatinous tissues at 312–377), at 2000 m ~490–500 (cf. gelatinous tissues at 355–385), at 3000 m ~590–600 (cf. gelatinous tissues at 467), and at 7000 m ~990–1000 (cf. gelatinous tissues at 945, Yancey et al., 2014; Linley et al., 2016). It should be noted that there would be an energetic cost associated with actively maintaining the ionic gradient needed to produce greater buoyancy (e.g., ion-regulating chloride cells in gelatinous tissues of leptocephali, Tsukamoto et al., 2009).

While most of the gelatinous tissues tested could aid fish buoyancy, our results suggest that this might not be the only function. Importantly, gelatinous tissues are found in some species with gas-filled swim bladders (e.g., Family Ophidiidae), indicating that buoyancy may not always be their primary adaptive role. Furthermore, gelatinous tissues are found in benthic flatfishes (Order Pleuronectiformes; e.g., *Embassichthys bathybius* and *Microstomus pacificus*), which would have less evolutionary pressure to develop positively buoyant tissues, as they spend more time resting on the seafloor than swimming. In several species, gelatinous tissues are concentrated ventrally, an unlikely position to provide positive buoyancy. Some bathypelagic fishes are within 0.5 and 1.2% (*Gonostoma elongatum* and *Xenodermichthys copei*) of neutral buoyancy without swim bladders or gelatinous layers, through reduced ossification and watery muscle tissue (Denton and Marshall, 1958) and some benthopelagic fishes lacking gas bladders also have watery muscle to aid in achieving neutral buoyancy (Drazen, 2007). In the hadal liparids, near neutral buoyancy seems also maintained by other means, including a large fatty liver and reduced bone ossification.

Alteration of Body Size & Shape. Watery gelatinous tissues may be used to increase body size at lower production cost than muscle tissue, a strategy noted earlier that has been proposed for some deep-sea invertebrates (e.g., Mitra and Zaman, 2016) and some larval fishes (e.g., Marliave and Peden, 1989). Adult deep-sea species may have evolved to retain this low growth cost

paedomorphic character in a food-poor environment. Some deep-sea fishes, including two flatfish in this study, also have very watery muscle tissue, which further reduce growth costs, though, in this case, by sacrificing locomotory capacity (Drazen, 2007). The gelatinous tissues are the extreme end of this continuum. They serve as low-growth-cost bulk tissues, allowing the animal to grow large, reducing the likelihood of predation, without alteration to locomotory muscle.

Gelatinous tissues could also act as fairing along the fish's tail, creating a better hydrofoil and improved swimming efficiency, especially in liparids and aphyonids. Davenport and Kjorsvik (1986) touched on this idea briefly, suggesting that there may be an exoskeletal function to gelatinous tissue in *Cyclopterus lumpus*. They note that the gelatinous tissue was more prominent in females than males, up to 18% of body mass, and show that the males used more high amplitude tail beats to swim than females. Our results suggest that this may be a much more broadly used strategy. Support for this concept is inferred from studies of tadpole swimming, where a 'fish-shaped' body required significantly less power to swim than a 'tadpole-shaped' body, due to a decrease in drag (Liu et al., 1996). The same authors also found that the tadpole morphology creates a 'dead water' zone where the tail meets the body, which decreases swimming efficiency (Liu et al., 1997). The tadpole shape is selected against in pond experiments where fish predators are present, further illustrating the advantage to losing those high drag zones (Johnson et al., 2015). The location of the gelatinous tissue, concentrated around the anterior of the body cavity and under the skin along the tail, suggests that it could act to counteract this effect (**Figure 5.2**). An optimization model of body shape in fishes showed the wide head and tapered tail to be an efficient shape for undulatory swimming (Eloy, 2013). We propose that the gelatinous tissues could allow the fish to reach this streamlined shape without producing more muscle, reducing the need for the high-amplitude, energetically expensive tail beats required of tadpole-shaped forms (Liu et al., 1997).

Material properties of the actual gelatinous tissues should also be analysed under deep-sea, especially hadal, temperatures and pressures, as even small changes in body shape and stiffness can make a large difference in swimming performance (e.g., Long et al., 2010, Lauder et al., 2012). Gelatinous tissues (which melt at room temperature) are likely stiffer at hadal conditions of cold temperatures and high pressures, and could provide an even better paddle for forward propulsion. Gelatinous tissues may change stiffness and shape with movement, as seen in other models of

undulatory swimming (e.g., McHenry et al., 1995). While further exploration of this hypothesis is needed, the improved performance of the robotic model with a gelatinous tissue analogue suggests that the presence of this layer could enhance swimming performance. The chemical composition of the gelatinous tissues show that they are inexpensive to form, but the benefit to structure and locomotory capacity could be significant, accounting for some of its prevalence across many deep-sea genera.

Conclusions. Our results suggest that gelatinous tissues are widely used by fishes, principally in deep-sea species, serving different roles both for individual fish and across families. Gelatinous tissues, which are primarily extracellular fluid, are present in fishes of very different life histories and behaviours, from the flatfish, *Microstomus pacificus*, to the hadal snailfish, *Notoliparis kermadecensis*. The varied location of gelatinous tissues, which are present in the trunk of some eelpouts (Zoarcidae), the snout of *Ateleopus japonicas* (Ateleopodidae), and directly below the skin in many snailfishes (Liparidae), also calls attention to potential functional complexity. Overall, gelatinous tissues seem to be a low-density, low-production cost method to increase body size and alter body shape and size, with adaptive advantages for both swimming efficiency and buoyancy with varied functions among species.

Contributors

Gerringer, M.E.[1], Drazen, J.C.[1], Linley, T.D.[2], Summers, A.P.[3], Jamieson, A.J.[2], Yancey, P.H.[4]

[1]Department of Oceanography, University of Hawai‘i at Mānoa, Honolulu, HI 96822, USA.
[2] School of Marine Science and Technology, Ridley Building, Newcastle University, Newcastle Upon Tyne, UK. NE1 7RU.
[3]Friday Harbor Labs, University of Washington, Friday Harbor, WA 98250, USA.
[4]Biology Department, Whitman College, Walla Walla, WA 99362, USA.

PHY and MEG designed and conducted the proximate chemistry study. Samples and video were collected by AJJ, JCD, PHY, TDL, and MEG. MEG and APS designed and implemented the robotic model experiment. TDL illustrated **Figure 5.2**. MEG, PHY, JCD, and TDL collected literature and at-sea survey observations of gelatinous tissues. MEG assembled the distribution tables and phylogenetic tree. All authors assisted in discussions of the ideas presented and the drafting and revising of the manuscript for both format and intellectual content.

Acknowledgements

The authors thank Jason Friedman (University of Hawai‘i) for running lipid analyses, Daniel Zajic (Whitman College) for assistance conducting *N. kermadecensis* ion analyses, Carrie Laxson (Whitman College) for collection help on the 2009 samples and shipboard buoyancy tests, Logan Peoples (UCSD) for his assistance with phylogenetic tree construction, and Amy Scott-Murray (Oceanlab, Aberdeen) for construction of the photogrammetry snailfish model. Thanks to Stephanie Crofts, Stacy Farina, Misty Paig-Tran, and the Friday Harbour Labs Functional Morphology and Biology of Fishes Course, 2014 for assistance with the robotic model. Draft was reviewed by Allen Andrews. The authors would also like to thank the captains and crews of the *RVs Kaharoa*, *Thompson*, *Falkor*, *Hakuho-Maru*, and *Point Sur*. We would like to thank our reviewers for useful and thoughtful feedback. Funding support was provided by the National Science Foundation grants OCE-0727135, OCE-1130712, OCE-1130494 and IOS-1256602. We are grateful for additional support contributed by New Zealand’s National Institute of Water and Atmospheric Research, the National Oceanic and Atmospheric Administration, Schmidt Ocean Institute, and the Stephen and Ruth Wainwright Endowment. M. Gerringer is grateful for the support of the NSF Graduate Research Fellowship Program. A. Jamieson and T. Linley are supported by the Marine Alliance for Science and Technology for Scotland (MASTS) pooling initiative.

References

Anderson, M., Hubbs, C., 1981. Redescription and osteology of the North-eastern Pacific fish *Derepodichthys alepidotus* (Zoarcidae). Copeia. 1981, 341–352. (doi:10.2307/1444223)

Anderson, M.E., 1994. Systematics and osteology of the Zoarcidae (Teleostei: Perciformes). Ichthyological Bulletin J.L.B. Smith Institute of Ichthyology 60:120 p.

Anderson, M.E., 2012. A new species of *Pachycara* Zugmayer (Teleostei: Zoarcidae) from off Monterey Bay, California, USA, with comments on two North Pacific *Lycenchelys* species. Zootaxa. 3559, 39–43.

Andriashev, A.P., Pitruk, D.L., 1993. A review of the ultra-abyssal (hadal) genus *Pseudoliparis* (Scorpaeniformes, Liparidae) with a description of a new species from the Japan Trench. Voprosy Iktiologii. 33, 325–330.

Andriashev, A., Stein D., 1998. Review of the snailfish genus *Careproctus* (Liparidae, Scorpaeniformes) in Antarctic and adjacent waters. Natural History Museum Los Angeles City Scientific Contributions 470, 1–63.

Andriashev, A.P., 1998. A review of recent studies of Southern Ocean Liparidae (Teleostei: Scorpaeniformes). Cybium 22(3), 255–266.

Bailey, D., Bagley, P., Jamieson, A., Collins, M., Priede, I., 2003 *In situ* investigation of burst swimming and muscle performance in the deep-sea fish *Antimora rostrata* (Günther, 1878). Journal of Experimental Marine Biology and Ecology 286, 295–311. (doi:10.1016/S0022-0981(02)00534-8)

Benson, D.A., Karsch-Mizrachi, I., Lipman, D.J., Ostell, J., Sayers, E.W., 2009 GenBank. Nucleic Acids Research 37. (doi:10.1093/nar/gkn723)

Betancur-R., R. et al., 2013. The tree of life and a new classification of bony fishes. *PLOS* Currents Tree of Life. Edition 1. (doi:10.1371/currents.tol.53ba26640df0ccaee75bb165c8c26288)

Bianchi, G., Carpenter, K.E., Roux, J.-P., Molloy, F.J., Boyer, D., Boyer, H.J., 1999. Field guide to the living marine resources of Namibia. FAO species identification guide for fishery purposes. Rome, FAO. 265 p.

Bligh, E., Dyer, W., 1959. A rapid method of total lipid extraction and purification. Canadian Journal of Biochemistry and Physiology 37, 911.

Burke, V., 1930. Revision of fishes of family Liparidae. Bulletin of the United States National Museum, 150, i–xii 1–204.

Busby, M., Cartwright, R., 2009. *Paraliparis adustus* and *Paraliparis bullacephalus*: two new snailfish species (Teleostei: Liparidae) from Alaska. Ichthyological Research 56, 245–252. (doi:10.1007/s10228-008-0090-x)

Chen, S., 2002. Fauna Sinica, Osteichthyes. Myctophiformes, Cetomimiformes, Osteoglossiformes. Fauna Sinica Series. Beijing: Science Press. 349p.

Chernova, N., 2001. A review of the genus *Psednos* (Pisces, Liparidae) with description of ten new species from the north Atlantic and southwestern Indian Ocean. Bulletin of the Museum of Comparative Zoology 155(10), 477–507.

Chernova, N., Møller, P., 2008. A new snailfish, *Paraliparis nigellus* sp. nov. (Scorpaeniformes, Liparidae), from the northern Mid-Atlantic Ridge – with notes on occurrence of *Psednos* in the area. Marine Biology Research 4, 369–375. (doi:10.1080/17451000802017507)

Collins, M. A., Priede, I.G., Bagley, P.M., 1999. *In situ* comparison of activity in two deep-sea scavenging fishes occupying different depth zones. Proceedings of the Royal Society B: Biological Sciences 266, 2011–2016. (doi:10.1098/rspb.1999.0879)

Davenport, J., Kjorsvik, E., 1986. Buoyancy of the lumpsucker *Cyclopterus lumpus*. Journal of the Marine Biological Association of the United Kingdom 66, 159–174. (doi:10.1017/S0025315400039722)

Denton, E. J., Marshall, N.B., 1958. The buoyancy of bathypelagic fishes without a gas-filled swim bladder. Journal of the Marine Biological Association of the United Kingdom 37, 753–767.

Drazen, J.C., 2007. Depth related trends in proximate composition of demersal fishes in the eastern North Pacific. Deep-Sea Research Part I: Oceanographic Research Papers 54, 203–219. (doi:10.1016/j.dsr.2006.10.007)

Drazen, J.C., Friedman, J.R., Condon, N.E., Aus, E.J., Gerringer, M.E., Keller, A.A., Clarke, E.M., 2015. Enzyme activities of demersal fishes from the shelf to the abyssal plain. Deep-Sea Research Part I: Oceanographic Research Papers 100, 117–126. (doi:10.1016/j.dsr.2015.02.013)

Dubois, M., Gilles, K., Hamilton, J., Rebers, P., Smith, F., 1956. Colorimetric method for determination of sugars and related substances. Analytical Chemistry 28, 350–356. (doi:10.1021/ac60111a017)

Eastman, J., Hikida, R., Devries, A., 1994. Buoyancy studies and microscopy of skin and subdermal extracellular matrix of the Antarctic snailfish, *Paraliparis devriesi*. Journal of Morphology 220, 85–101. (doi:10.1002/jmor.1052200108)

Eastman, J.T., Lannoo, M.J., 1998. Morphology of the brain and sense organs in the snailfish *Paraliparis devriesi*: Neural convergence and sensory compensation on the Antarctic shelf. Journal of Morphology 237, 213–236. (doi:10.1002/(SICI)1097-4687(199809)237:3<213::AID-JMOR2>3.0.CO;2-#)

Edgar, R.C., 2004. MUSCLE: multiple sequence alignment with high accuracy and high throughput. Nucleic Acids Research, 32(5), 1792-1797. (doi:10.1093/nar/gkh340)

Eloy, C., 2013. On the best design for undulatory swimming. Journal of Fluid Mechanics 717, 48–89. (doi:10.1017/jfm.2012.561)

Endo, H., Okamura, O., 1992. New records of the abyssal grenadiers *Coryphaenoides armatus* and *C. yaquinae* from the western North Pacific. Japanese Journal of Ichthyology 38(4), 433–437.

Fedorov, V.V., Chereshnev, I.A., Nazarkin, M.V., Shestakov, A.V., Volobuev, V.V., 2003 Catalog of marine and freshwater fishes of the northern part of the Sea of Okhotsk. Vladivostok: Dalnauka. 204 p.

Friedman, J., Condon, N., Drazen, J., 2012. Gill surface area and metabolic enzyme activities of demersal fishes associated with the oxygen minimum zone off California. Limnology and Oceanography 57, 1701–1710. (doi:10.4319/lo.2012.57.6.1701)

Froese, R., Pauly, D., 2015. FishBase [WWW Document]. World Wide Web Electron. Publ.

Fujii, T., Jamieson, A., Solan, M., Bagley, P., Priede, I., 2010. A large aggregation of liparids at 7703 meters and a reappraisal of the abundance and diversity of hadal fish. Bioscience 60, 506–515. (doi:10.1525/bio.2010.60.7.6)

Günther, A., 1887. Report on the deep-sea fishes collected by H. M. S. Challenger during the years 1873–76. Challenger Report 22.

Hart, J.L., 1973. Pacific fishes of Canada. Bulletin of the Fisheries Research Board of Canada 180, 740 p.

Jamieson, A.J., Fujii, T., Solan, M., Matsumoto, A.K., Bagley, P.M., Priede, I.G., 2009. Liparid and macrourid fishes of the hadal zone: *In situ* observations of activity and feeding behaviour. Proceedings of the Royal Society B: Biological Sciences 276, 1037–1045. (doi: 10.1098/rspb.2008.1670)

Johnson, J.B., Saenz, D., Adams, C.K., Hibbitts, T.J., 2015. Naturally occurring variation in tadpole morphology and performance linked to predator regime. Ecology and Evolution. *5*(15), 2991–3002. (doi:10.1002/ece3.1538)

Jung, A., Johnson, P., Eastman, J., Devries, A., 1995. Protein content and freezing avoidance properties of the subdermal extracellular matrix and serum of the Antarctic snailfish, *Paraliparis devriesi*. Fish Physiology and Biochemistry 14, 71–80.

Kai, Y., Orr, J., Sakai, K., Nakabo, T., 2011. Genetic and morphological evidence for cryptic diversity in the *Careproctus rastrinus* species complex (Liparidae) of the North Pacific. Ichthyological Research 58, 143–154. (doi:10.1007/s10228-010-0202-2)

Kenaley, C.P., DeVaney, S.C., Fjeran, T.T., 2013. The complex evolutionary history of seeing red: Molecular phylogeny and the evolution of an adaptive visual system in deep-sea dragonfishes (Stomiiformes: Stomiidae). Evolution 68(4), 996–1013. (doi:10.1111/evo.12322)

Kenaley, C.P., Stote, A., Flammang, B.E., 2014. The morphological basis of labriform rowing in the deep-sea bigscale *Scopelogadus beanii* (Percomorpha: Beryciformes). Journal of Experimental Marine Biology and Ecology 461, 297–305. (doi:10.1016/j.jembe.2014.07.024)

Knudsen, S.W., Møller, P.R., 2008. *Careproctus kidoi*, a new Arctic species of snailfish (Teleostei: Liparidae) from Baffin Bay. Ichthyological Research 55, 175–182. (doi:10.1007/s10228-007-0034-x)

Lannoo, M.J., Eastman, J.T., Orr, J.W., 2009. Nervous and sensory systems in sub-Arctic and Antarctic snailfishes of the genus *Paraliparis* (Teleostei: Scorpaeniformes: Liparidae). Copeia 2009, 732–739. (doi:10.1643/CG-08-157)

Lauder, G. V., Flammang, B., Alben, S., 2012. Passive robotic models of propulsion by the bodies and caudal fins of fish. Integrative and Comparative Biology 52, 576–87. (doi:10.1093/icb/ics096)

Leftwich, M., Tytell, E., Cohen, A., Smits, A., 2012. Wake structures behind a swimming robotic lamprey with a passively flexible tail. Journal of Experimental Biology 215, 416–25. (doi:10.1242/jeb.061440)

Letunic, I., Bork, P., 2006. Interactive Tree of Life (iTOL): an online tool for phylogenetic tree display and annotation. Bioinformatics 23(1), 127–128. (doi:10.1093/bioinformatics/btl529)

Linley, T.D., Gerringer, M.E., Yancey, P.H., Drazen, J.C., Weinstock, C.L., Jamieson, A.J., 2016. Fishes of the hadal zone including new species, *in situ* observations and depth records of Liparidae. Deep-Sea Research Part I: Oceanographic Research Papers 114, 99–110. (doi:10.106/j.dsr.2016.05.003)

Liu, H., Wassersug, R., Kawachi, K., 1996. A computational fluid dynamics study of tadpole swimming. Journal of Experimental Biology 199, 1245–60.

Liu, H., Wassersug, R., Kawachi, K., 1997. The three-dimensional hydrodynamics of tadpole locomotion. Journal of Experimental Biology 200, 2807–19.

Long, J.H. Jr., Porter, M.E., Root, R.G., Liaw, C.W., 2010. Go reconfigure: How fish change shape as they swim and evolve. Integrative and Comparative Biology 50(6), 1120–1139. (doi:10.1093/icb/icq066)

Luck, D.G., Pietsch, T.W., 2008. Observations of a deep-sea ceratioid anglerfish of the genus *Oneirodes* (Lophiiformes: Oneirodidae). Copeia 2008, 446–451. (doi:10.1643/CE-07-075)

Maddison, W., FitzJohn, R., 2015. The unsolved challenge to phylogenetic correlation tests for categorical characters. Systematic Biology 64(1), 127–136. (doi:10.1093/sysbio/syu070)

Marliave, J., Peden, A., 1989. Larvae of *Liparis fucensis* and *Liparis callyodon*: Is the "cottoid bubblemorph" phylogenetically significant? Fisheries Bulletin 87, 735–743.

Marsh, J., Weinstein, D., 1966. Simple charring method for determination of lipids. Journal of Lipid Research 7, 574–6.

Masuda, H.K., Amaoka, K., Araga, C., Uyeno, T., Yoshino, T., 1984. The fishes of the Japanese Archipelago. Vol. 1. Tokai University Press, Tokyo, Japan. 437 p.

McHenry, M.J., Pell, C.A., Long, J.H. Jr., 1995. Mechanical control of swimming speed: Stiffness and axial wave form in undulating fish models. Journal of Experimental Biology 198(11), 2293–2305.

McWilliam, H., Li, W., Uludag, M., Squizzato, S., Park, Y.M. Buso, N. Cowley, A.P., Lopez, R., 2013. Analysis tool web services from the EMBL-EBI. Nucleic Acids Research, 41, W597–W600. (doi:10.1093/nar/gkt376)

Miller, M.J., 2009. Ecology of anguilliform leptocephali: remarkable transparent fish larvae of the ocean surface layer. Aquatic BioScience Monographs 2, 1– 94. (doi:10.5047/absm.2009.00204.0001)

Miller, M.A., Pfeiffer, W., Schwartz, T., 2010. Creating the CIPRES Science Gateway for inference of large phylogenetic trees. Proceedings of the Gateway Computing Environments Workshop (GCE), New Orleans, LA pp 1–8.

Mitra, A., Zaman, S., 2016. Basics of Marine and Estuarine Ecology. Springer India, 481 p. (doi:10.1007/978-81-322-2707-6)

Møller, P.R., Knudsen, S.W., Schwarzhans, W., Nielsen, J.G., 2016. A new classification of viviparous brotulas (Bythitidae)—with family status for Dinematichthyidae—based on molecular, morphological, and fossil data. Molecular Phylogenetics and Evolution. 100, 391–408. (doi:10.1016/j.ympev.2016.04.008)

Near, T.J., Dornburg, A., Eytan, R.I., Keck, B.P., Smith, W.L., Kuhn, K.L., Moore, J.A., Price, S.A., Burbrink, F.T., Friedman, M., Wainwright, P.C., 2013. Phylogeny and tempo of diversification in the superradiation of spiny-rayed fishes. Proceedings of the National Academy of Sciences U.S.A. 110(31), 12738–12743. (doi:10.1073/pnas.1304661110)

Nielsen, J. G., 1986. Ophidiidae. p. 1158-1166. In P.J.P. Whitehead, M.-L. Bauchot, J.-C. Hureau, J. Nielsen, and E. Tortonese (eds.) Fishes of the North-eastern Atlantic and the Mediterranean. UNESCO, Paris. Vol. 3.

Nielsen, J.G., 1990. Ophidiidae. p. 564-573. In J.C. Quero, J.C. Hureau, C. Karrer, A. Post and L. Saldanha (eds.) Check-list of the fishes of the eastern tropical Atlantic (CLOFETA). JNICT, Lisbon; SEI, Paris; and UNESCO, Paris. Vol. 2.

Nielsen, J.G., 1998. Paxton, J.R., Eschmeyer, W.N., ed. Encyclopedia of Fishes. San Diego: Academic Press. p. 134. (ISBN 0-12-547665-5)

Nielsen, J.G., Cohen, D.M., Markle, D.F., Robins, C.R., 1999. Ophidiiform fishes of the world (Order Ophidiiformes). An annotated and illustrated catalogue of pearlfishes, cusk-eels, brotulas and other ophidiiform fishes known to date. FAO Fisheries Synopsis 125(18), 178p.

Ozaka, C., Yamamoto, N., Somiya, H., 2009. The aglomerular kidney of the deep-sea fish, *Ateleopus japonicus* (Ateleopodiformes: Ateleopodidae): Evidence of wider occurrence of the aglomerular condition in Teleostei. Copeia 2009, 609–617. (doi:10.1643/CP-08-131)

Parin, N.V., Fedorov, V.V., Sheiko, B.A., 2002. An annotated catalogue of fish-like vertebrates and fishes of the seas of Russia and adjacent countries: Part 2. Order Scorpaeniformes. Journal of Ichthyology 42(Suppl.1), S60–S135.

Peden, A.E., 1979. Meristic variation of *Lycodapus mandibularis* (Pisces: Zoarcidae) and oceanic upwelling on the west coast of North America. Journal of the Fisheries Research Board of Canada 36, 69–76.

Pfeiler, E., 1999. Developmental physiology of elopomorph leptocephali. Comparative Biochemistry and Physiology 123A, 113–128. (doi:10.1016/s1095-6433(99)00028-8)

Pietsch, T.W., 1986. Melanocetidae. p. 375–376. In M.M. Smith and P.C. Heemstra (eds.) Smith's sea fishes. Springer-Verlag, Berlin.

Prosser, C., Mackay, W., Kato, K., 1970. Osmotic and ionic concentrations in some Alaskan fish and goldfish from different temperatures. Physiological Zoology 43, 81–89.

R Core Development Team, 2015. R: A Language and Environment for Statistical Computing. R Found. Stat. Comput. Vienna, Au.

Russian Academy of Sciences, 2000. Catalog of vertebrates of Kamchatka and adjacent waters. 166 p.

Schneider, C.A., Rasband, W.S., Eliceiri, K.W., 2012. NIH Image to ImageJ: 25 years of image analysis. Nature Methods 9, 671–675. (doi:10.1038/nmeth.2089)

Scholander, P.F., 1954. Secretion of gases against high pressures in the swimbladder of deep sea fishes. Biological Bulletin 107, 260–277. (doi:10.2307/1538612)

Shinohara, G., Yabe, K., Nakaya, M., Anma, G., Yamaguchi, S., Amaoka, K., 1994. Deep-sea fishes collected from the North Pacific by the T/S Oshoro-Maru. Bulletin of the Faculty of Fisheries Hokkaido University 45(2), 48–80.

Smith, P.K., Krohn, R.I., Hermanson, G.T., Mallia, A.K., Gartner, F.H., Provenzano, M.D., Fujimoto, E.K., Goeke, N.M., Olson, B.J., Klenk, D.C., 1985. Measurement of protein using bicinchoninic acid. Analytical Biochemistry 150, 76–85. (doi:10.1016/0003-2697(85)90442-7)

Stamatakis, A., 2014. RAxML Version 8: A tool for phylogenetic analysis and post-analysis of large phylogenies. Bioinformatics 30, 1312–1313. (doi:10.1093/bioinformatics/btu033)

Stein, D.L., 1978. A review of the deepwater Liparidae (Pisces) from the coast of Oregon and adjacent waters. Proceedings of the California Academy of Sciences 127, 1–55.

Stein, D.L., Chernova, N., Andriashev, A.P., 2001. Snailfishes (Pisces: Liparidae) of Australia, including descriptions of thirty new species. Records of the South Australian Museum 53, 341–406. (doi:10.3853/j.0067-1975.53.2001.1351)

Stein, D.L., 2005. Descriptions of four new species, redescription of *Paraliparis membranaceus*, and additional data on species of the fish family Liparidae (Pisces, Scorpaeniformes) from the west coast of South America and the Indian Ocean. Zootaxa 1019, 1–25.

Tangorra, J., Phelan, C., Esposito, C., Lauder, G., 2011. Use of biorobotic models of highly deformable fins for studying the mechanics and control of fin forces in fishes. Integrative and Comparative Biology 51, 176–89. (doi:10.1093/icb/icr036)

Tsukamoto, K., Yamada, Y., Okamura, A., Kaneko, T., Tanaka, H., Miller, M.J., Horie, N., Mikawa, N., Utoh, T., Tanaka, S., 2009. Positive buoyancy in eel leptocephali: an adaptation for life in the ocean surface layer. Marine Biology 156, 835–846. (doi:10.1007/s00227-008-1123-8)

Vetter, R., Lynn, E., Costa, A., Garza, M., 1994. Depth zonation and metabolic adaptation in Dover sole, *Microstomus pacificus*, and other deep-living flatfishes: factors that affect the sole. Marine Biology 120, 145–159.

Withers, P., Hefter, G., Pang, T., 1994. Role of urea and methylamines in buoyancy of elasmobranchs. Journal of Experimental Biology 188, 175–89.

Yancey, P., Gerringer, M., Drazen, J., Rowden, A., Jamieson, A., 2014. Marine fish may be biochemically constrained from inhabiting the deepest ocean depths. Proceedings of the National Academy of Sciences U. S. A. 111, 4461–5. (doi:10.1073/pnas.1322003111)

Yancey, P., Lawrence-Berrey, R., Douglas, M., 1989. Adaptations in mesopelagic fishes. Marine Biology 103, 453–459. (doi:10.1007/BF00399577)

CHAPTER VI

Pseudoliparis swirei: A newly-discovered hadal liparid (Scorpaeniformes: Liparidae) from the Mariana Trench

Abstract

Pseudoliparis swirei sp. nov. is described from 37 individuals collected in the Mariana Trench at depths 6,898–7,966 m. The collection of this new species is the deepest benthic capture of a vertebrate with corroborated depth data. Here, we describe *P. swirei* and discuss aspects of its biology, distribution, and phylogenetic relationships to other hadal liparids based on analysis of three mitochondrial genes. *Pseudoliparis swirei* is almost certainly endemic to the Mariana Trench, as other hadal liparids appear isolated to a single trench or trench system in the Kermadec, Macquarie, South Sandwich, South Orkney, Peru-Chile, Kurile-Kamchatka and Japan trenches. The discovery of another hadal liparid species, apparently abundant at depths where other fish species are few and only found in low numbers, provides further evidence for the dominance of this family within the hadal fish fauna.

Introduction

The Liparidae (snailfishes, Scorpaeniformes), are probably the most geographically and bathymetrically widespread family of marine fishes, including more than four hundred species in about 30 genera with representatives in all oceans where water temperature is temperate to cold. The snailfishes have the widest depth range of any marine fish family (Chernova et al., 2004), with habitats ranging from the intertidal to depths exceeding 8,000 m (Linley et al., 2016). To date, different, likely endemic, liparid species have been found in seven trenches and troughs, including the Kermadec, Macquarie, South Orkney, South Sandwich, Peru-Chile, Japan, and Kurile-Kamchatka trenches with another species likely in the Puerto Rico Trench (Fujii et al., 2010; Pérês 1965). Recent advances in hadal sampling technology have allowed the observation and recovery of these animals and show them to be abundant in those trenches that have been systematically

studied (Jamieson et al., 2009; Fujii et al., 2010; Linley et al., 2016). The liparids are a notably successful hadal fish family, extending deeper and/or reaching higher densities than other hadal fishes.

During cruises of the *R/V Falkor* from 9 November to 10 December 2014 and the *R/V Shinyo-maru* from 20 January to 3 February 2017, baited traps collected 37 individuals of a new species of snailfish at depths from 6,898 to 7,966 m in the Mariana Trench. These specimens are probably the deepest collected fish from the ocean bottom with corroborating depth data (see notes on spurious records in Fujii et al., 2010), although another remarkable liparid species was filmed (but not recovered) on the same cruise at an even greater depth of 8,143 m (Linley et al., 2016). In this paper, we describe and name the new species that was collected and present aspects of its biology.

Materials & Methods

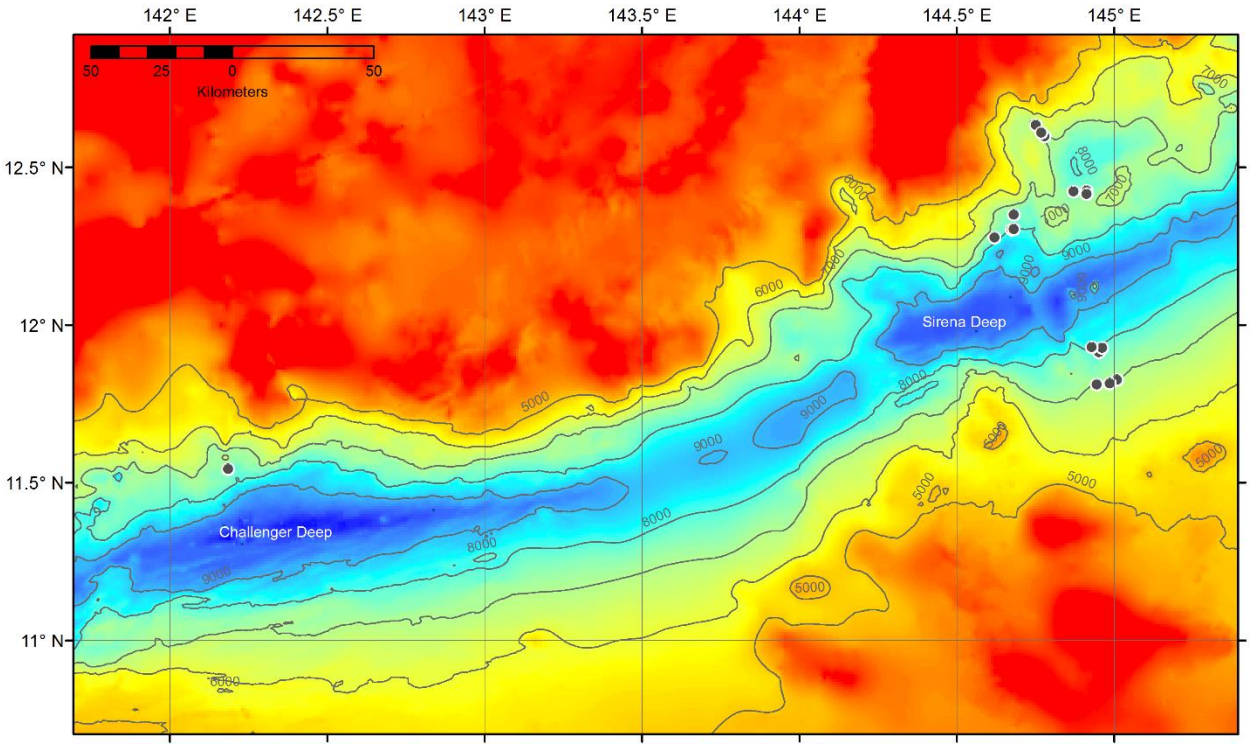

Figure 6.1. Map of collection locations within the Mariana Trench. Bathymetry courtesy of JAMSTEC. Isobaths are added between 5,000 and 9,000 m at 1,000 m intervals.

Specimens were collected using two free-falling traps (Linley et al., 2016) with steel ballast ejected for retrieval by acoustic release (IXSEA, France; Teledyne Benthos, USA). The holotype and most paratypes were collected in 2014, with one additional paratype collected on 29 Jan 2017 using the same methodology. Traps consisted of an aluminum or fiber glass frame lined with stiff plastic mesh covered with fine mesh netting to minimize specimen damage, attached to a mooring line with glass floatation spheres in 43 cm protective housings (Nautilus Marine Services, Germany) to provide buoyancy. Each trap was baited with mackerel in a nylon mesh bag, and included PVC funnel traps for amphipod collection. Collection sites are shown in **Figure 6.1** and site details are provided in **Table 6.1**.

Table 6.1. Collection information. Specimens collected on cruise FK141109 of the *RV Falkor* and SY1615 of the *RV Shinyo-maru*. Number of individual fish collected in each trap deployment (*n*) shown.

Deployment	Date	Latitude	Longitude	Depth (m)	*n*
TR05	15 Nov 2014	12.59786ºN	144.77854ºE	7062	1
TR06	16 Nov 2014	12.63390ºN	144.75080ºE	6914	1
TR07	18 Nov 2014	12.42347ºN	144.87058ºE	7497	8
TR08	19 Nov 2014	12.42556ºN	144.91171ºE	7509	4
TR09	21 Nov 2014	12.30274ºN	144.67388ºE	7929	1
TR10	23 Nov 2014	11.91280ºN	144.94450ºE	7841	3
TR12	25 Nov 2014	11.81070ºN	144.99450ºE	6898	1
TR13	26 Nov 2014	11.82600ºN	145.00880ºE	6974	3
TR19	6 Dec 2014	12.27660ºN	144.62020ºE	7626	2
TR20	7 Dec 2014	12.34950ºN	144.68130ºE	7652	4
WT03	16 Nov 2014	12.61026ºN	144.76839ºE	6961	3
WT04	18 Nov 2014	12.41505ºN	144.91187ºE	7495	1
WT06	21 Nov 2014	12.30370ºN	144.68038ºE	7949	1
WT07	23 Nov 2014	11.92730ºN	144.96200ºE	7907	1
WT08	24 Nov 2014	11.92970ºN	144.92880ºE	7966	1
WT09	25 Nov 2014	11.81470ºN	144.98580ºE	6949	2
FT02	29 Jan 2017	11.54290°N	142.18485°E	7581	1

Fin clips and tissue samples for genetic study were preserved in 95% EtOH. Additional tissue samples were frozen at -80°C for physiological studies. Individuals were fixed in 10% buffered formalin at sea and transferred after five months in stages to 75% EtOH. The specimens

are deposited at the Smithsonian National Museum of Natural History and the Scripps Institution of Oceanography Marine Vertebrate Collection.

Definitions of counts, measurements, and characters follow Stein et al. (2001), Andriashev (2003), and Stein (2012). Museum abbreviations follow Sabaj Perez (2014). Counts of vertebrae, dorsal, and anal fin rays and pre-dorsal fin lengths were obtained from radiographs of specimens. Pectoral and caudal fin ray counts were made by direct examination. Pectoral girdles were removed from four specimens and stained using alizarin red S (Taylor, 1967a; b). Whole specimens were temporarily stained with cyanine blue when necessary (Saruwatari et al., 1997).

Selected measurements (total length, standard length, pre-anal fin length, head length, eye width, snout width, and weight) were made immediately upon retrieval. Fresh and preserved measurements of the same characters in each fish were compared to estimate shrinkage caused by preservative osmolarity changes (e.g., Hay, 1982; Kristoffersen and Salvanes, 1998).

Counts are given as the mode, followed by the range in parentheses. Ratios for proportions are given as percent standard length (SL) and percent head length (HL) for the mean first, followed in parentheses by the range for all specimens. For characters that were damaged during preservation, fresh ratios are presented. Ratios taken from fresh measurements are indicated with an asterisk. Ratios taken from photographs of freshly caught specimens are indicated with two asterisks. All ratios are based on comparisons of like measurements, e.g., fresh head length to fresh standard length or preserved vs preserved. Data analysis was conducted using the program R (R Core Development Team, 2015) and figures were constructed using the package *ggplot2* (Wickam, 2009). Ontogenetic trends were investigated through fitted linear models and ANOVA (type-I sum of squares). Imprecision of very small orbit width measurements, leading to heteroscedasticity, was corrected through cubed weighted least squares relative to SL. Results were considered significant at an α of 0.05.

Sex was determined macroscopically. Eggs were removed from mature and maturing females. For the four females with sufficiently ripe eggs, all eggs were counted and those above 1.5 mm diameter were measured. For the remaining females with distinguishable eggs, maximum egg size was recorded.

DNA was extracted from epaxial muscle tissue from five individuals of *Pseudoliparis swirei* and five hadal liparids from the Kermadec Trench (collection described by Linley et al.,

2016) with the DNeasy Blood and Tissue Kit (Qiagen), following the manufacturer's protocols. Three mitochondrial gene fragments, 16S rRNA (16S, 1472 bp), cytochrome *b* (Cyt-*b*, 1007 bp) and cytochrome *c* oxidase subunit I (COI, 1399 bp) were amplified in polymerase chain reaction (PCR). PCR cycling included 35 cycles of denaturation at 95ºC for 30 seconds, annealing at 48ºC (16S) or 52ºC (Cyt-*b*, COI) for 30 seconds, and extension at 72ºC for 1 minute. Primers used included 16S_liparids_F (5'-CTA TTA ATA CCC CCA AAT ACC CC-3'), 16S_liparids_R (5'-CGA TGT TTT TGG TAA ACA GGC G-3'), and 16S_liparids_R2 (5'-GAT TTC ATC AGG TAG GGG GAG GGC-3') for 16S rRNA. For Cyt-*b*, primers were Cytb_liparids_F (5'-ATG GCA AGC CTA CGA AAA ACC CAC C-3'), Cytb_liparids_R (5'-TAT TCT CTA TGA AGC CGG TAA GGG-3'), and Cytb_liparids_R2 (5'-GGG TTA GTT GAG CCT GTT TCG TG-3'). COI primers were COI_liparids_F (5'GCC ATC CTA CCT GTG GCC ATC ACA CG-3'), COI_liparids_R (5'-AGT GGG ATA AAA CAA ATG CGG G-3'), as well as modified versions of the COI primers reported by Ward et al., (2005), Liparid_WardsF1 (5'-TCG ACT AAT CAC AAA GAC ATT GGC AC-3'), and Liparid_WardsR1 (5'-TAA ACT TCG GGA TGG CCA AAG AAT CA-3'). PCR products were purified using ExoSAP-IT *Express* (affymetrix, Thermo Fisher Scientific) and Sanger sequencing was performed on an ABI 3730XL with BigDye chemistry. Two sequencing primers were used in addition to PCR primers: 16S_liparids_I (5'-CCA AAA ACA TCG CCT CTT GTA CCC-3') for 16S and COI_liparids_I (5'-CTG ATT CTT TGG CCA TCC CGA AG-3') for COI.

Base calls were confirmed by aligning both strands in Geneious v7.1.8 (Kearse et al., 2012), with final alignments for each gene fragment generated by Multiple Sequence Comparison by Log-Expectation (MUSCLE; Edgar 2004; McWilliam et al., 2013). The best fit nucleotide substitution model for each alignment was evaluated by Bayesian Information Criterion (BIC), as implemented in jModelTest (Darriba et al., 2012; Guindon & Gascuel, 2003). The best models were found to be HKY+G for COI and Cyt-*b* and TPM2uf+G for 16S. Average pairwise genetic distances among species were calculated in MEGA6 (Tamura et al., 2013), using the closest available model, the Tamura-Nei model with gamma-distributed rate variation (α = 0.1813 [16S], 0.1889 [COI], 0.2314 [Cyt-*b*], model-averaged estimates). Because we included NCBI sequences of liparids *Careproctus rastrinus*, *C. colleti*, and *C. cypselurus* (GenBank Accession JF952697.1, FJ164433.1, AB565514.1, AB565517.1, AB565629.1; Zhang & Hanner, 2011; Steinke et al.,

2009; Kai et al., 2011), we trimmed our alignment to include only regions present for all species for genetic distance calculations (COI: 644 bp, Cyt-b: 744 bp, 16S: 699 bp).

Phylogenetic trees were inferred under maximum likelihood (ML) using Randomized Axelerated Maximum Likelihood (RAxML, GTRGAMMA model), with node support assessed by 1,000 bootstrap iterations (Stamatakis 2014). Bayesian phylogenetic inference was conducted in MrBayes 3.2 (Ronquist et al., 2012), using the GTR+gamma nucleotide substitution model. Markov Chain Monte Carlo (MCMC) sampling of the posterior distribution was conducted for 1 million generations, with sampling every 500 generations. Sequences from *Pseudoliparis belyaevi* from the Japan Trench (T.P. Satoh, unpublished data) were included in our alignments to assess placement of this new Mariana species into genus, with the smooth lumpfish, *Aptocyclus ventricosus* (GenBank Accession NC_008129.1; Miya et al., 2003), chosen as an outgroup. The Interactive Tree of Life (iTOL v3; Letunic & Bork 2007) was used for visualization of trees.

Results

***Pseudoliparis swirei* Gerringer & Linley 2017, sp. nov.**

Mariana snailfish: Linley et al., 2016

Mariana snailfish: Linley et al., 2017

Mariana snailfish/Mariana liparid: Gerringer et al., 2017

Diagnosis. *Pseudoliparis swirei* differs from the two other known *Pseudoliparis* species in the following characters. *Pseudoliparis swirei* differs from *P. belyaevi* in the presence of a distinct lower pectoral fin lobe, similar to that seen in *P. amblystomopsis*. *Pseudoliparis swirei* has more dorsal fin rays 55 (51–58) than *P. amblystomopsis* 49 (49–52), more anal fin rays 48 (43–49) compared to 43 (42–45), and more vertebrae 61 (56–62), compared to 55–57, although these ranges somewhat overlap. Head length is shorter in *P. swirei* (17.0–21.7 %SL) than *P. amblystomopsis* (21.6–24.0 %SL). Comparisons were made according to ranges presented by Andriashev and Pitruk (1993). *Pseudoliparis belyaevi* is known only from the Japan Trench, *P. amblystomopsis* from the Japan and Kurile-Kamchatka trenches, *P. swirei* only from the Mariana Trench.

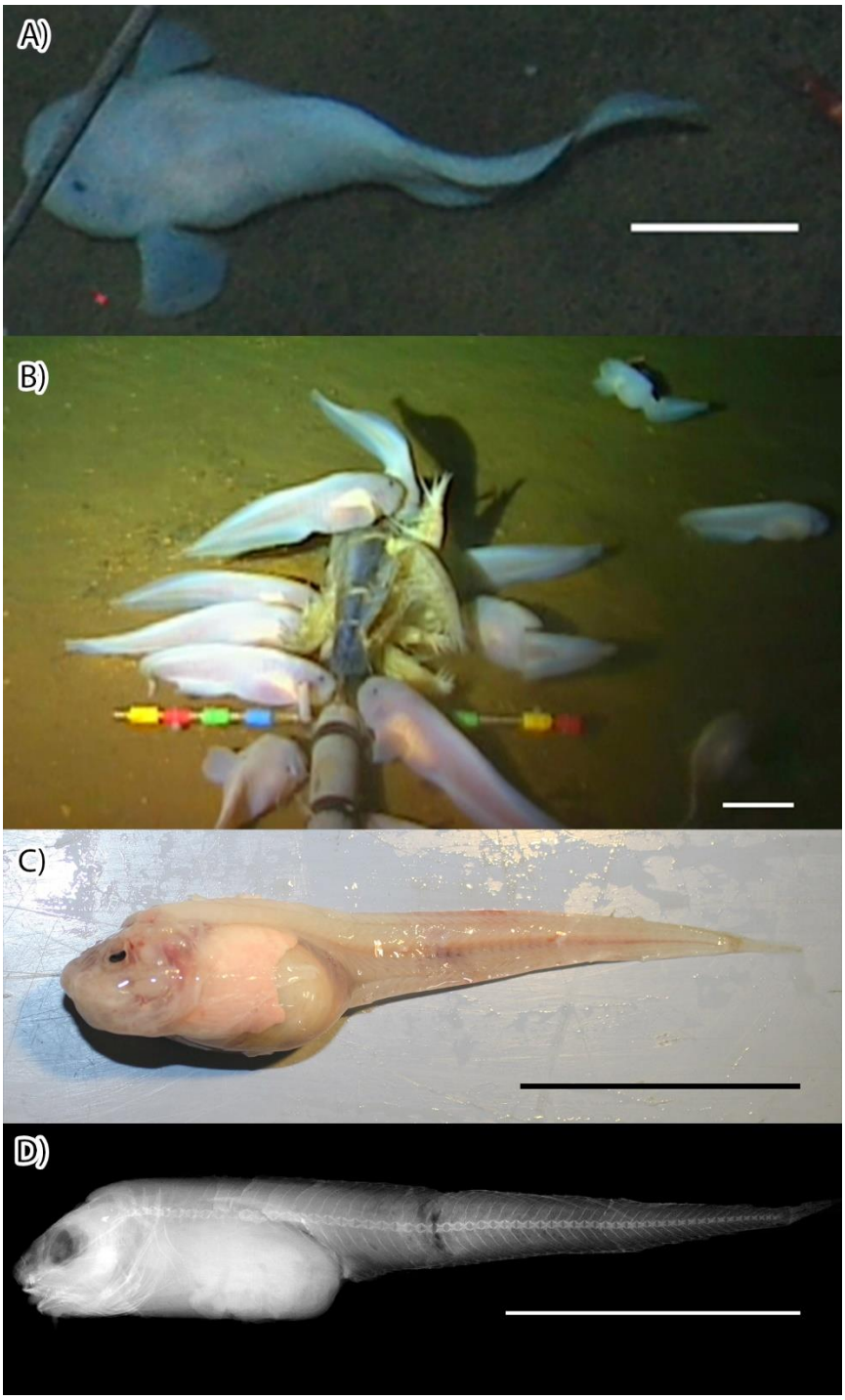

Figure 6.2. A) *In situ* photograph of *Pseudoliparis swirei* at 6198 m. B) a group at 7,485 m. C) Deck photograph of HADES #200049. D) Radiograph of HADES #200141. Image by Sandra Raredon. Scale indicator 5 cm.

Table 6.2. Measurements and counts of *Pseudoliparis swirei*. Measurements taken from preserved specimens, given in mm. Body depth measured from fresh photographs. Dorsal fin origin between vertebrae #, #. Maximum and minimum values (mean and standard deviation) shown for measurements. Counts show range (median). Number of specimens examined for individual characters (*n*).

	Holotype	**Holotype and Paratypes**	***n***
Measurements			
Standard Length	104.0	87.0–226.0 (151.3±38.8)	24
Total Length	112.0	95.0–237.0 (160.5±41.6)	21
Head Length	18.9	17.8–42.9 (31.2±8.0)	20
Head Depth at Occiput	~14	20.5–32.7 (27.3±6.2)	3
Head Width	13.1	2.6–41.4 (27.0±9.7)	11
Snout Length	6.7	5.6–15.2 (9.8±2.8)	26
Lower Lobe Distance		2.3–6.6 (4.7±1.4)	16
Body Depth	18.0	18.0–62.0 (41.0±11.0)	18
Orbit Width	3.5	2.8–6.1 (4.8±1.0)	23
Disk Length		2.9–9.0 (6.2±2.1)	14
Gill Opening		5.4–9.6 (8.1±2.4)	3
Upper Jaw Length	~8.7	8.1–20.6 (13.8±3.3)	31
Lower Jaw Length	8.2	6.6–19.3 (12.7±3.1)	31
Distance: Mandible to Disk	8.8	8.8–22.3 (15.2±3.7)	25
Distance: Snout to Anus	23.2	23.2–56.7 (41.1±13.5)	6
Distance: Mandible to Anus	21.0	21.0–47.5 (35.3±12.0)	5
Distance: Disk to Anus	9.5	9.5–33.5 (18.7±8.9)	5
Distance: Anus to Anal Fin	10.9	10.9–25.9 (18.4±6.3)	7
Length Upper Pectoral Fin Lobe	>15.6	14.2–33.4 (22.8±4.5)	28
Length Lower Pectoral Fin Lobe	8.9	7.3–22.9 (12.3±3.3)	22
Counts			
Total Vertebrae	58	56–62 (59)	19
Abdominal Vertebrae	12	11–14 (12)	18
Caudal Vertebrae	46	44–49 (46)	17
Dorsal Fin Origin		3–6 (4,5)	12
Dorsal Fin Rays	~52	51–58 (54)	11
Anal Fin Rays	≥44	43–49 (47)	15
Total Pectoral Rays	30	28–32 (30)	24
Pectoral Fin Rays (Upper Lobe)	20	18–23 (21)	26
Pectoral Rays (Notch)	5	3–6 (5)	27
Pectoral Fin Rays (Lower Lobe)	5	4–6 (5)	26
Total Caudal Fin Rays	13	11–14 (13)	20
Caudal Fin Rays (Upper)	5	4–6 (5)	21
Caudal Fin Rays (Lower)	6	4–7 (6)	21
Caudal Fin Rays (Auxiliary)	2	0–2 (1)	20
Pyloric Caeca		5–9 (7)	17

Table 6.3. Ratios of *Pseudoliparis swirei*. Preserved and fresh measurements presented. Body depth taken from photographs. Predorsal fin length measured from radiograph.

	%SL			%HL		
	Holotype	**Holotype and Paratypes**	***n***	**Holotype**	**Holotype and Paratypes**	***n***
Preserved						
Head Length	18.2	17.0–21.7 (19.8±1.1)	19			
Head Width	12.6	12.6–19.6 (15.8±2.5)	8	69.3	68.2–101.0 (81.0±11.5)	8
Snout Length	6.4	5.2–8.3 (6.5±0.7)	21	35.4	28.5–38.0 (32.9±2.6)	18
Orbit Width	3.4	2.3–4.4 (3.2±0.6)	17	18.5	12.1–20.1 (16.0±2.3)	16
Upper Jaw Length	~8.4	7.4–10.5 (9.1±0.8)	20	~46.0	38.3–52.2 (45.9±3.3)	17
Lower Jaw Length	7.9	6.5–10.6 (8.3±1.0)	20	43.4	33.7–53.2 (42.2±4.7)	17
Upper Pectoral Fin Length		12.6–19.8 (15.2±2.2)	21		60.2–95.4 (75.4±11.3)	16
Lower Pectoral Fin Length	8.6	6.3–12.1 (7.8±1.4)	16	47.1	30.0–61.6 (39.0±7.7)	14
Gill Opening		4.4–5.3 (5.0±0.5)	3		22.3–26.5 (24.9±2.3)	3
Disk Length		2.4–5.6 (3.9±0.9)	13		12.1–25.9 (20.0±4.0)	12
Distance: Disk to Anus	9.1	8.6–15.6 (10.8±3.2)	4	50.3	43.1–83.8 (59.0±21.7)	3
Distance: Mandible to Disk	8.5	7.7–13.7 (10.0±1.4)	20	46.6	39.8–59.8 (49.7±5.4)	17
Lower Lobe Distance		1.8–4.7 (3.1±0.9)	12		8.3–23.0 (15.2±4.7)	10
Predorsal Fin Length	32.0	22.7–32.6 (27.8±3.1)	13	176.4	118.1–176.4 (142.2±18.2)	13
Distance: Snout to Anus	22.3	22.3–29.3 (26.0±3.0)	6	122.8	114.6–143.3 (130.0±11.3)	5
Distance: Mandible to Anus	20.2	20.2–27.6 (24.3±3.4)	4	111.1	111.1–134.8 (120.1±12.8)	3
Distance: Anus to Anal Fin	10.5	8.7–15.9 (12.5±2.9)	5	57.7	46.5–66.6 (59.1±9.3)	4
Fresh						
Head Length	20.6	14.5–21.9 (18.7±1.8)	33			
Snout Length	7.2	4.3–9.3 (6.4±1.0)	33	35.0	26.3–45.5 (33.8±5.3)	37
Eye Width	2.1	0.9–2.9 (1.8±0.5)	33	10.0	5.3–15.4 (9.9±2.4)	37
Body Depth	18.6	18.6–31.2 (24.5±3.1)	18	90.0	90.0–156.8 (128.7±17.9)	18
Preanal Fin Length	37.1	36.5–49.5 (42.0±3.5)	33	180.0	180.0–295.8 (228.0±26.1)	37

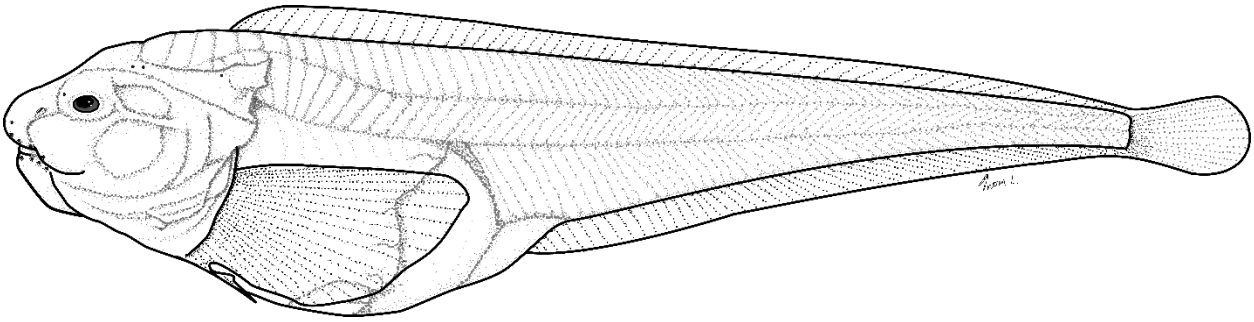

Figure 6.3. Lateral view of *Pseudoliparis swirei*. Combined representation of holotype, paratypes, and freshly captured images of paratype HADES #200133, juvenile, 151 mm. Drawings by Thomas D. Linley.

Description. Vertebrae 61 (56–62), dorsal-fin rays 55 (51–58), anal-fin rays 48 (43–49), caudal-fin rays 13 (11–14), pectoral-fin rays 30 (28–32), pectoral radials 4, pyloric caeca 7 (5–9). Ranges of measurements and counts are presented in **Table 6.2.** Ratios are presented in **Table 6.3**. All individual measurements and counts are available in **Supplementary Table 6.1**.

Head small, low, and wide, lateral profile anteriorly rounded and rising slowly to occiput, where the angle increases. Head depth about equal to body depth or lower, depending on abdominal fullness. Snout blunt, nostrils single, nares on horizontal with center of eye. Mouth broad, horizontal, subterminal, moderately large; upper jaw reaching to below middle of orbit, oral cleft reaching to below anterior edge of orbit. Teeth simple, sharp canines, innermost largest, arranged in approximately 9 (6–11 maxilla, 7–13 mandible) oblique, irregular rows of up to 20 (6–17 maxilla, 8–20 mandible) teeth each, forming a moderately wide band (2–4 teeth wide) in each jaw (**Figure 6.4**). Larger individuals had more teeth per row and more rows of teeth. Maxilla with prominent symphyseal gap, slight gap present in mandible. Pharyngeal teeth well developed, long, sharp, strongly fixed on globular tooth plates. Eye very small, about 10% head length. Orbit large, its dorsal margin well below that of head. Gill opening small, located completely above pectoral fin, width 5% SL. Opercular flap fleshy, broadly triangular, opercle terminates in two small spines below the flesh. Cephalic pores small, easily damaged; few remaining. Chin pores widely separated, lacking raised rims.

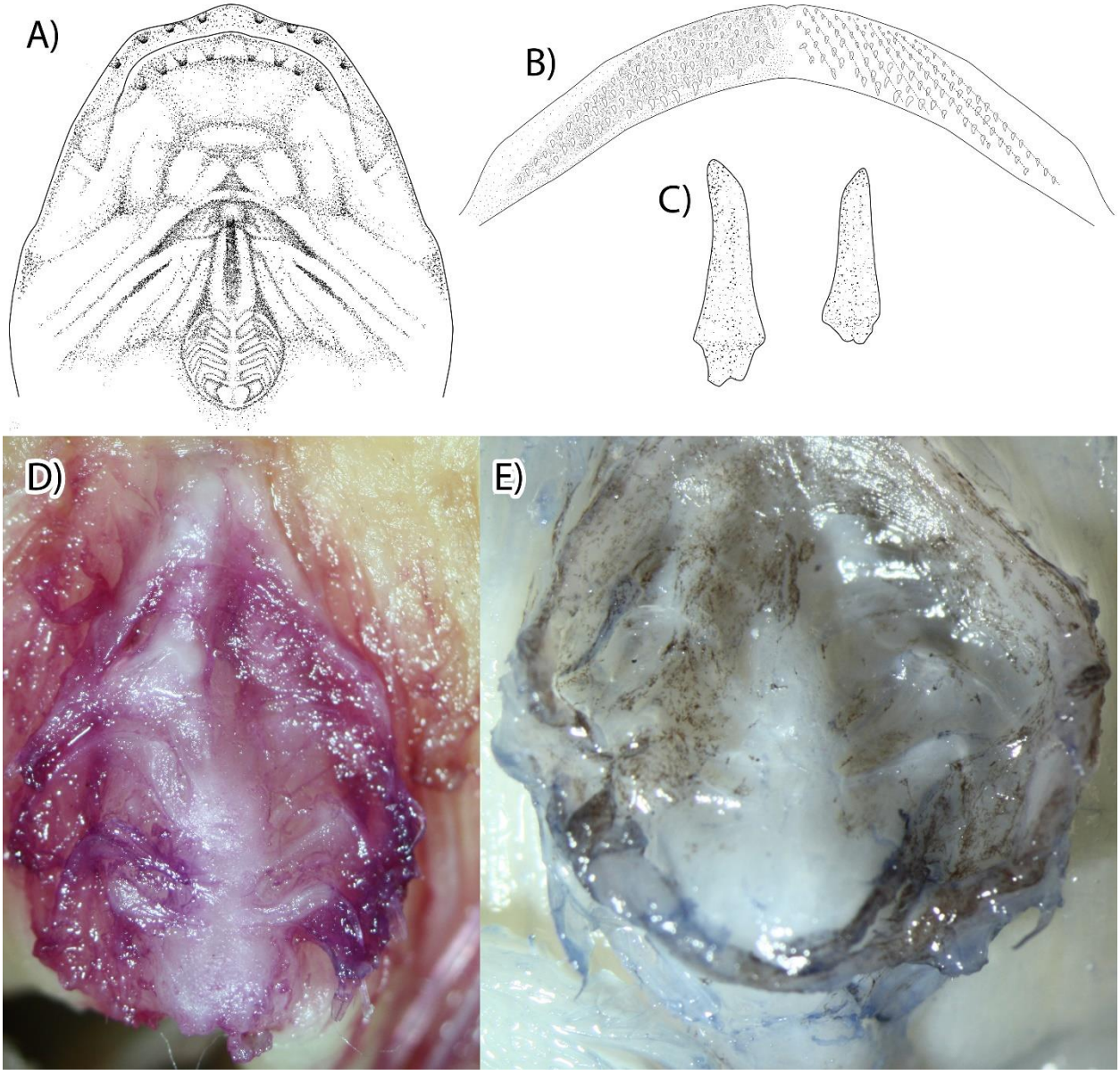

Figure 6.4. A) Ventral view drawing. B) Tooth pattern on maxillary jaw. Counted rows denoted on right side of image. C) Tooth structure of HADES Specimen #200024. D) Disk details of HADES #200025 stained with Alizarin Red S. E) Disk of HADES #200085 stained with Cyanine Blue.

Pectoral fin divided into lobes by a moderately deep notch, rudimentary rays absent. Notch rays 5 (3–6), clearly more widely spaced than those of upper and lower lobes, more so in larger individuals. Upper and lower lobe rays closely spaced. Dorsal-most pectoral fin ray on horizontal between level of upper jaw and lower margin of orbit. Symphysis of pectoral fins and anterior-most ray below rear of orbit. Upper lobe about 15.2% SL (12.6–19.8), lower about 7.8% SL (6.3–12.1). Upper lobe almost extending to anal fin origin, lower lobe distinct, reaching well behind disk to below middle of upper lobe base. Pectoral radials four, fenestra absent; of four specimens examined (#24, 27, 33, 96); one (#24) had (1+1+1+1), and three (#27, 33, 96) had (3+1) radials, generally round, notches and foramina absent (**Figure 6.5**). Radials gradually and irregularly decreasing in size from R1 (largest) to R4 (smallest). Scapula double-headed, posterior head larger and broader than anterior head, coracoid with broad head and long slender helve.

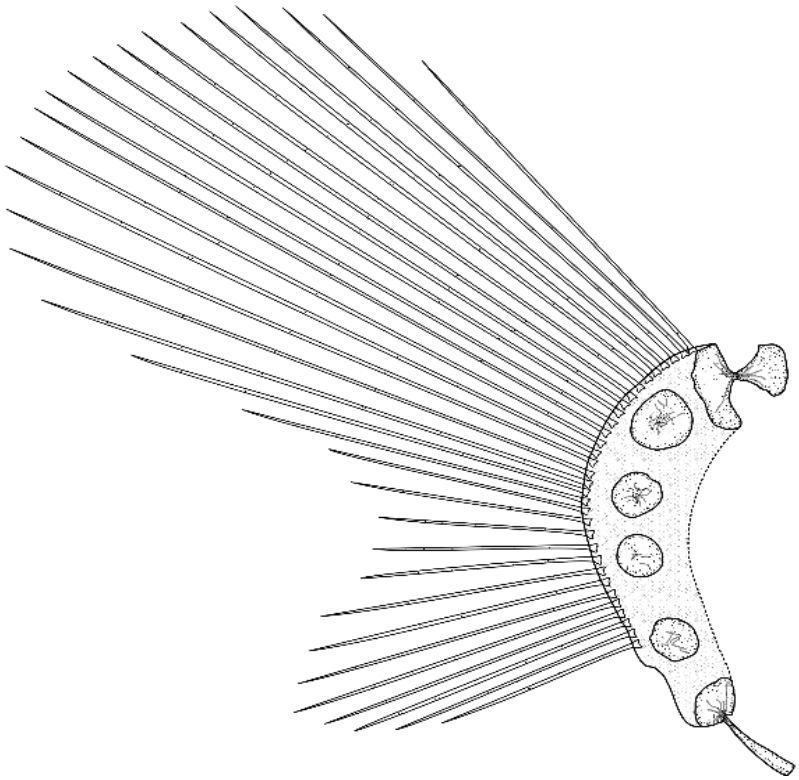

Figure 6.5. Pectoral girdle HADES #200027, female, 220 mm. Ventral HADES #200085, female, 225 mm. Scapula, radials 1–4, coracoid shown. Drawing by Thomas D. Linley.

Disk present, oval, longer than wide, below cheek and gill cavity between pectoral fin notches; well behind pectoral symphysis. Bones fully developed but weakly calcified; all elements present. Disk and pectoral girdle supported by a pair of clearly visible and strongly developed muscles extending anteriorly to pectoral symphysis, probably infracarinalis anterior (D.L. Stein, personal communication). Disk structure supporting a thin layer of tissue, often damaged or missing entirely; disk margin only slightly thicker than more central tissue. In cross section, disk rays clearly flattened as if to support disk margin.

Body depth dependent on reproductive state and fullness of stomach, usually much deeper than head depth, but shallow above vertebral column. Abdominal cavity long; peritoneum and body cavity extending to about 40% standard length. Total vertebrae 61 (56–62); anterior 13 (11–14), caudal 46 (44–49). In the 19 individuals in good enough condition to be radiographed, a double ray is present at or near anal fin first ray, usually between the second and third haemal spines of the caudal vertebrae. Pre-dorsal length about 27% SL (18.6–32.6), dorsal fin origin between fourth and fifth vertebrae (origin after vertebrae 3–5). Pre-anal fin length about 42% SL (36.3–49.5)*. Anus far posterior to disk, roughly 2/3 of distance from disk to anal fin origin. Pyloric caeca usually 7 (5–9), located left ventrally in body cavity; thick, digitate, usually separated into two distinct size classes, most commonly 4 short and 3 long, longest about 8.7% SL (5.9–11.7), shortest 3.7% SL (2.4–5.3). Longer caeca generally grouped together. Hypural with obvious suture; caudal fin most commonly of 13 (11–14) rays, ventral one or two often rudimentary. Skin thin, transparent; subdermal extracellular matrix (SECM; Eastman et al., 1994) thick below skin and between muscle bands. Total and standard lengths were approximately 10% shorter after preservation. The subdermal extracellular matrix is also lost after capture and preservation, resulting in changes to shape and proportion (**Chapter V**). With increased visual *in situ* techniques, reporting of both fresh and preserved specimen features will become increasingly useful.

The 37 individuals used for description varied in size from 89–235 mm SL, apparently covering a wide developmental range for the species. Some characters correlated significantly with ontogeny, explaining much of the variation in ratios. Both the upper and lower pectoral fin lobe lengths as a percentage of SL decreased significantly with increasing SL (upper: $F_{1,25}$=11.88,

$p<0.01$, $R^2=0.322$; lower $F_{1,23}=5.05$, $p<0.05$, $R^2=0.180$). Proportional orbit width decreased with increasing standard length ($F_{1,18}=26.25$, $p<0.01$, $R^2=0.593$).

In life, body pinkish-white, skin and peritoneum transparent; internal organs (liver, stomach, pyloric caeca) and muscles of trunk clearly visible through skin and thin abdominal wall. Anterior bundles of epaxial muscle thick, becoming less densely packed posteriorly. Some larger specimens with dusky skin on head. Pyloric caeca orange; most individuals entirely lacked both internal and external pigmentation. In alcohol, except for those with dusky heads, specimens uniformly pale.

Phylogenetic inference supports placement within the genus *Pseudoliparis*, with *P. swirei* more closely related to *P. belyaevi* of the Japan Trench than to the Kermadec Trench liparids (*Notoliparis kermadecensis, N. stewarti*). Phylogenetic relationships of *P. swirei* and closely-related species based on 16S, COI, and Cyt-*b* are presented in **Figure 6.6**, with estimates of evolutionary divergence among species reported in **Table 6.4**. Both the 16S and Cyt-*b* trees support placement of *P. swirei* as most closely related to *P. belyaevi* (>74% ML bootstrap support, >0.96 Bayesian posterior probability), with highly concordant topology. Genetic distances between the two *Pseudoliparis* species are 0.006% at Cyt-*b* and 0.007% at 16S (**Table 6.4**), with distances of 0.014% (Cyt-*b*) and 0.01% (16S) to the *Notoliparis* species. COI lacked sufficient polymorphism to resolve the relevant nodes, with low bootstrap support observed for the placement of *P. swirei* relative to P. *belyaevi* and *N. kermadecensis* (**Figure 6.6**). Genetic distances among species also were the lowest at COI, at < 1% or three nucleotide substitutions observed between the *Pseudoliparis* sequences. Sequences from *Pseudoliparis swirei, Notoliparis kermadecensis, Notoliparis stewarti* (this study) are available under GenBank accession numbers KY659176–KY659204 (**Supplementary Table 6.2**).

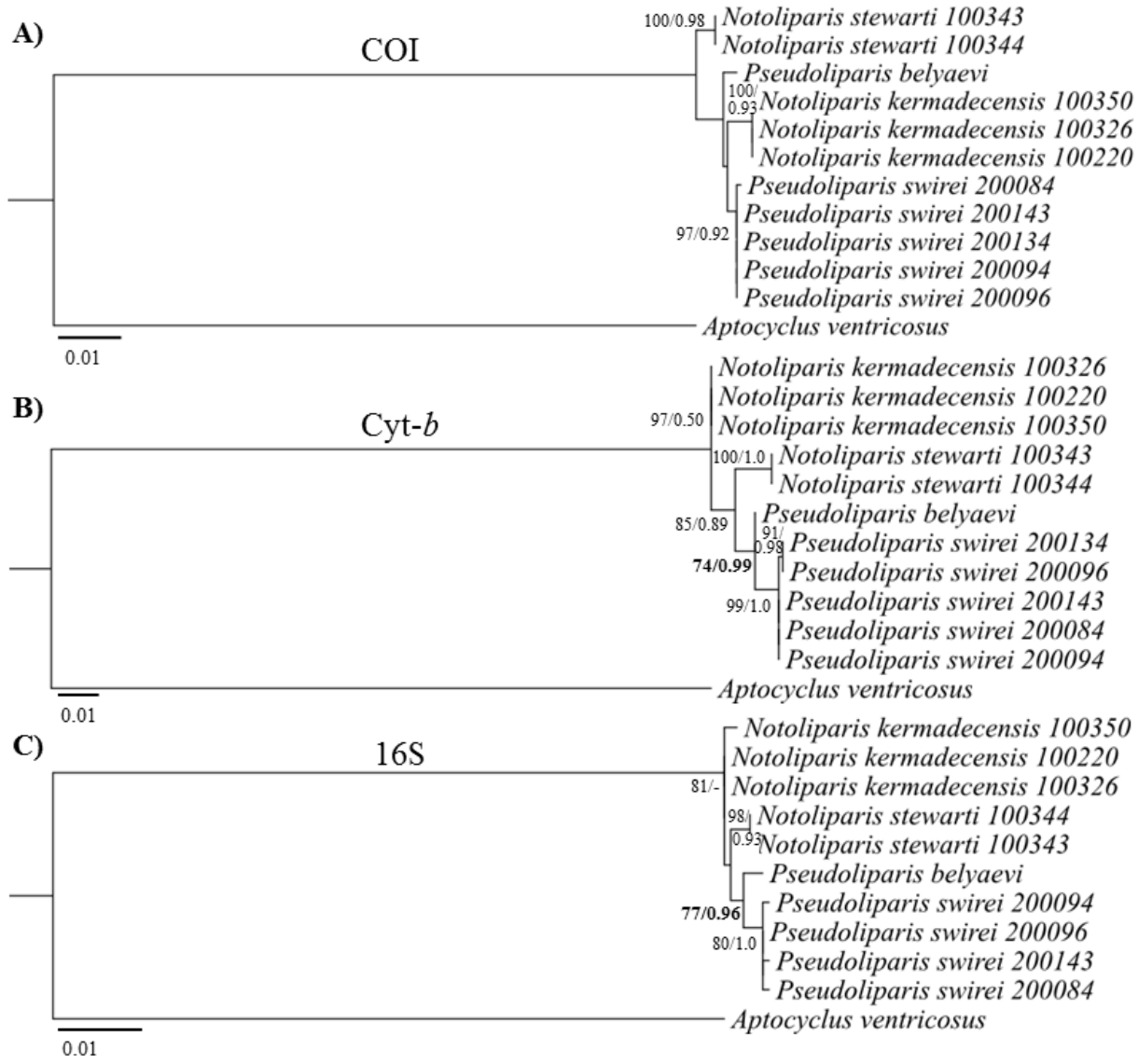

Figure 6.6. Phylogenetic relationships of *Pseudoliparis swirei* to closely related hadal liparids, *P. belyaevi* from the Japan Trench and *Notoliparis kermadecensis* and *Notoliparis stewarti* from the Kermadec Trench. Maximum likelihood (ML) trees based on A) cytochrome *c* oxidase subunit I (1399 bp), B) cytochrome *b* (1007 bp), and C) 16S rRNA (1472 bp). ML bootstrap support (>70%) and Bayesian posterior probability (>0.70) values are shown as ML/BI. Bold values indicate the node that supports placement of *P. swirei* sp. nov. within the genus *Pseudoliparis*. *Aptocyclus ventricosus* (GenBank accession NC008129.1) was used to root each tree.

Table 6.4. Evolutionary divergence between *Pseudoliparis swirei* and close relatives. Average genetic distance among species calculated for (A) cytochrome *c* oxidase subunit I (644 bp), (B) cytochrome *b* (744 bp), and (C) 16S rRNA (699 bp), based on the Tamura-Nei substitution model with gamma-distributed rate variation across sites. Sequences from *P. swirei*, *N. kermadecensis*, *N. stewarti* derive from this study, *P. belyaevi* is unpublished data from T. Satoh (National Museum of Nature and Science, Japan), sequences from *C. rastrinus*, *C. cypselurus*, *A. ventricosus* were from NCBI (GenBank Accession Numbers: AB565515.1, AB565517.1, AB565629.1, FJ164433.1, JF952697.1, NC_008129.1).

COI	*A. ventricosus*	*C. cypselurus*	*C. rastrinus*	*N. kermadecensis*	*N. stewarti*	*P. belyaevi*	*P. swirei*
A. ventricosus	***	0.648	0.505	0.359	0.353	0.391	0.373
C. cypselurus	0.648	***	0.173	0.121	0.121	0.12	0.13
C. rastrinus	0.505	0.173	***	0.139	0.138	0.136	0.133
N. kermadecensis	0.359	0.121	0.139	***	0.01	0.009	0.004
N. stewarti	0.353	0.121	0.138	0.01	***	0.015	0.01
P. belyaevi	0.391	0.12	0.136	0.009	0.015	***	0.005
P. swirei	0.373	0.13	0.133	0.004	0.01	0.005	***
Cyt-b	*A. ventricosus*	*C. colletti*	*C. rastrinus*	*N. kermadecensis*	*N. stewarti*	*P. belyaevi*	*P. swirei*
A. ventricosus	***	1.026	0.881	0.742	0.813	0.769	0.779
C. colletti	1.026	***	0.196	0.245	0.216	0.241	0.237
C. rastrinus	0.881	0.196	***	0.193	0.189	0.179	0.189
N. kermadecensis	0.742	0.245	0.193	***	0.015	0.01	0.014
N. stewarti	0.813	0.216	0.189	0.015	***	0.01	0.014
P. belyaevi	0.769	0.241	0.179	0.01	0.01	***	0.006
P. swirei	0.779	0.237	0.189	0.014	0.014	0.006	***
16S	*A. ventricosus*	*C. rastrinus*	*N. kermadecensis*	*N. stewarti*	*P. belyaevi*	*P. swirei*	
A. ventricosus	***	0.3	0.271	0.281	0.281	0.303	
C. rastrinus	0.3	***	0.075	0.075	0.072	0.08	
N. kermadecensis	0.271	0.075	***	0.003	0.008	0.01	
N. stewarti	0.281	0.075	0.003	***	0.008	0.01	
P. belyaevi	0.281	0.072	0.008	0.008	***	0.007	
P. swirei	0.303	0.08	0.01	0.01	0.007	***	

Reproduction. Holotype is immature. Ripe females had eggs up to 9.4 mm diameter, among the largest teleost eggs recorded (Tyler and Sumpter, 1996), 0.4 mm smaller than the largest record (Matallanas et al., 1990). The eggs were unsorted within gonad with the largest eggs free and interspersed within a matrix of smaller eggs. No developmental structures were visible within even the largest eggs. Two distinct size classes of eggs present with up to 23 large eggs (>5 mm) and up to 851 small eggs of less than half the diameter of the larger size class. There were rarely intermediate stages (**Figure 6.7**). Individuals with only small eggs had maximum egg sizes ranging from 0.7 to 1.4 mm. Genital papilla visible in freshly collected males, oriented anteriorly.

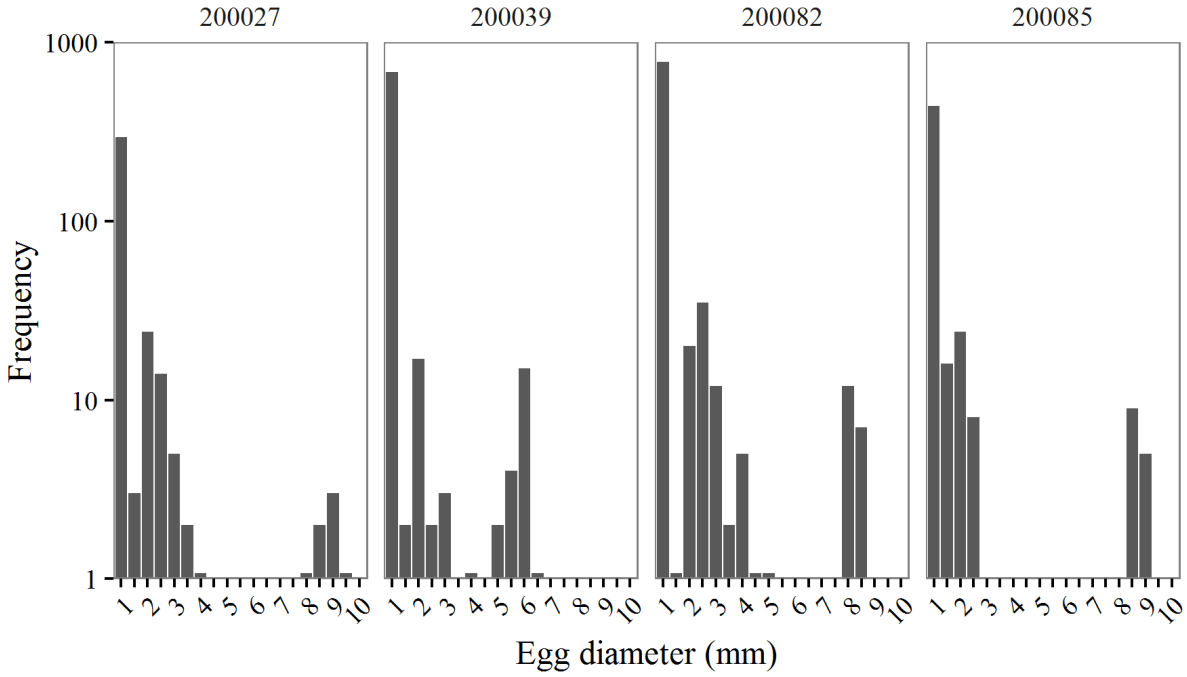

Figure 6.7. Egg sizes and frequencies from four individuals. Binned into 0.5 mm increments. Small peaks show 22, 23, 7, 14 large eggs for specimens HADES # 200027, 200039, 200082, 200085.

Distribution. Known only from the Mariana Trench at capture depths from 6898–7966 m, individuals likely this species were recognized in video at depths 6198–8098 m (Linley et al., 2016; Jamieson and Linley, unpublished data).

Etymology. The Mariana Trench famously houses the ocean's deepest point, at Challenger Deep, named for the *HMS Challenger* expedition which discovered the trench in 1875. Their deepest sounding of 8,184 m, then the greatest known ocean depth, was christened Swire Deep after Herbert Swire, the ship's First Navigating Sublieutenant (Corfield, 2003). We name this fish in his honor, in acknowledgment and gratitude of the crew members that have supported oceanographic research throughout history.

Discussion

Currently, the hadal liparid genera *Notoliparis* Andriashev 1975 and *Pseudoliparis* Andriashev 1955 are distinguished from one another only by the presence in the former (and absence in the latter) of a series of "extra" postcoronal and temporal cephalic pores (Andriashev & Pitruk, 1993). These pores are easily damaged or lost during sampling and recovery of specimens, in which case it is impossible to determine to which genus a specimen should be assigned. Andriashev himself noted that in at least one *Notoliparis* species, *N. macquariensis* Andriashev, the tiny posterior pores were only briefly visible in freshly caught specimens (Andriashev 1978). Due to the fragile skin and time spent in warm (up to 30°C) surface waters during recovery, very few of these pores remained in our material. In one individual (SY1615028), two postcoronal pores were visible (**Figure 6.8**). However, the skin had been damaged in such a way that temporal cephalic pores were lost. Other characters distinguishing the two genera overlap and cannot be used to assign a species to genus.

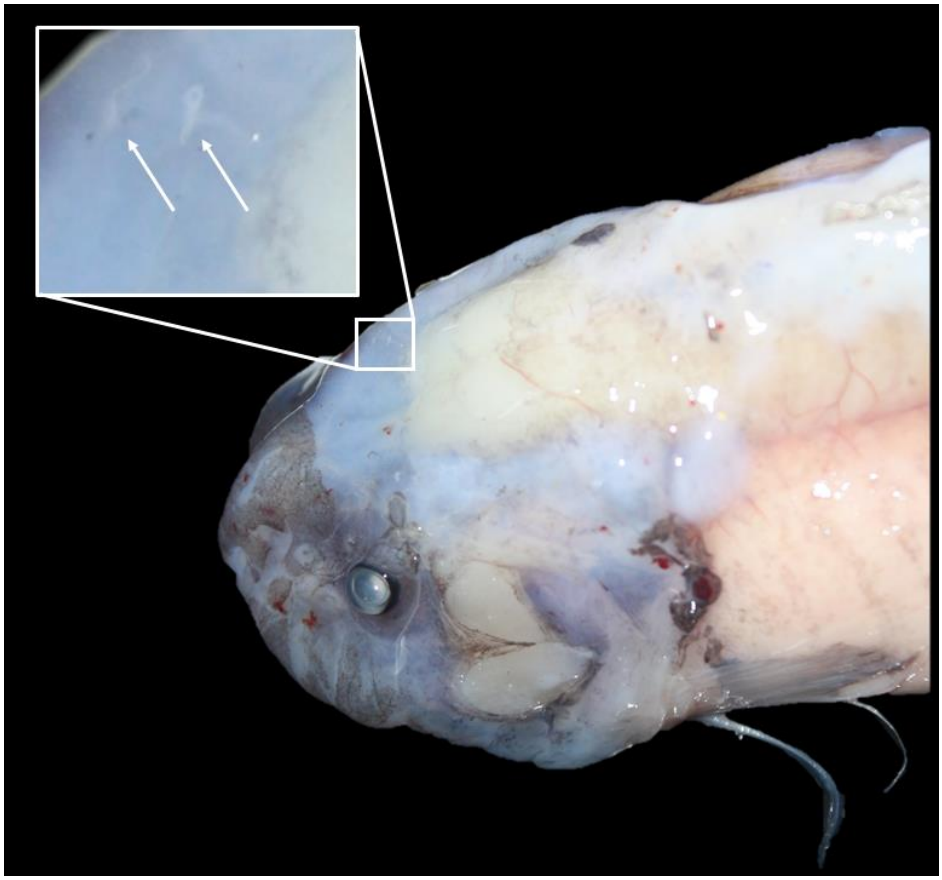

Figure 6.8. Postcoronal pores in freshly-caught specimen. Paratype SY1615028, male, head length 45 mm.

Given the uncertainty of the pore observations and without strong morphological justification for placement in either genus, we assign this new species to the genus *Pseudoliparis* on genetic grounds. Phylogenetic analysis supported a closer relationship between *P. swirei* sp. nov. and *Pseudoliparis belyaevi* in the Japan Trench than to hadal liparid populations in the Kermadec Trench (*N. kermadecensis*, *N. stewarti*; **Table 6.4**, **Figure 6.6**). Our molecular results also supported the distinction of two hadal liparid species in the Kermadec Trench as described by Stein (2016) - *Notoliparis kermadecensis* Nielsen and *Notoliparis stewarti* Stein, which appear to have overlapping distributions.

Our results also call into question the genus-level distinction between hadal liparids of *Pseudoliparis* and *Notoliparis*. The close genetic similarities between *Pseudoliparis* and

Notoliparis species, the fleeting and dubious nature of the distinguishing character of cephalic pores, and the behavioral and morphological consistencies between the two genera make it difficult to justify a division between these two groups. Aside from cephalic pore counts, the two genera overlap in meristic characters and counts (Stein, 2016; Andriashev & Pitruk, 1993). Further, in ecological studies, hadal liparids seem to fill very similar niches in their respective trenches (Jamieson et al., 2009; Fujii et al., 2010; Linley et al., 2016; Linley et al., 2017; Gerringer et al., 2017; **Chapter II**). Synonymizing these two hadal genera should be considered when genetic information on a greater number of *Notoliparis* and *Pseudoliparis* species are available.

Pseudoliparis swirei was abundant at depths of approximately 7000–8000 m in the Mariana Trench. Video records showed large aggregations of different-sized individuals were attracted to the bait (Linley et al., 2016) and fed on swarms of amphipods that also arrived (Linley et al., 2017; Gerringer et al., 2017; **Chapter II**). Smaller individuals were caught at greater depths (Linley et al., 2016). No individuals were seen at depths below 8,200 m, which is hypothesized to be the physiological depth limit for teleosts (Yancey et al., 2014). The discovery of yet another trench liparid species provides further evidence for the importance of this family within the hadal environment. This collection will allow further exploration of hadal endemism and the factors leading to the recurrent colonization of trenches by liparids.

Material Examined

Holotype. HADES #200060, immature, 97 mm SL, Stn. WT06, 12.3037°N, 144.6804°E, 7,949 m, 21 Nov 2014.

Paratypes. HADES #200021, male, 193 mm SL, Stn. TR05, 12.5979°N, 144.7785°E, 7,062 m, 15 Nov 2014. HADES #200024, sex unknown, 232 mm SL, #200025, female, 235 mm SL, Stn. WT03, 12.6103°N, 144.7684°E, 6,961 m, 16 Nov 2014. HADES #200027, female, 220 mm SL, Stn. TR06, 12.6339°N, 144.7508°E, 6,914 m, 16 Nov 2014. HADES #200033, sex unknown, 126 mm SL, Stn. WT04, 12.4151°N, 144.9119°E, 7,495 m, 18 Nov 2014. HADES #200036, sex

unexamined, 186 mm SL, #200037, sex unexamined, 89 mm SL, #200038, sex unexamined, 165 mm SL, #200039, female, 210 mm SL, #200040, female, 184 mm SL, #200041, sex unknown, 105 mm SL, #200042, sex unknown, 147 mm SL, #200043, female, 182 mm, Stn. TR07, 12.4235°N, 144.8706°E, 7,497 m, 18 Nov 2014. HADES #200047, male, 178 mm SL, #200048, male, 135+ mm SL, #200049, 128 mm SL, #200050, sex unexamined, ~100 mm SL, Stn. TR08, 12.4256°N, 144.9117°E, 7,509 m, 19 Nov 2014. HADES #200062, sex unknown, 16 mm head length Stn. TR09, 12.3027°N, 144.6739°E, 7,929 m, 21 Nov 2014. HADES #200070, female, 172 mm SL, #200071, sex unknown, 110 mm SL, #200072, juvenile, 119 mm SL, Stn. TR10, 11.9128°N, 144.9445°E, 7,841 m, 23 Nov 2014. HADES #200074, male, 145 mm SL, Stn. WT07, 11.9273°N, 144.9620°E, 7,907 m, 23 Nov 2014. HADES #200081, juvenile, 107 mm SL, Stn. WT08, 11.9297°N, 144.9288°E, 7,966, 24 Nov 2014. HADES #200084, female, 176 mm SL, #200085, female, 225 mm SL, Stn. WT09, 11.8147°N, 144.9858°E, 6,949 m, 25 Nov 2014. HADES #200087, female, 203 mm SL, Stn. TR12, 11.8107°N, 144.9945°E, 6,898 m, 25 Nov 2014. HADES #200094, female, 187 mm SL, #200095, female, 124 mm SL, #200096, female, 183 mm SL, Stn. TR13, 11.8260°N, 145.0088°E, 6,974, 26 Nov 2014. HADES #200133, juvenile, 151 mm SL, #200134, female, 161 mm SL, Stn. TR19, 12.2766°N, 144.6202°E, 7,626 m, 6 Dec 2014. HADES #200141, sex unexamined, 139 mm SL, #200142, male, 142 mm SL, #200143, female, 129 mm SL, #200144, juvenile, 119 mm SL, Stn. TR20, 12.3495°N, 144.6813°E, 7,652 m, 7 Dec 2014. #SY1615028, male, 210 mm SL, Stn. FT02, 11.5429°N, 142.1849°E, 7,581 m, 29 Jan 2017. SL measured fresh for all.

Contributors

Gerringer, M.E.[1], Linley, T.D.[2], Jamieson, A.J.[2], Goetze, E.[1], Drazen, J.D.[1]

[1]Department of Oceanography, University of Hawai‘i at Mānoa, Honolulu, HI 96822, USA.
[2]School of Marine Science and Technology, Ridley Building, Newcastle University, Newcastle Upon Tyne, UK. NE1 7RU

JCD, AJJ, TDL, and MEG collected specimens. MEG and TDL took meristic measurements and made counts. TDL produced the drawings. MEG and EG conducted genetic analyses. All authors contributed to the writing and editing of the manuscript.

Acknowledgements

This work was supported by the National Science Foundation Grant OCE #1130712, Schmidt Ocean Institute, and the Marine Alliance for Science and Technology for Scotland (MASTS). We are extremely grateful to T.P. Satoh (National Museum of Nature and Science, Japan) for *P. belyaevi* genetic data. The authors also express their gratitude to the NOAA Monument office for access to the Marianas Trench Marine National Monument, D. Stein (Oregon State University) for access to literature and taxonomic consultation, N. Chernova (ZIN) for access to Russian literature, S. Raredon (Smithsonian Institution) for obtaining radiographs of the specimens, Marilyn Dunlap and Tina Carvalho for providing dyes (University of Hawaii), Shaobin Hou and Xuehua Wan (University of Hawaii) for DNA sequencing, Adam Summers (University of Washington) for microCT images and the 3D model at the Karel F. Liem BioImaging Center, and the University of Guam for assistance in acquiring chemicals. G. Shinohara, National Museum of Nature and Science, Tokyo, loaned specimens of *P. amblystomopsis*. M. Gerringer is grateful for the support of NSF's Graduate Research Fellowship Program. T. Linley and A. Jamieson are supported by, and extend their thanks to, the MASTS pooling initiative. The MASTS Postdoctoral and Early Career Researcher Exchanges (PECRE) also supported T. Linley's travel expenses without which direct work on the specimens would not have been possible. We thank NOAA-NMFS Pacific Islands Fisheries Science Center, the Pacific Islands Regional Office, the Marine National Monuments Program, and E. Breuer (NOAA/NMFS), and NHK Japan Broadcasting Corporation for their assistance and collaboration. We extend also our heartfelt thanks to the captains and crews of the *R/V Falkor* and *R/V Shinyo-maru*, and participants in the HADES (HADal Ecosystems Studies) Program.

References

Andriashev, A., 1978. On the third species of the ultra-abyssal genus *Notoliparis* Andr. (Pisces. Liparidae), from the deepwaters of the Macquarie Trench, with some notes on zoogeographic and evolutionary significance of this discovery. Trudy Instituta Okeanologii Akademiia Nauk SSSR 112, 152–161.

Andriashev, A., 2003. Snailfishes (Liparidae, Scorpaeniformes) from the Southern Ocean and adjacent waters. In: Issledovaniya fauny morei (Study of Marine Fauna) St. Petersburg: Zoological Institute Ross. Akademiia Nauk.

Andriashev, A.P., Pitruk, D.L., 1993. A review of the ultra-abyssal (hadal) genus *Pseudoliparis* (Scorpaeniformes, Liparidae) with a description of a new species from the Japan Trench. Voprosy ikhtiologii 33, 325–330.

Chernova, N., Stein, D., Andriashev, A., 2004. Family Liparidae Scopoli 1777. California Academy of Sciences Annotated Checklists of Fishes 31.

Corfield, R., 2003. The silent landscape the scientific voyage of HMS Challenger. Washington, D.C.: Joseph Henry Press, Washington, D.C., 285 pp.

Darriba, D., Taboada, G.L., Doallo, R., Posada, D., 2012. jModelTest2: more models, new heuristics, and parallel computing. Nature Methods 9(8), 772. (doi:10.1038/nmeth.2109)

Eastman, J., Hikida, R., Devries, A., 1994. Buoyancy studies and microscopy of skin and subdermal extracellular matrix of the antarctic snailfish, *Paraliparis devriesi*. Journal of Morphology 220, 85–101. (doi:10.1002/jmor.1052200108)

Edgar, R.C., 2004. MUSCLE: Multiple sequence alignment with high accuracy and high throughput. Nucleic Acids Research 32, 1792–1797. (doi:10.1093/nar/gkh340)

Fujii, T., Jamieson, A., Solan, M., Bagley, P., Priede, I., 2010. A large aggregation of liparids at 7703 meters and a reappraisal of the abundance and diversity of hadal fish. BioScience 60, 506–515. (doi:10.1525/bio.2010.60.7.6)

Gerringer, M.E., Popp, B.N., Linley, T.D., Jamieson, A.J., Drazen, J.C., 2017. Comparative feeding ecology of abyssal and hadal fishes through stomach content and amino acid isotope analysis. Deep-Sea Research Part I: Oceanographic Research Papers. 121, 110–120. (doi:10.1016/j.dsr.2017.01.003)

Guindon, S., Gascuel, O., 2003. A simple, fast, and accurate method to estimate large phylogenies by maximum-likelihood. Systematic Biology 52, 696–704.

Hay, D.E., 1982. Fixation shrinkage of herring larvae: Effects of salinity, formalin concentration, and other factors. Canadian Journal of Fisheries and Aquatic Sciences 39, 1138–1143. (doi:10.1139/f91-215)

Jamieson, A. J., Fujii, T., Solan, M., Matsumoto, A. K., Bagley, P. M., Priede, I. G., 2009. Liparid and macrourid fishes of the hadal zone: *in situ* observations of activity and feeding behaviour. Proceedings of the Royal Society B: Biological Sciences, 276(1659), 1037–1045. (doi:10.1098/rspb.2008.1670)

Jamieson, A. J., Kilgallen, N., Rowden, A., Fujii, T., Horton, T., Lörz, A.-N., Kitazawa, K., Priede, I., 2011. Bait-attending fauna of the Kermadec Trench, SW Pacific Ocean: Evidence for an ecotone across the abyssal–hadal transition zone. Deep Sea Research Part I: Oceanographic Research Papers 58, 49–62. (doi:10.1016/j.dsr.2010.11.003)

Kai, Y., Orr, J.W., Sakai, K., Nakabo, T., 2011. Genetic and morphological evidence for cryptic diversity in the *Careproctus rastrinus* species complex (Liparidae) of the North Pacific. Ichthyological Research 58, 143–154. (doi:10.1007/s10228-010-0202-2)

Kearse, M., Moir, R., Wilson, A., Stones-Havas, S., Cheung, M., Sturrock, S., Buxton, S., Cooper, A., Markowitz, S., Duran, C., Thierer, T., Ashton, B., Mentjies, P., Drummond, A., 2012. Geneious Basic: an integrated and extendable desktop software platform for the organization and analysis of sequence data. Bioinformatics 28(12), 1647–1649. (doi:10.1093/bioinformatics/bts199)

Kristoffersen, J.B., Salvanes, A.G.V., 1998. Effects of formaldehyde and ethanol preservation on body and otoliths of *Maurolicus muelleri* and *Benthosema glaciale*. Sarsia 83, 95–102. (doi:10.1080/00364827.1998.10413675)

Letunic, I., Bork, P., 2007. Interactive Tree of Life (iTOL): an online tool for phylogenetic tree display and annotation. Bioinformatics 23, 127–8.

Linley, T.D., Gerringer, M.E., Yancey, P.H., Drazen, J.C., Weinstock, C.L., Jamieson, A.J., 2016. Fishes of the hadal zone including new species, *in situ* observations and depth records of Liparidae. Deep Sea Research Part I: Oceanographic Research Papers 114, 99–110. (doi:10.1016/j.dsr.2016.05.003)

Linley, T.D., Stewart, A.L., McMillan, P.J., Clark, M.R., Gerringer, M.E., Drazen, J.C., Fujii, T., Jamieson, A.J., 2017. Bait attending fishes of the abyssal zone and hadal boundary: community structure, functional groups and species distribution in the Kermadec, New Hebrides and Mariana trenches. Deep Sea Research Part I: Oceanographic Research Papers 121, 38–53. (doi:10.1016/j.dsr.2016.12.009)

Matallanas, J., Rucabado, J., Lloris, D., Olivar, M. P., 1990. Early stages of development and reproductive biology of the South-American eelpout *Austrolycus depressiceps* Regan, 1913 (Teleostei: Zoarcidae). Scientia Marina, 54(3), 257–261.

McWilliam, H., Li, W., Uludag, M., Squizzato, S., Park, Y.M., Buso, N., Cowley, A.P., Lopez, R., 2013. Analysis tool web services from the EMBL-EBI. Nucleic Acids Research 41, 597–600. (doi;10.1093/nar/gkt376)

Miller, M., Pfeiffer, W., Schwartz, T., 2010. Creating the CIPRES Science Gateway for inference of large phylogenetic trees. Proceedings of the Gateway Computing Environments Workshop (GCE), pp 1–8.

Miya, M., Takeshima, H., Endo, H., Ishiguro, N.B., Inoue, J.G., Mukai, T., Satoh, T.P., Yamaguchi, M., Kawaguchi, A., Mabuchi, K., Shirai, S.M., Nishida, M., 2003. Major patterns of higher teleostean phylogenies: a new perspective based on 100 complete mitochondrial DNA sequences. Molecular Phylogenetics and Evolution 26(1), 121–38. (doi:10.1016/S1055-7903(02)00332-9)

Pérês, J., 1965. *Aperçu sur les résultats de deux plongées effectuées dans le ravin de Puerto-Rico par le bathyscaphe Archimède.* Deep-Sea Research and Oceanographic Abstracts 12, 883–891.

Ronquist, F., Teslenko, M., van der Mark, P., Ayres, D.L., Darling, A., Höhna, S., Larget, B., Liu, L., Suchard, M.A., Huelsenbeck, J.P., 2012. MrBayes 3.2: Efficient Bayesian phylogenetic inference and model choice across a large model space. Systematic Biology 61(3), 539–542. (doi:10.1093/sysbio/sys129)

Sabaj Perez, M., 2014. Standard Symbolic Codes for Institutional Resource Collections in Herpetology and Ichthyology. Version 5.

Saruwatari, T., López, J.A., Pietsch, T.T.W., Lopez, J., Pietsch, T.T.W., 1997. Cyanine blue: A versatile and harmless stain for specimen observation. Copeia 1997, 840–841. (doi:10.2307/1447302)

Stamatakis, A., 2014. RAxML version 8 a tool for phylogenetic analysis and post-analysis of large phylogenies. 2010–2011.

Stein, D.L., 2012. Snailfishes (Family Liparidae) of the Ross Sea, Antarctica, and Closely Adjacent Waters. Zootaxa 3285, 1–120.

Stein, D.L., 2016. Description of a new hadal *Notoliparis* from the Kermadec Trench, New Zealand, and redescription of *Notoliparis kermadecensis* (Nielsen) (Liparidae, Scorpaeniformes). Copeia 104(4), 907–920. (doi:10.1643/CI-16-451)

Stein, D.L., Chernova, N., Andriashev, A.P., 2001. Snailfishes (Pisces: Liparidae) of Australia, including descriptions of thirty new species. Records of the Australian Museum 53, 341–406. (doi:10.3853/j.0067-1975.53.2001.1351)

Steinke, D., Zemlak, T.S., Gavin, H., Hebert, P.D.N., 2009. DNA barcoding fishes of the Canadian Pacific. Marine Biology 156(12), 2641–2647. (doi:10.1007/s00227-009-1284-0)

Tamura, K., Nei, M., 2993. Estimation of the number of nucleotide substitutions in the control region of mitochondrial DNA in humans and chimpanzees. Molecular Biology and Evolution 10, 512–526. (doi:10.1093/oxfordjournals.molbev.a040023)

Tamura, K., Stecher, G., Peterson, D., Filipski, A., Kumar, S., 2013. MEGA6: Molecular Evolutionary Genetics Analysis Version 6.0. Molecular Biology and Evolution 30, 2725–2729. (doi:10.1093/molbev/mst197)

Taylor, W.R., 1967a. An enzyme method of clearing and staining small vertebrates. Smithsonian Press, Washington, D.C.

Taylor, W.R., 1967b. Outline of a method of clearing and staining tissues with pancreatic enzymes and staining bones of small vertebrates. Turtox News 45.

R Core Development Team, 2015. R: A Language and Environment for Statistical Computing. R Foundation for Statistical Computing Vienna, Au.

Tyler, C. R., Sumpter, J. P., 1996. Oocyte growth and development in teleosts. Reviews in Fish Biology and Fisheries, 6(3), 287–318. (doi:10.1007/BF00122584)

Wickam, H., 2009. ggplot2: elegant graphics for data analysis.

Yancey, P., Gerringer, M., Drazen, J., Rowden, A., Jamieson, A., 2014. Marine fish may be biochemically constrained from inhabiting the deepest ocean depths. Proceedings of the National Academy of Sciences U. S. A. 111, 4461–5. (doi:10.1073/pnas.1322003111)

Zhang, J.-B., Hanner, R., 2011. DNA barcoding is a useful tool for the identification of marine fishes from Japan. Biochemical Systematics and Ecology 39(1), 31–42. (doi:10.1016/j.bse.2010.12.017)

CHAPTER VII

Conclusions: On the success of the hadal snailfishes

Ocean zones are divided based on the distinguishing physical features of the environment which govern ecological interactions of the communities therein (Hedgpeth, 1957). Differing light levels, bathymetry, nutrient inputs, temperatures, hydrostatic pressures, and other factors have resulted in the evolution of a vast diversity of organisms that are specially adapted to their given habitats. Of course, we cannot travel back to witness the evolutionary processes, to track the development of adaptations across geologic time. While some fossils provide clues into the history of life on earth, for many habitats, we can only infer the evolutionary success of organisms to their particular environment by what remains today. Through observation and experimentation, we slowly piece together the story, by narrowing and isolating selective factors as systematically as possible. Through multiple approaches and careful consideration, a picture may begin to emerge. By comparing specific taxa found in one zone to those in another, we can explore the factors that explain the community shifts we observe today.

The bathymetric shift from the abyssal plains to hadal trench slopes is accompanied by distinct changes in the local fauna (e.g., Wolff, 1959; Beliaev, 1989; Jamieson et al., 2011). For fishes, this divide is prominent (e.g., Linley et al., 2017). Abyssal communities are characterized by cosmopolitan, elongate fishes such as macrourids, ophidiids, synaphobranchids, ipnopids, and zoarcids (e.g., Wilson and Waples, 1983; Nielsen and Merrett, 2000; Milligan et al., 2016), while in many hadal trenches, a different family dominates—the liparids. Although liparids are found over a wide bathymetric range—from the intertidal through the abyss (Chernova et al., 2004)—their consistent abundance at hadal depths is striking. On the abyssal plain, snailfishes are not generally found in large groups, nor are they a prominent fish family by any means. Yet, in trench after trench, from the Kurile-Kamchatka in the north to the Kermadec in the south, to the Peru-Chile across the Pacific, large communities of apparently endemic snailfishes have been discovered (Nielsen, 1964; Jamieson et al., 2009; Fujii et al., 2010; Linley et al., 2016). Further,

in these hadal habitats, snailfishes seem to have replaced other families of larger fishes such as macrourids that are more abundant than liparids in abyssal and bathyal habitats. Clearly, these snailfishes are well-suited to the hadal zone. This dissertation explores potential factors driving this success of the snailfishes in hadal trenches.

Together, the present studies suggest that the drivers resulting in the notable success of the liparids in the hadal zone are complex and likely involve the interaction of several factors. Snailfishes may have a nutritional advantage in hadal trenches due to increased abundances of small crustacean prey such as amphipods. Fish taxa that rely on piscivory or scavenging, such as macrourids or synaphobranchids, might not see this advantage and may therefore not have the same evolutionary pressures to invade hadal depths. Stomach contents and stable isotope analyses in **Chapter II** supported this hypothesis. Although there may be increased food availability for some taxa, hadal depths are also characterized by extremely high hydrostatic pressures. Only organisms that have been able to adapt to these pressures would be able to live in the hadal zone—perhaps the most obvious factor limiting radiation to the greatest ocean depths (Günther, 1887). Adaptations to high pressure can take many forms, from maintenance of membrane fluidity to the accumulation of molecules that extrinsically support protein function (reviewed by Somero, 1992). **Chapter III** detailed an additional pressure adaptation – intrinsic changes in lactate dehydrogenase of hadal liparids and abyssal macrourids that allow the enzymes to function better at *in situ* pressures than at atmospheric pressure, a change not seen in shallower-living confamilials. This type of pressure adaptation allows these fishes to thrive at hadal depths. **Chapter IV** tested the hypothesis that life history plays a role in the success of the hadal liparids. This may be partially true. Hadal liparids were estimated to be relatively short-lived based on otolith growth zones, on the order of 15 years, which may be advantageous in the seismically active, high-disturbance environment of subducting trenches. However, the hypothesis that hadal liparids have benthic larvae—limiting dispersal and facilitating endemism—was not supported by thermal history reconstructions based on oxygen isotopic composition of otoliths. Unexpectedly, large changes in oxygen isotopic compositions suggest temperature changes of greater than 5°C across ontogeny for hadal liparids from both the Mariana and Kermadec trenches. **Chapter V** illustrated an

additional adaptation of liparids—gelatinous tissues that help the fishes maintain buoyancy and body shape at low energetic cost. As may be expected, these studies suggest that there are a multitude of factors that have led to the notable success of snailfishes in the hadal zone.

Although this doctoral research marks significant advancements in the understanding of the biology of hadal snailfishes, each of the factors explored here warrant further investigation. Few data exist on feeding ecology at hadal depths (e.g., Blankenship and Levin, 2007; **Chapter II**). **Chapter II** provided stomach contents data for two hadal snailfishes, showing that amphipods are the most important prey item in both species. For a less temporally-limited view of trophic ecology, $\delta^{15}N$ values of specific amino acids were also determined. From these, trophic levels were estimated to be near four for both hadal liparids. This study revealed previously unknown predator-prey relationships in the hadal zone—particularly that hadal liparids eat both swimming polychaetes (*Notoliparis kermadecensis* only) and decapods. Stomach content compositions and trophic positions were distinctly different for the abyssal and hadal species examined. This comparison was made using published data on abyssal species. However, data on the feeding habits of abyssal fishes are currently limited (reviewed by Drazen and Sutton, 2017). The comparison of the trophic ecology of abyssal and hadal species would benefit from a broader analysis of abyssal fish stomach contents and stable isotopic compositions. Additional detailed analysis should focus on the deepest living species of the families Ophidiidae, Zoarcidae, and Synaphobranchidae. A detailed functional morphology of abyssal and hadal fish feeding, similar to what has been conducted for Antarctic fishes (Bansode et al., 2014), may also further illuminate the role of trophic ecology in niche partitioning and depth zonation in these zones. In addition to a shift in feeding strategy—from certain abyssal fishes that bite and tear their food to suction-feeding in hadal fishes—functional morphology and modeling of suction feeding parameters may reveal differences in optimum prey sizes for abyssal and hadal species. A difference in optimum prey size in relation to prey availability may partially account for the abundance of liparids in the hadal zone in comparison to the ophidiids, which also suction feed but have only a shallow-hadal and abyssal range (Linley et al., 2017). Further, the strong pharyngeal jaw apparatus found in snailfishes from the Kermadec and Mariana trenches (Gerringer et al., 2017; **Chapter II**) likely

contributes to their ability to take advantage of large amphipod biomass at hadal depths. Detailed analysis of functional morphology of this pharyngeal jaw structure across the family Liparidae using extensive museum collections already in existence would further clarify the role of trophic ecology in the radiation of this family into the deep sea. Insight into the sensory strategies of abyssal and hadal fishes would also be useful toward this end. For example, an analysis of the relative brain lobe sizes of hadal liparids could reveal sensory adaptations in these species (Eastman and Lannoo, 1998; Wagner, 2002; Lisney and Collin, 2006). No records of bioluminescence yet exist at hadal depths, but the hadal liparids that have been collected do have developed eyes (Nielsen, 1964; **Chapter VI**).

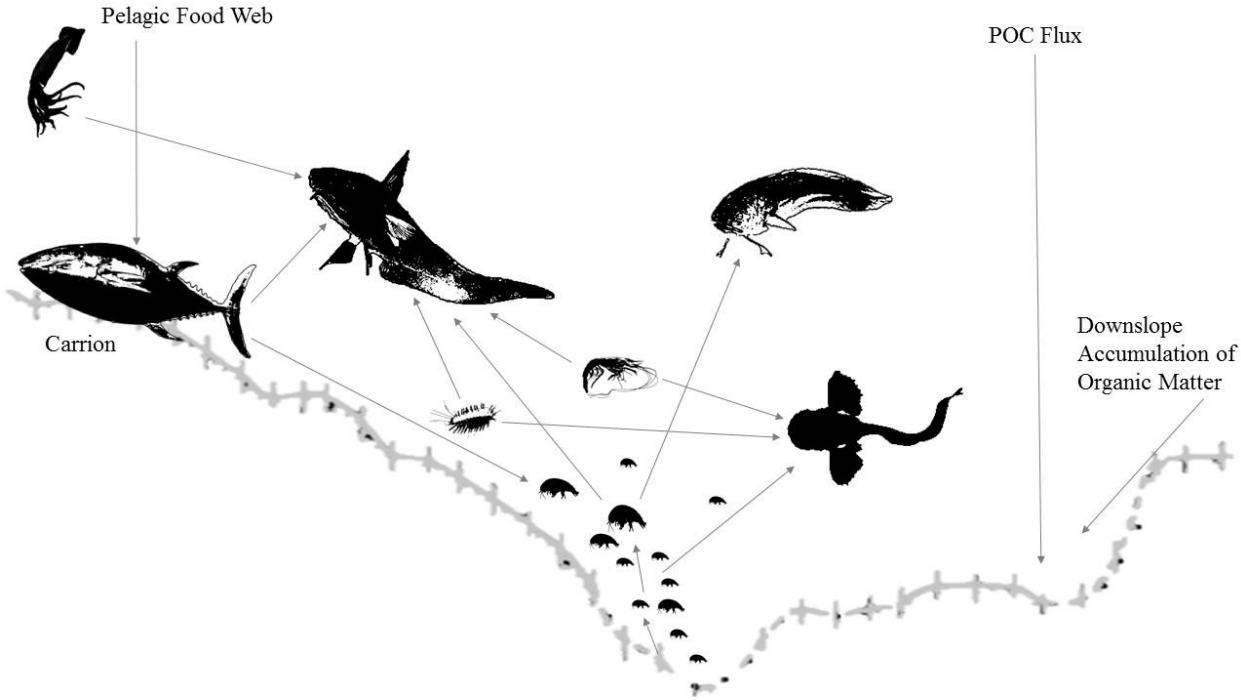

Figure 7.1. Preliminary generalized hadal food web derived from information presented here. Bathymetry based on Japan Trench (Fisher, 1954). Arrows indicate known trophic linkages. Organisms shown include squid, macrourids, ophidiids, liparids, decapods, polychaetes, and amphipods. Macrourids and ophidiids are part of the abyssal/upper edges of the hadal food web. POC: Particulate organic carbon. Drawings based on photos from MBARI, NOAA OER, Stuart Piertney, Alan Jamieson. Not to scale.

The data presented in **Chapter II** inform new understanding of trophic linkages in the hadal zone, with the eventual goal of assembling a hadal food web (i.e., **Figure 7.1**). Further research is necessary to construct a complete food web, however. Additional stomach contents and stable isotope analysis on other taxa—particularly amphipods, decapods, and holothurians—would be needed. Understanding the hadal food web is important not only as a matter of ecological interest, but for tracking global patterns of carbon turnover. The hypothesis that trenches act as sinks of organic matter has been largely accepted (George and Higgins, 1979; Danovaro et al., 2002; Itoh et al., 2011; Ichino et al., 2015). Many authors note that accumulation of organic material would be significant for global carbon cycling, but the details of this process demand further research (Glud et al., 2013; Oguri et al., 2013; Wenzhöfer et al., 2016).

Hadal liparids certainly employ a number of adaptations to high hydrostatic pressures, some of which are outlined in **Chapter III**. Lactate dehydrogenases from hadal snailfishes functioned better under *in situ* pressures than at atmospheric pressure, while the same enzyme from an intertidal snailfish was inhibited by pressure. Future study could investigate specific amino acid changes involved in maintaining this stability under pressure (e.g., Brindley et al., 2008). A crystallography approach could also be used to determine water dynamics and mechanisms involved in these reactions, which would provide additional insight into this pressure adaptation (Gross and Jaenicke, 1994; Shrestha et al., 2015; Foglia et al., 2016).

Metabolic enzyme activities have been used as proxies of metabolic rate in deep-sea fishes (e.g., Drazen et al., 2015), a technique that is complicated by the findings of **Chapter III**. Pressure effects on enzyme maximum activities, which we show vary by species, enzyme, and habitat, will need to be considered in future applications of these proxies. Hydrostatic pressure has been considered not to affect metabolic rate (e.g., Seibel and Drazen, 2007). However, these results show that pressure, like temperature, can control reaction rates of certain enzymes. Hadal depth pressures may affect metabolic rate. Future work should seek to clarify these effects. Pressure and temperature also have interacting effects on biomolecules (e.g., Dahlhoff and Somero, 1991; Somero, 1992). The interaction of these two factors is an interesting field of study that requires additional research. Eventually, it may be possible to develop a model that quantifies pressure and

temperature effects on a molecular level, allowing something like a growing degree-day-bar to be applied in discussions of metabolic rate (**Chapter III**).

Chapter IV provided the first data on the life history of hadal fishes using otolith growth zones and oxygen isotope analysis. Age estimates for hadal liparids ranged between five and sixteen years old. These estimates are younger than those estimated for the shallower-living liparid *Careproctus melanurus*, which revealed up to twenty-five annuli. Abyssal macrourids *Coryphaenoides armatus* and *C. yaquinae* were estimated to be up to twenty-nine and sixteen years old, respectively. In this study, growth rings were assumed to be annual, but validation methods were not feasible. Future research should seek to validate these estimates and the age reading protocol. Although many methods for validation exist (reviewed by Campana, 2001), most are not practical at abyssal or hadal depths. Lead-radium dating may be used to validate the ages of *Coryphaenoides armatus* and *C. yaquinae*, as was applied to other macrourids (Andrews et al., 1999), but this method requires nearly a gram of early otolith growth (core extraction of first few years) material for instrumental analysis. Hence, multiple individuals from discrete size or age classes would be needed to pool enough material. This type of analysis would likely require the combination of multiple collections to cover a thorough size range, but would be a valuable way to verify growth patterns in a common and important abyssal group. Validated life history data on these abyssal macrourids would also greatly inform discussions of the factors governing growth rate of deep-sea fishes (Cailliet et al., 2001; Drazen and Haedrich, 2012), potentially clarifying the role of variables such as temperature, pressure, and food supply.

The hadal snailfish otoliths and otolith collections themselves are smaller than current instrumental analysis limits would allow for lead-radium dating, even with sample pooling. Other validation methods such as mark/recapture or outer ring analysis across multiple seasons are also impractical at this time. However, there may be a way to validate age estimates for one group of hadal liparids due to recent, extremely unfortunate circumstances. Four months after the Tohoku-Oki earthquake and Fukushima Dai-ichi nuclear disaster, large amounts of ^{134}Cs were deposited into the Japan Trench and found at 7,500 m (Oguri et al., 2013). Cesium is one of the detectable trace elements present in fish otoliths (reviewed by Sturrock et al., 2012). If the radioactive cesium

signature were taken up by the hadal snailfishes in the Japan Trench near the known time of deposition in 2011, it may be possible to use this time-specific marker as a tracer in a similar manner to bomb radiocarbon of fishes (e.g., Andrews et al., 2012). Given the relatively short ages predicted for hadal snailfishes and half-life of ^{134}Cs (2.06 years), there would be a limited temporal opportunity for this kind of study. In addition to validating ages for fishes in the hadal zone, future work could explore patterns of age and growth in other taxa. For example, hadal amphipods could be aged based on the accumulation of lipofuscin pigment in the brain (Bluhm et al., 2001). These data would be valuable as they represent the end of the depth and pressure range for marine organisms, allowing for the thorough examination of these effects.

The thermal history reconstruction results presented in **Chapter IV** that were determined from oxygen isotopic fractionation within the otoliths were highly unexpected. Changes in the oxygen isotopic composition across the otoliths of two hadal liparids suggest large changes in habitat temperature across the life of the fishes, potentially reflecting a 5,000 m depth differential between larvae and adult populations, according to the established conversions (e.g., Thorrold et al., 1997; Høie et al., 2004; Chang et al., 2015). According to the published literature and our validation efforts, this change could not be explained by metabolically-mediated fractionation, pressure effects, excess protein accumulation, or instrumental drift. Although the suggestion that a hadal fish could have such a large vertical range throughout ontogeny is surprising, it cannot currently be refuted with the available data. If these snailfishes are indeed feeding in shallow waters before returning to the hadal zone, this is an incredible feat. Other fishes are known for similarly impressive migrations, salmon being the most famous example, but also the European eel *Anguilla anguilla* that travels across the Atlantic in a 5,000 km spawning migration (Aarestrup et al., 2009). Large vertical migrations also exist in other species, for example the jellynose fish *Ateleopus japonicus* (Shiao et al., 2017) or rattails (Lin et al., 2012). However, this would be one of the largest changes in hydrostatic pressure experienced by any metazoan and this finding certainly warrants further verification. The vertical migration suggested in *Careproctus melanurus* shows that other members of the family Liparidae likely display similar life history traits. Pressure effects, such as those explored in **Chapter III**, would need to be investigated with this added

complication. If hadal liparid larvae are indeed present at depths shallower than 1000 m, it should be possible to collect them by trawl. Although liparid larvae have few distinguishing characters (e.g., Kim et al., 1986; Marliave and Peden, 1989) and confirming identifications morphologically would be difficult, genetic analysis could be used. This technique has been successfully applied in a number of systems for larval identification (e.g., Hubert et al., 2010; Riemann et al., 2010). Data from the genetic markers (mitochondrial genes 16S, COI, and Cyt-b) analyzed in **Chapter VI** for *Notoliparis kermadecensis* and the newly-discovered species of hadal liparid from the Mariana Trench would allow for positive identification of hadal liparid larvae collected from shallower depths over the trench.

There are now a few hadal trenches known to have more than one species of apparently endemic hadal snailfish. The Japan Trench has both *Pseudoliparis belyaevi* and *Pseudoliparis amblystomopsis* (Andriyashev et al., 1993). Collections from the present studies have revealed two populations in the Kermadec Trench—*Notoliparis kermadecensis* and *Notoliparis stewarti* (Stein, 2016; **Chapter VI**). There are also two snailfish populations in the Mariana Trench—the newly-collected species described here and the ethereal snailfish, which remains uncollected (**Chapter VI**, Linley et al., 2016). Perhaps a pelagic larval stage provides a dispersal mechanism for these populations. Future phylogenetic analyses of multiple hadal liparids, building on the tree presented in **Chapter VI** would be valuable in understanding connectivity between hadal fish populations and evolutionary patterns of dispersal. Similar work has begun for hadal amphipods, which shows complex connectivity patterns and species overlap, particularly in the genus *Hirondellea* (Ritchie et al., 2015). While it may be tempting to think of hadal trenches as remote, isolated habitats, evidence increasingly shows that trenches are closely tied to the surrounding ocean systems, even accumulating man-made pollutants at high concentrations (Jamieson et al., 2017). It will be interesting to continue to explore how connected or distinct individual hadal trenches are from one another and the waters above, and whether these patterns vary across taxa.

Chapter V explored the distribution, composition, and functions of gelatinous tissues in deep-sea fishes, including the hadal snailfish. Robotic modeling results supported the hypothesis that gelatinous tissues may help certain deep-sea fishes maintain low-drag body shapes without

having to build up energetically costly muscle. Future research could test this hypothesis further—applying computational fluid dynamic modeling to test the effects of a gelatinous-tissue-streamlined body shape on drag profiles around both a stationary, and then undulatory swimming fish, similar to work that has been done for tadpoles (Liu et al., 1996, 1997). Some authors have noted that body shape in fishes becomes more elongate at greater depths (Ward and Mehta, 2010; Neat and Campbell, 2013). Future modeling could also test how the positioning of gelatinous tissues within the body relates to this elongation. The location of the gelatinous tissues also varies between species. It is more likely that the drag reducing effect of gelatinous tissues would occur when the tissues are present directly under the skin—as in the hadal snailfishes—rather than embedded within muscle bundles, as in the cusk eel *Spectrunculus grandis*. The hypothesis that there is a swimming kinematics advantage to gelatinous tissue would also benefit from a study of the material properties of gelatinous tissues under *in situ* pressures and temperatures. This study may have implications for the design of biomimetic soft-bodied robot forms, which could employ a similar strategy for drag reduction to that used by these deep-sea fishes.

Much of the comparative work in this dissertation was conducted on *Coryphaneoides armatus* and *C. yaquinae*, prominent abyssal macrourids. This comparison is justifiable. The macrourids are certainly an important abyssal group, with representatives in most ocean basins at a broad range of depths (e.g., Wilson and Waples, 1983; Jamieson et al., 2009). Because there is a diversity of fishes living at abyssal depths, however, this is an oversimplification of the interactions at play in structuring the fish communities at abyssal and hadal depths. In particular, this simplification likely undervalues the role of the cusk eels (Ophidiidae). Ophidiids are a largely understudied group, though they are wide-ranging and likely important members of the abyssal fish community (e.g., Nielsen and Merrett, 2000; Uiblein et al., 2008; Nielsen and Møller, 2011; Linley et al., 2017). Future research could focus on the biogeography and ecology of the deep-dwelling cusk eels- to address their role in the abyssal ecosystem. Other abyssal fish families could also be compared in more detail in future work, including the eelpouts (Zoarcidae), cutthroat eels (Synaphobranchidae), and tripodfishes (Ipnopidae), the latter of which are very poorly studies as they are not attracted to baited cameras or traps.

Overall, this research shows hadal liparids to be highly-specialized, endemic fishes that thrive in deep-sea trenches through a number of adaptations. Hadal liparids have been captured and described from the Kurile-Kamchatka Trench (Andriashev, 1955), Japan Trench (Andriashev, 1955; Andriashev and Pitruk, 1993), Kermadec Trench (Nielsen, 1964), and Peru-Chile Trench (Stein, 2005). In addition to these known species, there are likely undiscovered species of hadal liparids in unexplored trenches. In 1964, for example, those diving the Puerto Rico Trench in the bathyscaphe *Archimede* reported that "at 7,300 m the community was characterized by the abundance of a liparidid fish (*Careproctus*?: about 200 individuals)" (Pérês, 1965). While no photographs were taken, subsequent observations of other trenches give credence to the claim. Due to its geographic isolation from other hadal ecosystems, this finding would be of particular importance to the understanding of the adaptation and evolution of the planet's deepest-living vertebrates.

Exploration of the Puerto Rico Trench could also shed light on one of the most contentious reports in hadal research. In 1970, the fish *Abyssobrotula galathea* was collected in an otter trawl deployed to 8,370 m in the Puerto Rico Trench. This has since held the record for deepest living fish (Nielsen, 1977). However, this fish was caught in an open trawl and the validity of this report has been called into question (e.g., Jamieson et al., 2009), although it is impossible to disprove. It has been suggested that fish may be physiologically incapable of descending much further than 8,200 m, due to the constraints of pressure adaptation (Yancey et al., 2014). A survey of the fish fauna of the Puerto Rico Trench would help to settle this debate and provide further insight into the depth limit for fishes.

Recent hadal research, including the contributions of this dissertation, has been largely exploratory. The next phase of hadal research should strive for greater temporal and spatial understanding of deep-sea trenches. From the videos, images, and samples of the hadal zone so far, it is already clear that there is great topographic and faunal heterogeneity within individual trenches and between trenches. The factors driving these changes warrant further exploration. Further, much of the work done at hadal depths has been on bait-attending fauna, due to technical constraints. Although useful, this equipment provides a certain biased view of the community.

Alternative sampling and exploration methods, including remotely operated vehicles, will need to be employed to gain a more holistic view of hadal fauna and their physiology and ecology. Hadal science is by necessity highly collaborative and interdisciplinary work. It will take continued cooperation between a host of scientists and engineers across borders to further our understanding of these communities in the ocean's greatest depths and their role in the global ocean ecosystem.

Delving into hadal research provides the opportunity to reveal one of our planet's most extraordinary and least understood habitats. There is an innate human curiosity and attraction to understanding the extremes of life and pushing the extremes of technology. This perpetual drive for progress and exploration is something very fundamental to the human spirit. In many ways, trench exploration embodies these drives. Toward this aim, there is still much more to discover, and much further to go in understanding the incredible organisms with whom we share our planet.

References

Aarestrup, K., Økland, F., Hansen, M.M., Righton, D., Gargan, P., Castonguay, M., Bernatchez, L., Howey, P., Sparholt, H., Pedersen, M.I., McKinley, R.S., 2009. Oceanic spawning migration of the European eel *Anguilla anguilla*. Science 325(5948), 1660. (doi:10.1126/science.1178120)

Andrews, A., Cailliet, G., Coale, K., 1999. Age and growth of the Pacific grenadier (*Coryphaenoides acrolepis*) with age estimate validation using an improved radiometric ageing technique. Canadian Journal of Fisheries and Aquatic Sciences 56, 1339–1350.

Andrews, A.H., DeMartini, E.E., Brodziak, J., Nichols, J.S., Humphreys, R.L., 2012. A long-lived life history for a tropical deep-water snapper (*Pristipomoides filamentosus*): bomb radiocarbon and lead-radium dating as extensions of daily increment analyses in otoliths. Canadian Journal of Fisheries and Aquatic Sciences 69, 1850–1869.

Andriashev, A., 1955. A new fish of the snailfish family (Pisces, Liparidae) found at a depth of more than 7 kilometers. Trudy Instituta Okeanologii 12, 340–344.

Andriashev, A., Pitruk, D., 1993. A review of the ultra-abyssal (hadal) genus *Pseudoliparis* (Scorpaeniformes, Liparidae) with a description of a new species from the Japan Trench. Voprosy ikhtiologii 33, 325–330.

Bansode, M., Eastman, J., Aronson, R., 2014. Feeding biomechanics of five demersal Antarctic fishes. Polar Biology 35–40. (doi:10.1007/s00300-014-1565-z)

Beliaev, G., 1989. Deep-Sea Ocean Trenches and their Fauna.

Blankenship, L., Levin, L., 2007. Extreme food webs: Foraging strategies and diets of scavenging amphipods from the ocean's deepest 5 kilometers. Limnology and Oceanography 52, 1685–1697. (doi:10.4319/lo.2007.52.4.1685)

Bluhm, B.A., Brey, T., Klages, M., 2001. The autofluorescent age pigment lipofuscin: Key to age, growth and productivity of the antarctic amphipod *Waldeckia obesa* (Chevreux, 1905). Journal of Experimental Marine Biology and Ecology 258, 215–235. (doi:10.1016/S0022-0981(01)00214-3)

Brindley, A.A., Pickersgill, R.W., Partridge, J.C., Dunstan, D.J., Hunt, D.M., Warren, M.J., 2008. Enzyme sequence and its relationship to hyperbaric stability of artificial and natural fish lactate dehydrogenases. PloS One. 3(4), e2042. (doi:10.1371/journal.pone.0002042)

Cailliet, G., Andrews, A., Burton, E., Watters, D., Kline, D., Ferry-Graham, L., 2001. Age determination and validation studies of marine fishes: do deep-dwellers live longer? Experimental Gerontology 36, 739–764. (doi:10.1016/S0531-5565(00)00239-4)

Campana, S., 2001. Accuracy, precision, and quality control in age determination, including a review of the use and abuse of age validation methods. Journal of Fish Biology 59, 197–242. (doi:10.1006/jfbi.2001.1668)

Chang, N.N., Liu, E.Y., Liao, Y.C., Shiao, J.C., 2015. Vertical habitat shift of viviparous and oviparous deep-sea cusk eels revealed by otolith microstructure and stable-isotope composition. Journal of Fish Biology 86, 845–853. (doi:10.1111/jfb.12605)

Chernova, N., Stein, D., Andriashev, A., 2004. Family Liparidae Scopoli 1777. California Academy of Sciences Annotated Checklists Fishes 31.

Dahlhoff, E., Somero, G., 1991. Pressure and temperature adaptation of cytosolic malate-dehydrogenases of shallow-living and deep-living marine-invertebrates—evidence for high body temperatures in hydrothermal vent animals. Journal of Experimental Biology 159, 473–487.

Danovaro, R., Gambi, C., Della Croce, N., 2002. Meiofauna hotspot in the Atacama Trench, eastern South Pacific Ocean. Deep-Sea Research Part I: Oceanographic Research Papers 49, 843–857. (doi:10.1016/S0967-0637(01)00084-X)

Drazen, J., Haedrich, R., 2012. A continuum of life histories in deep-sea demersal fishes. Deep-Sea Research Part I: Oceanographic Research Papers 61, 34–42. (doi:10.1016/j.dsr.2011.11.002)

Drazen, J.C., Friedman, J.R., Condon, N.E., Aus, E.J., Gerringer, M.E., Keller, A.A., Elizabeth Clarke, M., 2015. Enzyme activities of demersal fishes from the shelf to the abyssal plain. Deep-Sea Research Part I: Oceanographic Research Papers 100, 117–126. (doi:10.1016/j.dsr.2015.02.013)

Drazen, J.C., Sutton, T.T., 2017. Dining in the deep: The feeding ecology of deep-sea fishes. Annual Reviews in Marine Science 9, 337–366. (doi:10.1146/annurev-marine-010816-060543)

Eastman, J.T., Lannoo, M.J., 1998. Morphology of the brain and sense organs in the snailfish *Paraliparis devriesi*: Neural convergence and sensory compensation on the Antarctic shelf. Journal of Morphology 237, 213–236. (doi:10.1002/(SICI)1097-4687(199809)237:3<213::AID-JMOR2>3.0.CO;2-#)

Fisher, R., 1954. On the sounding of trenches. Deep-Sea Research 2, 48–58.

Foglia, F., Hazael, R., Simeoni, G.G., Appavou, M., Moulin, M., Haertlein, M., Forsyth, V.T., Seydel, T., Daniel, I., Meersman, F., Mcmillan, P.F., 2016. Water dynamics in *Shewanella oneidensis* at ambient and high pressure using quasi-elastic neutron scattering. Nature Scientific Reports 6, 1–9. (doi:10.1038/srep18862)

Fujii, T., Jamieson, A., Solan, M., Bagley, P., Priede, I., 2010. A large aggregation of liparids at 7703 meters and a reappraisal of the abundance and diversity of hadal fish. Bioscience 60, 506–515. (doi:10.1525/bio.2010.60.7.6)

George, R., Higgins, R., 1979. Eutrophic hadal benthic community in the Puerto Rico Trench. Ambio Special Reports 51–58.

Gerringer, M.E., Popp, B.N., Linley, T.D., Jamieson, A.J., Drazen, J.C., 2017. Comparative feeding ecology of abyssal and hadal fishes through stomach content and amino acid isotope analysis. Deep-Sea Research Part I: Oceanographic Research Papers 121, 110–120. (doi:10.1016/j.dsr.2017.01.003)

Glud, R., Wenzhöfer, F., Middelboe, M., Oguri, K., Turnewitsch, R., Canfield, D., Kitazato, H., 2013. High rates of microbial carbon turnover in sediments in the deepest oceanic trench on Earth. Nature Geosciences 6, 284–288. (doi:10.1038/NGEO1773)

Gross, M., Jaenicke, R., 1994. Proteins under pressure. The influence of high hydrostatic pressure on structure, function and assembly of proteins and protein complexes. European Journal of Biochemistry 221, 617–630. (doi:10.1111/j.1432-1033.1994.tb18774.x)

Günther, A., 1887. Report on the deep-sea fishes collected by H. M. S. Challenger during the years 1873–76. Challenger Report 22.

Hedgpeth, J.W., 1957. Treatise on marine ecology and paleoecology. New York, New York.

Høie, H., Otterlei, E., Folkvord, A., 2004. Temperature-dependent fractionation of stable oxygen isotopes in otoliths of juvenile cod (*Gadus morhua* L.). ICES Journal of Marine Science 61, 243–251. (doi:10.1016/j.icesjms.2003.11.006)

Hubert, N., Delrieu-Trottin, E., Irisson, J.-O., Meyer, C., Planes, S., 2010. Identifying coral reef fish larvae through DNA barcoding: A test case with the families Acanthuridae and Holocentridae. Molecular Phylogenetics and Evolution 55, 1195–1203. (doi:10.1016/j.ympev.2010.02.023)

Ichino, M.C., Clark, M.R., Drazen, J.C., Jamieson, A., Jones, D.O.B., Martin, A.P., Rowden, A.A., Shank, T.M., Yancey, P.H., Ruhl, H.A., 2015. The distribution of benthic biomass in hadal trenches: A modelling approach to investigate the effect of vertical and lateral organic matter transport to the seafloor. Deep-Sea Research Part I: Oceanographic Research Papers 100, 21–33. (doi:10.1016/j.dsr.2015.01.010)

Itoh, M., Kawamura, K., Kitahashi, T., Kojima, S., Katagiri, H., Shimanaga, M., 2011. Bathymetric patterns of meiofaunal abundance and biomass associated with the Kuril and Ryukyu trenches, western North Pacific Ocean. Deep-Sea Research Part I: Oceanographic Research Papers 58, 86–97. (doi:10.1016/j.dsr.2010.12.004)

Jamieson, A., Fujii, T., Solan, M., Matsumoto, A., Bagley, P., Priede, I., 2009. Liparid and macrourid fishes of the hadal zone: *in situ* observations of activity and feeding behaviour. Proceedings of the Royal Society B: Biological Sciences 276, 1037–45. (doi:10.1098/rspb.2008.1670)

Jamieson, A., Kilgallen, N., Rowden, A., Fujii, T., Horton, T., Lörz, A.-N., Kitazawa, K., Priede, I., 2011. Bait-attending fauna of the Kermadec Trench, SW Pacific Ocean: Evidence for an ecotone across the abyssal-hadal transition zone. Deep-Sea Research Part I: Oceanographic Research Papers 58, 49–62. (doi:10.1016/j.dsr.2010.11.003)

Jamieson, A.J., Malkocs, T., Piertney, S.B., Fujii, T., Zhang, Z., 2017. Bioaccumulation of persistent organic pollutants in the deepest ocean fauna. Nature 1, 24–27. (doi:10.1038/s41559-016-0051)

Kim, Y.U., Park, Y.S., Myoung, J.G., 1986. Egg development and larvae of the snailfish, *Liparis tanakai* (Gilbert et Burke). Korean Journal of Fisheries and Aquatic Sciences 19, 380–386.

Lin, H.-Y., Shiao, J.-C., Chen, Y-G., Iizuka, Y., 2012. Ontogenetic vertical migration of grenadiers revealed by otolith microstructures and stable isotopic compositions. Deep-Sea Research Part I: Oceanographic Research Papers 61, 123–130. (doi:10.1016/j.dsr.2011.12.005)

Linley, T.D., Gerringer, M.E., Yancey, P.H., Drazen, J.C., Weinstock, C.L., Jamieson, A.J., 2016. Fishes of the hadal zone including new species, *in situ* observations and depth records of Liparidae. Deep-Sea Research Part I: Oceanographic Research Papers 114, 99–110. (doi:10.1016/j.dsr.2016.05.003)

Linley, T.D., Stewart, A.L., McMillan, P.J., Clark, M.R., Gerringer, M.E., Drazen, J.C., Fujii, T., Jamieson, A.., 2017. Bait attending fishes of the abyssal zone and hadal boundary: community structure, functional groups and species distribution in the Kermadec, New Hebrides, and Mariana trenches. Deep-Sea Research Part I: Oceanographic Research Papers 121, 38–53. (doi:10.1016/j.dsr.2016.12.009)

Lisney, T., Collin, S., 2006. Brain morphology in large pelagic fishes: a comparison between sharks and teleosts. Journal of Fish Biology 68, 532–554. (doi:10.1111/j.1095-8649.2006.00940.x)

Liu, H., Wassersug, R., Kawachi, K., 1997. The three-dimensional hydrodynamics of tadpole locomotion. Journal of Experimental Biology 200, 2807–19.

Liu, H., Wassersug, R., Kawachi, K., 1996. A computational fluid dynamics study of tadpole swimming. Journal of Experimental Biology 199, 1245–60.

Marliave, J., Peden, A., 1989. Larvae of *Liparis fucensis* and *Liparis callyodon*: Is the "cottoid bubblemorph" phylogenetically significant? Fisheries Bulletin 87, 735–743.

Milligan, R.J., Morris, K.J., Bett, B.J., Durden, J.M., Jones, D.O.B., Robert, K., Ruhl, H.A., Bailey, D.M., 2016. High resolution study of the spatial distributions of abyssal fishes by autonomous underwater vehicle. Nature Scientific Reports. 6, 26095. (doi:10.1038/srep26095)

Neat, F.C., Campbell, N., 2013. Proliferation of elongate fishes in the deep sea. Journal of Fish Biology. 83, 1576–1591. (doi:10.1111/jfb.12266)

Nielsen, J., 1977. The deepest living fish, *Abyssobrotula galatheae*, a new genus and species of oviparus ophidioids (Pisces, Brotulidae). Galathea Report 14, 41–48.

Nielsen, J., 1964. Fishes from depths exceeding 6000 meters. Galathea Report 7, 113–124.

Nielsen, J., Merrett, N., 2000. Revision of the cosmpolitan deep-sea Genus *Bassozetus* (Pisces: Ophidiidae) with two new species. Galathea Report 18, 7–56.

Nielsen, J.G., Møller, P.R., 2011. Revision of the bathyal cusk-eels of the genus *Bassogigas* (Ophidiidae) with description of a new species from off Guam, west Pacific Ocean. Journal of Fish Biology 78, 783–795. (doi:10.1111/j.1095-8649.2010.02892.x)

Oguri, K., Kawamura, K., Sakaguchi, A., Toyofuku, T., Kasaya, T., Murayama, M., Fujikura, K., Glud, R., Kitazato, H., 2013. Hadal disturbance in the Japan Trench induced by the 2011 Tohoku-Oki earthquake. Scientific Reports 3, 1915. (doi:10.1038/srep01915)

Pérês, J., 1965. *Aperçu sur les résultats de deux plongées effectuées dans le ravin de Puerto-Rico par le bathyscaphe Archimède.* Deep-Sea Research and Oceanographic Abstracts 12, 883–891. (doi:10.1016/0011-7471(65)90811-9)

Riemann, L., Alfredsson, H., Hansen, M.M., Als, T.D., Nielsen, T.G., Munk, P., Aarestrup, K., Maes, G.E., Sparholt, H., Petersen, M.I., Bachler, M., Castonguay, M., 2010. Qualitative assessment of the diet of European eel larvae in the Sargasso Sea resolved by DNA barcoding. Biology Letters 6, 819–822. (doi:10.1098/rsbl.2010.0411)

Ritchie, H., Jamieson, A.J., Piertney, S.B., 2015. Phylogenetic relationships among hadal amphipods of the superfamily Lysianassoidea: Implications for taxonomy and biogeography. Deep-Sea Research Part I: Oceanographic Research Papers 105, 119–131. (doi:10.1016/j.dsr.2015.08.014)

Shiao, J.-C., Sui, T.-D., Chang, N.-N., Chang, C.-W., 2017. Remarkable vertical shift in residence depth links pelagic larval and demersal adult jellynose fish. Deep-Sea Research Part I: Oceanographic Research Papers 121, 160-168. (doi:10.1016/j.dsr.2017/01.011)

Shrestha, U.R., Bhowmik, D., Copley, J.R.D., Tyagi, M., Leão, J.B., Chu, X.-Q., Klein, M.L., 2015. Effects of pressure on the dynamics of an oligomeric protein from deep-sea hyperthermophile. Proceedings of the National Academy of Sciences U. S. A. 112, 13886–13891. (doi:10.1073/pnas.1514478112)

Somero, G., 1992. Adaptations to high hydrostatic pressure. Annuual Review of Physiology 54, 557–577.

Stein, D., 2005. Descriptions of four new species, redescription of *Paraliparis membranaceus*, and additional data on species of the fish family Liparidae (Pisces, Scorpaeniformes) from the west coast of South America and the Indian Ocean. Zootaxa 1–25.

Stein, D.L., 2016. Description of a new hadal *Notoliparis* from the Kermadec Trench, New Zealand, and redescription of *Notoliparis kermadecensis* (Nielsen) (Liparidae, Scorpaeniformes). Copeia 104, 907–920. (doi:10.1643/CI-16-451)

Sturrock, A., Trueman, C., Darnaude, A., Hunter, E., 2012. Can otolith elemental chemistry retrospectively track migrations in fully marine fishes? Journal of Fish Biology 81, 766–95. (doi:10.1111/j.1095-8649.2012.03372.x)

Thorrold, S., Campana, S., Jones, C., Swart, P., 1997. Factors determining ^{13}C and ^{18}O fractionation in aragonitic otoliths of marine fish. Geochimica et Cosmochimica Acta 61, 2909–2919.

Uiblein, F., Nielsen, J., Møller, P., 2008. Systematics of the ophidiid genus *Spectrunculus* (Teleostei: Ophidiiformes) with resurrection of *S. crassus*. Copeia 542–551.

Wagner, H.J., 2002. Sensory brain areas in three families of deep-sea fish (slickheads, eels, and grenadiers): comparison of mesopelagic and demersal species. Marine Biology 141, 807–817.

Ward, A.B., Mehta, R.S., 2010. Axial elongation in fishes: using morphological approaches to elucidate developmental mechanisms in studying body shape. Integrative and Comparative Biology 50, 1106–19. (doi:10.1093/icb/icq029)

Wenzhöfer, F., Oguri, K., Middelboe, M., Turnewitsch, R., Toyofuku, T., Kitazato, H., Glud, R.N., 2016. Benthic carbon mineralization in hadal trenches: Assessment by *in situ* O_2 microprofile measurements. Deep-Sea Research Part I: Oceanographic Research Papers 116, 272-286. (doi:10.1016/j.dsr.2016.08.013)

Wilson, R., Waples, R., 1983. Distribution, morphology, and biochemical genetics of *Coryphaenoides armatus* and *C. yaquinae* (Pisces: Macrouridae) in the central and eastern North Pacific. Deep-Sea Research Part A: Oceanographic Research Papers 30, 1127–1145. (doi:10.1016/0198-0149(83)90092-4)

Wolff, T., 1959. The hadal community, an introduction. Deep-Sea Research 6, 95–124. (doi:10.1016/0146-6313(59)90063-2)

Yancey, P., Gerringer, M., Drazen, J., Rowden, A., Jamieson, A., 2014. Marine fish may be biochemically constrained from inhabiting the deepest ocean depths. Proceedings of the National Academy of Sciences U. S. A. 111, 4461–5. (doi:10.1073/pnas.1322003111)

APPENDIX

Supplementary Table 2.1. Collection information. Sex: female (f), male (m), juvenile (j) indicated.

Trench	Depth (m)	Sample Number	Species	Standard Length (cm)	Weight (g)	Sex
Kermadec	3601	100363	*Coryphaenoides armatus*	78.6	1930	f
Kermadec	3569	100368	*Coryphaenoides armatus*	69	1686	m
Mariana	6081	200015	*Coryphaenoides yaquinae*	23	40	j
Mariana	7062	200021	Mariana liparid	19.3	70	m
Mariana	6961	200024	Mariana liparid	23.2	160	
Mariana	6961	200025	Mariana liparid	23.5	150	f
Mariana	6914	200027	Mariana liparid	22		f
Mariana	7495	200033	Mariana liparid	12.6	45	
Mariana	7497	200039	Mariana liparid	21	150	f
Mariana	7497	200040	Mariana liparid	18.4	90	f
Mariana	7497	200041	Mariana liparid	10.5	15	j
Mariana	7497	200042	Mariana liparid	14.7	30	j
Mariana	7497	200043	Mariana liparid	28.8	90	f
Mariana	7509	200047	Mariana liparid	17.8	75	m
Mariana	7509	200048	Mariana liparid	13.5	25	m
Mariana	7929	200062	Mariana liparid		8	
Mariana	7841	200070	Mariana liparid	17.2	65	f
Mariana	7841	200071	Mariana liparid	11	15	j
Mariana	7841	200072	Mariana liparid	11.9	15	j
Mariana	7907	200074	Mariana liparid	14.5	30	m
Mariana	7966	200081	Mariana liparid	10.7	10	j
Mariana	6949	200084	Mariana liparid	17.6	65	f
Mariana	6949	200085	Mariana liparid	22.5	130	f
Mariana	6898	200087	Mariana liparid	20.3	90	f
Mariana	6974	200094	Mariana liparid	18.7	75	f
Mariana	6974	200095	Mariana liparid	12.4	15	f
Mariana	6974	200096	Mariana liparid	18.3	85	f
Mariana	7626	200133	Mariana liparid	15.1	35	j
Mariana	7626	200134	Mariana liparid	16.1	45	f
Mariana	7652	200142	Mariana liparid	14.2	40	m
Mariana	7652	200143	Mariana liparid	12.9	20	f
Mariana	7652	200144	Mariana liparid	11.9	20	j
Kermadec	7392	100162	*Notoliparis kermadecensis*	20.7	88	f
Kermadec	7392	100164	*Notoliparis kermadecensis*	16.7	76	m
Kermadec	7392	100165	*Notoliparis kermadecensis*	20.9	92	f
Kermadec	7515	100171	*Notoliparis kermadecensis*	18.3	80	m
Kermadec	7515	100172	*Notoliparis kermadecensis*	20.9	104	f
Kermadec	7515	100173	*Notoliparis kermadecensis*	12.9	26	j
Kermadec	7515	100175	*Notoliparis kermadecensis*	18.3	46	f
Kermadec	7515	100176	*Notoliparis kermadecensis*	15.9	50	f
Kermadec	7515	100177	*Notoliparis kermadecensis*	24.2	156	f
Kermadec	7200	100216	*Notoliparis kermadecensis*	23.6	182	f
Kermadec	7200	100217	*Notoliparis kermadecensis*	25.9	230	f
Kermadec	7200	100218	*Notoliparis kermadecensis*	20.2	110	
Kermadec	7200	100219	*Notoliparis kermadecensis*	18.2	68	j
Kermadec	7200	100220	*Notoliparis kermadecensis*	17.3	54	j
Kermadec	7251	100309	*Notoliparis kermadecensis*	20.8	108	m

Trench	Depth (m)	Sample Number	Species	Standard Length (cm)	Weight (g)	Sex
Kermadec	7251	100310	*Notoliparis kermadecensis*	21	94	m
Kermadec	7251	100311	*Notoliparis kermadecensis*	17.7	46	m
Kermadec	7251	100312	*Notoliparis kermadecensis*	16.8	54	m
Kermadec	7251	100313	*Notoliparis kermadecensis*	17.8	42	f
Kermadec	7251	100314	*Notoliparis kermadecensis*	20	74	f
Kermadec	7251	100315	*Notoliparis kermadecensis*	18.3	66	m
Kermadec	7251	100316	*Notoliparis kermadecensis*	19.4	66	f
Kermadec	7251	100317	*Notoliparis kermadecensis*	13.6	20	f
Kermadec	7187	100318	*Notoliparis kermadecensis*	18.4	66	f
Kermadec	7187	100319	*Notoliparis kermadecensis*	17.4	48	f
Kermadec	7187	100320	*Notoliparis kermadecensis*	22.2	124	f
Kermadec	6456	100326	*Notoliparis kermadecensis*	24.2	154	m
Kermadec	6456	100327	*Notoliparis kermadecensis*	23.5	168	m
Kermadec	6456	100328	*Notoliparis kermadecensis*	22	158	m
Kermadec	6456	100329	*Notoliparis kermadecensis*	29	200	f
Kermadec	7554	100338	*Notoliparis kermadecensis*	15.2		
Kermadec	7554	100339	*Notoliparis kermadecensis*	14.4		
Kermadec	7554	100340	*Notoliparis kermadecensis*	18		
Kermadec	7554	100341	*Notoliparis kermadecensis*	17.6	80	
Kermadec	7554	100342	*Notoliparis kermadecensis*	23.3	110	f
Kermadec	7554	100343	*Notoliparis kermadecensis*	22.2	132	f
Kermadec	7554	100344	*Notoliparis kermadecensis*	23.7	164	m
Kermadec	7227	100350	*Notoliparis kermadecensis*	22.2	120	m
Kermadec	4989	100083	*Pachycara sp.*	43.6	460	
Kermadec	4989	100084	*Pachycara sp.*	46.8	660	m
Kermadec	4817	100073	*Pyrolycus sp.*	42	508	f
Kermadec	3865	100036	*Spectrunculus grandis*	43.9	532	f
Kermadec	3601	100364	*Spectrunculus grandis*	29	170	
Kermadec	3601	100365	*Spectrunculus grandis*	26.9	106	j
Kermadec	3569	100371	*Spectrunculus grandis*	31.5	136	m
Kermadec	3569	100372	*Spectrunculus grandis*	28.2	142	m
Kermadec	3569	100376	*Spectrunculus grandis*	33	196	

Supplementary Table 2.2. Compound Specific Isotope Analysis of Individual Amino Acids and Bulk White Muscle Tissue Isotope Analysis Results. HADES Sample numbers listed. B1/B2 indicates batch number. $\delta^{15}N$ values presented in ‰ vs. AIR, δ13C in ‰ vs. V-PDB. Standard deviations from triplicate measurements of one sample.

	Coryphaenoides armatus						***Coryphaenoides yaquinae***					
	100038 (B2)		100363 (B2)		100367 (B2)		200008 (B1)		200151 (B1)		200152 (B2)	
	average	stdev	average	stdev	average	stdev	average	stdev	average	stdev	average	stdev
Alanine	31.82	0.18	33.04	0.37	33.38	0.14	29.19	0.35	29.30	0.19	31.72	0.38
Glycine	0.46	0.14	-0.32	0.49	3.53	0.94	-0.79	0.69	-1.54	0.50	-4.26	0.12
Threonine	-33.56	0.32	-32.39	0.50	-35.68	0.65	-35.52	0.40	-33.88	0.75	-31.74	0.98
Serine	4.52	0.34	3.10	0.38	5.20	0.50	3.61	0.75	5.64	0.26	-1.21	0.11
Valine	25.13	0.20	26.04	0.45	26.70	0.77	23.77	0.46	24.48	0.34	23.49	0.57
Leucine	28.28	0.14	29.48	0.02	29.93	0.18	25.59	0.29	26.06	0.14	28.01	0.08
Isoleucine	29.66	0.38	30.67	0.30	30.61	0.20	26.85	0.32	27.41	0.07	29.13	0.06
Norleucine	19.06	0.00	20.61	0.05	19.89	0.09	19.06	0.00	19.06	0.00	19.81	0.04
Proline	31.03	0.11	29.34	0.16	29.72	0.16	25.76	0.26	26.40	0.15	26.31	0.17
Aspartic acid	23.34	0.31	24.37	0.28	25.45	0.07	24.44	0.20	23.36	0.13	23.92	0.13
Methionine	9.53	0.33	8.71	0.77	12.96	0.22	8.17	0.37	7.86	0.09	9.60	0.36
Glutamic acid	30.85	0.06	32.76	0.06	32.86	0.12	29.64	0.10	30.33	0.09	31.06	0.06
Phenylalanine	2.43	0.58	2.65	0.29	3.97	0.42	1.16	0.34	0.43	0.56	2.28	0.51
Aminoadipic Acid	-6.20	0.00	-5.97	0.37	-5.03	0.13	-6.20	0.00	-6.20	0.00	-5.22	0.20
Tyrosine	6.90	0.67	3.26	0.34	9.28	0.04	6.64	0.24	5.53	0.32	7.65	0.58
Lysine	4.61	0.24	4.99	0.23	6.23	0.13	3.14	0.14	3.21	0.10	3.89	0.03
Source AA (Lys, Phe)	3.96	0.41	3.95	0.36	5.71	0.31	2.55	0.32	2.80	0.29	3.80	0.17
Trophic AA (Ala, Leu, Glu)	30.40	0.19	30.34	0.12	32.26	0.22	28.69	0.25	28.82	0.20	29.98	0.18
Trophic Position	5.14	0.17	5.13	0.11	5.16	0.18	5.08	0.20	5.06	0.17	5.09	0.12
Bulk Tissue δ15N	14.2		13.0				12.8		12.3			
Bulk Tissue δ13C	-18.9		-21.3				-18.0		-18.7			

	Spectrunculus grandis					
	100060 (B1)		100377 (B1)		100364 (B2)	
	average	stdev	average	stdev	average	stdev
Alanine	30.85	0.23	31.83	0.04	34.93	0.43
Glycine	3.56	0.87	6.20	0.30	7.23	0.52
Threonine	-31.01	0.62	-29.06	0.63	-30.12	0.54
Serine	8.13	0.38	11.41	0.16	12.29	0.46
Valine	23.63	1.03	25.82	0.70	27.56	0.37
Leucine	26.20	0.08	27.72	0.10	29.17	0.03
Isoleucine	28.07	0.41	28.77	0.31	30.63	0.34
Norleucine	19.47	0.04	19.37	0.10	20.76	0.18
Proline	28.54	0.46	32.39	0.25	31.40	0.11
Aspartic acid	22.74	0.61	24.46	0.06	25.08	0.12
Methionine	9.97	0.66	12.46	0.52	12.81	0.27
Glutamic acid	28.67	0.92	30.99	0.19	31.87	0.04
Phenylalanine	3.40	0.57	4.80	0.79	6.71	0.35
Aminoadipic Acid	-5.46	0.98	-5.40	0.06	-5.49	0.13
Tyrosine	13.15	0.33	12.58	0.26	14.06	0.66
Lysine	5.97	0.14	5.90	0.29	6.27	0.04
Source AA (Lys, Phe)	5.47	0.33	5.60	0.46	6.32	0.19
Trophic AA (Ala, Leu, Glu)	27.44	0.23	30.78	0.15	30.51	0.13
Trophic Position	4.32	0.19	4.90	0.15	4.72	0.11
Bulk Tissue δ15N	14.4		15.5			
Bulk Tissue δ13C	-19.1		-18.9			

	Notoliparis kermadecensis						**Mariana liparid**							
	100175 (B1)		100310 (B1)		100171 (B2)		200039 (B1)		200070 (B1)		200033 (B2)		200041 (B2)	
	average	stdev	average	stdev	average	stdev	average	stdev	average	stdev	average	stdev	average	stdev
Alanine	30.43	0.07	30.34	0.17	30.19	0.45	30.73	0.24	29.70	0.36	29.41	0.40	28.91	0.34
Glycine	7.75	0.24	6.36	0.26	8.86	0.22	7.68	0.34	7.78	0.19	9.96	0.18	10.58	0.31
Threonine	-22.02	0.96	-32.48	0.71	-30.18	0.79	-40.62	0.30	-38.93	0.86	-37.73	0.42	-37.97	0.76
Serine	10.40	0.91	11.83	0.05	12.42	0.49	-0.72	0.21	1.05	1.15	3.30	0.20	14.48	0.23
Valine			22.95	0.42	25.07	0.87	23.12	0.17	22.13	0.33	24.51	0.18	21.55	0.88
Leucine	26.97	0.36	27.85	0.08	29.71	0.08	28.29	0.21	27.20	0.48	27.32	0.20	26.97	0.33
Isoleucine			23.45	1.12	26.32	0.81	24.63	1.24	24.75	0.92	25.23	1.04	24.12	0.91
Norleucine	18.86	0.26	18.84	0.18	19.69	0.23	18.71	0.06	19.02	0.20	19.06	0.00	19.06	0.00
Proline	30.91	0.07	31.75	0.15	32.46	0.17	32.76	0.38	31.61	0.11	30.72	0.08	28.96	0.21
Aspartic acid	20.80	0.21	23.16	0.08	23.68	0.26	24.97	0.26	24.55	0.18	23.17	0.05	22.36	0.12
Methionine	16.42	0.91	15.18	0.10	15.92	0.11	14.74	0.22	16.45	0.17	15.34	0.54	13.80	0.20
Glutamic acid	25.84	0.19	30.05	0.23	29.71	0.08	30.46	0.19	29.84	0.31	29.16	0.07	28.38	0.17
Phenylalanine	7.29	0.62	3.51	0.54	4.15	0.46	3.71	0.27	3.09	0.36	4.70	0.29	2.48	0.19
Aminoadipic Acid	-4.88	0.08	-5.72	0.12	-5.57	0.53	-6.22	0.04	-5.73	0.15	-6.20	0.00	-6.20	0.00
Tyrosine			11.41	0.44	8.12	0.19	4.77	0.56	6.32	0.58	8.11	0.71	11.18	0.52
Lysine	8.81	0.42	9.80	0.10	9.36	0.30	7.23	0.15	7.24	0.05	6.63	0.18	6.46	0.04
Source AA (Lys, Phe)	8.19	0.50	8.77	0.30	7.29	0.43	5.99	0.31	6.78	0.20	5.89	0.33	5.77	0.18
Trophic AA (Ala, Leu, Glu)	28.85	0.22	28.89	0.21	29.75	0.19	29.81	0.27	29.11	0.35	28.76	0.22	28.15	0.29
Trophic Position	4.08	0.20	3.98	0.17	4.41	0.17	4.66	0.20	4.38	0.17	4.48	0.18	4.39	0.15
Bulk Tissue δ15N	14.2		12.8		13.3		13.4		13.6		14.4		13.2	
Bulk Tissue δ13C	-20.9		-21.4		-21.7		-19.8		-18.9		-19.5		-20.0	

Supplementary Table 4.1. Otolith collection information and age estimates of the snailfishes *Careproctus melanurus*, *Notoliparis kermadecensis*, and the Mariana liparid (Liparidae sp. nov.). Sex listed as female (f), male (m), juvenile (j), and unknown (u).

Location	Depth (m)	Sample ID	Species	Total Length (cm)	Standard Length (cm)	Body Mass (g)	Sex	Otolith Mass (mg)	Otolith Height (mm)	Otolith Width (mm)	Otolith Length (mm)	Age Estimate (years)
Kermadec	7392	100162	*Notoliparis kermadecensis*	22.2	20.7	88	f	1.1772	0.66	0.997	1.279	9
Kermadec	7392	100163	*Notoliparis kermadecensis*	23	21	106	f	1.566	0.76	1.118	1.325	
Kermadec	7392	100164	*Notoliparis kermadecensis*	18.5	16.7	76	m	0.8206	0.52	0.944	1.11	7
Kermadec	7392	100165	*Notoliparis kermadecensis*	23	20.9	92	f	0.8691	0.54	0.905	1.172	9
Kermadec	7515	100171	*Notoliparis kermadecensis*	20.2	18.3	80	m	0.9514	0.6	0.918	1.127	11
Kermadec	7515	100172	*Notoliparis kermadecensis*	22.9	20.9	104	f	0.3766	0.4	0.671	0.879	9
Kermadec	7515	100173	*Notoliparis kermadecensis*	13.9	12.9	26	j	0.6211	0.46	0.864	1.042	7
Kermadec	7515	100175	*Notoliparis kermadecensis*	20	18.3	46	f	0.6112	0.5	0.799	1.022	9
Kermadec	7515	100176	*Notoliparis kermadecensis*	17.6	15.9	50	f	0.9866	0.6	1.001	1.194	8
Kermadec	7515	100177	*Notoliparis kermadecensis*	26.4	24.2	156	f	0.9731	0.6	0.999	1.146	
Kermadec	7200	100216	*Notoliparis kermadecensis*	25.6	23.6	182	f	1.4915	0.66	1.142	1.314	14
Kermadec	7200	100217	*Notoliparis kermadecensis*	28	25.9	230	f	2.0052	0.8	1.311	1.539	13
Kermadec	7200	100218	*Notoliparis kermadecensis*	22.2	20.2	110	m	1.2195	0.64	1.13	1.434	10
Kermadec	7200	100219	*Notoliparis kermadecensis*	20.1	18.2	68	j	0.9694	0.54	1.123	1.162	10
Kermadec	7200	100220	*Notoliparis kermadecensis*	18.9	17.3	54	j	0.7725	0.42	1.103	1.184	
Kermadec	7251	100309	*Notoliparis kermadecensis*	23	20.8	108	m	0.7775	0.6	0.855	1.034	
Kermadec	7251	100310	*Notoliparis kermadecensis*	23.2	21	94	m	1.1667	0.62	1.041	1.264	11
Kermadec	7251	100311	*Notoliparis kermadecensis*	19.6	17.7	46	m	0.4803	0.46	0.765	0.948	7
Kermadec	7251	100312	*Notoliparis kermadecensis*	18.5	16.8	54	m	0.6882	0.54	0.861	1.11	10

Location	Depth (m)	Sample ID	Species	Total Length (cm)	Standard Length (cm)	Body Mass (g)	Sex	Otolith Mass (mg)	Otolith Height (mm)	Otolith Width (mm)	Otolith Length (mm)	Age Estimate (years)
Kermadec	7251	100313	*Notoliparis kermadecensis*	19.8	17.8	42	f	0.3773	0.42	0.729	0.895	8
Kermadec	7251	100314	*Notoliparis kermadecensis*	21.8	20	74	f	1.0887	0.69	0.936	1.278	9
Kermadec	7251	100315	*Notoliparis kermadecensis*	20.3	18.3	66	m	0.6553	0.51	0.841	1.032	8
Kermadec	7251	100316	*Notoliparis kermadecensis*	21.2	19.4	66	f	1.2014	0.63	1.18	1.304	10
Kermadec	7251	100317	*Notoliparis kermadecensis*	15.1	13.6	20	f	0.4997	0.47	0.746	1.051	6
Kermadec	7187	100318	*Notoliparis kermadecensis*	20.1	18.4	66	f	0.8214	0.62	0.817	1.175	10
Kermadec	7187	100319	*Notoliparis kermadecensis*	19	17.4	48	f	0.8679	0.55	0.975	1.217	8
Kermadec	7187	100320	*Notoliparis kermadecensis*	23.4	22.2	124	f	0.6307	0.55	0.89	1.05	12
Kermadec	6456	100326	*Notoliparis kermadecensis*	26.3	24.2	154	m	1.1579	0.62	1.095	1.3	14
Kermadec	6456	100328	*Notoliparis kermadecensis*	24.3	22	158	m	0.8312	0.53	0.981	1.265	10
Kermadec	6456	100329	*Notoliparis kermadecensis*	31.5	29	200	f	1.4822	0.71	1.19	1.397	15
Kermadec	7554	100338	*Notoliparis kermadecensis*	16.7	15.2	26*	u	0.7295	0.56	0.875	1.095	6
Kermadec	7554	100339	*Notoliparis kermadecensis*	16	14.4	28*	u	0.5707	0.48	0.811	1.19	7
Kermadec	7554	100340	*Notoliparis kermadecensis*	19.8	18	52*	u	0.9877	0.57	1.062	1.338	9
Kermadec	7554	100341	*Notoliparis kermadecensis*	19.5	17.6	80	u	0.8682	0.62	0.894	1.216	8
Kermadec	7554	100342	*Notoliparis kermadecensis*	25.6	23.3	110	f	0.9389	0.59	1.184	1.199	13
Kermadec	7554	100343	*Notoliparis kermadecensis*	25	22.2	132	f	0.8929	0.5	1.101	1.267	13
Kermadec	7554	100344	*Notoliparis kermadecensis*	26.4	23.7	164	m	0.9664	0.62	1.046	1.285	15
Kermadec	7227	100350	*Notoliparis kermadecensis*	24.3	22.2	120	m	0.8399	0.65	0.998	1.08	13
Mariana	7062	200021	Mariana liparid	21.5	19.3	70	m	0.7098	0.55	0.969	1.282	
Mariana	6961	200024	Mariana liparid	24.4	23.2	160	u	1.3421	0.68	1.265	1.547	10

Location	Depth (m)	Sample ID	Species	Total Length (cm)	Standard Length (cm)	Body Mass (g)	Sex	Otolith Mass (mg)	Otolith Height (mm)	Otolith Width (mm)	Otolith Length (mm)	Age Estimate (years)
Mariana	6961	200025	Mariana liparid	26	23.5	150	f	0.8675	0.49	0.964	1.237	10
Mariana	6914	200027	Mariana liparid		22		f	1.2999	0.64	1.088	1.33	12
Mariana	7495	200033	Mariana liparid	19	12.6	45	u	0.8599	0.51	0.931	1.047	
Mariana	7497	200039	Mariana liparid	23	21	150	f	1.4463	0.64	1.092	1.514	
Mariana	7497	200040	Mariana liparid	20.7	18.4	90	f	1.2243	0.73	1.027	1.142	11
Mariana	7497	200041	Mariana liparid	12.4	10.5	15	j	0.5207	0.39	0.923	0.955	5
Mariana	7497	200042	Mariana liparid	16.4	14.7	30	j	0.4779	0.47	0.757	0.844	7
Mariana	7497	200043	Mariana liparid	21.1		90	f	0.8499	0.58	0.891	1.078	
Mariana	7509	200047	Mariana liparid	19.4	17.8	75	m	0.806	0.57	0.875	0.986	9
Mariana	7509	200048	Mariana liparid	15	13.5	25	m	0.646	0.42	0.877	1.108	7
Mariana	7929	200062	Mariana liparid			8	u	0.305	0.45	0.688	0.838	
Mariana	7841	200070	Mariana liparid	19	17.2	65	f	0.9766	0.74	0.801	0.941	8
Mariana	7841	200071	Mariana liparid	12.3	11	15	j	0.3202	0.4	0.809	0.931	7
Mariana	7841	200072	Mariana liparid	13.4	11.9	15	j	0.4378	0.44	0.781	0.929	7
Mariana	7907	200074	Mariana liparid	16.3	14.5	30	m	0.5104	0.35	0.796	0.827	8
Mariana	7966	200081	Mariana liparid	12	10.7	10	j	0.4256	0.4	0.807	0.908	5
Mariana	6949	200084	Mariana liparid	19.5	17.6	65	f	1.2682	0.67	0.992	1.137	8
Mariana	6949	200085	Mariana liparid	24.7	22.5	130	f	0.7704	0.56	0.946	1.317	12
Mariana	6974	200094	Mariana liparid	20.5	18.7	75	f	0.8429	0.46	1.106	1.346	12
Mariana	6974	200095	Mariana liparid	13.7	12.4	15	f	0.4635	0.39	0.714	0.842	6
Mariana	6974	200096	Mariana liparid	20.1	18.3	85	f	0.7922	0.62	0.98	1.14	10
Mariana	7626	200133	Mariana liparid	16.7	15.1	35	j	0.4467	0.45	0.727	0.867	8

Location	Depth (m)	Sample ID	Species	Total Length (cm)	Standard Length (cm)	Body Mass (g)	Sex	Otolith Mass (mg)	Otolith Height (mm)	Otolith Width (mm)	Otolith Length (mm)	Age Estimate (years)
Mariana	7626	200134	Mariana liparid	17.2	16.1	45	f	0.8158	0.52	1.013	1.187	9
Mariana	7652	200142	Mariana liparid	15.9	14.2	40	m	0.6976	0.51	0.909	1.071	8
Mariana	7652	200143	Mariana liparid	13.7	12.9	20	f	0.3452	0.36	0.723	0.878	7
Mariana	7652	200144	Mariana liparid	13	11.9	20	j	0.5822	0.47	0.869	0.948	7
California	340	Cmel340.1	*Careproctus melanurus*		19.3	93	m	6.15	1.1	2.96	2.56	24
California	379	Cmel379.1	*Careproctus melanurus*		14.8	52	f	3.38	0.72	2.56	2.06	13
California	379	Cmel379.2	*Careproctus melanurus*		14.7	38	m	4.587	0.79	2.8	2.23	13
California	379	Cmel379.3	*Careproctus melanurus*		17.1	53	m	4.124	0.74	2.5	2.34	17
California	379	Cmel379.4	*Careproctus melanurus*		14.7	41	f	3.63	0.84	2.5	2.32	12
California	379	Cmel379.5	*Careproctus melanurus*		17.2	87	f	4.73	0.86	2.87	2.37	20
California	379	Cmel379.6	*Careproctus melanurus*		15.6	62	f	3.564	0.65	2.5	2.31	15
California	379	Cmel379.7	*Careproctus melanurus*		12.7	20	j	3.144	0.67	2.48	2.24	9
California	379	Cmel379.8	*Careproctus melanurus*		16.1	34	f	1.873	0.64	2.1	1.65	17
California	435	Cmel435.1	*Careproctus melanurus*		15.2	67	f	5.4	0.74	3.14	2.61	14
California	439	Cmel439.1	*Careproctus melanurus*		14.9	36	f	3.9	0.64	2.69	2.46	14
California	457	Cmel457.1	*Careproctus melanurus*		13.4	25	f	4.653	0.63	2.83	2.45	11
California	457	Cmel457.2	*Careproctus melanurus*		16	57	f	4.292	0.69	2.66	2.2	15
California	457	Cmel457.3	*Careproctus melanurus*		15.6	54	f	3.801	0.7	2.76	2.26	15
California	457	Cmel457.4	*Careproctus melanurus*		16.2	70	f	4.616	0.76	2.95	2.54	19
California	457	Cmel457.5	*Careproctus melanurus*		16	59	m	1.352	0.66	1.98	1.8	13
California	457	Cmel457.6	*Careproctus melanurus*		15.4	48	m	3.876	0.85	2.72	2.51	14
California	457	Cmel457.7	*Careproctus melanurus*		17.2	87	f	5.193	0.77	2.74	2.69	19

Location	Depth (m)	Sample ID	Species	Total Length (cm)	Standard Length (cm)	Body Mass (g)	Sex	Otolith Mass (mg)	Otolith Height (mm)	Otolith Width (mm)	Otolith Length (mm)	Age Estimate (years)
California	479	Cmel479.1	*Careproctus melanurus*		18.2	53	f	5.7	0.78	2.98	2.59	21
California	479	Cmel479.2	*Careproctus melanurus*		16.1	29	f	4	0.68	2.71	2.37	18
California	479	Cmel479.3	*Careproctus melanurus*		11.8	12	f	2.8	0.64	2.21	1.87	9
California	530	Cmel530.1	*Careproctus melanurus*		13.9	25	j	3	0.66	2.49	1.92	14
California	530	Cmel530.2	*Careproctus melanurus*		12.5	16	j	2.7	0.65	2.61	1.9	11
California	530	Cmel530.3	*Careproctus melanurus*		13.8	30	j	3.4	0.6	2.51	2.22	11
California	531	Cmel531.1	*Careproctus melanurus*		13.5	39	m	3.586	0.63	2.71	2.02	11
California	531	Cmel531.2	*Careproctus melanurus*		19.4	139	f	6.002	0.82	3.09	2.72	19
California	561	Cmel561.1	*Careproctus melanurus*		21.8	103	f	6.34	0.82	3.11	2.59	23
California	841	Cmel841.1	*Careproctus melanurus*		18	52	f	4.262	0.76	2.32	2.24	
California	841	Cmel841.2	*Careproctus melanurus*		11.8	8.1	j	2.196	0.62	2.17	1.72	10

Supplementary Table 4.2. Otolith collection information and age estimates from *Coryphaenoides armatus* and *Coryphaenoides yaquinae* (Family Macrouridae).

Pulse Cruise #	Date Collected	Specimen #	Otolith ID	Species	Total Length (cm)	Head Length (cm)	Body Mass (g)	Sex	Otolith Mass (g)	Otolith Height (mm)	Otolith Width (mm)	Otolith Length (mm)	Age Estimate (years)
24	2/17/1995	1	CA001	*Coryphaenoides armatus*	46	9.2	541	m	0.048	1.66	4.03	4.47	13
24	2/17/1995	5	CA002	*Coryphaenoides armatus*	53	9.8	669	m	0.057	1.67	3.94	5.68	10
24	2/17/1995	36	CA003	*Coryphaenoides armatus*	45	9.2	355	f	0.045	1.57	4.12	4.62	13
24	2/17/1995	3	CA004	*Coryphaenoides armatus*	52.5	10.2	571	f	0.063	1.77	4.76	5.08	17
24	2/17/1995	27	CA005	*Coryphaenoides armatus*	56	9.9	822	m	0.069	1.75	4.68	5.68	18
25	4/29/1995	7	CA006	*Coryphaenoides armatus*	56	8.8	722	m	0.071	1.92	4.59	5.75	14
35	9/1/1998	1.1	CA007	*Coryphaenoides armatus*	60.2	11.6	1010	f	0.061	1.79	4.23	5.44	12
36	12/20/1998	13.1	CA008	*Coryphaenoides armatus*	60.4	10.5	832	m	0.066	1.96	3.99	5.64	14
36	12/20/1998	14.1	CA009	*Coryphaenoides armatus*	70.5	15.0	3049	f	0.130	2.29	5.07	7.35	22
36	12/20/1998	4.1	CA010	*Coryphaenoides armatus*	73.1	12.2	1608	f	0.084	1.93	5	6	20
35	9/1/1998	22.1	CA011	*Coryphaenoides armatus*	80.5	14.1	2333	f	0.094	2.01	4.84	6.26	19
35	9/1/1998	14.1	CA012	*Coryphaenoides armatus*	80.7	14.6	3021	f	0.074	1.97	4.47	5.62	22
24	2/17/1995	7	CA013	*Coryphaenoides armatus*	50.5	9.3	484	m	0.045	1.6	3.6	4.6	10
24	2/17/1995	9	CA014	*Coryphaenoides armatus*	78.5	13.5	2810	f	0.114	2	5.3	6.6	22
24	2/17/1995	10	CA015	*Coryphaenoides armatus*	67.5	11.7	1341	f	0.078	1.9	4.4	5.5	15
24	2/17/1995	11	CA016	*Coryphaenoides armatus*	64	11.8	1780	f	0.096	2.2	4.7	5.7	16
24	2/17/1995	12	CA017	*Coryphaenoides armatus*	62	11.0	1021	m	0.077	1.7	4.9	5.4	15
24	2/17/1995	14	CA018	*Coryphaenoides armatus*	58	9.6	768	m	0.067	1.7	4.3	5.1	12
24	2/17/1995	17	CA019	*Coryphaenoides armatus*	58	10.0	652	m	0.071	1.6	4.6	6	11

Pulse Cruise #	Date Collected	Specimen #	Otolith ID	Species	Total Length (cm)	Head Length (cm)	Body Mass (g)	Sex	Otolith Mass (g)	Otolith Height (mm)	Otolith Width (mm)	Otolith Length (mm)	Age Estimate (years)
24	2/17/1995	21	CA020	*Coryphaenoides armatus*	51	9.2	563	m	0.072	1.3	5.3	5.6	13
24	2/17/1995	30	CA021	*Coryphaenoides armatus*	52	9.4	650	m	0.063	1.5	4.2	5.4	12
24	2/17/1995	32	CA022	*Coryphaenoides armatus*	54	9.4	568	m	0.051	1.5	4.1	5.2	10
24	2/17/1995	29	CA023	*Coryphaenoides armatus*	55	9.5	694	m	0.042	1	4.2	5.9	10
24	2/17/1995	25	CA024	*Coryphaenoides armatus*	49.5	9.0	416	m	0.051	1.6	4.6	4.3	11
24	2/17/1995	18	CA025	*Coryphaenoides armatus*	55.5	9.8	804	m	0.039	1.4	2.7*	5.7	11
24	2/17/1995	23	CA026	*Coryphaenoides armatus*	44	7.7	299	f	0.036	1.5	3.9	3.7	9
24	2/17/1995	26	CA027	*Coryphaenoides armatus*	48	8.5	495	m	0.058	1.8	3.7	5.6	9
24	2/17/1995	16	CA028	*Coryphaenoides armatus*	57.5	10.0	720	m	0.070	1.7	4.8	5.1	13
24	2/17/1995	28	CA029	*Coryphaenoides armatus*	55.5	9.6	720	m	0.057	1.6	4.4	4.7	13
24	2/17/1995	33	CA030	*Coryphaenoides armatus*	44.5	8.1	315	m	0.047	1.5	3.9	4.5	14
24	2/17/1995	35	CA031	*Coryphaenoides armatus*	48.5	9.6	375	f	0.038	1.5	4.4	3.5	13
24	2/17/1995	24	CA032	*Coryphaenoides armatus*	50	8.9	595	m	0.056	1.5	4.1	5.1	13
24	2/17/1995	15	CA033	*Coryphaenoides armatus*	59.5	10.0	960	m	0.076	1.7	4.7	5.6	15
24	2/17/1995	22	CA034	*Coryphaenoides armatus*	47	7.3	520	m	0.068	1.6	4.4	5.6	11
25	4/29/1995	2	CA035	*Coryphaenoides armatus*	47	10.2	683	m	0.079	1.7	4.7	5.5	16
25	4/29/1995	3	CA036	*Coryphaenoides armatus*	50	8.9	443	m	0.049	1.5	4	4.5	11
25	4/29/1995	4	CA037	*Coryphaenoides armatus*	55.5	9.7	635	m	0.056	1.5	4.2	5	11
25	4/29/1995	6	CA038	*Coryphaenoides armatus*	62	10.7	896	m	0.060	1.7	4.4	5.3	16
25	4/29/1995	9	CA039	*Coryphaenoides armatus*	59	10.2	789	m	0.071	1.6	4.1	6.2	12
25	4/29/1995	10	CA040	*Coryphaenoides armatus*	93.5	15.4	3220	f	0.126	2	5.1	6.9	29
27	11/16/1995	1	CA041	*Coryphaenoides armatus*	58.5	10.2	760	m	0.070	1.7	4.5	5.4	15
27	11/16/1995	3	CA042	*Coryphaenoides armatus*	57.5	9.8	687	m	0.072	1.6	4.5	5.5	13

Pulse Cruise #	Date Collected	Specimen #	Otolith ID	Species	Total Length (cm)	Head Length (cm)	Body Mass (g)	Sex	Otolith Mass (g)	Otolith Height (mm)	Otolith Width (mm)	Otolith Length (mm)	Age Estimate (years)
27	11/16/1995	5	CA043	*Coryphaenoides armatus*	60	9.9	823	m	0.070	1.6	4.7	5.6	13
27	11/16/1995	10	CA044	*Coryphaenoides armatus*	51	9.1	481	m	0.055	1.6	4	4.9	10
27	11/16/1995	13	CA045	*Coryphaenoides armatus*	59.5	10.3	862	m	0.064	1.6	4.3	5.1	12
27	11/16/1995	17	CA046	*Coryphaenoides armatus*	56.5	10.2	673	m	0.074	1.4	5	5.8	13
27	11/16/1995	19	CA047	*Coryphaenoides armatus*	53.5	9.2	542	m	0.051	1.6	3.8	4.4	11
27	11/16/1995	22	CA048	*Coryphaenoides armatus*	69.5	14.2	2980	f	0.101	1.9	4.7	6.9	21
27	11/16/1995	23	CA049	*Coryphaenoides armatus*	84	14.7	3280	f	0.084	1.8	5.1	5.4	27
29	1/31/1996	5	CA050	*Coryphaenoides armatus*	54.5	9.6	592	m	0.049	1.4	4.2	4.6	11
29	1/31/1996	7	CA051	*Coryphaenoides armatus*	58.2	10.7	863	m	0.074	1.7	4.3	5.8	15
29	1/31/1996	12	CA052	*Coryphaenoides armatus*	49.6	9.2	432	u	0.058	1.4	4.2	5.3	9
29	1/31/1996	13	CA053	*Coryphaenoides armatus*	44.9	8.6	460	u	0.056	1.6	4.2	5.1	8
29	1/31/1996	15	CA054	*Coryphaenoides armatus*	85.6	13.9	3125	f	0.054	1.3	4.5	4.8	22
30		1.1	CA055	*Coryphaenoides armatus*	79.4		2120	u	0.094	1.9	5.1	5.9	23
31	10/11/1996	1	CA056	*Coryphaenoides armatus*	55.5	10.0	651	m	0.075	1.7	4.2	6.2	13
31	10/11/1996	3	CA057	*Coryphaenoides armatus*	48.3	8.8	394	m	0.060	1.4	4.3	6	11
31	10/11/1996	5	CA058	*Coryphaenoides armatus*	53.8	9.0	444	m	0.054	1.5	3.9	4.7	13
31	10/11/1996	6	CA059	*Coryphaenoides armatus*	54	9.6	593	m	0.053	1.5	4.2	4.6	12
31	10/11/1996	7	CA060	*Coryphaenoides armatus*	57.3	10.0	683	m	0.071	1.7	4.5	5.2	13
31	10/11/1996	10	CA061	*Coryphaenoides armatus*	56.9	10.0	700	m	0.071	1.5	4.4	5.7	15
31	10/11/1996	11	CA062	*Coryphaenoides armatus*	54.7	9.4	541	m	0.059	1.4	4.3	5.2	12
31	10/11/1996	12	CA063	*Coryphaenoides armatus*	77.4	13.6	2210	f	0.109	2	5.2	6.2	19
31	10/11/1996	13	CA064	*Coryphaenoides armatus*	56.9	9.6	573	m	0.059	1.6	3.9	5.3	12
31	10/11/1996	14	CA065	*Coryphaenoides armatus*	55	9.7	614	f	0.068	1.5	4.9	5.2	14

Pulse Cruise #	Date Collected	Specimen #	Otolith ID	Species	Total Length (cm)	Head Length (cm)	Body Mass (g)	Sex	Otolith Mass (g)	Otolith Height (mm)	Otolith Width (mm)	Otolith Length (mm)	Age Estimate (years)
31	10/11/1996	15	CA066	*Coryphaenoides armatus*	52	9.7	501	m	0.058	1.5	4	5	13
31	10/11/1996	16	CA067	*Coryphaenoides armatus*	59.2	10.3	730	m	0.060	1.6	4.5	4.6	14
31	10/11/1996	18	CA068	*Coryphaenoides armatus*	53	9.2	571	m	0.061	1.7	4.3	5.3	11
31	10/11/1996	19	CA069	*Coryphaenoides armatus*	54.8	9.5	722	m	0.065	1.5	4	5.8	12
34	4/23/1998	1.1	CA070	*Coryphaenoides armatus*	57.2	10.3	693	m	0.059	1.4	4.2	5.3	13
34	4/23/1998	2.1	CA071	*Coryphaenoides armatus*	79	13.0	2439	f	0.092	1.8	4.9	5.9	19
34	4/23/1998	3.1	CA072	*Coryphaenoides armatus*	73.4	12.6	1915	f	0.121	2.1	5.5	6.1	20
34	4/23/1998	4.1	CA073	*Coryphaenoides armatus*	65.3	12.1	1662	f	0.080	1.5	4.9	5.6	17
34	4/23/1998	5.1	CA074	*Coryphaenoides armatus*	52.5	9.2	434	m	0.064	1.5	4.4	5.5	12
34	4/23/1998	6.1	CA075	*Coryphaenoides armatus*	77.4	14.2	2249	f	0.128	2	5.6	7.1	22
34	4/23/1998	7.1	CA076	*Coryphaenoides armatus*	58.2	10.9	1002	m	0.056	1.6	4	4.8	15
34	4/23/1998	8.1	CA077	*Coryphaenoides armatus*	59.3	10.5	914	m	0.063	1.7	4	5	
34	4/23/1998	9.1	CA078	*Coryphaenoides armatus*	86.1	14.2	2802	f	0.070	2	4.5	4.7	26
35	9/1/1998	2.1	CA079	*Coryphaenoides armatus*	73.6	13.6	1969	f	0.094	1.9	4.9	5.4	18
35	9/1/1998	3.1	CA080	*Coryphaenoides armatus*	53.4	9.8	593	m	0.064	1.6	4.4	5.2	12
35	9/1/1998	4.1	CA081	*Coryphaenoides armatus*	60.1	10.8	745	m	0.048	1.4	4.2	4.6	13
35	9/1/1998	5.1	CA082	*Coryphaenoides armatus*	56.8	10.1	580	m	0.067	1.6	4.5	5.4	15
35	9/1/1998	6.1	CA083	*Coryphaenoides armatus*	59.3	10.0	795	m	0.048	1.8	3.9	5	14
35	9/1/1998	7.1	CA084	*Coryphaenoides armatus*	50.5		431	m	0.059	1.6	4.4	5	11
35	9/1/1998	8.1	CA085	*Coryphaenoides armatus*	56.7	10.0	739	m	0.084	1.6	5.1	6.1	16
35	9/1/1998	9.1	CA086	*Coryphaenoides armatus*	68.4	12.3	1224	f	0.083	1.8	4.8	5.4	17
35	9/1/1998	10.1	CA087	*Coryphaenoides armatus*	53.6	10.7	822	m	0.080	1.7	5.2	5.2	12
35	9/1/1998	12.1	CA088	*Coryphaenoides armatus*	49.1	9.5	579	m	0.074	1.9	4.6	5.2	14

Pulse Cruise #	Date Collected	Specimen #	Otolith ID	Species	Total Length (cm)	Head Length (cm)	Body Mass (g)	Sex	Otolith Mass (g)	Otolith Height (mm)	Otolith Width (mm)	Otolith Length (mm)	Age Estimate (years)
35	9/1/1998	13.1	CA089	*Coryphaenoides armatus*	76	14.3	1598	u	0.096	1.9	4.7	6	19
35	9/1/1998	15.1	CA090	*Coryphaenoides armatus*	77.9	13.5	2398	f	0.106	2.1	5	6.9	18
35	9/1/1998	17.1	CA091	*Coryphaenoides armatus*	56.4	10.0	619	m	0.053	1.5	4.2	4.9	11
35	9/1/1998	18.1	CA092	*Coryphaenoides armatus*	72	12.9	1754	f	0.060	1.6	4.4	5	17
35	9/1/1998	19.1	CA093	*Coryphaenoides armatus*	56.3	9.9	631	m	0.065	1.7	4.2	5.3	11
35	9/1/1998	21.1	CA094	*Coryphaenoides armatus*	57.6	10.0	674	m	0.072	1.5	4.5	5.6	12
35	9/1/1998	23.1	CA095	*Coryphaenoides armatus*	52.8	9.5	518	m	0.070	1.6	4.6	5.7	11
35	9/1/1998	24.1	CA096	*Coryphaenoides armatus*	59.6	10.7	587	u	0.080	1.7	4.9	5.6	13
35	9/1/1998	25.1	CA097	*Coryphaenoides armatus*	55.9	9.9	615	u	0.102	2	5.4	5.9	
36	12/20/1998	1.1	CA098	*Coryphaenoides armatus*	57.6	10.2	778	m	0.058	1.7	4.2	4.9	
36	12/20/1998	2.1	CA099	*Coryphaenoides armatus*	64.3	10.6	922	m	0.072	1.6	4.5	5.7	
36	12/20/1998	3.1	CA100	*Coryphaenoides armatus*	69.3	12.2	1388	f	0.087	1.8	5	5.7	14
36	12/20/1998	5.1	CA101	*Coryphaenoides armatus*	52.8	9.3	497	m	0.044	1.6	3.9	3.9	11
36	12/20/1998	6.1	CA102	*Coryphaenoides armatus*	58.1	9.9	600	m	0.065	1.6	4.8	5.1	
36	12/20/1998	7.1	CA103	*Coryphaenoides armatus*	57.2	10.6	753	m	0.069	1.6	4.4	5.5	14
36	12/20/1998	10.1	CA104	*Coryphaenoides armatus*		10.0		u	0.052	2.3	4.9	6.1	
36	12/20/1998	11	CA105	*Coryphaenoides armatus*		9.9		u	0.082	1.7	4.9	5.8	11
36	12/20/1998	12	CA106	*Coryphaenoides armatus*		9.7		u	0.071	1.6	4.6	5.7	13
36	12/20/1998	15.1	CA107	*Coryphaenoides armatus*	55.7	10.1	694	m	0.079	1.4	4.8	6.4	
36	12/20/1998	16.1	CA108	*Coryphaenoides armatus*	60.5	10.1	668	m	0.058	1.4	4.1	5.1	15
36	12/20/1998	17.1	CA109	*Coryphaenoides armatus*	54	9.7	570	m	0.076	1.6	4.6	5.8	12
36	12/20/1998	18.1	CA110	*Coryphaenoides armatus*	85.5	14.9	3760	f	0.150	2.2	6.2	6.7	23
36	12/20/1998	19.1	CA111	*Coryphaenoides armatus*	55	9.5	595	m	0.052	1.5	4	4.8	11

Pulse Cruise #	Date Collected	Specimen #	Otolith ID	Species	Total Length (cm)	Head Length (cm)	Body Mass (g)	Sex	Otolith Mass (g)	Otolith Height (mm)	Otolith Width (mm)	Otolith Length (mm)	Age Estimate (years)
36	12/20/1998	20.1	CA112	*Coryphaenoides armatus*	54.9	10.0	635	f	0.065	1.6	4.1	5.4	13
36	12/20/1998	21.1	CA113	*Coryphaenoides armatus*	82.3	14.6	2301	f	0.100	1.8	6	6.1	24
36	12/20/1998	22.1	CA114	*Coryphaenoides armatus*	51.8	9.9	671	m	0.052	1.5	3.6	4.9	12
24	2/17/1995	2	CY001	*Coryphaenoides yaquinae*	47	9.3	380	f	0.046	1.53	4.44	4.67	9
24	2/17/1995	4	CY002	*Coryphaenoides yaquinae*	46.5	9.0	367	f	0.056	1.76	4.54	4.54	12
29	1/31/1996	9	CY003	*Coryphaenoides yaquinae*	38	7.4	202	f	0.025	1.34	3.6	3.84	7
29	1/31/1996	11	CY004	*Coryphaenoides yaquinae*	38.2	7.5	179	f	0.028	1.3	3.98	3.58	6
24	2/17/1995	34	CY005	*Coryphaenoides yaquinae*	51.5	9.9	554	f	0.062	1.66	4.71	5.01	10
29	1/31/1996	1	CY006	*Coryphaenoides yaquinae*	51.8	9.5	401	f	0.055	1.62	4.74	4.55	
27	11/16/1995	12	CY007	*Coryphaenoides yaquinae*	56	10.8	657	f	0.054	1.82	4.91	4.23	9
27	11/16/1995	14	CY008	*Coryphaenoides yaquinae*	56	10.7	558	f	0.043	1.62	4.41	4.37	10
24	2/17/1995	6	CY009	*Coryphaenoides yaquinae*	52	9.5	445	f	0.053	1.6	4.1	4.7	11
24	2/17/1995	19	CY010	*Coryphaenoides yaquinae*	53	10.9	592	f	0.049	1.5	4.4	4.9	12
24	2/17/1995	20	CY011	*Coryphaenoides yaquinae*	53	9.8	482	f	0.046	1.6	4.5	4.1	10
24	2/17/1995	37	CY012	*Coryphaenoides yaquinae*	43	7.9	232	f	0.034	1.3	3.8	3.7	8
24	2/17/1995	38	CY013	*Coryphaenoides yaquinae*	45	8.7	311	f	0.046	1.5	4.5	3.9	7
24	2/17/1995	31	CY014	*Coryphaenoides yaquinae*	50.5	9.7	424	f	0.044	1.4	4.6	4.1	11
25	4/29/1995	1	CY015	*Coryphaenoides yaquinae*	39.5	7.5	219	f	0.031	1.3	4.4	3.3	7
25	4/29/1995	5	CY016	*Coryphaenoides yaquinae*	52.5	10.1	505	f	0.051	1.6	4.7	4.3	13
25	4/29/1995	8	CY017	*Coryphaenoides yaquinae*	54	9.8	641	m	0.061	1.6	4.1	5.2	9
27	11/16/1995	2	CY018	*Coryphaenoides yaquinae*	49.5	9.8	492	f	0.035	1.4	4.6	3.6	8
27	11/16/1995	4	CY019	*Coryphaenoides yaquinae*	47	9.5	395	f	0.047	1.5	4.5	4.7	9

Pulse Cruise #	Date Collected	Specimen #	Otolith ID	Species	Total Length (cm)	Head Length (cm)	Body Mass (g)	Sex	Otolith Mass (g)	Otolith Height (mm)	Otolith Width (mm)	Otolith Length (mm)	Age Estimate (years)
27	11/16/1995	6	CY020	*Coryphaenoides yaquinae*	49.5	9.3	309	f	0.044	1.6	4	4.2	9
27	11/16/1995	7	CY021	*Coryphaenoides yaquinae*	54	10.9	589	f	0.077	1.7	4.7	5.2	13
27	11/16/1995	8	CY022	*Coryphaenoides yaquinae*	53.5	9.8	447	f	0.054	1.5	5	4.5	12
27	11/16/1995	9	CY023	*Coryphaenoides yaquinae*	47	8.8	332	f	0.044	1.4	4.4	3.8	11
27	11/16/1995	11	CY024	*Coryphaenoides yaquinae*	47	9.3	412	f	0.064	1.8	4.9	4.6	11
27	11/16/1995	15	CY025	*Coryphaenoides yaquinae*	48.5	8.9	382	f	0.039	1.5	4.2	3.5	12
27	11/16/1995	16	CY026	*Coryphaenoides yaquinae*	51	10.0	463	f	0.058	1.6	5	4.5	12
27	11/16/1995	18	CY027	*Coryphaenoides yaquinae*	43.5	8.2	314	f	0.040	1.5	3.9	4.1	9
27	11/16/1995	20	CY028	*Coryphaenoides yaquinae*	50	9.5	433	f	0.044	1.5	4.7	3.9	14
27	11/16/1995	21	CY029	*Coryphaenoides yaquinae*	65	11.9	1107	f	0.085	1.9	5.5	5	16
29	1/31/1996	3	CY030	*Coryphaenoides yaquinae*	42.4	8.2	291	f	0.029	1.2	4	3.5	9
29	1/31/1996	4	CY031	*Coryphaenoides yaquinae*	42.3	8.2	241	f	0.028	1.2	3.8	3.6	9
29	1/31/1996	6	CY032	*Coryphaenoides yaquinae*	45.1	9.1	376	f	0.034	1.3	4	4	10
29	1/31/1996	8	CY033	*Coryphaenoides yaquinae*	40.6	7.7	242	u	0.049	1.4	4.1	5.2	8
29	1/31/1996	10	CY034	*Coryphaenoides yaquinae*	38.5	7.4	209	f	0.029	1.3	3.7	3.7	7
29	1/31/1996	2	CY035	*Coryphaenoides yaquinae*	34.7	8.2	247	f	0.039	1.5	4.1	4.1	9
29	1/31/1996	14	CY036	*Coryphaenoides yaquinae*	47.2	9.1	410	f	0.043	1.5	4.7	4	12
31	10/11/1996	2	CY037	*Coryphaenoides yaquinae*	49.1	9.1	411	f	0.040	1.4	4.5	3.5	13
31	10/11/1996	4	CY038	*Coryphaenoides yaquinae*	52.1	9.6	447	f	0.046	1.7	4.4	3.8	11
31	10/11/1996	8	CY039	*Coryphaenoides yaquinae*	47.5	9.2	400	f	0.050	1.4	4.4	4.7	12
31	10/11/1996	9	CY040	*Coryphaenoides yaquinae*	40.5	7.8	231	m	0.033	1.4	4.1	3.7	8
31	10/11/1996	17	CY041	*Coryphaenoides yaquinae*	48.4	9.1	357	f	0.052	1.6	4.5	4.6	12
35	9/1/1998	20.1	CY042	*Coryphaenoides yaquinae*	54.4	10.1	481	f	0.056	1.7	4.7	4.5	14

Pulse Cruise #	Date Collected	Specimen #	Otolith ID	Species	Total Length (cm)	Head Length (cm)	Body Mass (g)	Sex	Otolith Mass (g)	Otolith Height (mm)	Otolith Width (mm)	Otolith Length (mm)	Age Estimate (years)
36	12/20/1998	8.1	CY043	*Coryphaenoides yaquinae*	40.2	9.1	260	f	0.040	1.4	4.3	4	9
36	12/20/1998	23.1	CY044	*Coryphaenoides yaquinae*	64.3	12.0		u	0.065	1.5	5	5.3	

Supplementary Table 5.1. Specimen information for gelatinous tissue samples tested. *N. kermadecensis* specimens were collected by free-vehicle trap (described Jamieson et al., 2013). Other specimens were collected by trawl (Drazen et al., 2015). Capture depth in metres. Collection dates noted. Standard length (SL) and Total length (TL) presented in centimeters, mass in grams.

Family	Species	Depth	Date	SL	TL	Mass	Sex
Liparidae	*Careproctus cypselurus*	1000	4.8.09		17.8	47.8	M
	Careproctus melanurus	750	10.2.09	15.5		24.47	F
		750	10.2.09	13.7	15.2	36.46	F
		1000	4.8.09		25.6	193.2	F
	Notoliparis kermadecensis	7000	11.29.11	24.5			
		7000	11.29.11	22.9			F
		7200	5.4.14	25.9	28	230	F
		7392	5.2.14	16.7	18.5	76	M
		7515	5.3.14	20.9	22.9	104	F
Ophidiidae	*Spectrunculus grandis*	2000	10.9.09	141	146	17463.3	
		4149	4.20.14	70	73.8	2128	F
Pleuronectidae	*Embassichthys bathybius*	1000	10.1.09	32.4	37.4	627.4	M
		1000	10.10.09	31.7	35	735.1	F
		1000	10.11.09	37.5	41.4	880.3	F
		1000	10.11.09	30.2	33.7	537.4	
	Microstomus pacificus	1000	10.1.09	46.6	50.4	1342.3	F
		1000	10.1.09	40.3	46.2	1127.1	F
		1000	10.1.09	43.7	48.5	1224.8	F
Zoarcidae	*Bothrocara brunneum*	1000	10.11.09	51	52.9	707	M
		2000	4.13.09	57.7	59.3	890.1	F
		2000	4.13.09		59.5	779.7	F
	Pachycara karenae	3000	10.8.09	35.6	37.4	503.6	F
		3000	10.8.09	34.7	36.6	450.8	M
		3000	10.8.09	37.7	38.5	501.6	F
	Pyrolycus sp.	4817	4.16.14	42	43.4	508	F

Supplementary Table 5.2. Species and gene sequences used in construction of phylogenetic tree showing distribution of gelatinous tissues (**Figure 5.2**). GenBank accession numbers and descriptions given. Depth ranges taken from FishBase (Froese and Pauly, 2015).

Species	Gelatinous Tissues	Minimum Depth (m)	Maximum Depth (m)	Mid Depth (m)	Family	Order	Accession Number
Acantholumpenus mackayi	no	0	200	100	Stichaeidae	Perciformes	
Amblyeleotris fasciata	no	4	20	12	Gobiidae	Perciformes	HQ536686.1
Anisarchus medius	no	30	100	65	Stichaeidae	Perciformes	HQ704778.3
Antimora microlepis	no	175	3048	1611.5	Moridae	Gadiformes	FJ164299.1
Antimora rostrata	no	1300	2500	1900	Moridae	Gadiformes	EU148073.1
Aptocyclus ventricosus	no	612	1700	1156	Cyclopteridae	Scorpaeniformes	AB795689.1
Arctogadus glacialis	no	0	1000	500	Gadidae	Gadiformes	LC146697.1
Astronesthes simulus	no				Stomiidae	Stomiiformes	GU071747.1
Ateleopus japonicus	yes	140	600	370	Ateleopodidae	Ateleopodiformes	KP267617.1
Atheresthes stomias	no	18	950	484	Pleuronectidae	Pleuronectformes	FJ164331.1
Balistes capriscus	no				Balistidae	Tetradontiformes	HQ167724.1
Bassozetus zenkevitchi	no	0	6930	3465	Ophidiidae	Ophidiiformes	FJ164347.1
Bathylagoides wesethi	no	25	1130	577.5	Bathylagidae	Argentiniformes	KJ190024.1
Bothrocara brunneum	yes	129	2570	1349.5	Zoarcidae	Perciformes	JQ354020.1
Brotula barbata	no	50	300	175	Ophidiidae	Ophidiiformes	
Callionymus filamentosus	no	5	100	52.5	Callionymidae	Perciformes	JQ797036.1
Careproctus canus	yes	244	434	339	Liparidae	Scorpaeniformes	FJ164432.1
Careproctus furcellus	yes	98	1270	684	Liparidae	Scorpaeniformes	FJ164446.1
Careproctus georgianus	yes	85	285	185	Liparidae	Scorpaeniformes	EU326329.1
Careproctus longipectoralis	yes		2037	1018.5	Liparidae	Scorpaeniformes	HQ712900.1
Careproctus melanurus	yes	89	2286	1187.5	Liparidae	Scorpaeniformes	FJ164451.1
Chauliodus macouni	yes	25	4390	2207.5	Stomiidae	Stomiiformes	JQ354039.1
Chauliodus sloani	no	494	1000	747	Stomiidae	Stomiiformes	KR086811.1
Coelorinchus fasciatus	no	400	800	600	Macrouridae	Gadiformes	EU074373.1
Citharichthys spilopterus	no	0	75	37.5	Paralichthyidae	Pleuronectformes	
Coryphaenoides acrolepis	no	900	1300	1100	Macrouridae	Gadiformes	FJ164488.1

Species	Gelatinous Tissues	Minimum Depth (m)	Maximum Depth (m)	Mid Depth (m)	Family	Order	Accession Number
Coryphaenoides armatus	no	282	5180	2731	Macrouridae	Gadiformes	EU148116.1
Coryphaenoides carapinus	no	384	5610	2997	Macrouridae	Gadiformes	EU148121.1
Coryphaenoides ferrieri	no	2525	3931	3228	Macrouridae	Gadiformes	JN640855.1
Coryphaenoides filifer	no	1285	2904	2094.5	Macrouridae	Gadiformes	
Coryphaenoides guentheri	no	831	2830	1830.5	Macrouridae	Gadiformes	
Coryphaenoides leptolepis	no	1900	3700	2800	Macrouridae	Gadiformes	EU148127.1
Coryphaenoides mediterraneus	no	1000	4262	2631	Macrouridae	Gadiformes	EU148128.1
Coryphaenoides yaquinae	yes	3400	5800	4600	Macrouridae	Gadiformes	GU440292.1
Coryphaneoides rupestris	no	400	1200	800	Macrouridae	Gadiformes	
Cyclopsetta panamensis	no	0	50	25	Paralichthyidae	Pleuronectformes	JX887475.1
Cyclopteropsis lindbergi	no	20	200	110	Cyclopteridae	Scorpaeniformes	AB917599.1
Cyclopterus lumpus	yes	50	868	459	Cyclopteridae	Scorpaeniformes	JN311802.1
Embassichthys bathybius	yes	41	1800	920.5	Pleuronectidae	Pleuronectformes	JQ354077.1
Epinephelus areolatus	no				Serranidae	Perciformes	JN208569.1
Epinephelus erythrurus	no				Serranidae	Perciformes	JN208607.1
Epinephelus fuscoguttatus	no				Serranidae	Perciformes	JN208616.1
Eptatretus cirrhatus	no	40	700	370	Myxinidae	Myxiniformes	KF144309.1
Eptatretus deani	no	103	2743	1423	Myxinidae	Myxiniformes	FJ164594.1
Ernogrammus hexagrammus	no	0	142	71	Stichaeidae	Perciformes	HQ704726.3
Eumicrotremus andriashevi	no	20	83	51.5	Cyclopteridae	Scorpaeniformes	AB917662.1
Eumicrotremus asperrimus	no	20	900	460	Cyclopteridae	Scorpaeniformes	AB795674.1
Eumicrotremus derjugini	no	50	930	490	Cyclopteridae	Scorpaeniformes	AM498309.1
Eumicrotremus orbis	no	0	575	287.5	Cyclopteridae	Scorpaeniformes	HQ712372.1
Eumicrotremus taranetzi	no	0	7	3.5	Cyclopteridae	Scorpaeniformes	AB917649.1
Eurypharynx pelecanoides	yes	1200	1400	1300	Eurypharyngidae	Saccopharyngiformes	KF681863.1
Gadella imberbis	no	200	800	500	Moridae	Gadiformes	KC015367.1
Gadomus longifilis	no	630	2165	1397.5	Macrouridae	Gadiformes	
Gadus chalcogrammus	no	183	1280	731.5	Gadidae	Gadiformes	HM421792.1
Genypterus brasiliensis	no	60	200	130	Ophidiidae	Ophidiiformes	

Species	Gelatinous Tissues	Minimum Depth (m)	Maximum Depth (m)	Mid Depth (m)	Family	Order	Accession Number
Glyptocephalus stelleri	no	15	800	407.5	Pleuronectidae	Pleuronectformes	KF386401.1
Gnatholepis scapulostigma	no	2	20	11	Gobiidae	Perciformes	HQ536707.1
Guttigadus latifrons	no	770	1875	1322.5	Moridae	Gadiformes	EU148219.1
Hexagrammos octogrammus	no	0	200	100	Hexagrammidae	Scorpaeniformes	AB755189.1
Hippoglossina stomata	no	30	137	83.5	Paralichthyidae	Pleuronectformes	JQ354124.1
Hippoglossoides dubius	no	10	600	305	Pleuronectidae	Pleuronectformes	JF952755.1
Hippoglossoides platessoides	no	90	250	170	Pleuronectidae	Pleuronectformes	EU513650.1
Hippoglossoides robustus	no	0	150	75	Pleuronectidae	Pleuronectformes	GU804873.1
Hippoglossus hippoglossus	no	50	2000	1025	Pleuronectidae	Pleuronectformes	EU513652.1
Hygophum proximum	no	0	1000	500	Myctophidae	Myctophiformes	KJ555400.1
Isopsetta isolepis	no	20	425	222.5	Pleuronectidae	Pleuronectformes	HQ712510.1
Istigobius rigillus	no	0	30	15	Gobiidae	Perciformes	HQ536672.1
Lampadena urophaos	no	50	1000	525	Myctophidae	Myctophiformes	KJ555408.1
Lamprogrammus niger	no	741	1500	1120.5	Ophidiidae	Ophidiiformes	JQ354156.1
Lepidion capensis	no	457	1152	804.5	Moridae	Gadiformes	HQ945968.1
Leptoclinus maculatus	no	2	607	304.5	Stichaeidae	Perciformes	HQ704751.3
Lethotremus awae	no	0	20	10	Cyclopteridae	Scorpaeniformes	AB795679.1
Lethotremus muticus	no	58	330	194	Cyclopteridae	Scorpaeniformes	AB917647.1
Leuroglossus schmidti	no	394	1800	1097	Bathylagidae	Argentiniformes	JQ354170.1
Liparis dennyi	no	73	223	148	Liparidae	Scorpaeniformes	JQ354179.1
Liparis fabricii	no	12	1800	906	Liparidae	Scorpaeniformes	AM498311.1
Liparis fucensis	no	225	388	306.5	Liparidae	Scorpaeniformes	KF918880.1
Liparis gibbus	no	100	200	150	Liparidae	Scorpaeniformes	KC015566.1
Liparis liparis	no	1	300	150.5	Liparidae	Scorpaeniformes	KJ204976.1
Liparis pulchellus	no	9	183	96	Liparidae	Scorpaeniformes	JQ354184.1
Liparis rutteri	no	0	73	36.5	Liparidae	Scorpaeniformes	JQ354186.1
Liparis tanakae	no	50	121	85.5	Liparidae	Scorpaeniformes	JF952785.1
Liparis nanus	no	0	910	455	Liparidae	Scorpaeniformes	FJ164719.1
Lophius americanus	no	0	668	334	Lophiidae	Lophiiformes	EU660712.1

Species	Gelatinous Tissues	Minimum Depth (m)	Maximum Depth (m)	Mid Depth (m)	Family	Order	Accession Number
Lophius piscatorius	no	20	1000	510	Lophiidae	Lophiiformes	EU660698.1
Lumpenus sagitta	no	0	425	212.5	Stichaeidae	Perciformes	HQ704784.3
Lycenchelys crotalinus	no	200	2816	1508	Zoarcidae	Perciformes	HQ704761.3
Lycodes raridens	no	10	400	205	Zoarcidae	Perciformes	HQ704788.3
Macrourus holotrachys	no	300	1400	850	Macrouridae	Gadiformes	JF265089.1
Macrourus whitsoni	no	600	1500	1050	Macrouridae	Gadiformes	JF265117.1
Malacocephalus laevis	no	300	750	525	Macrouridae	Gadiformes	JQ774539.1
Melanocetus johnsonii	yes	100	1500	800	Melanocetidae	Lophiiformes	
Melanogrammus aeglefinus	no	10	200	105	Gadidae	Gadiformes	LC146710.1
Microstomus pacificus	yes	10	1370	690	Pleuronectidae	Pleuronectformes	KP835305.1
Myctophum selenops	no	40	500	270	Myctophidae	Myctophiformes	KJ555435.1
Myxine glutinosa	no	30	1200	615	Myxinidae	Myxiniformes	Y15182.1
Nectoliparis pelagicus	yes	0	238	119	Liparidae	Scorpaeniformes	FJ164907.1
Neobythites sivicola	no	25	249	137	Ophidiidae	Ophidiiformes	KC442074.1
Nezumia sclerorhynchus	no	450	730	590	Macrouridae	Gadiformes	JQ774541.1
Ophidion holbrookii	no	0	75	37.5	Ophidiidae	Ophidiiformes	
Ophidion scrippsae	no	0	110	55	Ophidiidae	Ophidiiformes	
Opisthocentrus ocellatus	no	0	335	167.5	Stichaeidae	Perciformes	HQ704737.3
Paralichthys lethostigma	no	0	43	21.5	Paralichthyidae	Pleuronectformes	KM407611.1
Paralichthys squamilentus	no	1	230	115.5	Paralichthyidae	Pleuronectformes	KF930230.1
Paraliparis dactylosus	no	541	1000	770.5	Liparidae	Scorpaeniformes	KF918890.1
Paraliparis rosaceus	no	1050	3358	2204	Liparidae	Scorpaeniformes	FJ164980.1
Parophrys vetulus	no	0	550	275	Pleuronectidae	Pleuronectformes	EU752162.1
Pholidapus dybowskii	no	0	146	73	Stichaeidae	Perciformes	HQ704747.3
Photonectes brueri	no				Stomiidae	Stomiiformes	KF930258.1
Physiculus natalensis	no	433	500	466.5	Moridae	Gadiformes	JF494153.1
Physiculus rastrelliger	no	183	366	274.5	Moridae	Gadiformes	GU440460.1
Pleuronectes quadrituburculatus	no	0	600	300	Pleuronectidae	Pleuronectformes	HQ712726.1
Pleuronichthys decurrens	no	8	533	270.5	Pleuronectidae	Pleuronectformes	FJ165025.1

Species	Gelatinous Tissues	Minimum Depth (m)	Maximum Depth (m)	Mid Depth (m)	Family	Order	Accession Number
Pseudorhombus elevatus	no	7	200	103.5	Paralichthyidae	Pleuronectformes	JF494304.1
Raneya brasiliensis	no	40	150	95	Ophidiidae	Ophidiiformes	
Scopelopsis multipunctatus	no	3	2000	1001.5	Myctophidae	Myctophiformes	
Selachophidium guentheri	no	200	400	300	Ophidiidae	Ophidiiformes	GU804921.1
Spectrunculus grandis	yes	800	4300	2550	Ophidiidae	Ophidiiformes	KF930451.1
Stichaeus ochriamkini	no	14	99	56.5	Stichaeidae	Perciformes	HQ704745.3
Symbolophorus californiensis	no	557	1497	1027	Myctophidae	Myctophiformes	KJ555466.1
Tactostoma macropus	yes	30	2000	1015	Stomiidae	Stomiiformes	KJ190048.1
Thryssa kammalensis	no	1	20	10.5	Engraulidae	Clupeiformes	KF951618.1
Trachyrincus scabrus	no	395	1700	1047.5	Macrouridae	Gadiformes	KC015971.1
Trichiurus lepturus	no				Trichiuridae	Perciformes	EF607600.1

Supplementary Table 6.1. All counts and measurements used for the description of *Pseudoliparis swirei*. In order of ascending standard length. Holotype HADES #200060 in bold. *Fresh measurements. **Measurements taken from radiograph.

SAMPLE NUMBER	Date	Deployment	Latitude	Longitude	Depth (m)	Total Length* (mm)	Standard Length* (mm)	Pre-Anal Fin Length* (mm)	Pre-dorsal Fin Length (mm, from x-rav)	Head Length* (mm)	Eye Width* (mm)	Snout Length* (mm)	Total Weight* (g)
200037	18/11/2014	TR07	12.42347°N	144.87058°E	7497	99	89	35	22	13	2	5	15
200060	**21/11/2014**	**WT06**	**12.30370°N**	**144.68038°E**	**7949**	**109**	**97**	**36**	**33**	**20**	**2**	**7**	**7**
200041	18/11/2014	TR07	12.42347°N	144.87058°E	7497	124	105	43		23	3	7	15
200081	24/11/2014	WT08	11.92970°N	144.92880°E	7966	120	107	39		19	1	6	10
200071	23/11/2014	TR10	11.91280°N	144.94450°E	7841	123	110	42		20	2	7	15
200072	23/11/2014	TR10	11.91280°N	144.94450°E	7841	134	119	48		24	2	7	15
200144	7/12/2014	TR20	12.34950°N	144.68130°E	7652	130	119	48		21	2	7	20
200095	26/11/2014	TR13	11.82600°N	145.00880°E	6974	137	124	45		22	2	9	15
200049	19/11/2014	TR08	12.42556°N	144.91171°E	7509	143	128	50	38	25	3	7	20
200143	7/12/2014	TR20	12.34950°N	144.68130°E	7652	137	129	49	34	23	3	9	20
200048	19/11/2014	TR08	12.42556°N	144.91171°E	7509	150	135	58		22	3	10	25
200141	7/12/2014	TR20	12.34950°N	144.68130°E	7652	152	139	62		25	2	9	30
200142	7/12/2014	TR20	12.34950°N	144.68130°E	7652	159	142	70		30.5	3	10	40
200074	23/11/2014	WT07	11.92730°N	144.96200°E	7907	163	145	61		25	3	9	30
200042	18/11/2014	TR07	12.42347°N	144.87058°E	7497	164	147	62		28	2	9	30
200133	6/12/2014	TR19	12.27660°N	144.62020°E	7626	167	151	68		27	4	9	35
200134	6/12/2014	TR19	12.27660°N	144.62020°E	7626	172	161	67		33	4	15	45
200038	18/11/2014	TR07	12.42347°N	144.87058°E	7497	186	165	71	45	24	2	10	50

SAMPLE NUMBER	Date	Deployment	Latitude	Longitude	Depth (m)	Total Length* (mm)	Standard Length* (mm)	Pre-Anal Fin Length* (mm)	Pre-dorsal Fin Length (mm, from x-rav)	Head Length* (mm)	Eye Width* (mm)	Snout Length* (mm)	Total Weight* (g)
200070	23/11/2014	TR10	11.91280°N	144.94450°E	7841	190	172	73	44	30	3	8	65
200084	25/11/2014	WT09	11.81470°N	144.98580°E	6949	195	176	71		35	3	11	65
200047	19/11/2014	TR08	12.42556°N	144.91171°E	7509	194	178	81	55	37	3	13	75
200096	26/11/2014	TR13	11.82600°N	145.00880°E	6974	201	183	70		34	2	11	85
200040	18/11/2014	TR07	12.42347°N	144.87058°E	7497	207	184	87	46	36	3	10	90
200036	18/11/2014	TR07	12.42347°N	144.87058°E	7497	205	186	92		37	4	10.5	110
200094	26/11/2014	TR13	11.82600°N	145.00880°E	6974	205	187	76	48	36	3	10	75
200021	15/11/2014	TR05	12.59786°N	144.77854°E	7062	215	193	77	46	32	4	13	70
200087	25/11/2014	TR12	11.81070°N	144.99450°E	6898	223	203	82	56	38	2	11	90
200039	18/11/2014	TR07	12.42347°N	144.87058°E	7497	230	210	95	65	40	4	17	150
SY1615028	29/01/2017	FT02	11.54290°N	142.18485°E	7581	235	213	94		45	4	17	
200027	16/11/2014	TR06	12.63390°N	144.75080°E	6914		220	97		44	4	14	
200085	25/11/2014	WT09	11.81470°N	144.98580°E	6949	247	225	88	49	43	3.5	15	130
200024	16/11/2014	WT03	12.61026°N	144.76839°E	6961	244	232	105		37	4	10	160
200025	16/11/2014	WT03	12.61026°N	144.76839°E	6961	260	235	108	61	44	4	14	150
200033	18/11/2014	WT04	12.41505°N	144.91187°E	7495	190		79		33	3	12	45
200043	18/11/2014	TR07	12.42347°N	144.87058°E	7497	211		86	43	35	3.5	10	90
200050	19/11/2014	TR08	12.42556°N	144.91171°E	7509	116		42		19	2	5	10
200062	21/11/2014	TR09	12.30274°N	144.67388°E	7929			39		16	2	5	8

SAMPLE NUMBER	TL (mm)	SL (mm)	HL (mm)	Head Depth (mm)	Lower Lobe (mm)	Body Depth (mm, from photo)	Orbit Width (mm)	Snout Length (mm)	Head Width (mm)	Disk Length (mm)	Gill Opening (mm)
200037	95.0	87.0	17.8		4.1		2.9	5.7			
200060	**112.0**	**104.0**	**18.9**	**~14**		**18.0**	**3.5**	**6.7**	**13.1**		
200041	115.0	107.0			3.8	25.0		5.6			
200081	>110	>103	~16.2	~11			2.8	7.3	12.6		
200071	119.0	111.0	~20.6		3.2			6.5		3.4	
200072		~115	~22				4.1	7.9			
200144	124.0	112.0	21.8		2.3		3.7	7.7		4.5	
200095	138.0	123.0	20.9				~4.5	~8		2.9	
200049	132.0	123.0	24.2			29.0	4.0	8.0			5.4
200143	132.0	119.0	23.9				3.9	7.5	16.3	4.7	
200048	>129					30.0	4.1	10.1			
200141	143.0	132.0	27.2				5.4	8.6		3.3	
200142	151.0	138.0	~30		5.6	40.0	6.1	11.4		6.3	
200074	154.0	139.0	27.8				4.4	8.3		5.8	
200042	149.0	142.0						~9			
200133	153.0	143.0	28.9		6.2	37.0	5.8	7.0		6.9	
200134		155.0	33.6		2.8	39.0	5.0	12.4		8.7	
200038	181.0	163.0				36.0	4.4	10.0			
200070	~182	163.0	34.4			42.0	5.8	9.8	28.3		
200084	>178		~34.1			41.0	5.6	~12	23.9		
200047	185.0	169.0	35.0			46.0		10.9			
200096	>188	>173	~36				~5	~11			
200040	198.0	181.0	36.2		5.1	49.0		10.7	27.7		9.6
200036			~36		6.2	58.0	5.7	~10	29.5		
200094	196.0	178.0	36.3		6.0	50.0	5.0	11.9	~20.9	6.9	9.4
200021	~204	~184			5.5	44.0		~8.1			
200087	~212	~192	35.3		6.6	45.0	6.0	11.2	~27	8.8	
200039	220.0	211.0	41.0		6.0	62.0		14.4	41.4		
SY1615028	233	208	41.5	32.7		47	5.6	14	39.2	8.2	
200027			~40								
200085	237.0	215.0	40.0	20.5			5.4	15.2	31.8	7.4	
200024			~48				~8	~10			
200025		226.0	42.9	28.7	4.9		5.2	13.5	32.9	9.0	
200033	~188	~170									
200043	203.0	182.0	36.7		5.0		5.2	12.3			
200050		~100	~21		2.5		~3	~7			

SAMPLE NUMBER	Distance: Mandible to Disk (mm)	Distance: Snout to Anus (mm)	Distance: Mandible to Anus (mm)	Distance: Disk to Anus (mm)	Distance: Anus to Anal Fin (mm)	Upper Jaw Length (mm)	Lower Jaw Length (mm)	# Rows of Teeth on Upper Jaw	Maximum # Teeth Per Row on Upper Jaw	Width (# of Teeth) Upper Jaw	# Rows of Teeth on Lower Jaw	Maximum # Teeth Per Row on Lower Jaw	Width (# of Teeth) Lower Jaw
200037	~10.3	25.5	24.0	~11.3	11.7	8.1	7.6	~7	12	4	>6	>10	3
200060	**8.8**	**23.2**	**21.0**	**9.5**	**10.9**	**~8.7**	**8.2**	**7**	**8**	**4**	**8**	**11**	**4**
200041	9.9					9.1	~9	~6	~7	2	~8	~12	3
200081	~9.2					10.7	9.8						
200071	10.7					9.2	9.7	>5			9	~7	3
200072	10.5							6	6	3	9		3
200144	10.3					10.1	9.6				8	12	~3
200095	12.5					10.9	9.7	7	10	3	9	12	4
200049	13.3					10.7	~10	~9	>6	3	9	12	4
200143	12.0					11.0	10.0	>6	>5	>2	~8	10	3
200048	13.9					11.7	10.4	8	8	4	10	9	4
200141	14.9	~41	~37.6	~18.4	~19.4	13.8	12.1	9	8	4	10	14	4
200142	14.3					13.2	12.4	8	>9	4	10 - 11	15	4 - 5
200074	~16					13.4	14.8	9	>8	4	10	17	4
200042							10.4	8	~10	4	~13	12	4
200133	14.7	~49	~47	~26	~9	~10.2	~9.1	8 - 9	10	4	10	16	4
200134	15.9	~43	~40	~17	~20	15.5	13.9	10	>11	4	>8	~14	4
200038	22.3	46.0	43.2	16.2	25.9	16.3	13.7	~8	14	4	~14	>12	~4
200070	20.0					15.8	13.3	8	~10	4	11	15	4
200084	~18		~42	~18	~22	16.8	15.5	8	12	4 - 5	8	11	4
200047					23.3	16.5	16.7	9	8	4	13	12	4
200096						16.5	13.3	10	10	4	9	7 - 9	4
200040	16.5	48.0				17.2	12.9	9	15	4 - 5	12	19	4
200036	16.7	~44	40.6	16.2	24.3	15.7	15.3	9	12	4	8	8	4
200094	18.5	~48	~45.9	~22.3	~14.5	15.9	14.2	9	14	4	~11	15	4

SAMPLE NUMBER	Distance: Mandible to Disk (mm)	Distance: Snout to Anus (mm)	Distance: Mandible to Anus (mm)	Distance: Disk to Anus (mm)	Distance: Anus to Anal Fin (mm)	Upper Jaw Length (mm)	Lower Jaw Length (mm)	# Rows of Teeth on Upper Jaw	Maximum # Teeth Per Row on Upper Jaw	Width (# of Teeth) Upper Jaw	# Rows of Teeth on Lower Jaw	Maximum # Teeth Per Row on Lower Jaw	Width (# of Teeth) Lower Jaw
200021	15.0					16.3	14.6	10	11	4	11	16	4 - 5
200087	17.6					16.0	15.9	9 - 10	12	4	13	15	4
200039	16.3	47.0				15.7	13.8	9	11	4	11	20	4
SY1615028	21.7	56.7	47.5	17.9									
200027						18.8	19.3	10	10	4	8	12	4
200085	20.0	~62	~58	33.5	18.6	16.9	15.4	9	10	4 - 5	>10	~14	4
200024						~15.9	~17.8	10	20	4 - 5	7 - 8	15	4 - 5
200025	17.3					20.6	17.9						
200033						12.7	12.0	9	9	3 - 4	8	12	4
200043	17.2	~44.2	~41	~18.4	~24.6	15.5	14.4	9	11	4	12 - 13	14	4
200050		~35	~32		14.1	9.0	10.4				10	8	4
200062						9.0	6.6	7		3	7		

SAMPLE NUMBER	Total # Vertebrae	# Abdominal Vertebrae	# Caudal Vertebrae	Dorsal Fin Origin (Between Vertebrae #, #)	# Dorsal Fin Rays	# Anal Fin Rays	Extra Ray at Anal Origin	Total # Pyloric Caecae	# Short Pyloric Caecae	Minimum Pyloric Caeca Length (mm)	# Long Pyloric Caecae	Maximum Pyloric Caeca Length (mm)	Sex	Maximum Egg Size (mm)	# Eggs (Large, Small)	Condition
200037	61					~51	Yes									Undissected
200060	**58**	**12**	**46**		**~52**	**≥44**	**Yes**									**Undissected**
200041	>56			4, 5	51	43		~5	~3	4.5	~2	8.1	Juvenile			Poor
200081								9	6	2.8	3	7.3	Juvenile			Poor
200071	60	12	48		>51	48	Yes	>6	6	5.5	0	6.6	Juvenile			Poor
200072																Poor
200144	59	12	47	4, 5	53	48	Yes	7	4	5.9	3	9.7	Juvenile			Good
200095													Female			Poor
200049	57	12	45		52	44	Yes									Poor
200143	61	~11	~50		>41	~48		~6	4	3.9	2	9.1	Female			Fair
200048	>51	11	>40	4, 5	>49	>42	Yes	~5	~2	4.6	~3	10.3	Male?			Poor
200141	57	13	44			~46	Yes									Undissected
200142								7	4	7.2	3	14.1	Male			Fair
200074	61	13	48	4, 5	>54	47	Yes	7	4	4.4	3	9.3	Male			Poor
200042													Juvenile			Poor
200133								8	5	3.5	3	12.6	Juvenile			Poor
200134								8	1	5.7	7	13.4	Female			Poor
200038	60	13	47	5, 6	54	48	Yes									Undissected
200070	59	13	46		>54	46	Yes	8	5	5.6	3	15.2	Female			Good
200084								6		8.0		13.6	Female	0.7		Poor
200047	58	14	44	4, 5	53	43	Yes	7	4	8.9	3	19.8	Male			Fair
200096								~7	4	5.6	>2	12.0	Female			Poor
200040	60	13	47		>54	48	Yes	7	5	8.7	2	17.6	Female			Fair

SAMPLE NUMBER	Total # Vertebrae	# Abdominal Vertebrae	# Caudal Vertebrae	Dorsal Fin Origin (Between Vertebrae #, #)	# Dorsal Fin Rays	# Anal Fin Rays	Extra Ray at Anal Origin	Total # Pyloric Caecae	# Short Pyloric Caecae	Minimum Pyloric Caeca Length (mm)	# Long Pyloric Caecae	Maximum Pyloric Caeca Length (mm)	Sex	Maximum Egg Size (mm)	# Eggs (Large, Small)	Condition
200036																Undissected
200094	59	13	46	3, 4	55	46	Yes	7	4	9.5	3	18.0	Female	0.9		Good
200021	62	13	49	5, 6	58	49	Yes	7	4	7.4	3	17.7	Male			Poor
200087	59	13	46	4, 5	54	~46	Yes	~6	4	5.5	2	15.3	Female	1.4		Good
200039	60	11	49	4, 5	55	47	Yes	7	5	6.7	2	17.9	Female	6.4	23, 705	Fair
SY1615028													Male			Undissected
200027								7	5	5.3	2	18.0	Female	9.4	7, 344	Poor
200085	61	12	49		56	48	Yes	7	4	5.6	3	15.4	Female	9.2	14, 486	Good
200024																Poor
200025	57	12	45	~5, 6	>52	47	Yes	~7	5	7.1	2	15.6	Female	8.5	22, 851	Good
200033								>3				~13.4				Poor
200043	56	12	44	4, 5	55	43	Yes	7	4	6.1	3	18.3	Female	1.2		Fair
200050								5	3		2					Fair
200062																Poor

SAMPLE NUMBER	Length Upper Pectoral Fin Lobe (mm)	Length Lower Pectoral Fin Lobe (mm)	Total # Pectoral Rays (Left)	# Pectoral Rays on Upper Lobe (Left)	# Notch Rays (Left)	# Pectoral Rays on Lower Lobe (Left)	Total # Pectoral Rays (Right)	# Pectoral Rays on Upper Lobe (Right)	# Notch Rays (Right)	# Pectoral Rays on Lower Lobe (Right)	Total # Caudal Rays	# Upper Caudal Rays	# Lower Caudal Rays	# Auxiliary Caudal Rays
200037	14.2	7.3	28	18	5	5	28	18	5	5	11	4	6	1
200060	**>15.6**	**8.9**	**>27**	**20**			**30**	**20**	**5**	**5**	**13**	**5**	**6**	**2**
200041	19.7	~9	29	19	5	5	>25				>10			
200081														
200071	18.2	8.6	30	20	5	5	28	20	4	4	13	6	6	1
200072	19.8	~7.7	30	20	4	6		~15	5		14	6	7	1
200144	14.5	>9.8	30	20	5	5	29	19	5	5	13	6	6	1
200095	19.2	~12	>23				~27	~17	5	5				
200049	22.3	14.9	31	20	5	6	31	21	5	5				
200143	~16	9.3	30	20	5	5	>25	20	5		11	5	5	1
200048	20.2	~9	>20				>21	>15	6	5				
200141	20.7	>6.6	32	21	5	6	31	21	5	5	13	6	6	1
200142	23.6	11.2	31	21	5	5	29	18	5	6	11	5	6	0
200074	21.5	10.2	30	20	5	5	30	20	5	5	13	5	6	2
200042	21.0	9.8	32	21	6	5	29	19	5	5				
200133	25.1	11.5	30	20	5	5	30	20	5	5	13	5	6	2
200134	20.9	13.6	30	21	5	4	~30							
200038	20.5	10.2	~30	20	5	~5	32	21	5	6	14	6	6	2
200070	20.7	11.8	>20				>22				~10	4	4	2
200084	23.6	16.3	29	19	5	5	>25	>15	~6	4				
200047	33.4	~12	~33	~22	6	5	>26				12	5	6	1
200096	~19.4	~15.8	29	23	3	4	~26	~18	4	4	11	5	6	0
200040	~21	12.5	31	21	5	5	30	21	4	5	12	5	6	1
200036	27.3	22.9	31	22	4	5	31	22	4	5	12	5	7	0

SAMPLE NUMBER	Length Upper Pectoral Fin Lobe (mm)	Length Lower Pectoral Fin Lobe (mm)	Total # Pectoral Rays (Left)	# Pectoral Rays on Upper Lobe (Left)	# Notch Rays (Left)	# Pectoral Rays on Lower Lobe (Left)	Total # Pectoral Rays (Right)	# Pectoral Rays on Upper Lobe (Right)	# Notch Rays (Right)	# Pectoral Rays on Lower Lobe (Right)	Total # Caudal Rays	# Upper Caudal Rays	# Lower Caudal Rays	# Auxiliary Caudal Rays
200094	24.3	13.8	31	21	5	5	31	21	5	5	12	5	5	2
200021	25.0	12.7	31	21	5	5	30	21	4	5	13	5	6	2
200087	~24	10.6	29	19	5	5	29	19	5	5				
200039	26.8	14.2	30	21	5	4	32	21	5	6	14	6	6	2
SY1615028	29.1	15.1												
200027	>31.4		~26						3	5				
200085	28.0	~21	~31	~20	6	5	29	20	4	5	>6			
200024	~28.1													
200025	28.5	~17	32	21	5	6	32	21	5	6				
200033	25.1		>11								13	6	7	~1
200043	28.9	12.1	31	21	5	5	>27				13	5	6	2
200050	17.5	13.9	30	21	4	5	30	21	4	5	>10	>5	>5	
200062							30	20	5	5				

SAMPLE NUMBER	HL % SL	HW % SL	Snout % SL	Eye % SL*	Orbit % SL	Upper Jaw % SL	Lower Jaw % SL	Upper Pectoral Lobe % SL	Lower Pectoral Lobe % SL	Gill Opening % SL
200037	20.5		6.6	2.2	3.3	9.3	8.7	16.3	8.4	
200060	**18.2**	**12.6**	**6.4**	**2.1**	**3.4**	**~8.4**	**7.9**		**8.6**	
200041	21.9*		5.2	2.9		8.5	~8.4	18.4	~8.4	
200081	17.8*		5.6*	0.9						
200071	~18.6		5.9	1.8		8.3	8.7	16.4	7.7	
200072	~19.1		~6.9	1.7	~3.6			~17.2	~6.7	
200144	19.5		6.9	1.7	3.3	9.0	8.6	12.9		
200095	17.0		~6.5	1.6	~3.7	8.9	7.9	15.6	~9.8	
200049	19.7		6.5	2.3	3.3	8.7	~8.1	18.1	12.1	4.4
200143	20.1	13.7	6.3	2.3	3.3	9.2	8.4	~13.4	7.8	
200048	16.3*		7.4*	2.2						
200141	20.6		6.5	1.4	4.1	10.5	9.2	15.7		
200142	~21.7		8.3	2.1	4.4	9.6	9.0	17.1	~8.1	
200074	20.0		6.0	2.1	3.2	9.6	10.6	15.5	7.3	
200042	19.0*		~6.3	1.4			7.3	14.8	6.9	
200133	20.2		~4.9	2.6	4.1	~7.1	~6.4	17.6	8.0	
200134	21.7		8.0	2.5	3.2	10.0	9.0	13.5	8.8	
200038	14.5*		6.1	1.2	2.7	10.0	8.4	12.6	6.3	
200070	21.1	17.4	6.0	1.7	3.6	9.7	8.2	12.7	7.2	
200084	19.9*		6.3*	1.7						
200047	20.7		6.4	1.7		9.8	9.9	19.8	~7.1	
200096	18.6*		6.0*	1.1						
200040	20.0	15.3	5.9	1.6		9.5	7.1	~11.6	6.9	5.3
200036	19.9*		5.6*	2.2						
200094	20.4	~11.7	6.1	1.6	2.8	8.9	8.0	13.7	7.8	5.3
200021	16.6*		6.7*	2.1		~8.9	~7.9	~13.6	~6.9	
200087	~18.4	~14.1	~5.8	1.0	~3.1	~8.3	~8.3	~12.5	~5.5	
200039	19.4	19.6	6.8	1.9		7.4	6.5	12.7	6.7	
SY1615028	20	18.8	6.9	2.0	2.7	11.0	9.9	14.0	7.3	
200027	20.0*		6.4*	1.8						
200085	18.6	14.8	7.1	1.6	2.5	7.9	7.2	13.0	~9.8	
200024				1.7						
200025	19.0	14.6	6.0	1.7	2.3	9.1	7.9	12.6	~7.5	
200033						~7.5	~7.1	~14.8		
200043	20.2		6.8		2.9	8.5	7.9	15.9	6.6	
200050	~21.0		~7.0		~3.0	~9.0	~10.4	~17.5	~13.9	

SAMPLE NUMBER	Disk Length % SL	Disk-anus Distance %SL	Mandible-Disk Distance % SL	LLD % SL	Body Depth % SL**	PreD % SL	preA % SL*	Snout to Anus % SL	Mandible to Anus % SL	Anus to Anal Fin % SL
200037		~13.0	~11.8	4.7		25.8	39.3	29.3	27.6	13.4
200060		**9.1**	**8.5**		**18.6**	**32.0**	**37.1**	**22.3**	**20.2**	**10.5**
200041			9.3	3.6	23.8		41.0			
200081							36.4			
200071	3.1		9.6	2.9			38.2			
200072			~9.1				40.3			
200144	4.0		9.2	2.1			40.3			
200095	2.4		10.2				36.3			
200049			10.8		22.7	31.0	39.1			
200143	3.9		10.1			28.8	38.0			
200048					22.2		43.0			
200141	2.5	~13.9	11.3			18.6	44.6	~31.2	~28.5	~14.7
200142	4.6		10.4	4.1	28.2		49.3			
200074	4.1		~11.5				42.1			
200042							42.2			
200133	4.8	~18.2	10.3	4.3	24.5		45.0	~34.3	~32.9	~6.3
200134	5.6	~11.0	10.3	1.8	24.2		41.6	~27.7	~25.8	~12.9
200038		9.9	13.7		21.8	27.5	43.0	28.2	26.5	15.9
200070			12.3		24.4	26.8	42.4			
200084					23.3		40.3			
200047					25.8	32.6	45.5			13.8
200096							38.3			
200040			9.1	2.8	26.6	25.6	47.3	26.5		
200036					31.2		49.5			
200094	3.9	~12.5	10.4	3.4	26.7	27.1	40.6	~27.0	~25.8	~8.1
200021			~8.2	~3.0	22.8	~24.9	39.9			
200087	~4.6		~9.2	~3.4	22.2	~29.2	40.4			
200039			7.7	2.8	29.5	31.0	45.2	22.3		
SY1615028	4.0	8.6	10.4		23.0			27.3	22.8	
200027							44.1			
200085	3.4	15.6	9.3			22.7	39.1	~28.8	~27.0	8.7
200024							45.3			
200025	4.0		7.7	2.2		26.8	46.0			
200033										
200043		~10.1	9.5	2.7		23.8		~24.3	~22.5	~13.5
200050				~2.5				~35.0	~32.0	~14.1

SAMPLE NUMBER	HW % HL	Snout % HL	Eye % HL*	Orbit % HL	Upper Jaw % HL	Lower Jaw % HL	Upper Pectoral Lobe % HL	Lower Pectoral Lobe % HL	Gill Opening % HL	Disk Length % HL
200037		32.0	15.4	16.3	45.5	42.7	79.8	41.0		
200060	**69.3**	**35.4**	**10.0**	**18.5**	**~46.0**	**43.4**		**47.1**		
200041		30.4*	13.0							
200081	~77.8	~45.1	5.3	~17.3	~66.0	~60.5				
200071		~31.5	10.0		~44.7	~47.1	~88.3	~41.7		~16.5
200072		~35.9	8.3	~18.6			~90.0	~35.1		
200144		35.3	9.5	17.0	46.3	44.0	66.5			20.6
200095		~38.3	9.1	~21.5	52.2	46.4	91.9	~57.4		13.9
200049		33.1	12.0	16.5	44.2	~41.3	92.1	61.6	22.3	
200143	68.2	31.4	13.0	16.3	46.0	41.8	~66.9	38.9		19.7
200048		45.5*	13.6							
200141		31.6	8.0	19.9	50.7	44.5	76.1			12.1
200142		~38.0	9.8	~20.3	~44.0	~41.3	~78.7	~37.3		~21.0
200074		29.9	12.0	15.8	48.2	53.2	77.3	36.7		20.7
200042		32.1*	7.1							
200133		~24.2	14.8	20.1	~35.3	~31.5	86.9	39.8		23.9
200134		36.9	12.1	14.9	46.1	41.4	62.2	40.5		25.9
200038		41.7*	8.3							
200070	82.3	28.5	10.0	16.9	45.9	38.7	60.2	34.3		
200084	~70.1	~35.2	8.6	~16.4	~49.2	~45.5	~69.2	~47.7		
200047		31.1	8.1		47.1	47.7	95.4	~34.3		
200096		~30.6	5.9	~13.9	~45.9	~36.9	~53.9	~43.8		
200040	76.5	29.6	8.3		47.5	35.6	~58.0	34.5	26.5	
200036	~81.9	~27.8	10.8	~15.8	~43.7	~42.5	~75.8	~63.6		
200094	~57.6	32.8	8.3	13.8	43.8	39.1	66.9	38.0	25.9	19.0
200021		40.6*	12.5							
200087	~76.5	31.7	5.3	17.0	45.3	45.0	~68.0	30.0		24.9
200039	101.0	35.1	10.0		38.3	33.7	65.4	34.6		
SY1615028	94.5	34.7	8.9	13.5			70.1	36.4		19.8
200027			9.1		~46.9	~48.3				
200085	79.5	38.0	8.1	13.5	42.3	38.5	70.0	~52.5		18.5
200024			10.8							
200025	76.7	31.5	9.1	12.1	48.0	41.7	66.4	~39.6		21.0
200033		36.4*	9.1							
200043		33.5	10.0	14.2	42.2	39.2	78.7	33.0		
200050		~33.3	10.5	~14.3	~42.9	~49.5	~83.3	~66.2		
200062		31.3*	12.5							

SAMPLE NUMBER	Disk-anus Distance %HL	Mandible-Disk Distance %HL	LLD % HL	Body Depth % HL**	PreD % HL	preA % HL*	Snout to Anus % HL	Mandible to Anus % HL	Anus to Anal Fin % HL
200037	~63.5	~57.9	23.0		126.3	269.2	143.3	134.8	65.7
200060	**50.3**	**46.6**		**90.0**	**176.4**	**180.0**	**122.8**	**111.1**	**57.7**
200041				108.7		187.0			
200081		~56.8				205.3			
200071		~51.9	~15.5			210.0			
200072		~47.7				200.0			
200144		47.2	10.6			228.6			
200095		59.8				204.5			
200049		55.0		116.0	157.6	200.0			
200143		50.2			143.4	213.0			
200048				136.4		263.6			
200141	~67.6	54.8			90.5	248.0	~151.5	~138.2	~71.3
200142		~47.7	~18.7	131.1		229.5			
200074		~57.6				244.0			
200042						221.4			
200133	~90.0	50.9	21.5	137.0		251.9	~169.6	~162.6	~31.1
200134	~50.6	47.3	8.3	118.2		203.0	~128.0	~119.0	~59.5
200038				150.0		295.8			
200070		58.1		140.0	127.1	243.3			
200084	~52.8	~52.8		117.1		202.9		~123.2	~64.5
200047				124.3	157.6	218.9			66.6
200096						205.9			
200040		45.6	14.1	136.1	127.8	241.7	132.6		
200036	~45.0	~46.4	~17.2	156.8		248.6	~122.2	~112.8	~67.5
200094	~61.4	51.0	16.5	138.9	133.1	211.1	~132.2	~126.4	~39.9
200021				137.5		240.6			
200087		49.9	18.7	118.4	158.9	215.8			
200039		39.8	14.6	155.0	159.4	237.5	114.6		
SY1615028	43.1	52.3		114.0			136.6	114.5	
200027						220.5			
200085	83.8	50.0			122.0	204.7	~155.0	~145.0	46.5
200024						283.8			
200025		40.3	11.4		141.4	245.5			
200033						239.4			
200043	~50.1	46.9	13.6		118.1	245.7	~120.4	~111.7	~67.0
200050			~11.9			221.1	~166.7	~152.4	~67.1
200062						243.8			

Supplementary Table 6.2. GenBank NCBI accession information for data collected in this study.

Species	Gene	Specimen ID	Accession Number
Notoliparis kermadecensis	16S	100220	KY659190
Notoliparis kermadecensis	16S	100326	KY659189
Notoliparis kermadecensis	16S	100350	KY659186
Notoliparis kermadecensis	COI	100220	KY659180
Notoliparis kermadecensis	COI	100326	KY659179
Notoliparis kermadecensis	COI	100350	KY659176
Notoliparis kermadecensis	Cyt-*b*	100220	KY659198
Notoliparis kermadecensis	Cyt-*b*	100326	KY659197
Notoliparis kermadecensis	Cyt-*b*	100350	KY659195
Notoliparis stewarti	16S	100343	KY659188
Notoliparis stewarti	16S	100344	KY659187
Notoliparis stewarti	COI	100343	KY659178
Notoliparis stewarti	COI	100344	KY659177
Notoliparis stewarti	Cyt-*b*	100343	KY659204
Notoliparis stewarti	Cyt-*b*	100344	KY659196
Pseudoliparis swirei	16S	200084	KY659194
Pseudoliparis swirei	16S	200094	KY659193
Pseudoliparis swirei	16S	200096	KY659192
Pseudoliparis swirei	16S	200143	KY659191
Pseudoliparis swirei	COI	200084	KY659185
Pseudoliparis swirei	COI	200094	KY659184
Pseudoliparis swirei	COI	200096	KY659183
Pseudoliparis swirei	COI	200134	KY659182
Pseudoliparis swirei	COI	200143	KY659181
Pseudoliparis swirei	Cyt-*b*	200094	KY659202
Pseudoliparis swirei	Cyt-*b*	200096	KY659201
Pseudoliparis swirei	Cyt-*b*	200134	KY659200
Pseudoliparis swirei	Cyt-*b*	200143	KY659199
Pseudoliparis swirei	Cyt-*b*	200084	KY659203

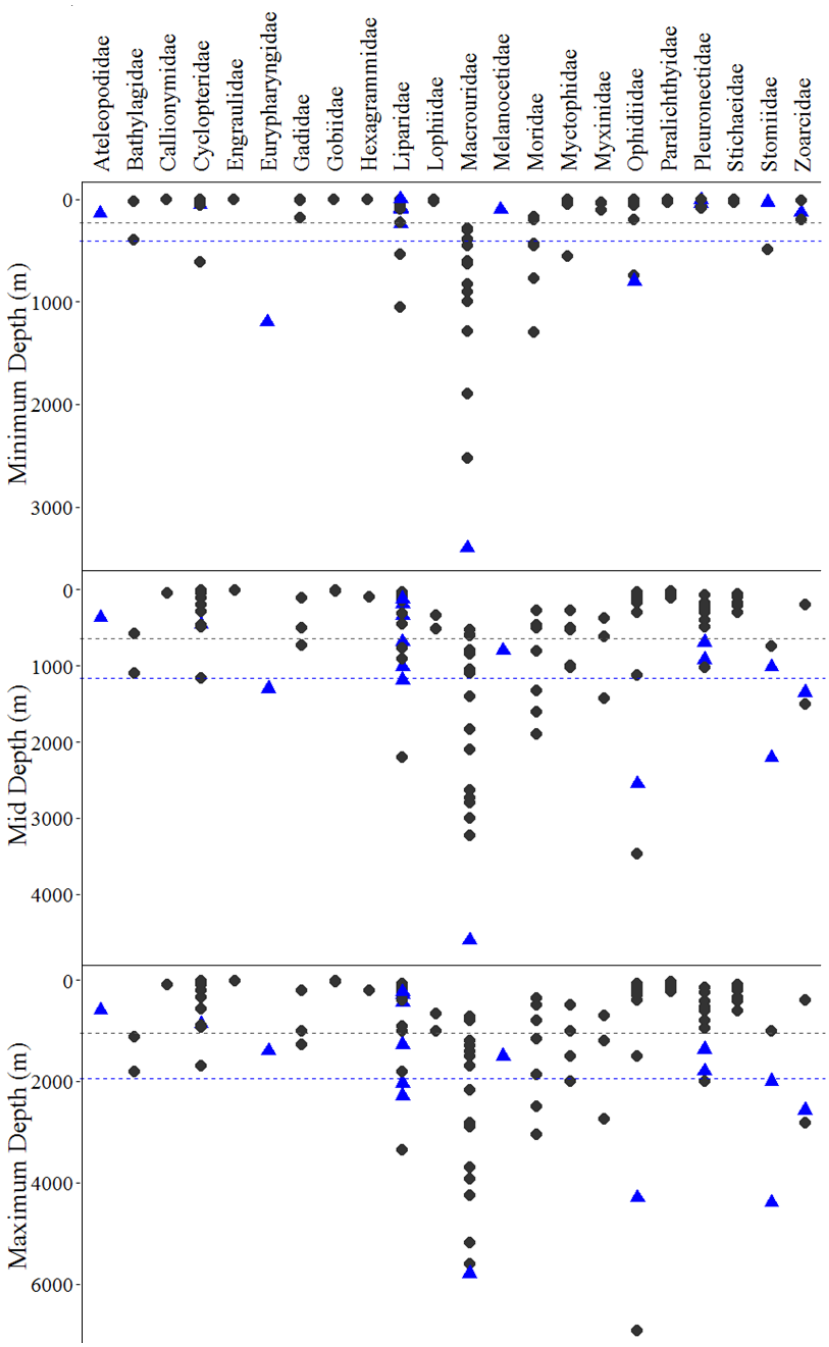

Supplementary Figure 5.1. Depth ranges of species with and without gelatinous tissues compared in the present study. Species with gelatinous tissues shown in blue triangles, those without gelatinous tissues grey circles. Grouped by family. Average depths of species with (blue) and without (grey) gelatinous tissues shown as dotted line.